## NOTICE

The quality of this microform is heavily dependent upon the quality of the original thesis submitted for microfilming. Every effort has been made to ensure the highest quality of reproduction possible.

If pages are missing, contact the university which granted the degree.

Some pages may have indistinct print especially if the original pages were typed with a poor typewriter ribbon or if the university sent us an inferior photocopy.

Previously copyrighted materials (journal articles, published tests, etc.) are not filmed.

Reproduction in full or in part of this microform is governed by the Canadian Copyright Act, R.S.C. 1970, c. C-30.

## AVIS

La qualité de cette microforme dépend grandement de la qualité de la thèse soumise au microfilmage. Nous avons tout fait pour assurer une qualité supérieure de reproduction.

S'il manque des pages, veuillez communiquer avec l'université qui a conféré le grade.

La qualité d'impression de certaines pages peut laisser à désirer, surtout si les pages originales ont été dactylographiées à l'aide d'un ruban usé ou si l'université nous a fait parvenir une photocopie de qualité inférieure.

Les documents qui font déjà l'objet d'un droit d'auteur (articles de revue, tests publiés, etc.) ne sont pas microfilmés.

La reproduction, même partielle, de cette microforme est soumise à la Loi canadienne sur le droit d'auteur, SRC 1970, c. C-30.

# THE ISOTOPE GEOCHEMISTRY AND ORIGINS OF FRACTURE CALCITES IN THE GRENVILLE GNEISSES, CHALK RIVER, ONTARIO

A thesis submitted to the School of Graduate Studies in partial fulfillment of the requirements for the degree of Doctor of Philosophy in Geology.

by

DENNIS JAMES BOTTOMLEY

DERRY LABORATORY
OTTAWA-CARLETON GEOSCIENCE CENTRE AND
DEPARTMENT OF GEOLOGY
UNIVERSITY OF OTTAWA
OTTAWA, CANADA, 1988

ISBN 0-315-46730-4

UNIVERSITÉ D'OTTAWA
UNIVERSITY OF OTTAWA

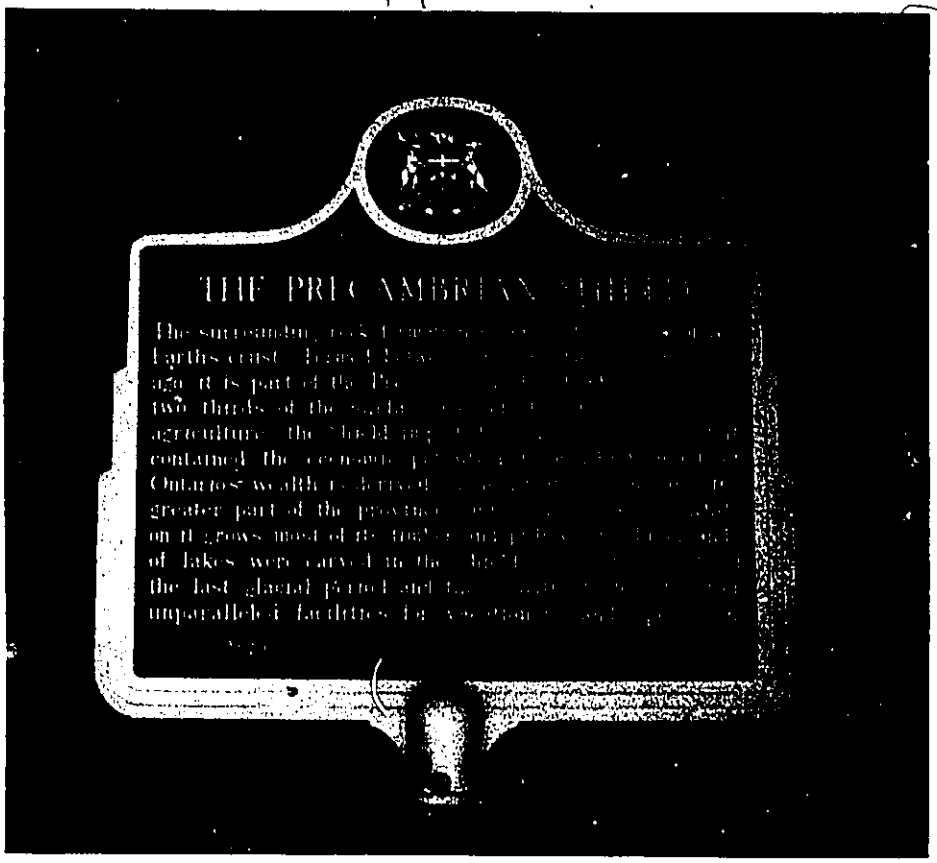

Historical Plaque at Bala, Ontario

Historically the Precambrian Shield has been a major factor in the settlement and economic development of Ontario. More recently its inherent ecological importance has become recognized and valued. In the next decade the federal government will decide whether a site on the Shield will be selected as a repository for Canada's nuclear fuel waste. It is incumbent on geoscientists that site selection be based on a firm geologic understanding of the medium and it is hoped that this thesis will make a small contribution to this effort.

# ABSTRACT

The Chalk River area of the Grenville structural province in eastern Ontario has been a centre for geoscience research in the Canadian Nuclear Fuel Waste Management Program (CNFWMP) of Atomic Energy of Canada Ltd. to determine whether plutonic rocks of the Precambrian Shield are suitable for the disposal of spent nuclear fuel waste. Drill core from this site has revealed that the bedrock (primarily monzonitic orthogneiss) is extensively fractured. Calcite is a particularly abundant fracture-infilling mineral in the core and it exhibits a variety of occurrences which indicates that calcite precipitation has occurred under variable hydrogeochemical conditions. Calcite is commonly associated with chlorite, quartz, and pyrite in sealed veins of hydrothermal origin, but it also occurs as flaky coatings or as fine crystallites in fractures that are presently open to ground water circulation. Chemical and isotopic analyses of these calcites, associated infillings, and host rocks have been conducted to determine the paleohydrogeology of this site.

Rubidium-strontium dating of the monzonitic gneiss indicates an emplacement age of 1345±22 Ma with an initial $^{87}Sr/^{86}Sr$ ratio of 0.70368. The Sr isotopic compositions of the calcites are relatively uniform, regardless of texture or occurrence, with a mean value (0.7090) that is significantly less radiogenic than the present day whole rock values. It is probable that the occurrence of calcite in these rocks is linked

to a period of late Proterozoic hydrothermal activity, possibly associated with incipient rifting of the Ottawa-Bonnechere graben system.

Concentrations of Fe and Mn in bulk calcite samples are generally between $10^3$ and $10^4$ ppm but most calcites have <200 ppm of Sr and Na. Cathodoluminescence spectroscopy, in conjunction with microprobe analyses, show significant variations in Mn and Fe concentrations in individual calcite veins indicating that hydrothermal fluid compositions were not uniform during calcite precipitation. Moreover, younger generations of calcites have formed on precursor hydrothermal calcite substrates in reactivated fractures. However, chondrite-normalized rare earth element (REE) patterns for the monzonitic gneisses and calcites are similar and are characterized by enrichment in the light rare earth elements. This suggests that the REE contents of the calcites, which are several times larger than in the gneisses, were derived from the host rocks.

The calcites exhibit a broad range in $\delta^{18}O$ with most values between 13 and 24°/oo (SMOW). A small group of calcites is significantly depleted in $^{18}O$, with values as low as -0.6°/oo. There is no strong, well-defined depth trend in the $\delta^{18}O$ values but large variations occur between closely spaced fractures and within individual fractures. Most sealed vein calcites have $\delta^{18}O$ values of <17°/oo, while flaky calcites in open fractures are generally much heavier. The $\delta^{13}C$ contents of the calcites are less variable, with most values be-

tween -5 and -8°/oo (PDB) although several values are lighter (minimum value -13.5°/oo).

Fracture pyrite is present as fine grained patches or disseminated cubes in calcite and chlorite and has $\delta^{34}S$ values that vary widely from -25 to +46°/oo (CDT). This range, as well as the highly positive $\delta^{34}S$ values, were likely produced by a Rayleigh distillation process in which the amount of S removed from solution by sulphide precipitation was a significant fraction of the total S in the initial solution. This indicates that at least semi-closed conditions existed within some fractures with respect to the transport of hydrothermal solutions. The negative $\delta^{34}S$ values of the pyrite, in association with $\delta^{13}C$ values near -7°/oo for unexchanged calcites, suggest that these minerals precipitated from a hydrothermal solution of near neutral pH and of moderately reducing oxygen fugacity ($f_{O_2} \sim 10^{-37}$). Isotopic geothermometers for coexisting calcite and dolomite yield conflicting hydrothermal temperatures, but the best estimate based on the Mg-calcite solvus geothermometer, is about 300°C.

After the period of hydrothermal activity, the calcites recrystallized and exchanged isotopically with meteoric ground waters resulting in a shift to $^{18}O$-rich but $^{13}C$-depleted calcites. The magnitude and direction of these shifts is controlled by temperature, the initial $\delta^{18}O$ and $\delta^{13}C$ of the calcite, the $\delta^{18}O$ of the ground water, the concentration and speciation of the dissolved inorganic carbon (DIC), the $\delta^{13}C$ of the DIC, and the time-integrated water/rock ratio of the flow system.

Because flow in fractured plutonic rock is primarily through channels along the fractures, calcites are influenced by highly variable water/rock ratios which results in non-uniform $\delta^{18}O$ values even at the scale of individual fractures. At Chalk River, the present ground water flow system acts as an open system with respect to water (and hence O) but as a closed system with respect to C. Calcites with the lightest $\delta^{13}C$ values have experienced time-integrated water/rock mole ratios approaching $10^5$. The presence of $^{14}C$ in these recrystallized calcites indicates that isotopic exchange is an active process at the present time.

Fracture calcites from the East Bull Lake gabbro-anorthosite pluton exhibit $\delta^{18}O - \delta^{13}C$ relationships similar to the Chalk River calcites, suggesting low temperature isotopic exchange may be a common phenomenon in fractured plutonic rock. However, fracture calcites in the White Lake trondhjemite are relatively rich in $^{13}C$ because of the contribution from sedimentary C in surrounding carbonate rocks at the time of intrusion. Consequently isotopic shifts resulting from recent exchange with meteoric waters are more difficult to resolve in such environments.

The stable isotopic compositions of fracture calcites may be useful in the CNFWMP for identifying masses of plutonic rock that have been relatively less permeable to ground water flow on a time-integrated basis. Moreover, the data suggest that flow in plutonic rocks would be more accurately described by discrete fracture flow models rather than by those based on an equivalent porous medium approach.

## ACKNOWLEDGEMENTS

I am indebted to my thesis supervisor, Professor J. Veizer, and gratefully acknowledge his support, encouragement, and insight without which this study could not have been completed.

I wish also to thank J. Loop, P. Middlestead, R. Hartree, G. Mrazek, W. Schmiedel, and G. St. Jean (University of Ottawa) and J.W. Card and J. Stevenson (Carleton University) for technical and analytical assistance during the course of my research. Electron microprobe and SEM facilities at the Canada Centre for Mineral and Energy Technology (EMR) and the Geological Survey of Canada were made available through the courtesy of P. Mainwaring and A.G. Plant, respectively. M. Bonardi kindly and cheerfully performed the electron microprobe analyses at the G.S.C. Several samples were also examined with the SEM in the Chemistry Department, University of Ottawa by T. Wrzesniewska.

Funding for this research was provided by Atomic Energy of Canada Ltd., who also provided access to the rock core for sampling, and by a Natural Sciences and Engineering Council grant to J. Veizer.

A special word of appreciation is offered to Eleanor Zurbrigg for her understanding.

# TABLE OF CONTENTS

TABLE OF CONTENTS (cont'd.)

TABLE OF CONTENTS (cont'd.)

TABLE OF CONTENTS (cont'd.)

# LIST OF TABLES

LIST OF TABLES (cont'd.)

# LIST OF FIGURES

LIST OF FIGURES (cont'd.)

LIST OF FIGURES (cont'd.)

LIST OF FIGURES (cont'd.)

LIST OF FIGURES (cont'd.)

LIST OF FIGURES (cont'd.)

# 1.0 INTRODUCTION

One of the major tasks of the Canadian Nuclear Fuel Waste Management Program (CNFWMP) is to ascertain whether spent nuclear fuel waste can be safely disposed of in plutonic rock of the Canadian Precambrian Shield (Wushcke et al., 1985). To this end five sites on the Shield were selected by Atomic Energy of Canada Ltd. as centres for geoscience research into the generic geologic properties of crystalline plutonic rocks to depths of up to 1 km. Because ground water transport is the only feasible process by which radionuclides from buried nuclear waste could return to the biosphere, the hydrogeologic characteristics of fractured rock, the hydrogeochemistry, and the nature of ground water flow systems in the Shield are elements of fundamental importance in this research program. The five AECL research areas are the Chalk River and White Lake plutons of the Grenville Structural Province in Ontario and the East Bull Lake (near Massey, Ontario), Eye-Dashwa Lakes (Atikokan, Ontario) and Lac du Bonnet (Whiteshell, Manitoba) batholiths of the Superior Province (Fig. 1).

The National Hydrology Research Institute of Environment Canada was the lead organization responsible for conducting the hydrogeologic investigations at some of the sites during the earliest days of the program. As a result I had the opportunity to study the hydrogeochemistry at the Chalk River, Whiteshell, and East Bull Lake Research Areas (Bottomley et al., 1984 a, b; 1986). Although the rocks at these sites are silicates, the dissolution of carbonates, which are present as fracture mine-

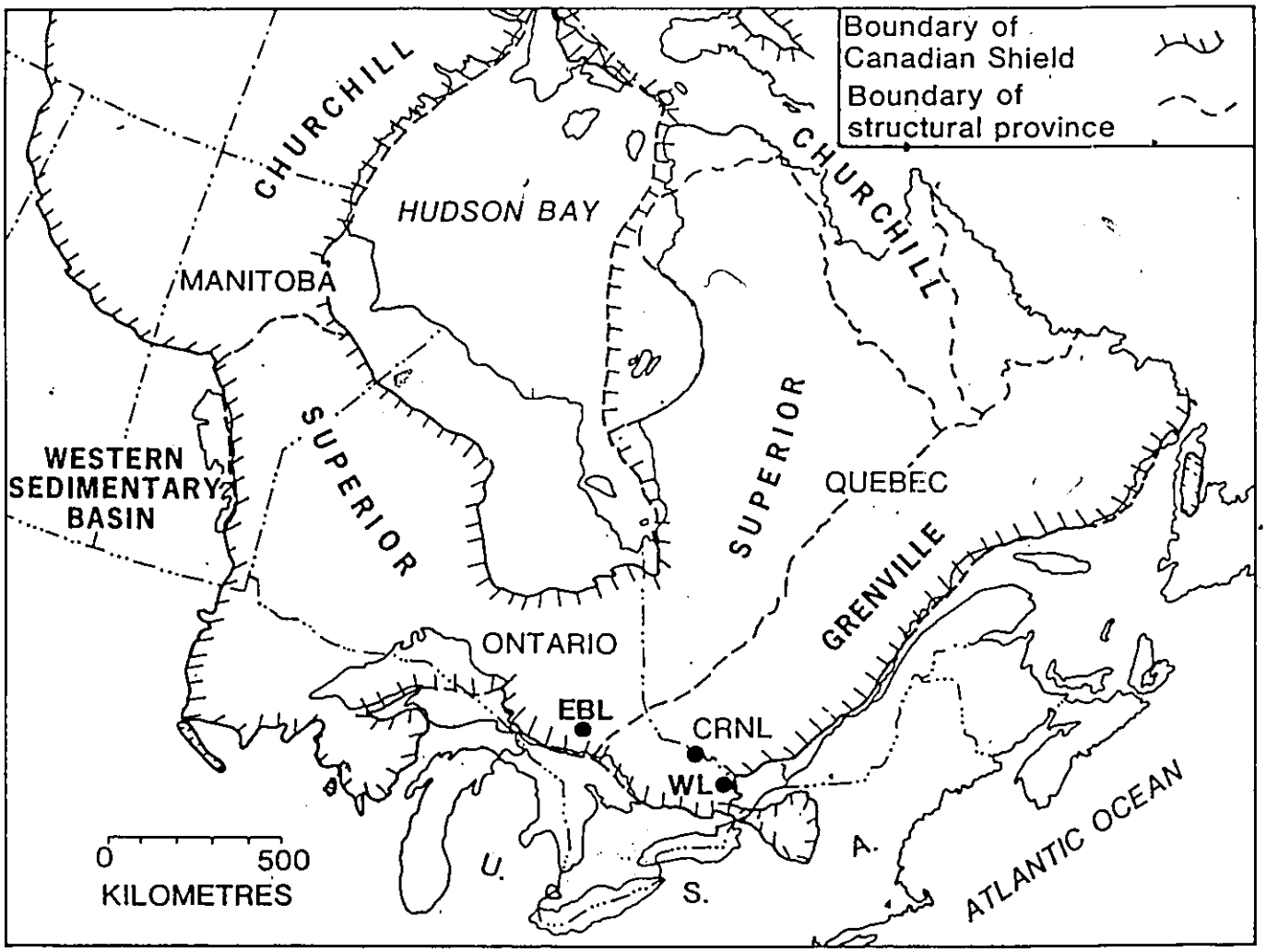


Fig. 1. Locations of AECL research areas discussed in this study. These areas are the Chalk River Nuclear Laboratories (CRNL), and the East Bull Lake (EBL) and White Lake (WL) plutons.

rals in the bedrock as well as components of the glacial drift at some sites, was found to be an important process in controlling the chemistry of the ground water to depths of 300-400 m. Characteristically the ground water at these depths is at or near saturation with respect to calcite. In spite of its common occurrence as a fracture mineral in core from all of the research areas, and its obvious importance as a control on the ground water chemistry, the origins of the fracture calcite and the nature of its interactions with present day ground waters have not been previously studied in detail in the CNFWMP.

Calcite contains several elements whose concentrations or isotopic compositions may be useful in determining its age of deposition and the nature and origin of the fluids from which it formed (Larson and Tullbourg, 1984; Milton and Brown, 1987). This in turn provides useful information on the paleohydrogeology of these sites and on the suitability of such rock to contain waste disposed within them.

Numerous studies by H.P. Taylor Jr. and co-workers have shown that the intrusion of batholiths into permeable country rocks frequently initiates convective hydrothermal systems involving large volumes of meteoric water (Criss and Taylor, 1986). Extensive oxygen isotopic exchange between the silicate minerals of these plutons and heated meteoric water often occurs. Sverjensky (1981) has extended these concepts to the isotopic alteration of Mississippi Valley Type carbonate rocks by hydrothermal formation waters and Taylor and Bucher-Nurminen (1986) have documented the nature of O and C isotopic exchange

reactions between marble and metasomatic fluids at temperatures near 400°C. Low temperature, diagenetic isotopic exchange between marine carbonate sediments and meteoric water or sea water has been demonstrated during the transformation of aragonite, high-Mg calcite and low-Mg calcite into diagenetic low-Mg calcite (Brand and Veizer, 1980; Al-Aasm and Veizer, 1986; Majid and Veizer, 1986). Isotopic exchange between deep sea foraminifera and marine pore water has been suggested by Killingly (1983). However low temperature (<25°C) isotopic exchange between meteoric waters and fracture calcites in plutonic rocks and achievement of isotopic equilibrium have not been convincingly demonstrated. Evidence for isotopic exchange in these rocks is worth collecting because this process may enable quantification of the time-integrated flux of meteoric water through their fracture networks.

Fracture calcite is particularly abundant in rock core from the Chalk River Research Area. I have therefore selected this site for detailed chemical and isotopic analyses of the calcite and associated fracture minerals and host rock. Additional analyses have been performed on calcites from the East Bull Lake and White Lake plutons to support the conceptual model of calcite isotopic evolution developed on the basis of the Chalk River data. Specifically the objectives of this thesis are to:

1) describe the occurrences and textures of fracture calcites in the Chalk River core;

2) determine the chemical and isotopic compositions of these calcites;

3) explain the age and origins of the calcite and to propose a model that accounts for the observed compositional variations;

4) test this model against fracture calcite data from the East Bull Lake and White Lake plutons, and,

5) suggest how such a model may be useful in identifying rock masses that may be the most suitable for the containment of radioactive waste over geologic time scales (at least $\sim 10^4$ years).

# 2.0 GEOLOGICAL SETTINGS

## 2.1 CHALK RIVER RESEARCH AREA

The Chalk River research area is located on the property of the Chalk River Nuclear Laboratories (CRNL) of AECL about 200 km northwest of Ottawa (Fig. 2). It is situated within the Ontario Gneiss Belt of the Grenville Structural Province of the Precambrian Shield and lies within the Ottawa-Bonnechère Graben system which is a large seismically active northwest striking fault system (Kay, 1942). The Ottawa River follows the Mattawa River Fault which defines the northern boundary of the graben system (Lumbers, 1972). The Ottawa-Bonnechère Graben system is about 60 km wide and is bounded on the northeast by the Laurentian Highlands and on the southwest by the Madawaska Highlands. Numerous fault blocks and dykes are present within this zone. Kumarapelli and Saull (1966) have suggested this graben and the St. Lawrence River valley form part of an ancient rift system stretching from Newfoundland to Lake Superior, and Burke and Dewey (1973) have proposed that the graben may be the failed arm of a triple junction system. The Chalk River pluton is situated near the northeastern edge of the large Algonquin batholith and these two intrusives may be genetically related (Schwerdtner and Lumbers, 1980). Silver et al. (1977) have suggested emplacement of the Algonquin batholith 1.4-1.5 Ga ago may be linked to the period of transcontinental anorogenic plutonism in North America.

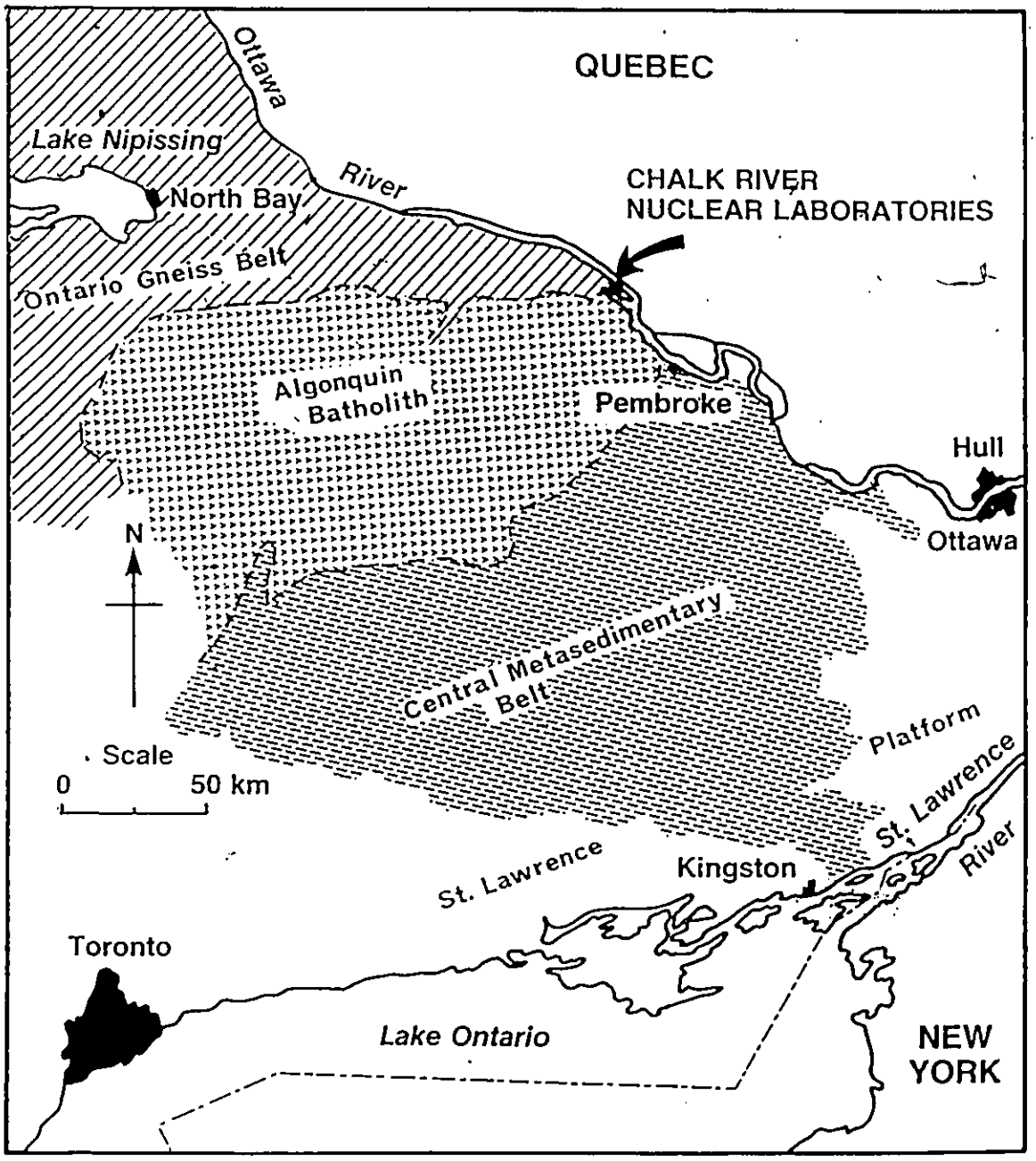


Fig. 2. Location of the CRNL research area showing the general regional geology of southeastern Ontario.

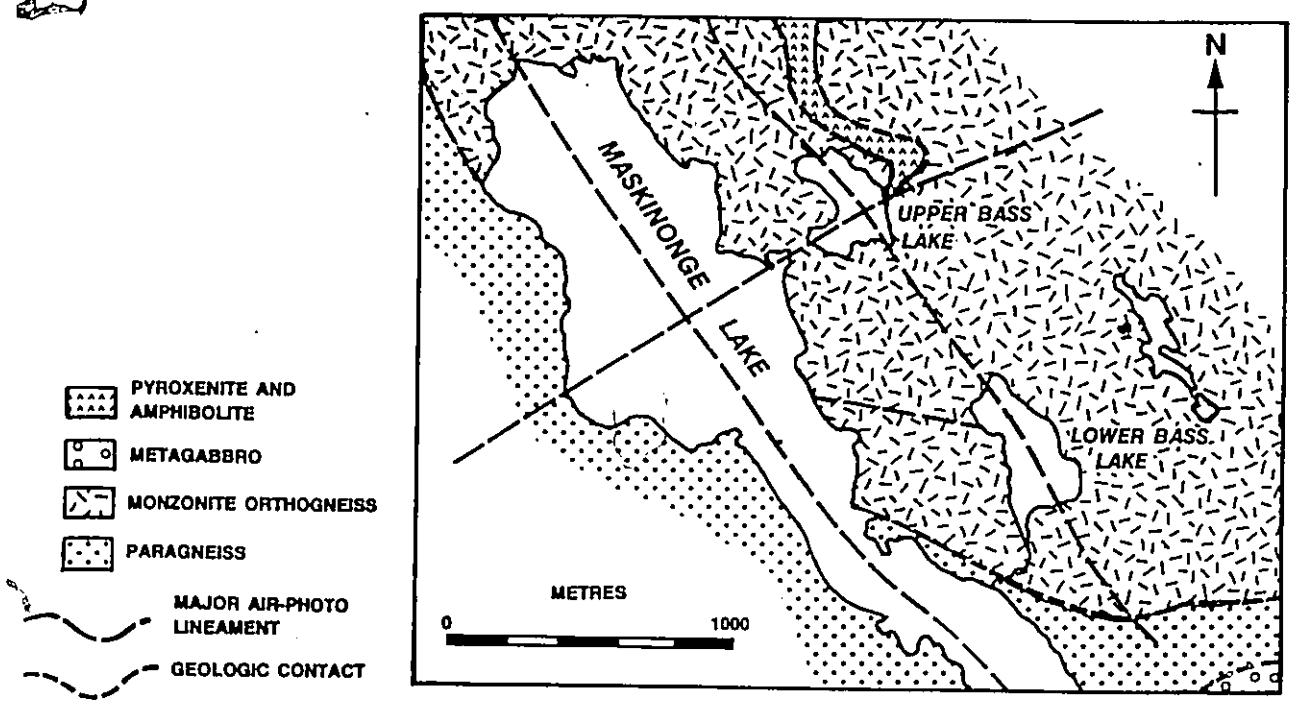


Fig. 3 General geology of the CRNL research area.

The area of investigation is located on the east side of Maskinonge Lake (Fig. 3) which lies on the eastern recumbent limb of a large north to northwest trending antiform (Brown and Rey, 1987). The axis of this antiform is located several kilometers to the west of the study area and the axial plane dips steeply to the northeast. Upright folding followed the earlier phase of recumbent folding and produced upright folds about east-west trending axes. Polyphase deformation has resulted in complexly fractured bedrock. Numerous northwest trending faults pass through the area which are crosscut by a later set of east-northeast trending faults.

The oldest rocks in the area are paragneisses which lie along the west side of Maskinonge Lake and which form the core of the northwest trending antiform. East of Maskinonge Lake the rocks are principally monzonitic orthogneiss which lie structurally above the paragneiss. The orthogneisses are sheet-like bodies which intruded the paragneiss (Dugal and Kamineni, 1987). Metagabbro is irregularly distributed as pod-shaped bodies along the contact between the paragneiss and orthogneiss. Granitic pegmatite, aplite, and diabase dikes intrude the gneisses and are the youngest rocks in the area. A small area of amphibolite and pyroxenite occurs on the northeast side of Upper Bass Lake. Although the orthogneisses are primarily monzonitic, Dugal and Kamineni (1987) recognize five varieties of orthogneiss at CRNL which, in increasing order of abundance, are as follows: 1) quartz syenitic gneiss, 2) gabbroic and monzogabbroic gneiss, 3) quartz monzodioritic and dioritic gneiss, 4) granitic and

granodioritic gneiss, and 5) monzonitic and quartz monzonitic gneiss. Plagioclase (oligoclase) is the most abundant mineral in the monzonitic rocks averaging about 45 modal per cent (Hamilton, 1984). Other major minerals are potassium feldspar (25%), quartz (9%), hornblende (5%), almandine garnet and biotite (4% each), and clinopyroxene (3%). Accessory primary minerals ($\leq$1%) include apatite, zircon, opaques (magnetite and ilmenite), allanite, and titanite.

The rocks at Chalk River have been regionally metamorphosed during the Grenville Orogeny to the upper amphibolite or granulite facies. Dugal and Kamineni (1987) estimate the temperature of regional metamorphism to have been around 650-750°C at pressures of 4 to 5 kb (400 to 500 MPa). The metamorphic peak of the Grenvillian event is commonly taken to be about 1100 Myr (Baer, 1981) but magmatism continued along the Ottawa graben during the Phanerozoic as recently as at least the Carboniferous (Higgins, 1982). Recent seismic experiments have shown that the Moho is very disturbed along major portions of the Ottawa graben and that there is evidence for a rise of high velocity material at its base (Mereu et al., 1986).

Between 1977 and 1983 ten NQ-3 and five HQ-3 inclined boreholes were drilled at the CRNL site (Fig. 4). The boreholes range from 48.5 to 704.3 m in length and have provided a total of approximately 2960 m of core. A summary of borehole technical details is presented in Table 1. Boreholes CR2, CR3, CR4, CR5, CR9, and FS17 were drilled to intersect major structural discontinuities and therefore the frequency of fracturing

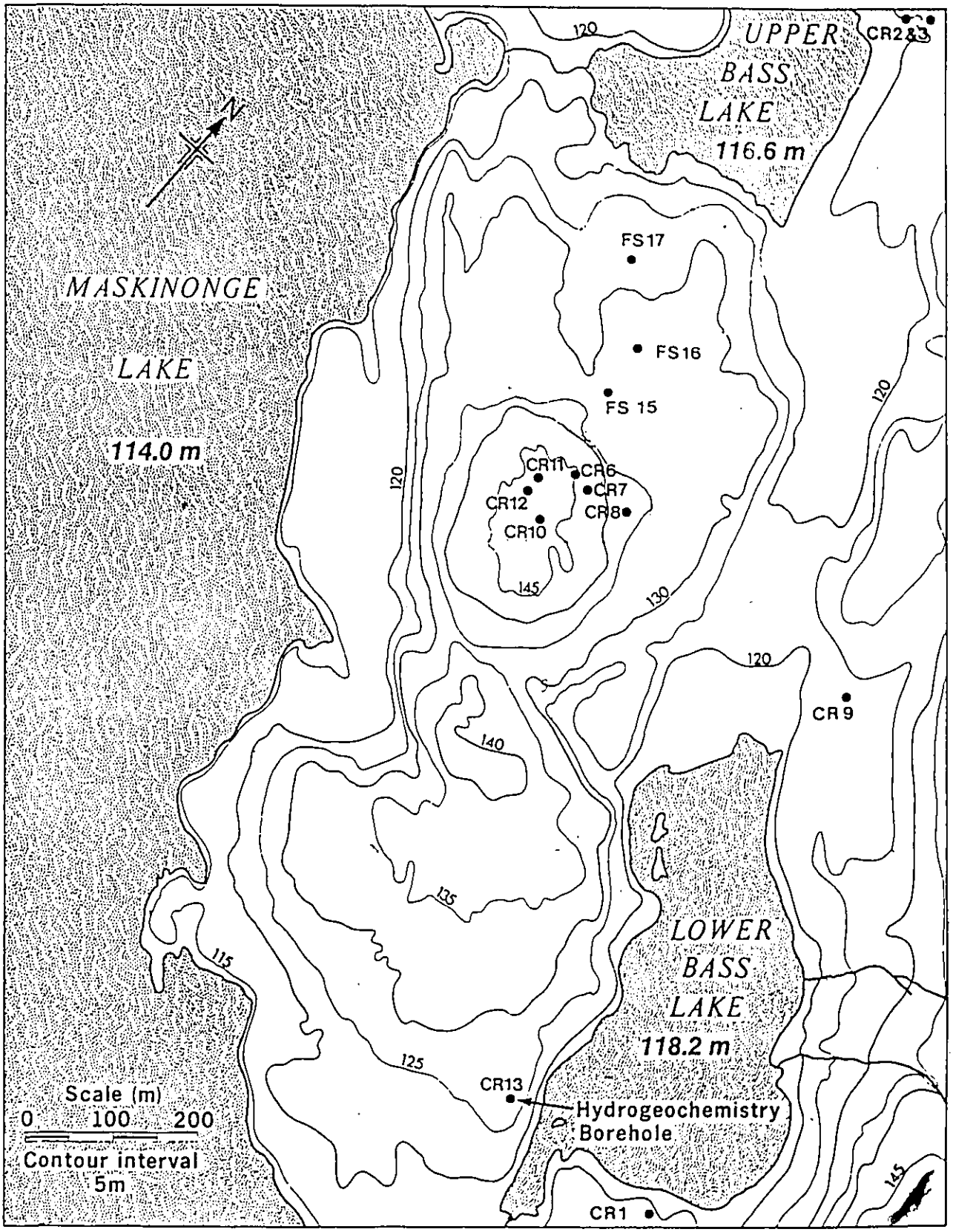


Fig. 4 Locations of CRNL cored boreholes sampled in this study and hydrogeochemistry borehole (air percussion drilled) CR13.

Table 1 - Technical details of the Chalk River research area cored boreholes (modified after Dugal and Kamineni, 1987)

| Borehole No. (year of drilling) | Type of Borehole | Length of Borehole (m) | Vertical Depth of Borehole (m) | Starting Trend/ Plunge |
|---|---|---|---|---|
| CR1 (1977) | NQ-3 | 270.6 | 250.4 | N16°/79°NNE |
| CR2 (1977) | NQ-3 | 213.8 | 185.1 | N133°/60°SE |
| CR3 (1977) | NQ-3 | 160.6 | 150.9 | N135°/70°SE |
| CR4 (1978) | HQ-3 | 113.4 | 102.8 | N134°/65°SE |
| CR5 (1978) | HQ-3 | 230.4 | 199.6 | N314°/60°NW |
| CR6 (1978) | NQ-3 | 305.5 | 293.5 | N184°/75°S |
| CR7 (1978) | NQ-3 | 153.4 | 148.1 | N184°/76°S |
| CR8 (1979) | NQ-3 | 306.3 | 292.3 | N245°/75°SW |
| CR9 (1979) | NQ-3 | 704.3 | 571.5 | N235°/60°SW |
| CR10 (1980) | NQ-3 | 112.8 | 112.8 | vertical |
| CR11 (1980) | NQ-3 | 106.7 | 106.7 | vertical |
| CR12 (1980) | NQ-3 | 121.0 | 121.0 | vertical |
| FS15 (1983) | HQ-3 | 48.5 | 48.5 | vertical |
| FS16 (1983) | HQ-3 | 50.3 | 50.3 | vertical |
| FS17 (1983) | HQ-3 | 60.8 | 60.8 | vertical |

observed in the core is higher for these boreholes. The average fracture frequency for all boreholes is about 15 fractures per metre and the bedrock is considered to be well to highly fractured (Dugal and Kamineni, 1987). The fractures usually contain one or more infilling minerals with chlorite and calcite dominant. Pyrite, sericite, epidote, iron oxides, clay minerals and rock fragments are also present. Crosscutting relationships indicate epidote is the oldest infilling followed by chlorite and sericite (Dugal and Kamineni, 1987). Calcite and pyrite occur toward the centre of chlorite-lined fractures indicating that they formed subsequent to chlorite formation.

The hydrogeology of the CRNL site to depths of about 300 m has been studied in detail and is described by Raven (1980), Davison (1981), Davison et al. (1982), Bottomley et al. (1984), Novakowski et al. (1985a,b), and Raven (1986). The hydraulic conductivity of fractured crystalline rock is primarily a function of fracture aperture, spacing, continuity, and interconnectivity. Equivalent rock mass hydraulic conductivity values determined from borehole hydraulic testing range from about $2.4 \times 10^{-4}$ m $s^{-1}$ to $2.9 \times 10^{-12}$ m $s^{-1}$ and reflect the variability in the geometry of the fracture system (Raven, 1980). Effective equivalent fracture apertures are also highly variable ranging between 1 and 500 μm. The most permeable pathways at CRNL are associated with discrete fracture zones associated with faulting and which are extremely important in the development of both local and regional scale flow systems.

The chemistry of the CRNL bedrock ground water to depths of about 500 m has been described by Bottomley et al. (1984a, b) and is based primarily on detailed studies in air-percussion drilled borehole CR-13. Briefly, the shallow ground water in the upper ~50 m at CRNL is of the $Ca/HCO_3$ type. This evolves to $Na/HCO_3$ water (probably via ion exchange reactions) which is present to depths of 200-250 m. Both water types are saturated with respect to calcite. Dilute Na/Cl ground water is present from 250 m to at least 350 m, and is apparently due to the presence of a component of Champlain Sea water which covered much of the CRNL area about 11,000 years ago following deglaciation (Catto et al., 1981). These authors estimate the Champlain Sea had a salinity of 12-16$^{o}$/oo in this region. Below 350 m the ground water chemistry appears to revert to the $Na/HCO_3$ type although drilling fluid contamination in the borehole may have obscured the true chemical nature of the ground water at depth. Bedrock ground water chemistry at CRNL is summarized in Table 2.

## 2.2 EAST BULL LAKE RESEARCH AREA

The East Bull Lake pluton is located about 35 km east of Elliot Lake, Ontario in the Superior Structural Province of the Precambrian Shield (Fig. 1). The pluton is comprised primarily of gabbro and anorthosite and has a maximum depth of about 780 m with the shape of a layered lopolith. Kamineni et al. (1984) have divided the pluton into 12 rock units. The thickest unit is a basal anorthosite approximately 400 m thick

Table 2 - Ground water chemistry at CRNL as measured in hydrogeochemistry borehole CR-13
(modified after Bottomley et al., 1984)

| Depth (m) | $Ca^{2+}$ | $Mg^{2+}$ | $Na^{+}$ | $K^{+}$ | $Sr^{2+}$ | $HCO_3^{-}$ | $SO_4^{-2}$ | $Cl^{-}$ | $Br^{-}$ | $F^{-}$ | Si | $Fe\ ugL^{-1}$ | $Mn\ ugL^{-1}$ | pH | $E_H$ (mV) | T (°C) | $ImeqL^{-1}$ cations | $ImeqL^{-1}$ anions | S.I.* calcite |
|---|---|---|---|---|---|---|---|---|---|---|---|---|---|---|---|---|---|---|---|
| 86 | 17.0 | 2.8 | 36.0 | 0.4 | 0.9 | 158.0 | 8.0 | 1.0 | <0.2 | 0.4 | 3.8 | <50 | <20 | 8.5 | +350 | 7.5 | 2.68 | 2.81 | 0.24 |
| 217 | 13.6 | 1.8 | 92.0 | 1.0 | 0.7 | 93.0 | 19.0 | 98.0 | 0.6 | 2.5 | 5.0 | <50 | 30 | 8.5 | +190 | 8.5 | 4.85 | 4.82 | -0.07 |
| 248 | 15.5 | 1.7 | 96.6 | 0.8 | 0.5 | 91.0 | 23.6 | 121.0 | 1.9 | 2.3 | 5.0 | <40 | <10 | 8.3 | +350 | 9.3 | 5.15 | 5.51 | -0.23 |
| 341 | 35.1 | 2.4 | 209.0 | 1.1 | 1.7 | 50.1 | 53.8 | 325.0 | 3.0 | 2.5 | 3.5 | <50 | 30 | 7.9 | +330 | 10.7 | 11.11 | 11.24 | -0.56 |
| 423 | 15.3 | 2.8 | 69.6 | 2.6 | 0.5 | 155.0 | 21.9 | 36.8 | 0.3 | 0.7 | 3.5 | 120 | <30 | 7.3 | +325 | 12.0 | 4.10 | 4.07 | -0.92 |
| 486 | 8.1 | 1.5 | 91.9 | 5.8 | 0.3 | 171.0 | 8.2 | 48.1 | 0.5 | 0.7 | 3.5 | 160 | <30 | 8.3 | -100 | 12.2 | 4.68 | 4.37 | -0.22 |
| 576 | 18.6 | 2.8 | 53.0 | 2.8 | 0.6 | 159.0 | 8.8 | 29.0 | <0.1 | 0.7 | 6.0 | 280 | 40 | 8.1 | 0 | 13.0 | 3.56 | 3.64 | 0.00 |

Measurements in mg $L^{-1}$ unless otherwise indicated.

*Saturation index with respect to calcite; S.I. = log ($IAP/K_T$) when IAP and $K_T$ are the ion activity product and the equilibrium constant, respectively, for the reaction $CaCO^3 \rightleftharpoons Ca^{2+} + CO_3^{2-}$ .

which grades upward into gabbroic anorthosite and a rhythmic layered anorthosite-gabbro unit. A troctolite unit, which is partly serpentinized, and highly fractured and permeable at its base separates the rhythmic layered unit from overlying layered crescummulate, and massive gabbro rock units.

The age of the pluton is about 2500 Ma based on a U-Pb age of 2480 +10/-5 Ma for baddeleyite ($ZrO_2$) fractions in a gabbro sample (Krogh et al., 1984) and a Sm-Nd age of 2472 ±70 Ma for the troctolite unit (Kamineni et al., 1987). The pluton is cut by numerous mafic dikes which have reported K-Ar ages ranging from 1.65 to 1.98 Ga (Kamineni et al., 1985). The pluton is underlain by gneissic rocks, granodiorites, and metavolcanics of Archean age.

The petrology, primary mineralogy, alteration and fracture infilling mineralogy of the pluton is described in Kamineni et al. (1985), Ejeckam et al. (1985), James and Born (1985), Kamineni (1986), and Kamineni et al. (1986) and is briefly summarized here. The EBL pluton is estimated to have crystallized at 1050°C (Kamineni et al., 1985) with clinopyroxene and plagioclase the most common primary minerals in the gabbro units, accompanied by olivine and orthopyroxene in the troctolite unit. The anorthite content of the plagioclase varies between bytownite and labradorite in the lower rock units and between labradorite and andesine in the units above the troctolite.

The clinopyroxene in the upper rock units is almost totally replaced by calcic amphiboles (hornblende, actinolitic hornblende, and actinolite) which frequently form an alteration

rim around a clinopyroxene core. However, unaltered pyroxene is present in parts of the troctolite unit. Dating of this secondary hornblende by the $^{40}Ar/^{39}Ar$ method indicates an age of 1800-1900 Ma which correlates well with a period of mafic dyke intrusion into the pluton (Kamineni et al., 1987).

The metamorphism responsible for the amphibole formation is believed to have occurred in the temperature range of 400 to 600°C at 100 to 200 MPa within the epidote-amphibolite/greenschist metamorphic facies (Kamineni, 1986). This metamorphism was pervasive and was also responsible for the formation of biotite, epidote, clinozoisite and chlorite. Other alteration minerals are the result of low grade, retrogressive metamorphism controlled by fluid circulation through fractures. Both prehnite-pumpellyite facies and lower temperature zeolite facies mineral assemblages (laumontite and analcime with calcite) have been recognized as well as low temperature clays, iron oxyhydroxides and gypsum. The prehnite-pumpellyite facies formed at a temperature of 200-300°C and the zeolite facies at temperatures of less than 200°C although the minimum temperature of laumontite formation is not well constrained. Laumontite is formed from the alteration of the plagioclase which, in some large fracture zones, has resulted in plagioclase albitization (Kamineni et al., 1985). Serpentinization of the troctolite is considered by Kamineni et al. (1985) to be the result of prehnite-pumpellyite facies metamorphism. Minor amounts of fracture chlorite also formed in this facies.

Kaolinite is the major low temperature clay mineral present but its formation is apparently not widespread and is concentrated in specific fracture zones. Similarly gypsum has only been identified in fractures between 265 and 300 m in borehole EBL-3. Vermiculite has been identified in core from EBL-3 but it is believed to have formed at relatively high temperatures in the prehnite-pumpellyite facies.

Four cored boreholes (EBL-1 to 4) and fourteen air-percussion boreholes (P.1 to 14) were drilled into the pluton (Fig. 5). Borehole EBL-1 is vertical and was drilled to a depth of 851 m to determine the thickness of the pluton. Serpentinized troctolite is present from 164-210 m and granitic basement rocks were encountered at 770 m in this borehole. Borehole EBL-2 is inclined at 71-75° and has a length of 836 m and was drilled to investigate the geology and hydrogeology of the 050 and 130 lineaments (Fig. 5). The troctolite zone extends from 51-122 m in this borehole. Borehole EBL-3 is inclined at 57-60° and has a length of 441 m and was drilled into highly fractured and altered rock associated with the Folson Lake Fault. Borehole EBL-4 was drilled to investigate an area that is relatively remote from major surface structural lineaments. The borehole is inclined at 65-69° and has a length of 489 m. The troctolite unit occurs from 119 to 185 m and as in EBL-1 and 2 is partly serpentinized.

The fourteen air-percussion holes range in depth from 38-99 m. Boreholes P-1, P-3, and P-4 provide shallow intersections with the 130 lineament while boreholes P-2, P-5, P-6, P-8

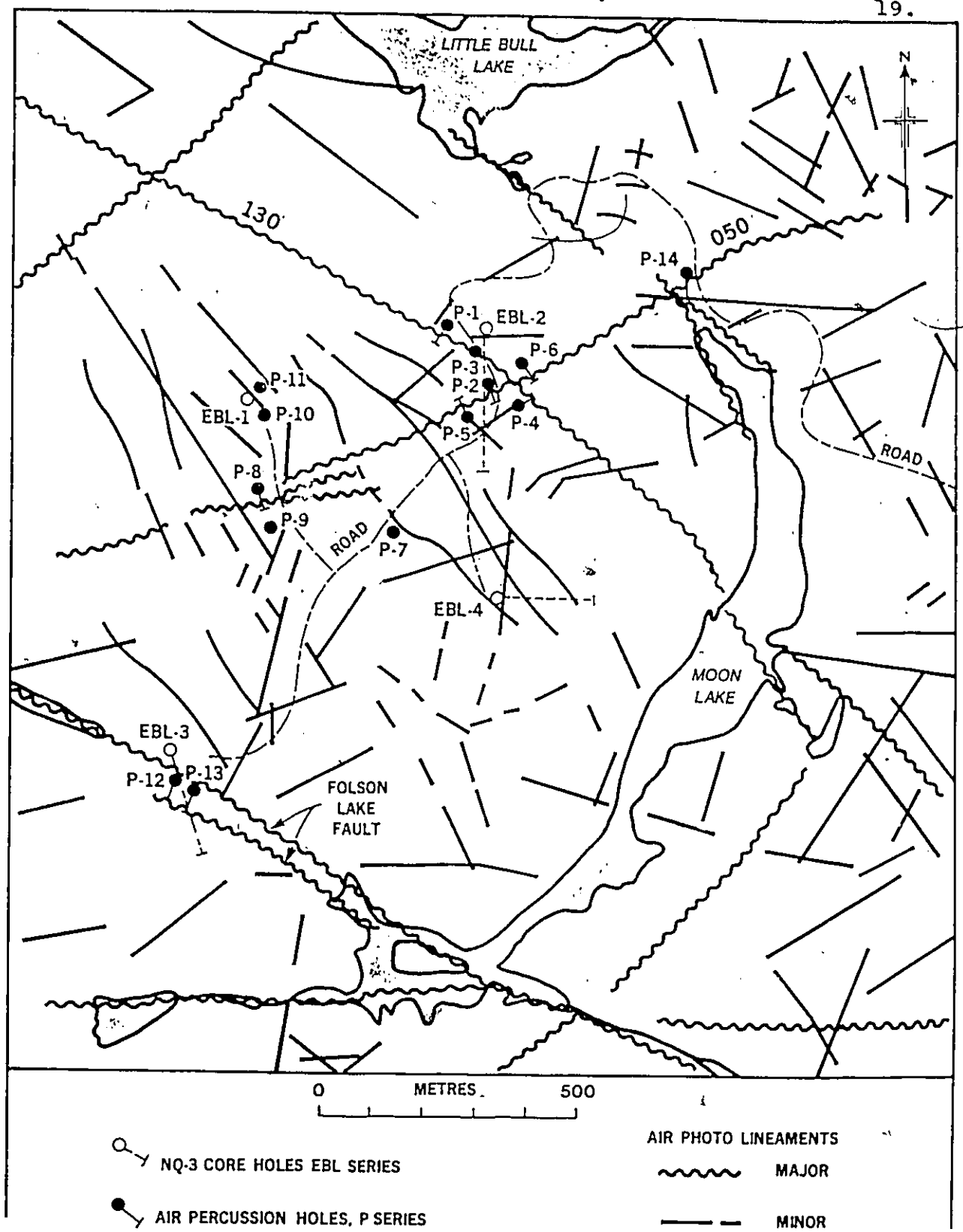


Fig. 5. Locations of EBL cored boreholes (EBL1-4) and air percussion drilled boreholes (P1-P14)(From Raven et al., 1987).

and P-14 intersect the 050 lineament. Boreholes P-12 and P-13 were drilled to shallow depths into the Folson Lake Fault zone.

There are several major structural discontinuities or lineaments transecting the pluton, most notably the 050 and 130 lineaments, and the Folson Lake Fault (Fig. 5). The 130 lineament is associated with a northwest striking mafic dyke whereas the 050 lineament likely reflects the presence of a large fracture zone or fault. Both lineaments dip steeply to the north. The Folson Lake Fault is a large regional fault that strikes northwesterly through the area. The hydraulic conductivity of the rock mass ranges from about $10^{-8}$ m $s^{-1}$ near the surface to less than $10^{-12}$ m $s^{-1}$ at depths greater than 400-500 m (Raven et al., 1987). However, fracture zones associated with the 050 and 130 lineaments have average hydraulic conductivities of 0.6 - 1.0 x $10^{-7}$ m $s^{-1}$. Major, low dipping fracture zones associated with the base of the troctolite and anorthosite units have similar, high hydraulic conductivity values.

Ground water sampling was conducted in all cored and air-percussion boreholes and the hydrogeochemistry of the pluton has been described in Bottomley et al. (1986). Three chemical types of ground water are present in the EBL pluton. In the recharge area of the local flow system (near borehole EBL-1) $Ca/HCO_3$ water is present which rapidly evolves by cation exchange reactions to high pH (~10) $Na/HCO_3$ water along the direction of ground water flow. The discharge areas for this local system are along the Folson Lake Fault and along the topographic depression created by the intersection of the 050 and 130 linea-

ments. Below a depth of about 350 m saline Na/Cl water is present which, on the basis of its chemistry and hydraulic head, is believed to be part of a deep regional ground water flow system. The ground water chemistry from all boreholes is listed in Table 3.

## 2.3 WHITE LAKE RESEARCH AREA

The White Lake pluton is located about 65 km west of Ottawa on the northwest side of White Lake (Fig. 6). It was the first site to be assigned research area status in the CNFWMP and the first and only research area to be abandoned because of public opposition to nuclear waste disposal related research in the area. Consequently only a limited amount of hydrogeologic work was done at this site which included the diamond drilling of four 30 m deep boreholes, one 38 m borehole and one inclined 79 m borehole (Dugal et al., 1979).

The White Lake pluton is located within the Central Metasedimentary Belt of the Grenville Province and its geochemistry and petrogenesis have been described by Somers (1984). The pluton is a granitic-trondhjemite which Lumbers (1982) has assigned to the biotite suite of plutonic rocks in this belt. It is prekinematic with respect to regional metamorphism having an age of between 1.3 and 1.0 Ga (Lumbers, 1982) and is intrusive into the marbles of the Grenville Supergroup metasedimentary rocks. Because of its uniformly low Rb/Sr ratio (0.05-0.09), it has not been possible to date this pluton by the Rb/Sr method (Bell and Blenkinsop, 1980). The pluton has a

Table 3 - Summary of representative ground water analyses (major and minor elements) for the P-series and EBL-cored boreholes, East Bull Lake.

Concentrations are in mg $L^{-1}$. Alkalinity is as mg $L^{-}$ $HCO_3^-$ and $P_{CO_2}$ Values are Calculated. C.B. denotes Charge Balance. (modified after Bottomley et al., 1986)

| Borehole and Sample Depth Interval (m) | $Ca^{2+}$ | $Mg^{2+}$ | $Na^{+}$ | $K^{+}$ | $Sr^{2+}$ | Alk | $SO_4^{2-}$ | $Cl^{-}$ | $F^{-}$ | $Br^{-}$ | Si | Fe | Mn | pH | S.I.$_c$ † | log $PCO_2$ (atm.) | C.B. (%) |
|---|---|---|---|---|---|---|---|---|---|---|---|---|---|---|---|---|---|
| P-1 | 32-53.3 | 1.9 | 0.1 | 53 | 0.4 | 0.06 | 139 | 6.7 | 0.6 | <0.1 | 0.06 | 7.3 | 0.11 | <0.04 | 9.1 | -0.17 | -4.08 | 0.2 |
| P-2 | 24.5-38.1 | 1.7 | 0.2 | 55 | 0.4 | 0.06 | 131 | 9.0 | 0.8 | <0.1 | 0.05 | 8.6 | <0.04 | <0.04 | 9.6 | 0.10 | -4.69 | 3.0 |
| P-3 | 0-16 | 17.3 | 3.8 | 24 | 0.8 | 0.14 | 127 | 8.6 | 1.0 | 0.2 | 0.04 | 7.0 | 0.37 | 0.12 | 7.3 | -0.98 | -2.28 | 1.0 |
| P-3 | 16-38.1 | 1.1 | 0.2 | 58 | 0.5 | 0.06 | 155 | 7.5 | 0.8 | 0.5 | 0.05 | 10.5 | <0.04 | <0.04 | 9.3 | -0.20 | -4.26 | 2.9 |
| P-4 | 0-35 | 25.0 | 4.7 | 8 | 1.6 | 0.06 | 103 | 3.6 | 0.9 | <0.1 | 0.05 | 6.6 | <0.04 | <0.04 | 7.7 | -0.51 | -2.77 | 6.2 |
| P-5 | 0-22 | 5.1 | 0.7 | 44 | 1.0 | 0.06 | 123 | 3.0 | 1.0 | 0.3 | 0.03 | 6.8 | 0.06 | <0.04 | 8.9 | 0.02 | -3.87 | 3.2 |
| P-5 | 88.5-97.6 | 1.6 | 0.3 | 59 | 0.3 | 0.06 | 149 | 6.0 | 1.2 | <0.1 | 0.03 | 9.1 | <0.04 | <0.04 | 9.4 | 0.01 | -4.40 | 0.3 |
| P-6 | 0-68 | 15.4 | 3.8 | 26 | 0.6 | 0.06 | 120 | 10.0 | 0.6 | 0.3 | 0.04 | 4.0 | <0.04 | <0.04 | 8.4 | 0.05 | -3.41 | 0.4 |
| P-7 | 0-39.6 | 22.8 | 1.1 | 3.9 | 0.9 | 0.12 | 68 | 12.0 | 0.6 | <0.1 | 0.04 | 5.2 | <0.04 | <0.04 | 9.0 | 0.53 | -4.29 | 1.5 |
| P-8 | 0-20 | 12.2 | 1.4 | 3.1 | 2.0 | 0.12 | 69 | 6.2 | 0.9 | <0.1 | <0.02 | 4.8 | 0.18 | 0.05 | 6.5 | -2.17 | -1.74 | 17.0 |
| P-9 | 0-12 | 15.8 | 2.2 | 4.4 | 0.6 | 0.06 | 63 | 5.7 | 0.5 | <0.1 | 0.11 | 8.0 | 0.53 | 0.05 | 6.2 | -2.39 | -1.48 | 1.3 |
| P-9 | 12-43.2 | 19.3 | 3.2 | 19 | 10.7 | 0.09 | 109 | 29.6 | 1.2 | <0.1 | 0.14 | 8.4 | 0.30 | 0.05 | 7.3 | -1.01 | -2.35 | 2.3 |
| P-10 | 0-34.5 | 19.2 | 4.5 | 5.5 | 0.7 | 0.06 | 82 | 11.2 | 2.8 | <0.1 | 0.09 | 9.4 | 0.04 | 0.06 | 6.1 | -2.31 | -1.27 | 6.2 |
| P-10 | 34.5-38.5 | 24.9 | 5.8 | 8.4 | 0.4 | 0.09 | 115 | 12.5 | 2.1 | <0.1 | 0.12 | 9.0 | 0.15 | 0.08 | 6.6 | -1.57 | -1.62 | 2.5 |
| P-10 | 66.3-70.3 | 20.7 | 5.5 | 10.6 | 0.7 | 0.06 | 123 | 12.0 | 1.6 | <0.1 | 0.11 | 8.0 | 0.26 | 0.06 | 7.8 | -0.42 | -2.80 | 8.1 |
| P-10 | 82-98.7 | 19.2 | 4.2 | 17.8 | 1.0 | 0.09 | 112 | 12.5 | 1.1 | <0.1 | 0.11 | 7.7 | <0.04 | 0.05 | 7.6 | -0.67 | -2.63 | 0.5 |
| P-11 | 0-49.2 | 32.4 | 7.3 | 9.5 | 6.8 | 0.20 | 157* | 12.5 | 1.3 | 0.2 | 0.08 | 7.0 | 0.23 | 0.25 | 6.8 | -1.15 | -1.70 | 1.3 |
| P-12 | 0-37 | 5.9 | 1.6 | 45 | 13.2 | 0.11 | 110 | 34.5 | 0.7 | 0.2 | 0.05 | 4.0 | 0.07 | 0.06 | 9.4 | 0.44 | -4.53 | 3.3 |
| P-12 | 38-48.6 | 4.1 | 0.9 | 40 | 6.8 | 0.12 | 116 | 18.0 | 0.9 | 0.4 | 0.13 | 6.8 | 0.08 | 0.05 | 8.9 | -0.08 | -3.95 | 2.8 |
| P-13 | 0-22 | 6.9 | 1.9 | 35 | 7.9 | 0.13 | 105 | 17.0 | 1.2 | 0.1 | 0.11 | 9.3 | <0.04 | 0.04 | 9.0 | 0.18 | -4.10 | 2.6 |
| P-14 | 0-43.3 | 23.1 | 5.5 | 2.6 | 1.6 | 0.15 | 93 | 5.9 | 0.2 | <0.1 | 0.10 | 6.7 | 0.13 | 0.08 | 7.5 | -0.78 | -2.61 | 3.2 |
| | 147-298 | 2.4 | 0.4 | 84 | 0.5 | 0.06 | 197* | 4.3 | 17.9 | <0.1 | 0.10 | 12.5 | <0.04 | <0.04 | 9.4* | 0.29 | -4.28 | 0.3 |
| EBL-1 | 204-213 | 2.6 | 0.7 | 76 | 0.04 | 0.06 | 190 | 3.5 | 17.8 | <0.1 | 0.17 | 13.5 | 0.56 | <0.02 | 9.9 | 0.57 | -4.88 | 2.4 |
| | 298-512 | 5.5 | 0.1 | 233 | 0.8 | 0.10 | 66 | 17.8 | 321 | <0.1 | 1.60 | 14.7 | 0.14 | <0.04 | 10.2 | 0.45 | -6.05 | 0.5 |
| | 504-642 | 8.5 | 0.3 | 205 | 0.10 | 0.09 | 69 | 14.5 | 310 | 0.6 | 1.66 | 19.3 | 0.06 | 0.02 | 9.8 | 0.55 | -5.40 | 4.2 |
| | 0-75 | 20.0 | 6.3 | 16 | 0.7 | 0.12 | 144 | 29 | 4.0 | <0.1 | 0.17 | 5.4 | 18.7 | 0.82 | 6.5 | -1.70 | -1.43 | 2.9 |
| | 75-248 | 0.4 | 0.6 | 65 | 0.2 | 0.06 | 157 | 9.9 | 10.9 | 0.4 | 0.04 | 12.1 | 1.13 | <0.04 | 10.4 | -0.13 | -5.83 | 3.4 |
| EBL-2 | 111-126 | 3.0 | 1.0 | 66 | 2.4 | 0.06 | 172 | 3.4 | 6.8 | <0.1 | 0.04 | 10.2 | 0.58 | <0.02 | 10.1 | 0.70 | -5.29 | 1.7 |
| | 248-460 | 0.5 | 0.3 | 7.4 | 0.5 | 0.06 | 130 | 21.5 | 31 | <0.1 | 0.3 | 14.4 | 0.30 | <0.04 | 9.7* | -0.34 | -4.84 | 2.6 |
| | 460-616 | 228 | 1.6 | 570 | 1.1 | 1.53 | 38 | 11.4 | 1237 | 1.6 | 3.3 | 4.4 | 0.12 | 0.13 | 8.0* | 0.12 | -3.55 | 0.8 |
| EBL-3 | 0-443 | 25.7 | 6.0 | 16 | 0.4 | 0.19 | 125 | 3.7 | 1.2 | 0.1 | 0.05 | 4.6 | <0.04 | 0.14 | 7.5 | -0.62 | -2.49 | 7.1 |
| | 0-120 | 13.3 | 4.8 | 15 | 0.9 | 0.06 | 96 | 9.0 | 0.8 | 0.1 | 0.05 | 7.7 | 3.20 | 0.22 | 6.7 | -1.79 | -1.79 | 1.4 |
| | 105-117 | 1.3 | 2.9 | 60 | 0.8 | 0.06 | 150 | 2.9 | 3.1 | 0.1 | 0.02 | 8.9 | 0.10 | <0.02 | 9.1* | -0.31 | -4.05 | 6.0 |
| EBL-4 | 120-198 | 1.6 | 0.6 | 78 | 0.4 | 0.06 | 23 | 1.6 | 1.7 | 0.4 | 0.03 | 15.8 | <0.04 | <0.04 | 10.0 | 0.44 | -4.99 | 1.2 |
| | 198-396 | 3.6 | 0.9 | 72 | 0.4 | 0.06 | 186* | 2.0 | 30.7 | 0.3 | 0.04 | 12.8 | <0.04 | <0.04 | 10.2* | 0.83 | -5.43 | 7.8 |
| | 429-456 | 455 | 2.2 | 1160 | 3.4 | 6.2 | 14 | 108 | 2580 | 0.6 | 10.8 | 9.2 | 0.13 | <0.02 | 8.5 | 0.23 | -4.53 | 1.2 |

† S.I.$_c$ = calcite saturation index = log IAP/$K_T$ where IAP = ion activity product and $K_T$ is the equilibrium constant for the reaction

$$CaCO_3 \rightleftharpoons Ca^{2+} + CO_3^{2-}$$

* Lab analysis - other values are field measurements.

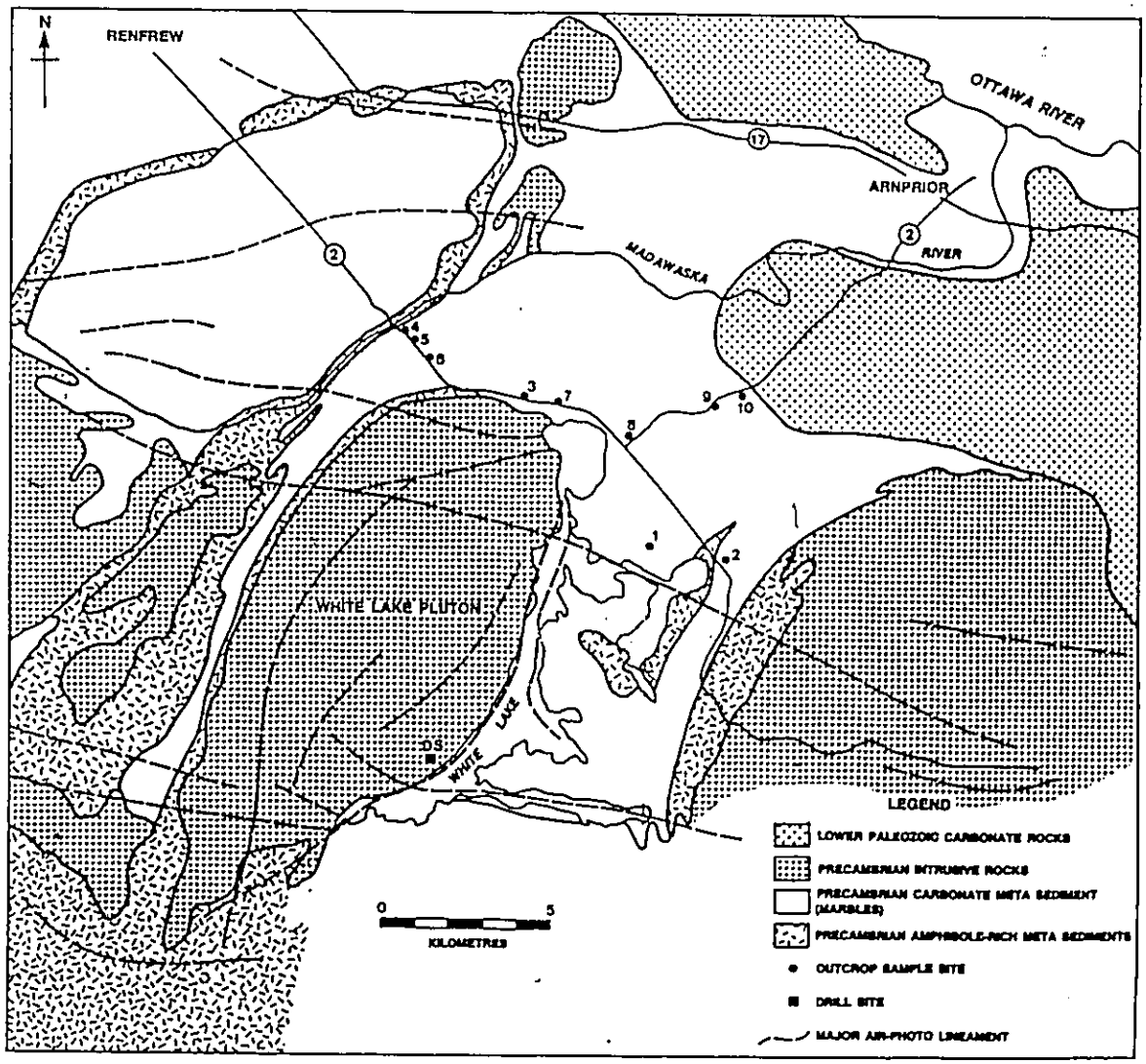


Fig. 6. General geology of the White Lake pluton showing location of the drill site (DS) and marble outcrop sampling sites (1-10).

$\delta^{18}O$ of 7.3±0.6°/oo (SMOW) (Wu and Kerrich, 1986) which is typical of trondhjemitic rocks in this part of the Grenville and which has been interpreted as indicating these rocks formed from a primary magma generated in the lower crust or upper mantle.

The pluton has a well developed gneissosity and veins and lenses of potassic granite pegmatite and feldspathic amphibolite are abundant. Fracture spacing in core from the boreholes varies from 0.25 cm to 2 m, depending on the location of shear zones and highly fractured areas (Dugal et al., 1979).

Calcite is the dominant fracture infilling but chlorite, sericite, clay minerals, and pyrite are also present. Hematitic staining is heavy in the highly sheared zones. Hydraulic testing and ground water sampling were not conducted in the boreholes.

Because this pluton is intrusive into carbonate rocks, $CO_2$ produced by decarboration or dissolution reactions could be convectively transported into the fractures of the cooling pluton and the C precipitated in fracture calcites. Therefore White Lake fracture calcites and the marble country rock were analyzed to determine whether sedimentary C would have to be considered as a C source for fracture calcites in plutons that are intrusive into metasedimentary formations.

# 3.0 THEORETICAL CONSIDERATIONS CONCERNING THE ORIGIN AND ISOTOPE GEOCHEMISTRY OF FRACTURE CALCITES

## 3.1 WATER/ROCK INTERACTIONS AND THE FORMATION OF LOW TEMPERATURE SECONDARY MINERALS

In shallow meteoric ground water flow systems in fractured plutonic rock there are three major water/rock interactions controlling the chemistry of the ground water:

a) dissolution of carbonates that are present either in the fractures or in unconsolidated surficial deposits or sedimentary rocks mantling the basement rocks. This may lead to reprecipitation of secondary calcite;

b) exchange reactions between solutes in the ground water and adsorbed cations primarily on clay minerals in the fractures. This process may be a major control on the chemical evolution of ground water;

c) incongruent dissolution of primary rock-forming silicate minerals which (unlike processes (a) and (b)) results in the formation of a secondary relatively Al-rich silicate mineral. An example of this type of reaction is the dissolution of albite by carbonic acid to produce kaolinite:

(1) $$2NaAlSi_3O_8 + 11\ H_2O + 2CO_2 \rightleftharpoons Al_2Si_2O_5(OH)_4 + 2Na^+ + 2HCO_3^- + 4H_4SiO_4.$$

The solubility of Al is very low except in very low or very high pH waters and thus is largely conserved in the secondary mineral. The low solubility of Al enables relative mineral stability relationships to be depicted on two-dimensional phase diagrams (Drever, 1982), examples of which are shown in Fig. 7 to 10 (at 25°C). The chemical compositions of CRNL and EBL ground waters have been plotted on these diagrams in order to determine which minerals should be the most stable in contact with these waters.

For the system $CaO-Al_2O_3-SiO_2-H_2O$ either kaolinite or Ca-smectite is expected to be the most stable phase in contact with the CRNL ground waters (Fig. 7). In contrast, the EBL ground waters show a progression from kaolinite in contact with shallow, relatively low pH recharge ground waters to smectite and/or laumontite in the evolved $Na/HCO_3$ and deep saline Na/Cl ground waters. Kaolinite and laumontite are present in fractures of the EBL core but smectite has not been identified by XRD analysis. Laumontite, which is particularly abundant in the anorthosite unit, generally forms under hydrothermal conditions (<300°C) but the minimum temperature of its formation is not well constrained. Laumontite formation has been reported at temperatures as low as 50°C (Boles and Coombs, 1977) and laumontite of apparent authigenic origins has been found in deep sea sediments (Sands and Drever, 1978) which implies that even lower temperatures than 50°C are possible for laumontite formation. The apparent stability of laumontite in contact with the $Na/HCO_3$ ground waters at EBL is probably a consequence of the high pH

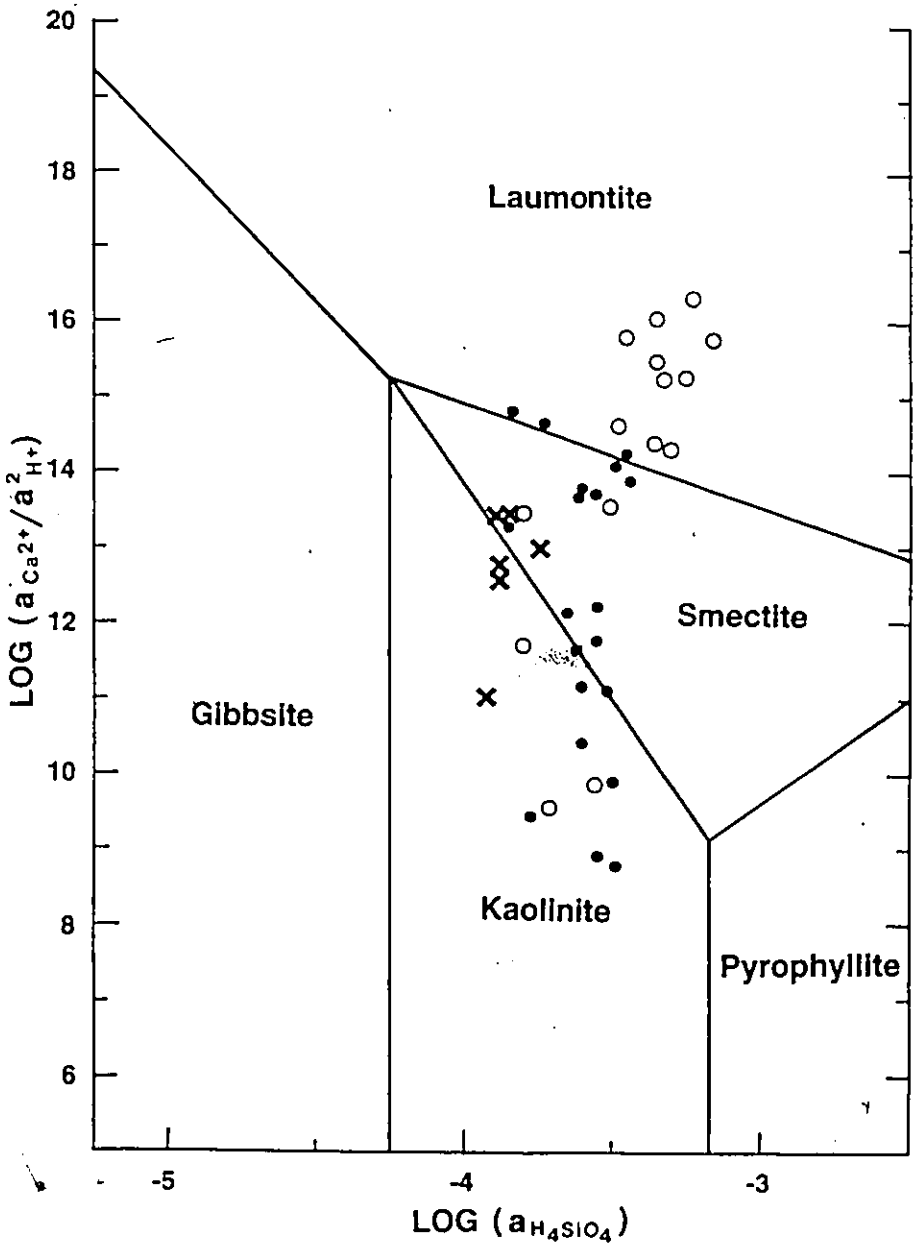


Fig. 7. Stability diagram for the system $CaO-Al_2O_3-SiO_2H_2O$ at 25°C (after Drever, 1982). Ground waters are plotted as crosses (CRNL), solid dots (EBL P-series boreholes) and open circles (EBL cored boreholes).

of the waters (up to pH 10.4) rather than an indication of active, present day laumontite formation. Nevertheless, laumontite crystallization as the result of recent water/rock interactions cannot be precluded.

For the system $Na_2O$-$Al_2O_3$-$SiO_2$-$H_2O$ kaolinite is again predicted to be the most stable phase in contact with the CRNL ground waters and the shallow EBL ground waters (Fig. 8). The geochemically evolved $Na/HCO_3$ waters and the saline Na/Cl waters at EBL should be in equilibrium with albite. Albite has been observed in fractures in the anorthosite and has been attributed to albitization of plagioclase with concomitant formation of laumontite:

$$(2) \qquad NaAlSi_3O_8 \cdot CaAl_2Si_2O_8 + 3\ SiO_2 + 2H_2O + Na^+ \rightleftharpoons 2NaAlSi_3O_8 + 0.5CaAl_2Si_4O_{12} \cdot 4H_2O + 0.5\ Ca^{2+}$$

Therefore, as in the case of laumontite the stability of albite in these waters does not necessarily mean that it is forming from present day albitization.

A Sr isotope study of the EBL pluton including ground waters and fracture calcites and laumontite was conducted by McNutt et al. (1987). The $^{87}Sr/^{87}Sr$ ratios of the calcite and laumontite are relatively constant at 0.7125 and are more radiogenic than present day whole rock values which are generally less than 0.710. McNutt et al. (1987) have suggested that the high ratios for the calcite and laumontite could reflect Sr isotope exchange between a parent hydrothermal fluid and K-rich secondary fracture minerals such as amphibole and biotite

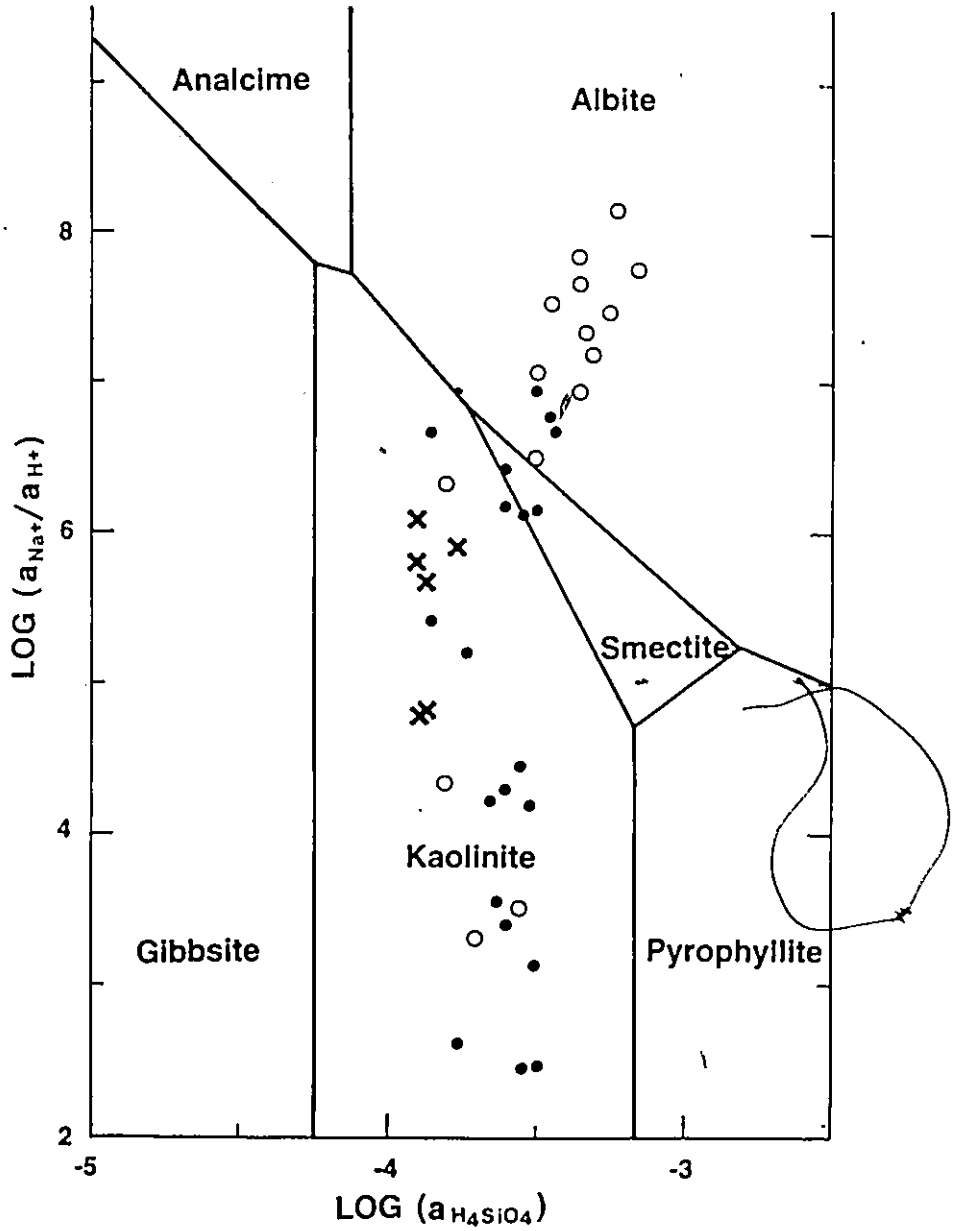


Fig. 8. Stability diagram for the system $Na_2O$-$Al_2O_3$-$SiO_2$-$H_2O$ at 25°C (after Drever, 1982). Ground waters are plotted as crosses (CRNL), solid dots (EBL P-series boreholes) and open circles (EBL cored boreholes.

which formed during the earlier metamorphic event of 1800-1900 Ma ago. They have suggested an early Phanerozoic age for these calcites based on the assumption that the laumontite associated with the calcite formed in response to burial metamorphism conditions imposed by Early Paleozoic sedimentation on the Precambrian craton. Crosscutting relationships indicate that laumontite-bearing fractures are less than about 900 Ma old (McNutt et al., 1987) but there is no minimum age estimate.

Because the $Na/HCO_3$ and Na/Cl waters have essentially the same $^{87}Sr/^{86}Sr$ ratio as the calcite and laumontite, McNutt et al. (1987) have suggested that dissolution of these minerals may be controlling the Sr isotopic composition of these ground waters. However, laumontite is apparently stable in the deep EBL ground waters and therefore dissolution of this mineral is an unlikely control on the Sr isotopic composition. Instead of an earlier fracture mineral control on the isotopic composition of the laumontite and calcite, it is possible that these minerals (and albite) precipitated from the Na/Cl water that is now found only at depth in the pluton but which at one time may have infiltrated the entire rock mass. Such an intrusion would have filled most of the exchangeable cation sites on clay minerals with $Na^+$ as well as imparted its isotopic signature on the exchangeable $Sr^{2+}$ population of the fracture minerals. This model would appear most suited for explaining the similarities in the Sr isotopic compositions of the $Na/HCO_3$ and Na/Cl waters despite their large difference in $Sr^{2+}$ concentrations

and the differences in age and origin of these waters. In other words, the Sr isotopic composition of the $Na/HCO_3$ water is likely in equilibrium with and controlled by the isotopic composition of the exchangeable $Sr^{2+}$ in the fractures.

For the system $MgO-Al_2O_3-SiO_2-H_2O$ kaolinite is predicted to be the most stable phase in contact with both the CRNL ground waters and most of the shallow EBL ground waters based on the mineral stability diagram of Nesbitt (1980) (Fig. 9). Chlorite is predicted to be in equilibrium with the deeper $Na/HCO_3$ and Na/Cl ground waters at EBL. However if the solubility relationships of other magnesium silicates such as talc, sepiolite and serpentine are considered (Fig. 9), then it is apparent that many of the ground waters are highly supersaturated with respect to talc and therefore if chlorite formed from these waters it would be metastable with respect to talc. This is also true for serpentine and sepiolite.

Talc has been identified in fractures of the CRNL core but chlorite and serpentine are the major Mg silicate fracture minerals in the EBL core. These minerals, however, are predominantly of ancient hydrothermal origins (Kamineni et al., 1985). Serpentinization primarily occurs in the troctolite unit and is considered to be the result of prehnite-pumpellyite facies metamorphism. Convincing evidence for significant low temperature Mg silicate formation at EBL is lacking.

A stability diagram for the system $K_2O-Al_2O_3-SiO_2-H_2O$ is shown in Fig. 10. Kaolinite and muscovite/illite are predicted to be stable secondary minerals in equilibrium with the

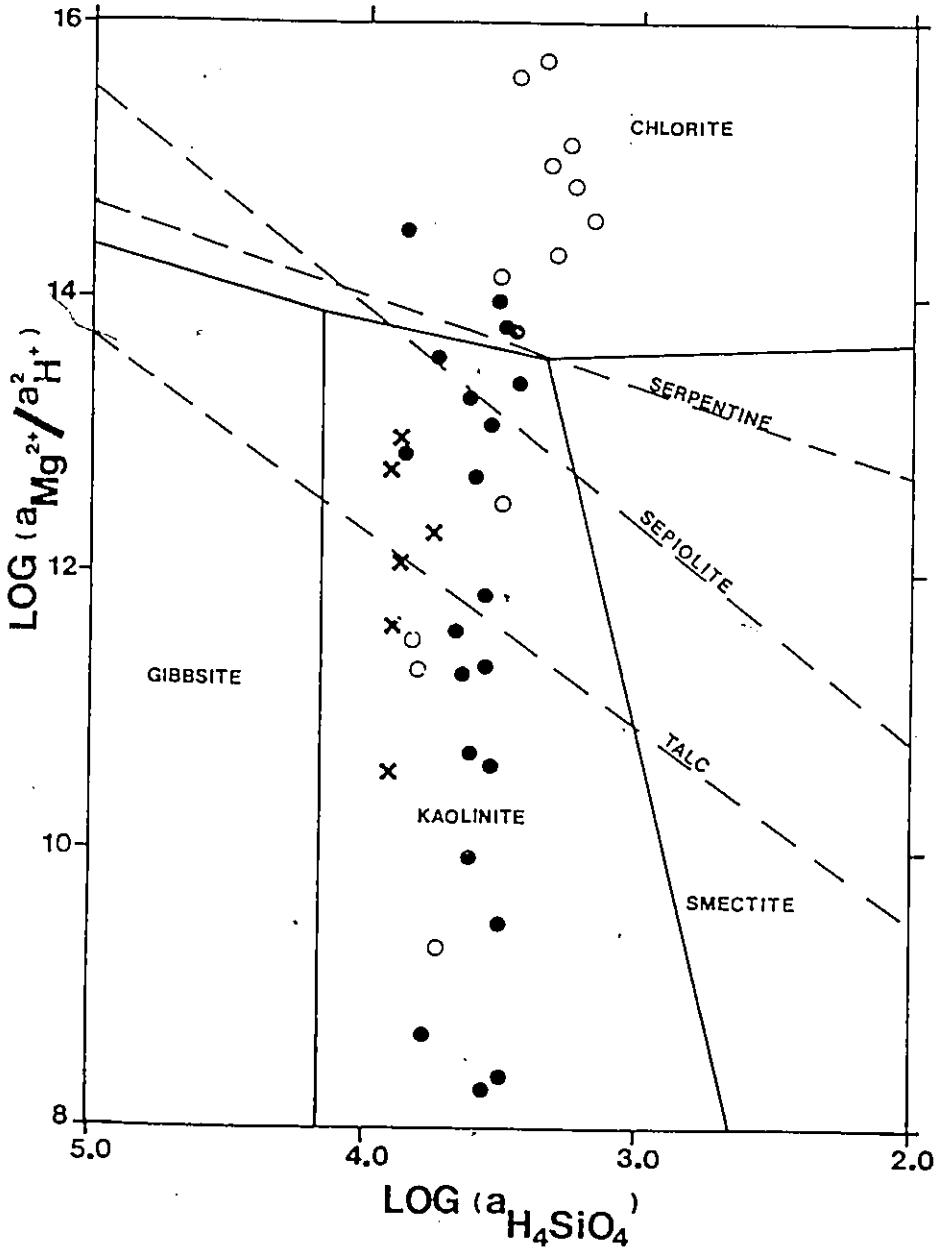


Fig. 9. Stability diagram for the system $MgO-Al_2O_3-SiO_2-H_2O$ at 25°C (after Nesbitt, 1980). Talc, sepiolite, and serpentine stability boundaries are from Drever, 1982. Ground waters are plotted as crosses (CRNL), solid dots (EBL P-series boreholes) and open circles (EBL cored boreholes).

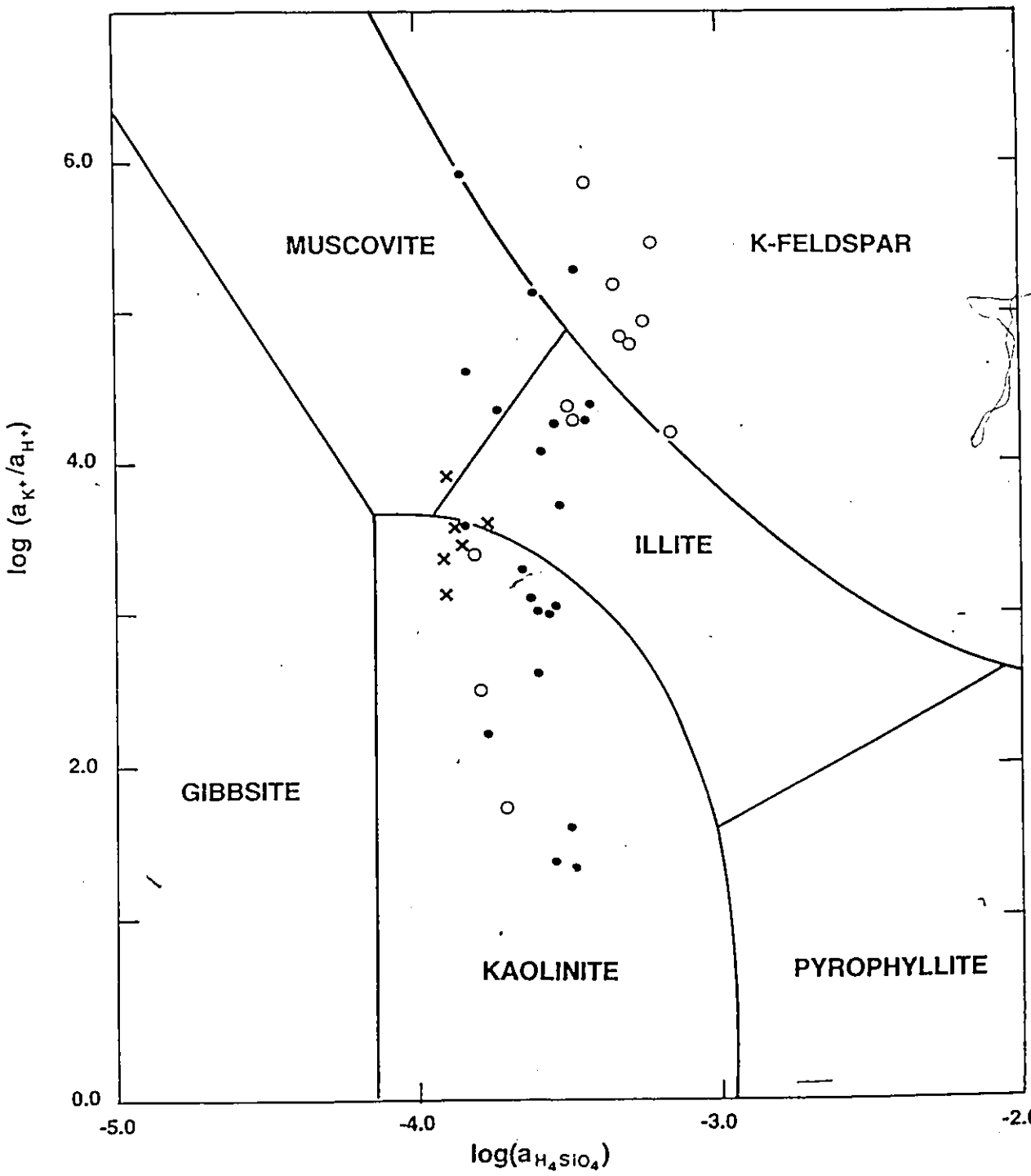


Fig. 10. Stability diagram for the system $K_2O$-$Al_2O_3$-$SiO_2$-$H_2O$ at 25°C (after Drever, 1982). Ground waters are plotted as crosses (CRNL), solid dots (EBL P-series boreholes) and open circles (EBL cored boreholes).

CRNL ground waters. The deeper EBL ground waters are supersaturated with respect to K feldspar so this mineral along with kaolinite and muscovite/illite are predicted to be stable at this site. Sericite is present in the CRNL fractures but not at EBL. Adularia is present in EBL fractures but it is of ancient hydrothermal origins (Kamineni et al., 1985). Adularia from the Folson Lake fault gave a $^{40}Ar/^{39}Ar$ age of 940 ± 3 Ma (McNutt et al., 1987). Low temperature K feldspar formation has not been observed.

Stability diagrams predict which minerals should be thermodynamically stable in contact with the ground waters. However, kinetic considerations may be such that mineral nucleation and precipitation or crystallization from amorphous precursors may be extremely slow, especially in low temperature ground water systems. For example, all the CRNL and EBL ground waters are supersaturated with respect to quartz (which has a solubility of $10^{-4}$M at 25°C and pH <9) but are undersaturated with respect to amorphous silica (solubility $2 \times 10^{-3}$M). Although quartz is present in hydrothermal vein calcite it is not precipitating from the present day ground waters. Quartz precipitation in low temperature (<25°C) sedimentary or diagenetic environments is a rare occurrence. The same kinetic constraints are also applicable to the formation of feldspar minerals.

The trends in the major ion compositions of the CRNL and EBL ground waters are shown in the ternary diagrams of Figs. 11 and 12. Shallow ground water at both sites is of the $Ca/HCO_3$ type which evolves primarily by ion exchange to the $Na/HCO_3$ type

both laterally along the direction of ground water flow and with increasing depth. The Na/Cl water present at both sites is not a geochemically evolved daughter of the $Na/HCO_3$ water but is the result of the infiltration of saline water into the plutons from external reservoirs. At CRNL the Na/Cl water is thought to represent a small component of Champlain Sea water that infiltrated the subsurface following deglaciation.

However the Na/Cl water at EBL is much more saline than the Na/Cl water at CRNL with a maximum measured TDS of 4.3 g $L^{-1}$. This deep saline water at EBL appears to be part of a deep regional saline ground water flow system. This interpretation is based on borehole hydraulic head measurements and on the chemical and isotopic characteristics of the saline water (Raven et al., 1987; Bottomley et al., 1986). In particular, the Br/Cl ratios (both of which are conservative elements) of the EBL saline waters range from 0.003 to 0.005. These ratios are close to those of sea water (0.0034) and sedimentary formation waters (0.002-0.007) but lower than the ratios in deep brines (0.006-0.013) from mines on the Canadian Shield (Frape et al., 1984). Ratios significantly higher than sea water have been attributed to leaching of saline fluid inclusions or halogen-bearing silicate minerals (Kamineni, 1987).

In summary it can be concluded that mineral reactions with postglacial ground waters at CRNL thermodynamically favour the formation of kaolinite and illite, Ca-smectite, or talc. Kaolinite is predicted to be particularly abundant because of its stability in all the chemical systems considered (Figs.

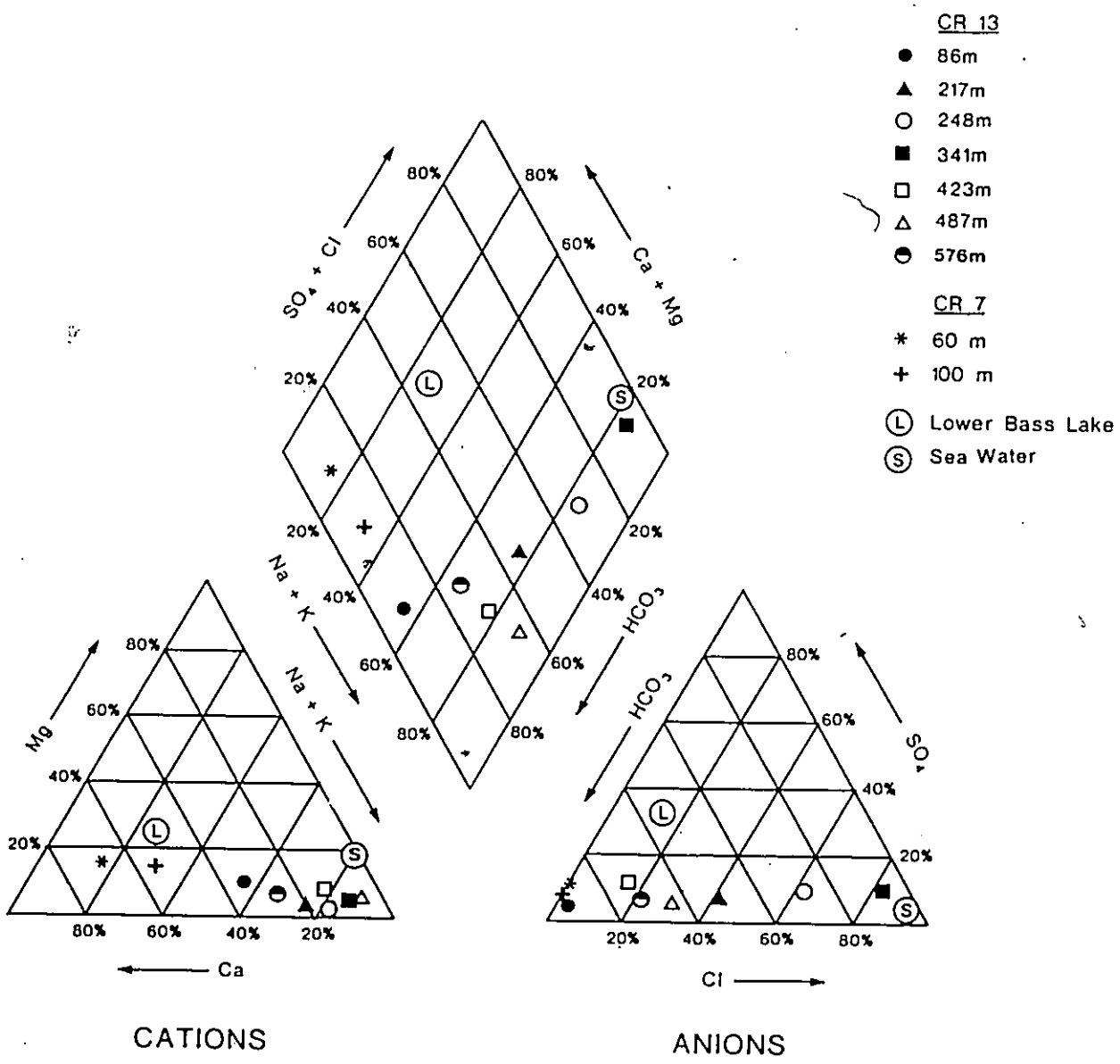


Fig. 11. Trilinear diagram showing the major ion compositions of CRNL ground waters (after Bottomley et al., 1984).

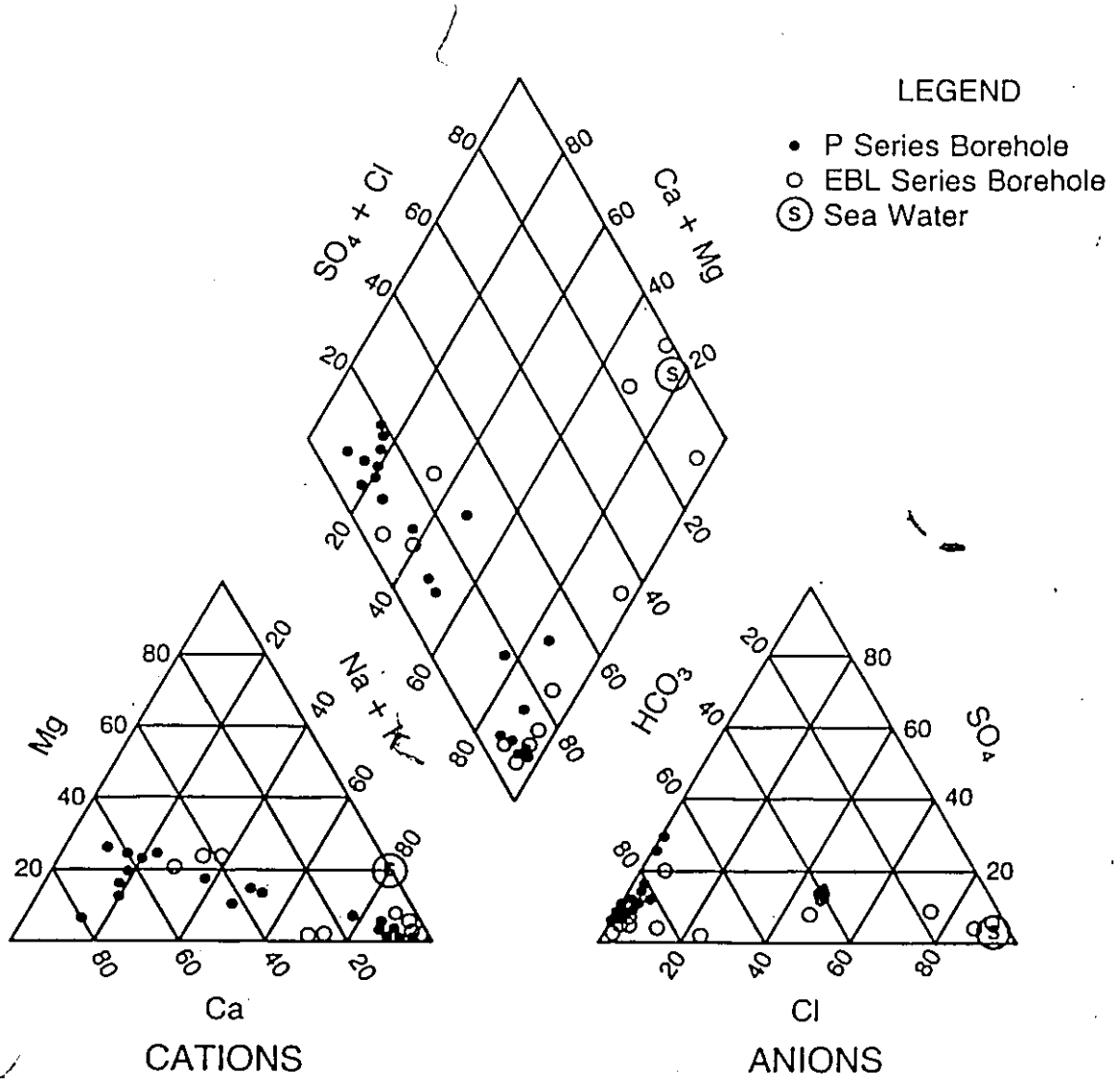


Fig. 12. Trilinear diagram showing the major ion compositions of EBL ground waters.

7-10). However, discrete infillings of kaolinite have not been observed presumably because of low temperature kinetic inhibition of its formation. Kaolinite has been observed as an alteration product of feldspar adjacent to rather than within fractures of the Eye-Dashwa pluton, Atikokan (Kamineni and Stone, 1983) and this may be its principal mode of formation at CRNL as well. In subsequent chapters it will be shown that calcite recrystallization is a more active process than the incongruent dissolution of silicates. This process has had a major impact on the chemical and C and Sr isotopic composition of the ground water and on the $\delta^{18}O$ and $\delta^{13}C$ compositions of the recrystallized calcite itself. Exchange reactions involving the adsorption of $Ca^{2+}$ and the release of $Na^{+}$ is the other major mineral-water interaction process at CRNL.

## 3.2 MINOR AND TRACE ELEMENT COMPOSITIONS OF SECONDARY CALCITES

Minor or trace elements in calcites are potentially useful indicators of the chemistry, and hence the nature, of the fluids from which they precipitated. If the element of interest substitutes for Ca in the calcite lattice then the incorporation of this element may be explained in terms of the partitioning theory (McIntire, 1963; Kinsman, 1969; Veizer, 1983 a, b). The distribution coefficient for the substituting element is defined as:

$$k_t = \frac{(m_t/m_c)_s}{(m_t/m_c)_\ell} \qquad (3)$$

where m is moles, t is the substituting element, c is the major element (in this case Ca), ℓ is the solution, and s is the solid. In other words, the mole ratio of the substituting element to Ca in calcite should be controlled by the distribution coefficient and the mole ratio in solution. For elements with a $k_t > 1$ the precipitated calcite will contain higher concentrations of these elements, relative to Ca, than the solution from which it precipitated. The opposite is true for elements with a $k_t < 1$. Suggested $k_t$ values, modified after Veizer (1983a), are listed in Table 4 for elements of interest in this study. Because distribution coefficients for some elements may vary with temperature, rates of calcite precipitation (Lorens, 1981), solution chemistry (Pingitore and Eastman, 1986), and growing crystal surfaces (Reeder et al., 1987), these values should be considered only as estimates of the direction and magnitude of elemental enrichment or depletion in calcite relative to the solution from which they precipitated. However, it is evident that Fe, Mn, and Zn will be enriched in calcite relative to the solution from which they precipitated, and Sr, Mg, and Na will be depleted. In particular, Sr and Mn may be useful in identifying the origins of calcite deposition because their distribution coefficients are reasonably well known and markedly different in direction. They also tend to be located mainly in the carbonate lattice as opposed to the associated insoluble residue or, in the case of Na, in interstitial lattice positions (Ishikawa and Ichikuni, 1984). Moreover, ground waters of different origin (meteoric, marine, or magmatic) may have very

Table 4 - Recommended distribution coefficients ($k_t$) for selected minor or trace elements in directly precipitated calcite (modified after Veizer, 1983a).

| ELEMENT | RECOMMENDED $k_t$ | REFERENCE |
|---|---|---|
| Sr | 0.13 | Kinsman (1969) |
| | 0.06* | Pingitore and Eastman (1986) |
| Na | 0.00002-0.00003 | Moller et al. (1976) |
| Mg | 0.015-0.045 | Gascoyne (1983) |
| Fe | 1-20 | Veizer (1974) |
| Mn | 6-16 | Bodine et al. (1965) |
| | | Michard (1968) |
| Zn | 5.5 | Dardenne (1967) |

* recommended value for solutions with Sr/Ca ratios (molar) $>0.3 \times 10^{-3}$

different Sr/Ca and Mn/Ca ratios which may be recorded in the calcites. Hence it is necessary to know what these ratios are in different subsurface waters if the origin of the calcite is to be inferred from its chemistry. Nevertheless, minor and trace elements have proven very useful in describing the diagentic transformation of marine carbonate sediments (Brand and Veizer, 1980; Majid and Veizer, 1986; Al-Aasm and Veizer, 1986), and therefore may be expected to be useful in investigations of the origins of fracture calcites.

The shapes of chondrite-normalized rare earth element (REE) patterns in fracture calcites should be controlled by source materials, solution chemistry, and water-rock interactions (Graf, 1984). However, since the REE as a group exhibit similar chemical behaviour, REE patterns are insensitive to changes in total concentration of all REE, changes in flow regime, or changes in precipitation rate. Rare earth elements with ionic radii closest to that of $Ca^{2+}$ such as $Ce^{+3}$, $Pr^{+3}$, and $Nd^{+3}$ should be enriched in calcite relative to other REE especially Lu which has the smallest ionic radius (Morgan and Wandless, 1980). However, since all REE are strongly complexed by $CO_3^{2-}$ and $Cl^-$, mineral-solution distribution coefficients of REE may be reduced to lower values than those for pure water (Graf, 1984). Both the degree and direction of fractionation in the distribution coefficients for REE as the result of complexation are apparently sensitive to the carbonate-chloride ratio in solution.

## 3.3 ISOTOPIC COMPOSITIONS OF OXYGEN AND CARBON IN GROUND WATERS

This thesis is mainly concerned with the stable isotopes of oxygen, which is the most abundant element in carbonate and silicate minerals, and with carbon. Oxygen has three stable isotopes in the following abundance (Garlick, 1969):

$^{16}O$ = 99.763%, $^{17}O$ = 0.0375% and $^{18}O$ = 0.1995%.

However it is the $^{18}O/^{16}O$ ratio which is generally determined because of the greater mass difference and higher abundance of these isotopes. Carbon has only two stable isotopes, $^{12}C$ (98.89%) and $^{13}C$ (1.11%).

Relative isotope concentrations with respect to standards can be measured very accurately with double collecting mass spectrometers. Stable isotope values are reported in $\delta(^{o}/oo)$ notation with the $\delta$ value being defined as:

$$(4) \qquad \delta^{o}/oo = \left( \frac{R(sample) - R(standard)}{R(standard)} \right) \times 10^{3}$$

where $R = {}^{18}O/{}^{16}O$ or $^{13}C/^{12}C$. The internationally accepted standard for $^{18}O$ is Standard Mean Ocean Watar (SMOW) or the Pee Dee Belemnite (PDB) carbonate standard, the latter also being the standard for $^{13}C$.

### 3.3.1 Oxygen Isotopes

Ground water may be of meteoric, connate, or juvenile origins. Thus the O isotopic composition of ground water can vary widely, a fact which can be used to identify the nature of the water responsible for secondary mineral formation in fractured rock. The isotopic characteristics of different sources of ground water are briefly reviewed in this section and the compositions of the present day CRNL and EBL ground waters are described and discussed.

#### 3.3.1.1 meteoric water

Meteoric water is derived from ocean water which has (by definition) $\delta^{18}O$ and $\delta^{2}H$ concentrations very near $0^{o}/oo$ (SMOW) at the present time. Because of equilibrium and kinetic fractionation factors associated with the evaporation of water from the surface of the ocean, water vapour is significantly depleted in $^{18}O$ and $^{2}H$ relative to ocean water. The condensation of water in equilibrium with water vapour and its subsequent removal from a cloud results in an isotopic relationship between vapour and liquid described by the Rayleigh distillation equation (Broecker and Oversby, 1971):

$$\frac{R}{R_o} = f^{(\alpha-1)} \qquad (5)$$

where $R_o$ = $^{18}O/^{16}O$ ratio of the vapour prior to condensation

$R$ = $^{18}O/^{16}O$ ratio of the remaining vapour

$f$ = fraction of the vapour remaining

$\alpha$ = isotopic fractionation factor between liquid and vapour phases.

Thus the first rain to form from ocean-derived water vapour should have an isotopic composition similar to that of ocean water and this in fact is what is obsesrved in low latitude marine rains. However, as the number of condensation stages increase the vapour becomes progressively more depleted in heavy isotopes as does the isotopic composition of the rain that subsequently condenses from it. Moreover, both the condensation process and the isotopic fractionation factor between liquid and vapour depend on temperature. Therefore, the latitude, altitude, and season of precipitation all influence the isotopic composition of precipitation through the temperature effect. The net effect is that continental precipitation is depleted in $^{18}O$ and $^{2}H$ compared to marine and coastal precipitation and the magnitude of this depletion is directly related to the nature of the cooling process of the original vapour mass. Figure 13 shows very generally the average $^{2}H$ and $^{18}O$ concentrations for meteoric surface waters in North America (Drever, 1982). The isotopically light meteoric water in inland regions of Canada where the CRNL and EBL areas are located is clearly evident and is attributable to the previously described climatological and geographic factors.

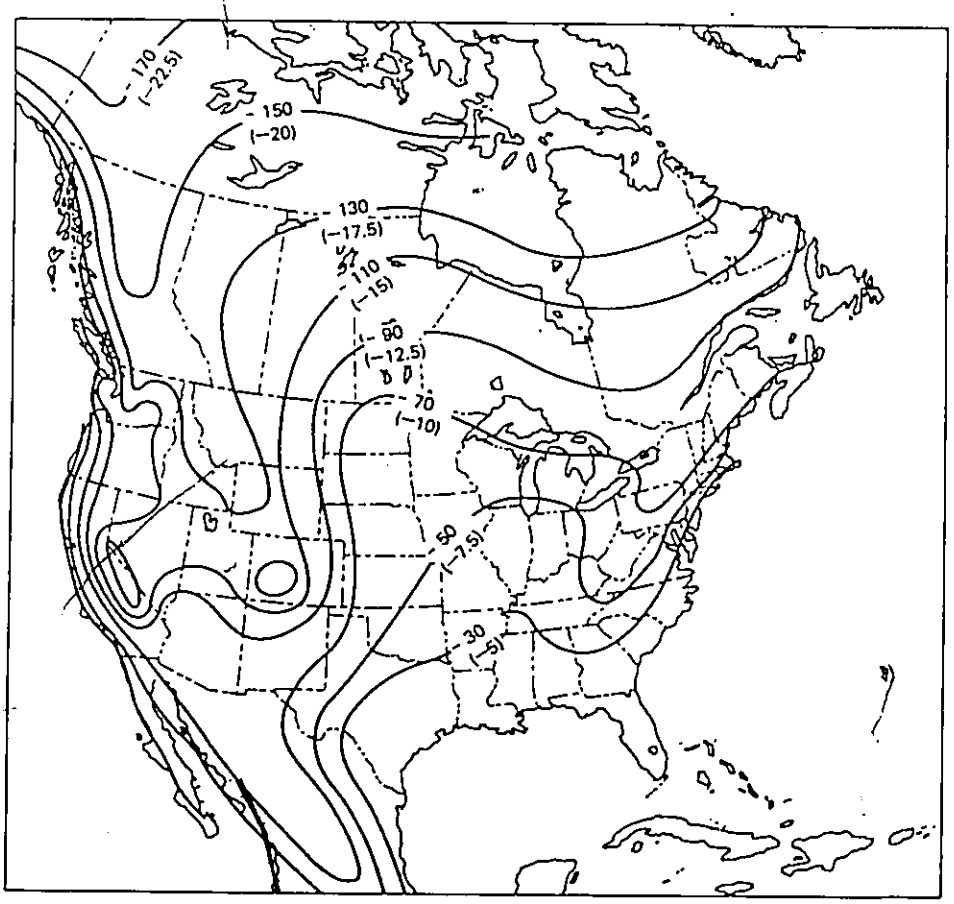


Fig. 13. Mean annual deuterium and oxygen-18 (parentheses) concentration contours for meteoric water in North America (from Drever, 1982, adapted after Sheppard et al., 1969).

Craig (1961) showed that on a global basis the $^{18}O$ and $^{2}H$ contents of meteoric waters were related by the "global meteoric water line" equation:

$$(6) \qquad \delta^{2}H = 8\ \delta^{18}O + 10^{o}/oo$$

This equation is of general validity for most continental localities although the slope (8) and intercept or the deuterium excess ($+10^{o}/oo$) of this relationship do vary regionally. Furthermore evaporation of rainwater before or during infiltration can preferentially increase the $^{18}O$ of ground water recharge relative to $^{2}H$ resulting in a slope of less than 8. It is also known that if recharge occurs preferentially during a certain season the $\delta^{18}O$ of ground water will be weighted toward the $\delta^{18}O$ of the precipitation during that season rather than reflect the annual average $\delta^{18}O$ of the precipitation. Nevertheless ground waters of meteoric origin are sufficiently depleted in $^{18}O$ and $^{2}H$ relative to other sources to impart a characteristic isotopic signature to secondary minerals formed by low temperature chemical interactions between ground water and silicate minerals in igneous rocks.

3.3.1.2 connate water

North American formation waters (i.e. interstitial water in sediments) were at one time believed to represent connate or original sea water trapped in sediment pores at the time of deposition. However, isotopic studies of these brines (Clayton et al., 1966; Hitchon and Friedman, 1969) have shown that chemically modified meteoric waters are a major component of these brines. On $\delta^{18}O$-$\delta^{2}H$ plots formation waters do not follow the meteoric water line but rather exhibit $^{18}O$ enrichment relative to $^{2}H$. As a consequence formation waters from a given sedimentary basin plot on a trend line that has a slope of less than 8 and an intercept with the meteoric water line that is indicative of the isotopic composition of the precipitation at the time of recharge (Fig. 14).

The $\delta^{18}O$ of ocean water has been relatively constant ($\pm 1$-$2^{o}/oo$) at least since the beginning of the Mesozoic (Taylor, 1974) although there is evidence that the $\delta^{18}O$ of the pre-Silurian ocean may have been as much as $5.5^{o}/oo$ lighter than SMOW (Brand and Veizer, 1981; Veizer et al., 1986). In contrast the $\delta^{18}O$ of the highest salinity oil-field formation waters range between +5 to $+10^{o}/oo$. This enrichment has been attributed to low temperature (as low as 10°C) isotopic exchange with $^{18}O$ rich marine carbonate rocks ($\delta^{18}O$ = +25 to $+30^{o}/oo$) over long periods of geologic time in systems with low water/rock ratios. In high water/rock environments the $\delta^{18}O$ of marine carbonates may be shifted to less positive values. In contrast ground water in contact with igneous rocks ($\delta^{18}O$ = +5 to $+10^{o}/oo$) at tempera-

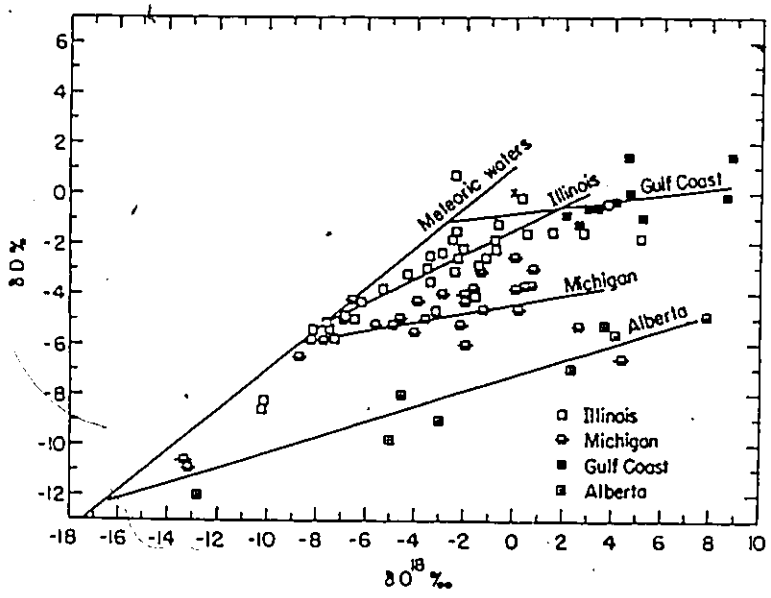


Fig. 14. Oxygen 18-deuterium plot of some North American formation waters (Clayton et al., 1966). The position of the intercept of the $^{18}O$-$^{2}H$ line for each basin approximates the present day isotopic composition of meteoric water in each region.

tures below about 150°C should experience little $^{18}O$ shift unless perhaps water/rock ratios are extremely low (Truesdell and Hulston, 1980). It should be noted that altered meteoric thermal waters exhibit an oxygen isotopic shift from the meteoric water without a comparable hydrogen shift. This is because the hydrogen content of the major rock forming minerals is too low to affect the deuterium content of the water.

3.3.1.3 juvenile water

Juvenile water is defined as water derived from the mantle that has never been in contact with meteoric waters. Uncontaminated juvenile waters have probably never been sampled. Juvenile water is not the same as magmatic waters which are solutions that have thoroughly exchanged chemically and isotopically at magmatic temperatures (about 700°C to 1100°C) with a magma system or an igneous rock body (Hoefs, 1973). Magmatic waters have no unique origin since juvenile, meteoric, and formation water components are all possible. Most igneous rocks have $\delta^{18}O$ values of between +5 and +10°/oo and $\delta^{2}H$ values of between -50 and -85°/oo (Taylor, 1974). Insofar as magma can only exist between about 700°C and 1100°C, Taylor (1974) has defined "primary magmatic water" as water in equilibrium with "normal" igneous rocks at temperatures >700°C. Because isotopic fractionations between water and minerals are very small at these high temperatures the isotopic composition of primary magmatic water is similar to that of normal igneous rocks. Hydrothermal waters are waters heated to temperatures that are

less than magmatic. Such waters are nongeneric and do not have a unique isotopic signature. However, hydrothermal waters of meteoric origins can be expected to exhibit an $^{18}O$ shift to higher values because of isotopic exchange with rocks. Metamorphic water is water of any origin that equilibrated with or was released from metamorphic rocks undergoing dehydration (Sheppard, 1986).

3.3.1.4 CRNL and EBL ground waters

The isotopic compositions of the CRNL and EBL ground waters are given in Tables 5 and 6. The $^{18}O$ and $^{2}H$ compositions are plotted in Figs. 15 and 16. The CRNL ground waters plot near the global meteoric water line of Craig (1961) but the dilute Na/Cl waters at depths of about 200-350 m are approximately $2^{o}/oo$ lighter in $\delta^{18}O$ than the shallow (<50 m) ground waters. This indicates that the deeper waters were either recharged under cooler climatic conditions or that a small component of glacial meltwater is present in these waters (Bottomley et al., 1984). If the former reason is responsible then the mean annual recharge temperature was about 3°C cooler than present if the temperature coefficient of $0.7^{o}/oo\ °C^{-1}$ is correct (Dansgaard, 1964).

At EBL most of the shallow ground waters sampled from the P-series boreholes have $\delta^{18}O$ values of -11 to $-12^{o}/oo$ and plot near the global meteoric water line (Fig. 16). An obvious exception is borehole P-5 which contains anomalously light ground water that is $6^{o}/oo$ lighter ($-17.8^{o}/oo$) in the bottom

Table 5. Isotopic composition of ground water in CRNL borehole CR13 (from Bottomley et al., 1984)

| Depth (m) | $\delta^{18}O$ SMOW | $\delta^{2}H$ SMOW | $^{3}H$ (T.U.) | $^{14}C$ (pmC) | $\delta^{13}C$ PDB | $\delta^{34}S(SO_4)$ CDT | $\delta^{18}O(SO_4)$ SMOW | $^{234}U/^{238}U$ A.R. |
|---|---|---|---|---|---|---|---|---|
| 86 | -12.1 | -84 | 0±8 | 49.4 | -15.7 | +12.7 | +9.6 | 3.7 |
| 217 | -13.5 | -95 | 0±8 | 21.8 | -14.6 | +25.5 | +12.5 | 1.7 |
| 248 | -13.1 | -93 | 0±8 | 13.9 | -14.3 | +29.7 | +9.9 | 1.8 |
| 341 | -12.9 | -94 | 0±8 | 33.6 | -13.8 | +30.4 | +14.0 | 1.7 |
| 423 | -12.1 | -93 | 316±9 | 41.4 | -18.5 | +14.7 | +8.3 | 1.9 |
| 486 | -11.0 | -81 | 615±13 | 64.0 | -18.0 | +36.6 | +12.6 | 1.7 |
| 576 | -11.8 | -83 | 512±13 | 70.1 | -17.5 | +25.8 | +15.4 | 1.6 |

$\delta^{13}C$ and $\delta^{34}S(SO_4)$ results are expressed in conventional $\delta$(‰) notation relative to the Pee Dee Belemnite (PDB) standard and Canyon Diablo troilite standard, respectively. $^{234}U/^{238}U$ results are activity ratios (A.R.). Tritium results are in tritium units (T.U.) where 1 T.U. = 1 $^{3}H$ atom in $10^{18}H$ atoms.

Table 6. Isotopic composition of EBL ground waters. N.D. denotes "not detected" (modified after Bottomley et al., 1986)

| Borehole and Sample Depth Interval (m) | | $^{18}O°/oo_{SMOW}$ * | $^{2}H°/oo_{SMOW}$ | $^{3}H(T.U.)$ + | $^{34}S°/oo\text{-}SO_4^{2-}{}_{CDT}$ | $^{18}O°/oo\text{-}SO_4^{2-}{}_{SMOW}$ | $^{13}C°/oo_{PDB}$ | $^{14}C°/o$ ♦ $_{MOD}$ |
|---|---|---|---|---|---|---|---|---|
| P-1 | 32-53.3 | -11.8 | -82.2 | N.D. | +4.0 | +3.5 | -17.6 | 7.8 |
| P-2 | 24.5-38.1 | -11.9 | -86 | 20 | - | - | -14.5 | 30.0 |
| P-3 | 0-16 | -11.9 | -85.1 | 44 | +4.6 | +6.5 | -22.0 | 14.2 |
| P-3 | 16-38.1 | -12.0 | -87.2 | N.D. | +6.8 | +7.5 | -14.2 | 12.0 |
| P-4 | 35-55 | -11.5 | -88 | 50 | +3.5 | +6.4 | - | - |
| P-5 | 0-22 | -15.8 | -124 | N.D. | +16.0 | +8.7 | -12.8 | 75 |
| P-5 | 88.5-97.6 | -17.8 | -136 | 26 | +21.2 | +6.2 | - | 32.7 |
| P-6 | 0-68 | -11.7 | -80.9 | 49 | +3.7 | +8.8 | -17.1 | 25.3 |
| P-7 | 0-39.6 | -10.2 | -73 | 59 | +10.1 | +6.1 | - | - |
| P-8 | 0-20 | -10.5 | -76.9 | 77 | +8.2 | +5.7 | -20.5 | N.D. |
| P-9 | 0-12 | -11.6 | -80.7 | 53 | +3.7 | +5.2 | -22.3 | 100 |
| P-9 | 12-43.2 | -11.6 | -83.9 | 62 | - | - | - | - |
| P-10 | 0-34.5 | -11.5 | -79.1 | 69 | +6.3 | +8.9 | -23.9 | 132 |
| P-10 | 34.5-38.5 | -11.3 | -78.5 | 53 | +5.8 | +7.0 | -21.1 | 117 |
| P-10 | 66.3-70.3 | -11.2 | -79.1 | 37 | +1.6 | +9.1 | -20.5 | 79 |
| P-10 | 82-98.7 | -11.2 | -79.8 | 22 | +8.4 | +7.1 | -19.4 | 63 |
| P-11 | 0-49.2 | -11.2 | -81.3 | 33 | +11.2 | +9.8 | -25.1 | - |
| P-12 | 0-37 | -11.6 | -80.2 | 18 | +13.5 | +10.8 | -17.3 | - |
| P-12 | 38-48.6 | -12.0 | -83.0 | 19 | +11.6 | +9.7 | -17.2 | 52 |
| P-13 | 0-22 | -11.9 | -84.2 | N.D. | +4.0 | +10.2 | -16.1 | 69 |
| P-14 | 0-43.3 | -11.8 | -82.6 | 92 | +3.4 | +3.4 | -17.5 | 35 |
| | 147-298 | -13.8 | -111 | 72 | - | - | -15.2 | 38 |
| EBL-1 | 204-213 | -13.5 | -99.2 | 28 | - | +11.4 | -15.7 | 29.3 |
| | 298-512 | -12.4 | -95 | 13 | - | - | -18.9 | - |
| | 504-642 | -13.3 | -95 | 20 | +13.9 | +11.3 | - | - |
| | 0-75 | -10.4 | -74.6 | 53 | - | - | - | - |
| | 75-248 | -14.1 | -103.4 | 15 | - | - | - | - |
| EBL-2 | 111-126 | -16.3 | -120.4 | N.D. (4.3) | +2.7 | +11.3 | -11.9 | 12.1 |
| | 248-460 | -13.5 | -103.2 | 34 | - | - | - | - |
| | 460-616 | -8.7 | -65.4 | 48 | +6.9 | +6.8 | - | - |
| EBL-3 | 0-443 | -11.4 | -79.8 | 66 | - | - | -18.9 | 39 |
| | 0-120 | -10.9 | -76.7 | 25 | - | - | -19.2 | 44 |
| | 105-117 | -12.9 | -93.9 | N.D.(N.D.) | - | +12.1 | - | 23.4 |
| EBL-4 | 120-198 | -15.0 | -104.9 | N.D. | +4.6 | +8.7 | -11.9 | - |
| | 198-396 | -14.1 | -103.8 | 23 | - | - | - | - |
| | 429-456 | -11.9 | -80.3 | 13(8.9) | +18.2 | +9.8 | - | - |

* Stable isotope concentrations are expressed in the conventional $\delta°/oo$ notation relative to the Standard Mean Ocean Water (SMOW), Pee Dee belemnite (PDB), or Canon Diablo Troilite (CDT) standards.

\+ T.U. - tritium unit (1 T.U. = 1 $^{3}H$ atom in $10^{18}H$ atoms). Precision is ± 10 T.U. except for enriched samples (brackets) where the precision is ±1 T.U.

♦ $^{14}C$ expressed as per cent modern carbon.

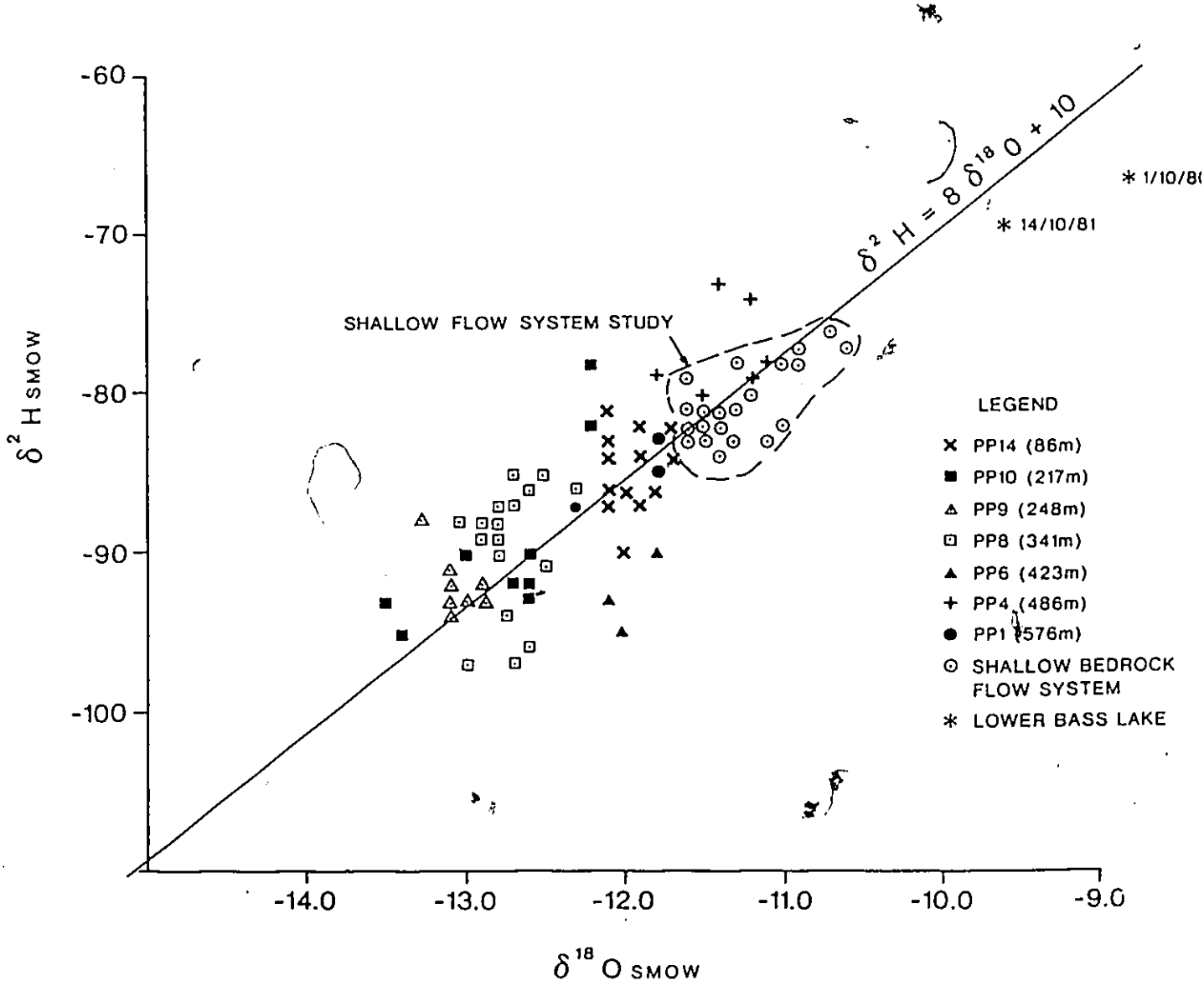


Fig. 15. Oxygen 18-deuterium plot of ground waters from borehole CR13 and from shallow bedrock boreholes at CRNL (Bottomley et al., 1984).

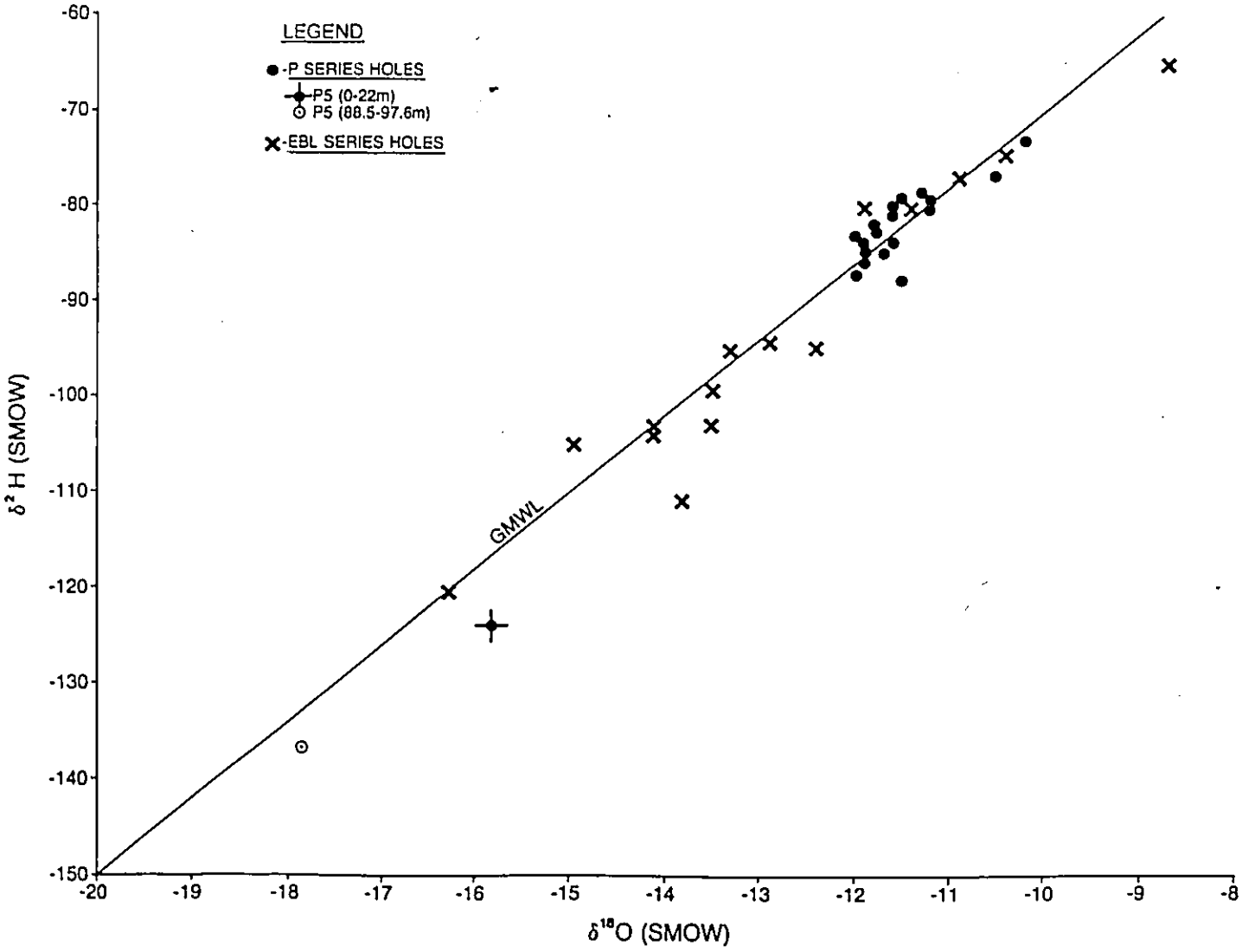


Fig. 16. Oxygen 18-deuterium plot of EBL ground waters.

zone (88.5-97.6 m) than the other P-series ground waters. This borehole intersects the 050 lineament and probably penetrates the upper part of the troctolite unit. Ground water in the high permeabililty zone at the base of the troctolite unit in the EBL-cored boreholes is also significantly lighter isotopically than the shallow ground water from the P-series boreholes. The lightest water was sampled from borehole EBL-2 at 111-126 m. This isotopically light $Na/HCO_3$ water from the troctolite is thus of a different origin than the isotopically heavier $Na/HCO_3$ waters sampled in the shallow P-series boreholes. Because the mean annual air temperature at EBL is only 4°C the very light ground water sampled from P-5 and EBL-2 (111-126 m) probably indicates a glacial meltwater component is present in these waters. If temperature alone was responsible for these light waters, an unreasonably cool mean air temperature of <0°C would be calculated using the temperature coefficient of Dansgaard (1964).

The saline Na/Cl water sampled in EBL-4 is isotopically heavier than the deeper $Na/HCO_3$ waters and is similar to the shallow ground water from the P-series boreholes. This suggests the Na/Cl water is not derived from the geochemical evolution of the overlying $Na/HCO_3$ water but rather is part of a deep regional flow system. This scenario is supported by hydraulic head measurements in EBL-4 at the basal contact of the EBL pluton which show the hydraulic head at this depth is lower than adjacent Moon Lake. Raven et al. (1987) proposed that the

Folson Lake Fault is a regional high hydraulic conductivity, low hydraulic head fracture zone that channels deep ground water from the pluton to the southeast. In contrast, ground water in the troctolite flows to the northeast and likely discharges at surface in the topographic depression between the northeast end of Moon Lake and Little Bull Lake (Fig. 5). The isotopically light ground water present in this region of the troctolite probably represents a significant glacial meltwater recharge component that has not yet been flushed from the fracture zone since post glacial re- establishment of the shallow flow system in the pluton.

Carbon isotope modelling has been performed on the EBL ground waters using the ISOTOP subroutines of Reardon and Fritz (1978) in conjunction with WATEQF, a code for the calculation of ionic species distributions and mineral saturation indices in natural waters (Plummer et al., 1976). Ground water from the basal troctolite in EBL-2 is computed to have a $^{14}C$ age of about 9500 years. This age is consistent with the interpretation based on the stable isotope data that this water recharged shortly after the region was deglaciated. This same model calculated an age of about 12,000 years for the low $^{18}O$ dilute Na/Cl water from CRNL. Therefore ground water in the upper ~400 m at both sites was recharged during the Holocene.

### 3.3.2 Carbon Isotopes

Unlike O and H, which are components of the water molecule, C is present as a dissolved solute usually in the form of an inorganic carbon compound. The isotopic composition of this dissolved inorganic carbon (DIC) is very much dependent on the origin of the ground water and its subsurface pathways.

Carbon dissolved in meteoric ground water is usually a mixture of carbon derived from soil zone $CO_2$, which dissolves in infiltrating precipitation and carbon from the dissolution of carbonate minerals. Soil zone $CO_2$, which is generated both from the decay of buried organic matter and from root respiration of living plants, typically has a $\delta^{13}C$ of $\sim -25^{o}/oo$ for plants having the Calvin photosynthetic cycle. Vegetation in southern regions of the Canadian Shield follows the Calvin cycle. The soil zone is a large reservoir of $CO_2$ with partial pressures as much as $10^2$ larger than the atmosphere $CO_2$ pressure. Carbonate minerals in aquifers are typically composed of, or derived from, marine sedimentary rocks and have an average $\delta^{13}C$ value near $0^{o}/oo$ that has varied by only $\pm 2^{o}/oo$ over the Phanerozoic (Veizer et al., 1980).

Ground water open to constant replenishment of $CO_2$ from the soil zone will have $\delta^{13}C$ values controlled by this source of $CO_2$ even if shallow subsurface carbonate mineral dissolution has occurred. If the ground water is closed with respect to the soil zone $CO_2$ then dissolution of carbonate

minerals will increase the $\delta^{13}C$ value of the ground water DIC. The final $^{13}C$ content will depend on the initial $P_{CO_2}$ of the water and its degree of saturation with respect to calcite or dolomite. A good discussion of the controls on the C isotope geochemistry of ground waters is given by Wigley (1975). Except for ground water near the water table in recharge zones, closed $CO_2$ conditions will exist unless other subsurface sources of $CO_2$ are present (i.e. organic carbon or $CH_4$ oxidation). The $\delta^{13}C$ contents of ground waters in closed $CO_2$ environments that are at or near calcite saturation are typically between -10 and $-16^{o}/oo$.

## 3.4 CONTROLS ON THE ISOTOPIC COMPOSITION OF SECONDARY MINERALS

The stable isotopic composition of a secondary mineral formed as the result of a chemical interaction between an aqueous phase and pre-existing primary mineral phases is a function of:

1. the isotopic composition of the aqueous phase,
2. the temperature of secondary mineral formation,
3. the equilibrium isotopic fractionation factor between the mineral and aqueous phase,
4. the degree to which isotopic equilibrium between the two phases is attained,
5. the isotopic mass balance between the aqueous and solid phases (i.e. the water/rock ratio) and,

6. the extent of subsequent isotopic exchange between the newly formed mineral and aqueous phases following crystallization.

In heterogeneous mineral-fluid systems, isotope exchange can occur through surface reactions such as solution-precipitation or through formation of new phases by chemical reactions, and by diffusion through grains (Cole and Ohmoto, 1986). However, diffusion controlled isotope exchange is a relatively slow process and makes a negligible contribution to the overall isotopic exchange during mineral-fluid interactions. For the calcite-water system isotopic exchange occurs primarily through solution-precipitation mechanisms provided the system is in chemical disequilibrium. In the case of oxygen, metal-oxygen bonds in the mineral must be broken to affect this exchange (O'Neil, 1977). The rate of isotopic exchange by the mechanism is controlled primarily by temperature, grain size and shape, and water/mineral mass ratio. At relatively low temperatures (<300°C) reaction rates for O isotope exchange between carbonates and water are much greater than for silicates (Cole and Ohmoto, 1986). The decrease in reaction rate is linear with decreasing temperature but experimental exchange reactions involving calcite recrystallization have not been conducted at temperatures of <~200°C. However, numerous field investigations of the diagenesis of sedimentary carbonates have convincingly shown that low temperature isotopic exchange between carbonate minerals and pore water (involving solution-reprecipitation) is a common phenomenon in sedimentary environments and therefore

should be expected in fractured rock as well as in other environments where chemical equilibrium between calcite and ground water can not be maintained.

The stable isotope equilibrium fractionation between two substances A and B is defined as:

$$(7) \qquad \alpha_{A-B} = \frac{R_A}{R_B} = \frac{1{,}000 + \delta_A}{1{,}000 + \delta_B}$$

At equilibrium $\alpha$ is closely related to the equilibrium constant for the isotope exchange reaction between two substances. Therefore like chemical equilibrium constants isotopic fractionation factors are a function of temperature but the isotopic properties of minerals depend most importantly on the nature of the chemical bonds within the minerals. A discussion of the factors affecting isotopic properties of minerals can be found in O'Neil (1977).

Fractionation factors have been determined for many of the major rock forming minerals by laboratory exchange experiments. These experiments are usually conducted at relatively high temperatures because exchange reactions are slow at low temperatures. Therefore there is some uncertainty as to the validity of extrapolating experimentally determined fractionation factors to low temperature environments. Equilibrium fractionation factors can be calculated in some instances if data on the vibrational frequencies of molecules are available (O'Neil, 1977). Emperical fractionation curves can also be constructed from data for natural mineralogical assemblages (Taylor, 1974).

Values of $\alpha$ are generally close to unity, typically 1.00X. Therefore isotopic fractionations are generally referred to the value of X or the "per mil fractionation". Since $10^3 \ln (1.00X) \approx X$, $10^3 \ln \alpha$ is the "per mil fractionation". Therefore

$$\Delta_{A-B} = \delta_A - \delta_B \approx 10^3 \ln \alpha_{A-B}$$

provided the $\Delta$ and $\delta$ values are both less than about 10.

The relationship between the equilibrium fractionation factor and temperature can be expressed by the equation:

(8) $$10^3 \ln \alpha = A(10^6 T^{-2}) + B$$

where A and B are constants and T is the temperature (°K).

Oxygen isotope fractionation factors for several minerals that can be formed in low temperature minerals are listed in Table 7. These fractionation factors are expressed in the form $10^3 \ln \alpha = AT^{-2} + B$. It is evident from this table that at equilibrium, secondary minerals formed at relatively low temperatures will be enriched in $^{18}O$ compared to the water they formed in.

The oxygen isotope fractionation between calcite and water is:

(9) $$10^3 \ln \alpha = 2.78\ (10^6 T^{-2}) - 2.89$$

(O'Neil et al., 1969)

Therefore calcite is enriched in $^{18}O$ by about $32^o/oo$ relative to the water from which it precipitates at 10°C. However the enrichment factor decreases to about $17^o/oo$ at 100°C and only $5^o/oo$ at about 320°C. The large difference in $\alpha$ as a function

Table 7. Some mineral-water oxygen isotope fractionation factors expressed in the form $10^3 \ln \alpha = AT^{-2} + B$.

| Mineral | Temperature Range °C | $10^6A$ | B | Reference |
|---|---|---|---|---|
| Quartz | 200-500 | 3.38 | -3.40 | Clayton et al. (1972) |
| | 250-500 | 3.34 | -3.31 | Matsuhisa et al. (1979) |
| Muscovite | 400-650 | 2.38 | -3.89 | O'Neil and Taylor (1969) |
| Albite (Alk. feldspar) | 400-500 | 2.39 | -2.51 | Matsuhisa et al. (1979) |
| | 350-800 | 2.91 | -3.41 | O'Neil and Taylor (1969) |
| Anorthite | 350-800 | 2.15 | -3.82 | O'Neil and Taylor (1969) |
| | 400-500 | 1.49 | -2.81 | Matsuhisa et al. (1979) |
| Kaolinite | not specified | 2.5 | -2.87 | Eslinger (1971) |
| | 172-319 | 2.05 | -3.85 | Kulla and Anderson (1978) |
| | empirical | 2.53 | -4.90 | Taylor (1974) |
| Illite | 160-270 | 2.43 | -4.82 | Eslinger and Savin (1973) |
| Smectite | 0-270 | 2.67 | -4.82 | Yeh and Savin (1977) |
| Mixed layer illite/smectite | 0-270 | 2.43+0.24E | -4.82 | Yeh and Savin (1977) |
| Serpentine | not specified | 0.6 | -5.4 | Wenner and Taylor (1971) |
| Chlorite | not specified | 1.56 | -4.70 | Wenner and Taylor (1971) |
| Calcite | 0-700 | 2.78 | -3.39* | O'Neil et al. (1969) |

* based on the former value of $\alpha_{CO_2 - H_2O} = 1.0407$ rather than the present value of 1.0412.

of temperature is useful in differentiating calcites formed under hydrothermal conditions from those of low temperature origins.

The carbon isotopic composition of hydrothermal calcite is dependent on the total carbon concentration in solution and its isotopic composition, the pH and $f_{O_2}$ (oxygen fugacity) of the solution, and temperature (Ohmoto, 1972). This is the result of the partitioning of C between various dissolved carbon species ($H_2CO_3$, $CO_2$ (g), $HCO_3^-$ and $CO_3^{2-}$) each having a different fractionation factor with respect to calcite, and the fact that either calcite or graphite may be the stable solid phase depending on solution chemistry. The presence of methane is an additional possible complication because of the large fractionation factor between $CH_4$ and $CO_2$.

In cool, meteoric ground water, however, calcite precipitation usually occurs at alkaline pH values where the dominant inorganic carbon species is the bicarbonate ion. The fractionation factor between calcite and bicarbonate has been measured to be $1.85 \pm 0.23^{o}/oo$ at 20°C with a temperature dependency of only $0.035 \pm 0.013^{o}/oo/°C$ at 20°C (Emrich et al., 1970). As temperature increases the fractionation factor decreases. Therefore calcite precipitating from cool meteoric ground water should normally be no more than $2\text{-}3^{o}/oo$ heavier in $^{13}C$ than the dissolved inorganic carbon. This assumes, however, that the amount of C removed in the calcite is small compared to the amount in solution and that the system is open

with respect to the replenishment of carbon. If this were not the case then the C isotopic composition of precipitating calcite will follow a Rayleigh distillation model (Fritz et al., 1979) with the result that the calcite will become progressively depleted in $^{13}C$ as the residual bicarbonate concentration becomes smaller. This is a closed system with respect to carbon.

## 3.5 ISOTOPE EXCHANGE IN OPEN AND CLOSED SYSTEMS AS A FUNCTION OF WATER/ROCK RATIOS

Isotopic exchange of $^{18}O$ and $^{2}H$ between hydrothermal fluids and intrusive igneous rocks has been well established by H.P. Taylor and co-workers (Taylor, 1971, 1974 and 1977; Turi and Taylor, 1971; Sheppard and Taylor, 1974; Magaritz and Taylor, 1976; Forester and Taylor, 1977; Criss and Taylor, 1983; and others). The heat associated with the intrusions can establish large-scale and long-lived convection systems if the intrusions are emplaced into permeable country rocks. Isotopic analyses of these intrusive rocks have shown they are low in $^{18}O$ compared to the uniform $\delta^{18}O$ values (+5.5 to +10$^{o}$/oo) of most unaltered volcanic and plutonic igneous rocks (Taylor, 1974) as the result of high temperature isotopic exchange with convectively-driven, low $^{18}O$ meteoric ground waters. This isotope depletion occurs after the intrusion has cooled sufficiently to solidify and fracture allowing penetration of meteoric water from the surrounding country rocks.

Isotopic exchange between hydrothermal fluids and carbonate host rocks has been proposed to explain the isotopic variations in the $^{13}C$ and $^{18}O$ of gangue calcite from Mississippi Valley Type Pb-Zn deposits (Sverjensky, 1981). Taylor and Bucher-Nurminen (1986) have also modelled the isotopic variations in metasomatic carbonates in terms of isotopic exchange between metasomatic fluids and carbonate wallrock. Unlike the case of O isotopic exchange between water and silicate rocks, modelling of C isotopic exchange between water and carbonate requires a knowledge of the predominant C-bearing species in solution and its concentration. In order to describe the rate of change of the $\delta^{13}C$ relative to the $\delta^{18}O$ of the secondary calcite, it is also necessary to know whether the system is open or closed with respect to O and C, the isotopic composition of the fluid and wallrock, the temperature of exchange, and the water/rock ratio of the system.

Closed systems with respect to water occur when the mass of fluid involved in the exchange reactions is fixed. This can occur in fracture systems that trap the fluid within the fracture porosity as the result of fracture sealing caused by secondary fracture mineral formation. On a larger scale, convective hydrothermal systems approximate closed system behaviour because of fluid recirculation controlled by thermal gradients. Open systems involve only a "single pass" of fluid through a system which is thus open to an external source of fluid replenishment. The isotopic composition of the fluid in a perfectly

open system is controlled by the isotopic composition of the external fluid reservoir. Cool meteoric ground water flow systems in fractured rock are "open" systems to water circulation.

Regardless of whether the system is open or closed the isotopic composition of secondary calcite, forming as the result of water/carbonate rock interactions, is highly dependent on the water/rock (w/r) ratio. If the w/r ratio is small the system is rock-dominated and the isotopic composition of the secondary calcite will be similar to that of the carbonate wall rock. At higher w/r ratios the system is water-dominated and the $^{18}O$ composition of the calcite will approach the equilibrium isotopic composition at that temperature. However, the magnitude of the $^{13}C$ shift is highly dependent on the C concentration of the water.

In a closed system the fluid and rock are in equilibrium at all times and hence the $\delta^{18}O$ of the secondary calcite (cc) and the w/r ratio for the system can be determined from mass balance considerations:

$$(10) \quad r\,\delta\,{}^{18}O_{cc}{}^{i} + w\,\delta\,{}^{18}O_{H_2O}{}^{i} = r\,\delta\,{}^{18}O_{cc}{}^{f} + w\,\delta\,{}^{18}O_{H_2O}{}^{f}$$

where r and w refer to rock and water, respectively and i and f are initial and final values respectively. If it is assumed that $\delta^{18}O_{H_2O}$ is determined by isotopic equilibration with the calcite then

$$(11) \quad w/r = \frac{\delta\,{}^{18}O_{cc}{}^{f} - \delta\,{}^{18}O_{cc}{}^{i}}{\Delta_r^w + \delta\,{}^{18}O_w{}^{i} - \delta\,{}^{18}O_{cc}{}^{f}}$$

where w/r is the atomic mass ratio for O in the water reservoir to rock reservoir and $\Delta_r^w$ is the O isotopic fractionation factor between the calcite and water. Since there are 3 moles of oxygen in each mole of calcite it is necessary to multiply the w/r ratio by 3 in order to calculate the mole ratio of water to rock in the system. This assumes that calcite is the only mineral phase involved in isotopic exchange reactions, which is a reasonable assumption for many low temperature environments.

For carbon isotope exchange in a closed system the mole ratio of carbon in the water reservoir ($m_c$) to carbon in the rock reservoir ($m_r$) is described by the equation:

$$(12) \qquad \frac{m_c}{m_r} = \frac{\delta\,{}^{13}C_{cc}{}^{f} - \delta\,{}^{13}C_{cc}{}^{i}}{\Delta_r^w + \delta\,{}^{13}C_c{}^{i} - \delta\,{}^{13}C_{cc}{}^{f}}$$

where $\Delta_r^w$ is the $^{13}C$ fractionation factor between calcite and the predominant C species in solution and $\delta^{13}C_c^i$ is the initial $^{13}C$ composition of this species. The mole ratio of water to rock can be calculated from the C mole ratio:

$$(13) \qquad \frac{w}{r} = \frac{m_c}{m_r} \times \frac{n_c}{x_c}$$

where $n_c$ = number of moles of C for each mole of carbonate mineral. For calcite $n_c = 1$ and $x_c$ is the number of moles of dissolved C per mole of water.

In an open system the isotopic composition of the secondary calcite is calculated from an integrated form of the mass balance equation (Taylor, 1977). For O isotope exchange the equation is:

$$(14) \qquad \frac{w}{r} = \ln \left[ \frac{\delta\,{}^{18}O_w{}^{i} + \Delta_r^w - \delta\,{}^{18}O_{cc}{}^{i}}{\delta\,{}^{18}O_w{}^{i} + \Delta_r^w - \delta\,{}^{18}O_{cc}{}^{f}} \right]$$

A similar equation is applicable for C isotope exchange but the concentration of dissolved C must also be included in the equation:

$$(15) \qquad X_c \cdot \frac{m_c}{m_r} = \ln \left[ \frac{\delta\,{}^{13}C_c{}^{i} + \Delta_r^w - \delta\,{}^{13}C_{cc}{}^{i}}{\delta\,{}^{13}C_c{}^{i} + \Delta_r^w - \delta\,{}^{13}C_{cc}{}^{f}} \right]$$

In previous studies Phanerozoic marine carbonates have comprised the wallrock that has been subjected to isotopic exchange with hydrothermal fluids. These rocks are typically rich in $^{18}O$ (20-30°/oo) and $^{13}C$ (0±2°/oo) relative to high temperature calcites of magmatic origin (Hoefs, 1973; Veizer et al., 1980). In contrast, mantle derived C as found in carbonatites, diamonds, $CO_2$ inclusions in oceanic basalt, and dissolved $CO_2$ in submarine hot springs from hydrothermal vents typically has $\delta^{13}C$ values of -5 to -8°/oo (Stakes and O'Neil, 1982). At hydrothermal temperatures the $^{13}C$ fractionation factor between calcite and aqueous bicarbonate is <1°/oo and hence the $^{13}C$ composition of magmatic calcites will closely resemble that of the mantle C source. Moreover, hydrothermal calcites derived from meteoric waters will also be light in $^{18}O$ relative to marine carbonates because of the dominating effect of the decrease in the $^{18}O$ fractionation factor between calcite and water at higher temperatures.

Figure 17 shows the expected trend in the isotopic composition of calcite formed from the interaction of a hydrothermal fluid with marine carbonate rocks (Sverjensky, 1981). In

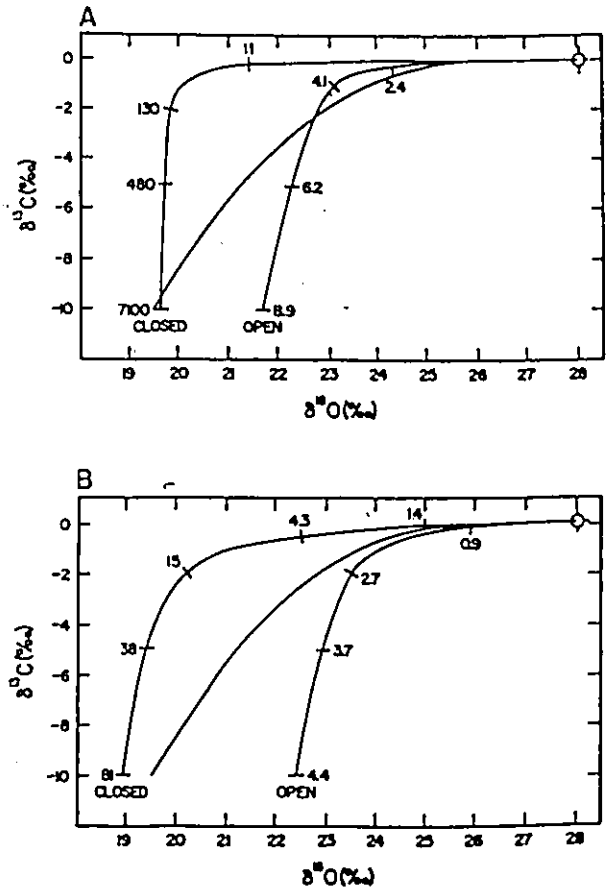


Fig. 17. Two models from Sverjensky (1981) showing the isotopic evolution of calcites from Mississippi Valley zinc-lead deposits as a function of water/rock mole ratios in open and closed systems. In "A" the initial water has a $\delta^{18}O = 3^{o}/oo$ and a $\delta^{13}C_{HCO_3^-} = -12^{o}/oo$. In "B" the initial water has a $\delta^{18}O_{HCO_3^-} = 2^{o}/oo$ and a $\delta^{13}C_{HCO_3} = -80^{o}/oo$ (oxidized methane).

this example bicarbonate is the dominant C species and a $\delta^{13}C$ value of $-12^{o}/oo$ has been assumed. Similar trends have been observed by Taylor and Bucher-Nurminen (1986) for the alteration of marine carbonate rock by a metasomatic fluid in which $CO_2$ with a $\delta^{13}C$ of $-5^{o}/oo$ was the predominant C species and at temperatures of 400-500°C. Isotope trends from both studies show a decrease in $\delta^{13}C$ and $\delta^{18}O$ values with increasing w/r ratios and the magnitude of the exchange, at a given w/r ratio, is greater for open than closed systems. The curvature of the trends is controlled by the concentration of C in solution. At low C concentrations complete O isotopic exchange occurs before significant C isotopic exchange takes place resulting in "L"-shaped isotopic trends. Isotopic exchange reactions between calcite and water almost certainly require the breaking of C-O bonds in order to significantly change the isotopic composition of the precursor calcite (O'Neil, 1977). Calcite that has recrystallized through multiple solution-reprecipitation cycles should, therefore, be highly susceptible to isotopic alteration.

Hydrothermal calcites precipitated in fractures during ancient periods of hydrothermal activity might also be expected to experience subsequent isotopic shifts if the calcite recrystallizes in contact with cool meteoric ground waters. However, because hydrothermal calcites are relatively light in $^{18}O$ compared to marine carbonates and because $^{18}O$ fractionation factors between calcite and water are large at low temperatures, recrystallization should result in an $^{18}O$ increase in the calcite unless the $\delta^{18}O$ of the water is very low. Moreover, since the

$\delta^{13}C$ of the DIC in meteoric ground waters is frequently lighter than mantle C values, recrystallization should also lead to a decrease in the $\delta^{13}C$ of the calcite with increasing w/r ratios. However, this tendency is somewhat counterbalanced by the low C concentrations in most meteoric ground waters. In crystalline rocks the dissolved C is predominantly in the form of bicarbonate but concentrations in excess of $5x10^{-3}$ molal are rare. This contrasts sharply with the concentration of $10^{-1}$ molal assumed by Sverjensky (1981) in the construction of Fig. 17. Low temperature, although a positive influence in fostering high fractionation factors, may be a negative influence if it hinders the kinetics of calcite recrystallization.

It is perhaps surprising that isotopic effects associated with the low temperature recrystallization of hydrothermal calcites have not been well documented. This is most likely because such isotopic trends have not been extensively looked for. Vein calcite devoid of economic mineralization in common shield rocks, for example, is not likely to draw much research interest, never mind research funding. Recently this situation has changed in Canada with the interest in locating a safe site in "ordinary" Precambrian plutonic rock for the disposal of high level nuclear waste. Isotope effects associated with vein calcite recrystallization may provide a means of estimating time-integrated meteoric water/rock ratios and thus provide information on the long term flux of meteoric groundwater through these rock masses. No other chemical or isotopic means of quantifying this paleoflux of meteoric water have been developed.

## 3.6 GROUND WATER FLOW IN FRACTURED ROCK

In crystalline plutonic rock ground water flow occurs primarily via the interconnected fracture porosity which comprises a small percentage (~1%) of the total bulk rock porosity (Norton and Knapp, 1977). As a first approximation the relation between the flow rate and fracture aperture is described by the smooth, parallel plate model which assumes flow is laminar and that the plates are uniformily separated. If this is the case then the cubic law holds (Raven and Gale, 1985):

(16) $$Q/\Delta H = C(2b)^3$$

where $Q/\Delta H$ = flow rate per unit head through the fracture

$2b$ = effective fracture aperture

$C$ = constant

The fracture permeability ($K_f$) or hydraulic conductivity is determined by the following equation:

(17) $$K_f = \frac{\rho g (2b)^3}{12\mu}$$

where $\rho$ = fluid density

$g$ = acceleration of gravity

$\mu$ = dynamic viscosity of the fluid

It is clear from the cubed relationship between fracture aperture and permeability that most of the flow occurs in the largest fractures. Natural fractures, however, rarely have uniform separations. Moreover fracture asperities and secondary mineral infillings formed by rock-water interactions result in rough rather than smooth fracture surfaces. Fracture roughness may reduce the flow rate from that predicted by the smooth parallel plate model by increasing frictional resistance between separated fracture surfaces or by creating tortuous flow paths

where the two fracture surfaces contact each other (Raven and Gale, 1977). Tortuosity results in increased streamline length and consequently lower hydraulic gradient and flow rate.

Novakowski et al. (1985) concluded from interborehole tracer experiments at CRNL (between boreholes CR6 and CR11) that intrafracture apertures are highly variable and that flow channeling leads to significant velocity variations along the plane of flow. Similar conclusions were reached by Rasmuson and Neretnieks (1986) from tracer experiments in fractured plutonic rock in Sweden. Computer modelling (Brown, 1987) has also verified that fracture roughness may result in large deviations of aperture-flow rate relationships from that predicted by the parallel plate model.

It is reasonable to expect that the formation of fracture minerals is a major cause of flow channeling in fractures. Certain portions of individual fractures may be totally filled with secondary minerals while other parts are devoid of significant infilling. Mega fluid inclusions could form that are isolated from the actual flow channels. Tectonic forces could re-open sealed fractures and seal open fractures and such processes could repeat themselves continuously over geologic time. Therefore intrafracture time-integrated water/rock ratios may be highly variable. Fracture calcite recrystallizing in such a dynamic environment may thus experience non-uniform isotopic shifts determined by the variability in time-integrated water/rock ratios. If this is the case intrafracture variability in the isotopic composition of the calcite may be large even over short distances along the plane of the fracture.

# 4.0 METHODS

## 4.1 CHEMICAL

Calcite samples were extracted from fracture surfaces using either a chisel or an electrical lapidary drill. The samples were then ground to approximately 200 mesh size using a Progressive Exploration rock pulverizer fitted with ceramic grinding plates or, for smaller samples, a mortar and pestel. Initially there was some concern that the drilling and coring of the samples might result in contamination of the calcite. Therefore the first set of CRNL samples were rinsed with $10^{-4}$M $L^{-1}$ $Al(NO_3)_3$ solution to remove any exchangeable cations present as suggested by Reardon and Reimer (1982). This rinsing was done in a glass Millipore vacuum filtration flask. The samples were then transferred to glass beakers and oven dried at 115°C. Subsequent analyses of duplicate samples showed that calcite samples rinsed with the $Al(NO_3)_3$ solution were not measureably dissimilar (chemically) from unrinsed samples. Therefore the rinsing procedure was not followed for later sample sets.

Approximately 0.5-1.0 g of dried powder from each sample was placed in a glass beaker and digested for 1-2 hr in 25 mL of 6% (V/V) HCl. The samples were then filtered in the Millipore filtration flask through a Whatman 43 ashless filter paper placed directly on top of a Millipore 0.45 µm nitrocellulose filter paper. Reference rock samples, blanks, and

duplicate samples were treated in the same manner. The filtrates were transferred to 60 mL nalgene bottles for chemical analyses by atomic absorption spectrophotometry. The weight of the insoluble residue (I.R.) retained on the ashless filter paper was determined following combustion of the filter paper and residue in clean, pre-weighed porcelain crucibles in a muffle furnace at approximately 800°C for 2 hours. Concentrations of Ca, Mg, Na, Fe, Mn, and Sr were determined on a Varian AA-175 Series spectrophotometer (AAS). Interelement interferences were reduced by the addition of $Sr(NO_3)_2$ to samples analyzed for $Ca^{2+}$ and $Mg^{2+}$ and by KCl to samples analyzed for $Sr^{2+}$ and $Na^{+}$. Results are expressed on an insoluble residue-free basis. Details of the technique, instrumentation, precision, and accuracy have been described by Veizer et al. (1978) and Brand and Veizer (1980).

Two polished thin sections of sealed calcite-filled fractures and one open fracture were examined by scanning electron microscopy at the Canada Centre for Mineral and Energy Technology. Concentrations of Ca, Mg, Na, Fe, Mn, and Sr were analyzed by wavelength analysis using a JEOL microprobe and compared to analyses by AAS of the same samples. An additional three polished thin sections of vein calcites were analyzed by a Cameca microprobe at the Geological Survey of Canada as well as ten patchy varieties of calcites from open fractures which were mounted and polished on a single slide.

Several calcite and whole rock samples were analyzed for rare earth elements. Calcite samples were prepared and digested in the same fashion as those analyzed for minor and trace elements. These samples were then evaporated to dryness and taken up in 50 mL of 1N $HNO_3$. Whole rock samples were crushed to about 200 mesh using the jaw and plate crushers. Approximately 1 g of whole rock powder from each sample was added to a teflon digestion beaker and reacted with about 6 mL of perchloric acid and 20 mL of HF acid (37-40%). The digestions were heated until incipient dryness, cooled, and taken up with 50 mL of 1N $HNO_3$. The samples were then passed through glass columns (2 mm I.D.) packed with 22 cm of DOWEX AG-50W (100-200 mesh) ion exchange resin for separation of the rare earth elements from the sample and were subsequently eluted from the resin with 50 mL of 6N $HNO_3$ and 50 mL of 8N $HNO_3$. This 100 mL volume of eluant was then evaporated to dryness and taken up with 25 mL of 0.1N $HNO_3$ containing 3000 $\mu g\ mL^{-1}$ of Li. These solutions were then analyzed on a Beckman Spectraspan V sequential direct current (argon) plasma atomic emission spectrophotometer (DCP-AES). Two ground water samples (80-90 mL) from CRNL were also analyzed for REE.

A number of whole rock samples were analyzed by X-ray fluorescence (XRF) on a Philips 1410 automated XRF at the University of Ottawa following preparation of fused discs comprised of 1.3 g of $Li_2B_4O_7$, $Li_2CO_3$ and sample. Accuracies and precisions are generally better than 5 relative per cent for major elements (Veizer et al., 1983c). Whole rock samples

analyzed for Sr isotopes had Rb/Sr ratios precisely analyzed by dedicated XRF at Carleton University following preparation of sample pellets with boric acid.

## 4.2 ISOTOPIC

The O and C isotopic ratios of the calcites were determined by mass spectrometry on $CO_2$ produced by reacting about 20 mg of sample (50-90% calcite) with 100% $H_3PO_4$ at 25°C for at least 12 hr.. The isotopic compositions of dolomite in mixed carbonate samples were determined on $CO_2$ produced after allowing the reaction to continue overnight at 50°C and following previous extraction of calcite-derived $CO_2$ after 4 hr of reaction at 25°C (Epstein et al., 1964). The $^{18}O$ and $^{13}C$ analyses were performed with a VG Isogas SIRA 12 mass spectrometer at the University of Ottawa. The precision and accuracy of this technique is 0.1°/oo for both isotopes. Most of the $CO_2$ samples were collected and stored in glass break seals prior to analysis although earlier samples were stored in glass sample tubes fitted with teflon valves. The $CO_2$ samples were purified of water vapour and liquid nitrogen non-condensible gases on the carbonate extraction line prior to sample collection.

Oxygen isotope fractionation factors for $H_3PO_4$ released $CO_2$ from calcite at 25°C of 1.01025 (Friedman and O'Neil, 1977) and from dolomite at 50°C of 1.01065 (Rosenbaum and Sheppard, 1986) have been used in the calculations of isotopic values.

The S isotopic compositions of fracture pyrites were measured on $SO_2$ produced by the thermal combustion of $FeS_2$ with $Cu_2O$ at about 1100°C. The analyses were performed on a Micro-

mass 602E mass spectrometer at the University of Ottawa. The precision and accuracy for the procedure is $0.2^{o}/oo$. As with $CO_2$, $SO_2$ was purified of water vapour, $CO_2$, and non-condensible gases prior to collection of the $SO_2$ in break seals.

Strontium was separated from fracture calcite and whole rock samples for isotope analyses using ion exchange chromatography. Calcite samples were digested as previously described and between 1 and 3 mL (depending on $Sr^{2+}$ concentration) of digestion sample were added to glass columns (1.1 cm ID) packed with Bio Rad AG50W-X8 cation exchange resin (200-400 mesh, hydrogen form). The resin was eluted with about 70 mL of 2.5N HCL to remove $Ca^{2+}$ and other ions prior to the elution of the $Sr^{2+}$ fraction with about 30 mL of 2.5N HCl. The 2.5N HCl was prepared from 6.4N distilled HCl provided by Carleton University. The exact volume increment containing the $Sr^{2+}$ fraction was determined for each of the four columns used by calibration with a suitable Sr standard solution prior to the actual sample separations. The collected solutions were evaporated to dryness at low temperature in teflon evaporation dishes then taken up in 2 mL of 2.5N HCl and transferred to cylindrical teflon sample holders. The solutions were again evaporated to dryness, covered with parafilm, and analyzed by a Finnigan-MAT 261 multicollector mass spectrometer at Carleton University (Bell and Blenkinsop, 1984).

Whole rock samples (approximately 200 mg) for Sr isotope analyses were dissolved in approximately 10 mL of HF and

3 mL of perchloric acid in teflon beakers. The solutions were taken to dryness and then re-dissolved in 2 mL of distilled, deionized water and centrifuged for approximately 10 min in disposable plastic vials. Centrifuging separated any perchlorate salts to the bottom of the vial. The solutions above the precipitate were transferred back to the evaporating dishes, dried, then taken up in 2 mL of 2.5N HCl. The samples were again centrifuged and then the clear solutions (~2 mL) were added directly to the exchange columns.

Stable isotope results are expressed in conventional ($\delta^{o}$/oo) notation relative to the Pee Dee Belemnite (PDB) carbonate standard for $^{13}C$ and Standard Mean Ocean Water (SMOW) for $^{18}O$. The Canyon Diablo troilite (CDT) is the standard for $^{34}S$ measurements. The NBS 987 standard for Sr analysis gives a $^{87}Sr/^{86}Sr$ ratio of 0.71023 ± 0.00003 and the Eimer and Amend standard a value of 0.70802 ± 0.00003 on the Carleton mass spectrometer. Reproducibility of the $^{87}Sr/^{86}Sr$ ratios is 0.004% of the quoted value at the 2$\sigma$ level.

Several calcite samples were analyzed for $^{14}C$ by accelerator mass spectrometry at the Isotrace Laboratory of the University of Toronto. Carbonate samples are converted to acetylene and cracked to graphite material suitable for sputtering in a cesium beam. The $^{14}C$ atoms are converted to negative ions and counted directly by mass spectrometry. For samples younger than 10,000 years BP a precision of 1% or better

is possible by averaging the results of two machine-ready targets measured on different occasions (Beukens et al., 1986). At ages of 40,000 years BP the precision is about 7‰. Each measurement is compared to two NBS oxalic acid I standards and all measurements are corrected for natural, sample preparation, and sputtering fractionations. The preferred sample size is approximately 5 mg of carbon which is at least two orders of magnitude smaller than that required for conventional $^{14}C$ analyses.

# 5.0 CALCITE OCCURRENCES AND TEXTURES

Fracture calcites in CRNL core exhibit a variety of textures and structures which suggest they formed under different physicochemical conditions. A photograph of typical fractured CRNL core exhibiting several occurrences of fracture calcite is shown in Plate I.

Calcite is frequently present in veins that are sealed with fracture infilling minerals. The thicknesses of these veins range from hairline widths to as much as ~1 cm and are present in all rock types. Examples of sealed calcite veins as viewed under the petrographic microscope are shown in Plate II. Black chlorite is often present between calcite in the centre of the fracture and the host rock showing that calcite precipitation followed fracture chlorite formation (Plate III). This is clearly evident under both the petrographic microscope and scanning electron microscope (Plate IV). Other minerals present in the calcite vein are quartz, K feldspar, and pyrite. The mixed carbonate-silicate mineral assemblage of these veins is apparent from Ca and Si imaging using back scattered X-ray imaging under the SEM (Plate IV). Compositional zoning is present in some calcite veins as illustrated in Plate V. Electron microprobe analyses of the dark chevron-like features indicated that these areas are highly depleted in Mn (0.04%) compared to the non-zoned regions of the vein (0.8%). The dark oval-shaped objects in the SEM image are quartz inclusions.

Calcite occurs as lenses along sealed fractures and as a breccia matrix in highly altered hematite-rich fracture zones (Plate VI). Dolomite sometimes accompanies calcite in these brecciated zones. In some fracture zones calcified lithic fragments are present. Alteration of the wall rock is a common feature of the calcite vein occurrences and usually takes the form of a ferric iron oxidation zone near the fracture surface (Plate VII). The zeolite mineral laumontite has been observed with calcite in closed fractures but these are rare occurrences. Plate VIII shows binocular microscope photographs of prismatic laumontite crystals in a calcite matrix which suggests their formation is coeval.

Calcic pyroxene phenocrysts in a diabase dyke encountered by borehole CR2 have been almost totally replaced by calcite. This can be clearly seen under cathodoluminescence (Plate IX). Because the diabase dykes are undeformed and were intruded following the Grenville orogeny (Dugal and Kamineni, 1987) the hydrothermal activity responsible for calcification of the pyroxene must post-date orogenesis.

The fracture mineral associations, textures, and wall-rock alteration thus point to a hydrothermal origin for the sealed calcite veins and carbonatized host rock. This is discussed further in a later section.

Calcite is also present in a variety of forms in open fractures. Occasionally it occurs as coarse, subhedral to euhedral crytals that have grown in a pre-existing void space

(Plate X). More frequently, however, the calcite is present as patches, flakes, or fine grained granular aggregates sometimes accompanied by fine cubes, patches or aggregates of pyrite (Plate XI and XII). Examples of slickensided calcite and pyrite patches have been observed (Plate XIII) which indicate they formed prior to some tectonic event that caused displacement of the host rock along the fracture surface. A scanning electron microscope examination of an open fracture revealed that the calcite can also be present as rhombohedral crystallites which, in this example, are associated with flaky aggregates of chlorite apparently forming from the alteration of K feldspar (Plate XIV).

Patchy and flaky varieties of open fracture calcite have been observed overlying thick, massive vein calcite (Plate XV). Fractures sealed with hydrothermal vein calcite may have been reactivated by subsequent tectonism allowing interactions between calcite and meteoric ground water which could redistribute vein calcite by recrystallization involving solution-reprecipitation processes. Support for such a model may be present in the chemical and isotopic compositions of fracture calcites as discussed in a later section.

The same types of fracture calcite observed in the CRNL core are also present in core from the East Bull Lake and White Lake research areas albeit with much less frequency. Vein calcite frequently accompanied by fine grained white to pink laumontite is common in the EBL core (Plate XVI). Calcite is also

present as fine grained patches or flakes on open fractures and as thin "papery" coatings. Finely disseminated pyrite is sometimes present in the calcite (Plate XVII). Coarse-grained euhedral-subhedral crystals of calcite are rare at EBL.

Fracture calcite at White Lake is often associated with hematitic staining of the wallrock. In open fractures the calcite is usually present as fine grained patches and sometimes is associated with pyrite or overlies an earlier generation of calcite. Sealed vein calcite is present and crosscuts veins of granitic material (Plate XVIII).

# 6.0 CHEMICAL AND ISOTOPIC RESULTS

## 6.1 CHEMICAL COMPOSITION OF CHALK RIVER GNEISSES AND ASSOCIATED ROCKS

Chemical analyses of representative rock types from CRNL are listed in Table 8. In a plot of the alkalinity ratio versus $SiO_2$ (Wright, 1969) the samples fall within the calc-alkaline or alkaline fields (Fig. 18a). Rocks of monzonitic composition predominate at the CRNL site so it is likely that the average alkalinity ratio of the orthogneiss falls near the calc-alkaline/alkaline boundary. Variations in the $K_2O$-$Na_2O$-CaO contents of these rocks are shown in Fig. 18b. The gabbro and pyroxenite rocks are relatively rich in CaO and the pegmatite, syenitic orthogneiss and paragneiss are rich in $K_2O$. The remaining orthogneiss samples tend to have approximately equal concentrations of these elements.

Variations in the alkali and alkaline earth trace element (Ba, Sr, and Rb) contents are shown in Fig. 18c. With the exception of the pyroxenite and gabbro from CR9, Ba is the predominant trace element in other CRNL rock types. Ratios of Ba/Sr are large ranging from 3.0 to 12.9 (excluding the pyroxenite and CR9 gabbro). Concentrations of Rb are low and, with the exception of the pegmatite sample, Rb/Sr ratios are $<0.4$. Depletion of Rb and other volatile, large ion lithophile elements is a common feature of granulite facies terrains in the Grenville (Rudnick et al., 1985; Arima et al., 1986).

Table 8. Chemical composition of CRNL whole rock samples. All samples were analyzed at the University of Ottawa except for Sr and Rb values shown in brackets which were determined at Carleton.

| | CR9 448.3 m Quartz Monzonitic Gneiss | CR9 574.2 m Quartz Monzonitic Gneiss | CR9 233.6 m Quartz Monzodioritic Gneiss | CR8 58.0 m Granodioritic Gneiss | CR8 184.5 m Granitic Gneiss | CR8 73.6 m Dioritic Gneiss | CR8 121.1 m Pegmatite | PS15 42.6 m Metagabbro | CR1 108.4 m Syenitic Gneiss | CR2 22.3 m Pyroxenite | CR14 29.1 m Paragneiss | CR9 642.0 m Metagabbro |
|---|---|---|---|---|---|---|---|---|---|---|---|---|
| $SiO_2$ (wt.%) | 62.05 | 58.97 | 62.36 | 70.81 | 58.60 | 65.86 | 73.67 | 50.37 | 54.61 | 47.96 | 74.37 | 43.87 |
| $Al_2O_3$ | 17.75 | 16.69 | 17.49 | 15.21 | 18.86 | 17.15 | 14.01 | 13.72 | 19.43 | 11.74 | 13.30 | 12.13 |
| $Fe_2O_{3T}$ | 6.70 | 8.91 | 5.58 | 2.61 | 6.32 | 3.60 | 1.12 | 15.66 | 8.99 | 10.43 | 1.01 | 18.73 |
| MgO | 1.94 | 0.88 | 1.05 | 0.56 | 1.12 | 0.90 | 0.40 | 2.61 | 2.55 | 13.02 | 0.43 | 5.34 |
| CaO | 3.46 | 3.91 | 4.47 | 2.49 | 3.31 | 3.55 | 0.95 | 6.93 | 2.11 | 12.12 | 0.98 | 9.28 |
| $Na_2O$ | 3.30 | 3.94 | 4.23 | 2.95 | 4.04 | 3.86 | 2.93 | 2.85 | 2.34 | 1.45 | 2.78 | 3.00 |
| $K_2O$ | 3.22 | 5.07 | 3.31 | 5.13 | 5.00 | 3.84 | 6.22 | 3.21 | 7.36 | 0.77 | 6.09 | 1.18 |
| $TiO_2$ | 0.80 | 0.93 | 0.66 | 0.30 | 0.77 | 0.51 | 0.13 | 2.82 | 1.10 | 0.36 | 0.15 | 7.08 |
| $P_2O_5$ | 0.30 | 0.25 | 0.14 | 0.07 | 0.17 | 0.15 | 0.00 | 1.78 | 0.32 | 0.00 | 0.10 | 0.45 |
| MnO | 0.11 | 0.16 | 0.09 | 0.04 | 0.14 | 0.07 | 0.02 | 0.23 | 0.20 | 0.17 | 0.02 | 0.19 |
| S | 0.03 | 0.01 | 0.06 | 0.00 | 0.03 | 0.02 | 0.01 | 0.07 | 0.00 | 0.02 | 0.01 | 0.05 |
| Ba(ppm) | 1641 | 2859 | 1416 | 1544 | 6273 | 1169 | 579 | 2151 | 4481 | 192 | 2255 | 186 |
| Cr | 17 | 17 | 28 | <10 | 10 | 17 | 10 | 13 | 24 | 829 | 24 | 16 |
| Zr | 493 | 908 | 507 | 171 | 888 | 263 | 16 | 358 | 710 | 43 | 156 | 270 |
| Sr | 411(440) | 338(359) | 465(484) | 348(342) | 530(542) | 391(408) | 176(174) | 277(304) | 348(365) | 285(310) | 383(386) | 289 |
| Rb | 67(71.5) | 95(103.7) | 53(61.4) | 119(119.0) | 95(100.4) | 88(92.9) | 157(156.1) | 50(65.9) | 76(86.7) | <10(11.6) | 117(125) | 21 |
| Y | 32 | 38 | 40 | 24 | 33 | 37 | 13 | 68 | 35 | 22 | 17 | 40 |
| Nb | 10 | 14 | <10 | <10 | 12 | <10 | 12 | 12 | 18 | <10 | <10 | 17 |
| Zn | 71 | 114 | 88 | 48 | 70 | 52 | 20 | 162 | 24 | 104 | 10 | 156 |
| Ni | <10 | <10 | <10 | <10 | <10 | <10 | <10 | <10 | <10 | 27 | <10 | 40 |
| V | 37 | 39 | 28 | <10 | 27 | 22 | <10 | 126 | 39 | 291 | <10 | 527 |
| Total | 99.99 | 101.23 | 99.75 | 100.44 | 99.27 | 99.76 | 99.56 | 100.64 | 99.68 | 98.31 | 99.58 | 101.54 |
| K/Rb | 398.57 | 443.07 | 518.14 | 361.12 | 441.34 | 366.51 | 330.82 | 533.67 | 803.96 | 1281.87 | 435.85 | 464.70 |
| Rb/Sr | 0.16(0.162) | 0.28(0.290) | 0.11(0.127) | 0.34(0.346) | 0.18(0.186) | 0.22(0.23) | 0.90(0.895) | 0.18(0.22) | 0.22(0.238) | 0.02(0.038) | 0.31(0.32) | 0.07 |
| Ba/Sr | 4.00 | 8.46 | 3.05 | 4.45 | 11.84 | 2.99 | 3.31 | 7.77 | 12.91 | 0.68 | 5.89 | 0.65 |

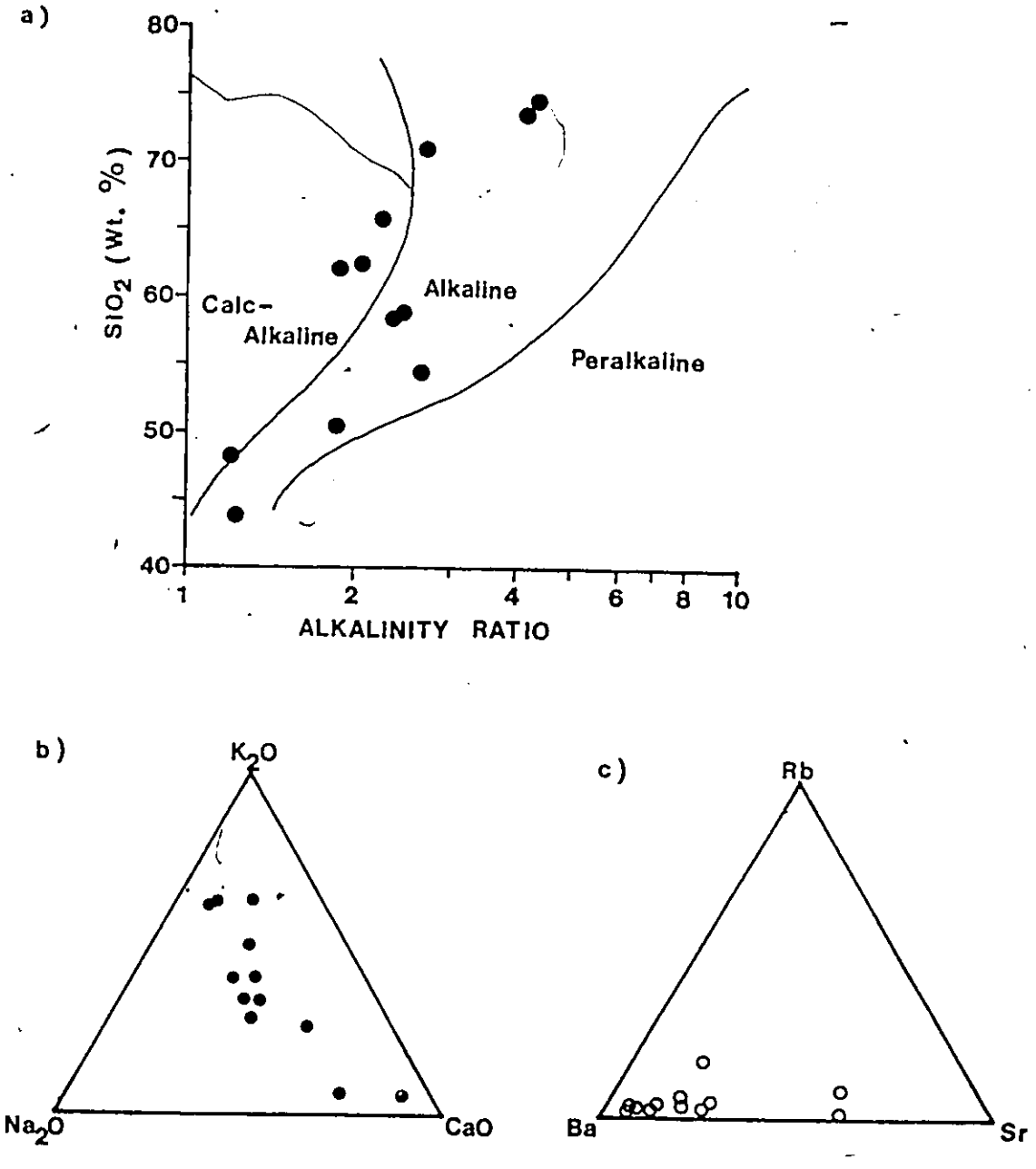


Fig. 18. a) Plot of $SiO_2$ vs. the alkalinity ratio for CRNL whole rock samples b) Ternary plot of whole rock $K_2O$-$Na_2O$-CaO compositions c) Ternary plot of whole rock Rb-Ba-Sr compositions. In "a" alkalinity ratio = $(Al_2O_3 + CaO + Total\ Alkalis)/(Al_2O_3 + CaO - Total\ Alkalis)$.

Total iron concentrations in the CRNL rocks range from about 1% in the paragneiss to 18.7% in the CR9 gabbro. Concentrations of 5-10% are more typical for the orthogneiss rocks as a whole. Manganese concentrations are relatively low (<0.3% MnO).

The chemical composition of the orthogneiss is similar to that of comparable rocks from the nearby Algonquin batholith (Wu and Kerrich, 1986) which suggests a possible co-genetic origin for these plutons. Schwerdtner and Lumbers (1982) suggested the Chalk River pluton is one of several small plutons on the periphery of the Algonquin batholith whose emplacement may be related to the diapiric remobilization of the batholith during the Grenville orogeny. As the emplacement age of the Algonquin batholith is 1.4-1.5 Ga (Wu and Kerrich, 1986) one might expect the Chalk River pluton to have a slightly younger Rb/Sr age reflecting its emplacement during the Grenville orogeny. Alternatively the age may reflect that of the metamorphic event itself if it "re-set" the Rb/Sr systematics.

## 6.2 CHEMICAL COMPOSITION OF CHALK RIVER CALCITES

The minor and trace element chemistry (ppm) of the CRNL calcites, determined by AAS and expressed on an insoluble residue free basis, is shown by the histograms in Fig. 19 and tabulated in Appendix A. Microprobe analyses of vein calcites are listed in Table 9 and analyses of patchy, flaky calcites from

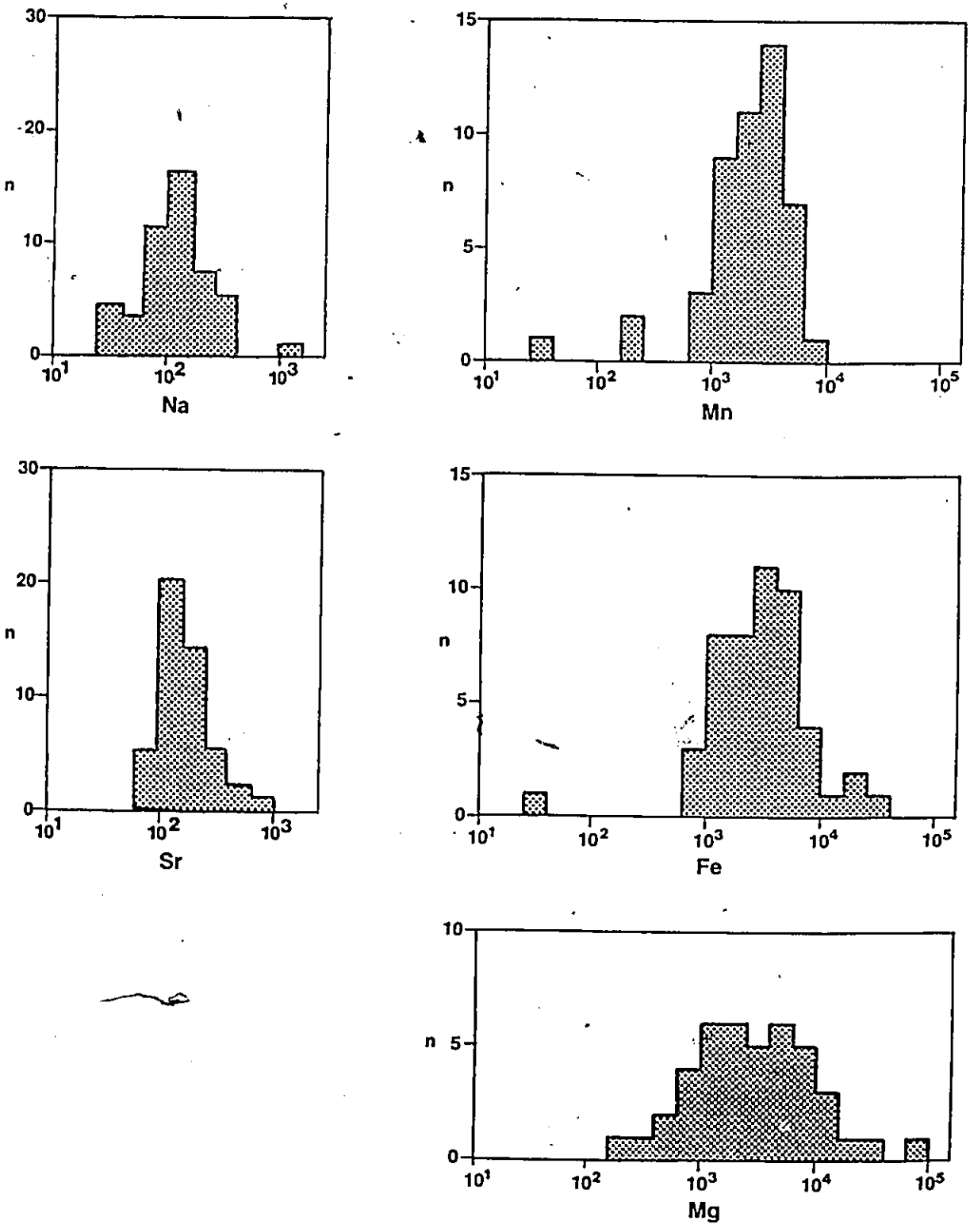


Fig. 19. Histograms of minor element compositions of CRNL calcites.

Table 9. Microprobe analyses of CRNL vein carbonates. Mg concentrations are in ppm except for the dolomite values which are in wt %.

| Borehole and Depth (m) | | Ca (%) | Mg ppm | Mn ppm | Fe ppm |
|---|---|---|---|---|---|
| CR7-137.34 | - P1 | 40.0 | <300 | 510 | <300 |
| | - P2 | 39.5 | <300 | 300 | <300 |
| | - P3 | 39.7 | <300 | 580 | <300 |
| | - P4 | 38.9 | <300 | 2480 | 310 |
| | - P5 | 40.3 | <300 | <300 | <300 |
| | - P6 | 39.5 | <300 | 430 | <300 |
| | - P7 | 39.8 | <300 | 1040 | 320 |
| | - P8 | 40.4 | <300 | 320 | <300 |
| | - P9 | 38.6 | <300 | 2250 | <300 |
| | - P10 | 38.5 | 320 | 2900 | 510 |
| | - P11 | 39.8 | <300 | <300 | <300 |
| | - P12 | 38.8 | <300 | 370 | <300 |
| | - P13 | 39.0 | <300 | <300 | <300 |
| CR9-574.33 | - P1 | 40.1 | 390 | 8710 | 870 |
| | - P2 | 39.1 | <300 | 3100 | 390 |
| | - P3 | 39.4 | <300 | 2400 | <300 |
| | - P4 | 40.1 | <300 | 5700 | 720 |
| | - P5 | 38.8 | <300 | 1250 | 390 |
| | - P6 | 39.0 | 310 | 4150 | 730 |
| | - P7 | 39.3 | 540 | 5040 | 1850 |
| | - P8 | 40.0 | 400 | 3560 | 1190 |
| | - P9 | 38.8 | 330 | 3930 | 970 |
| CR12-26.12 | - P1 | 40.1 | N.D. | 1000 | 1000 |
| | - P2 | 37.3 | 6000 | 2000 | 4000 |
| | - P3 | 40.4 | 4000 | 5000 | 5000 |
| | - P4 | 39.8 | 2000 | 2000 | 2000 |
| | - P5 | 39.5 | 1000 | 5000 | 1000 |
| FS15-13.82 | - P1 | - | 3000 | 8000 | 4000 |
| | - P2 | - | 4000 | 400 | 2000 |
| CR3-130.3 | -P1 | 39.6 | 370 | 2560 | 380 |
| | -P2 | 38.4 | <300 | 2410 | 710 |
| | -P3 | 38.6 | 3180 | 8940 | 1950 |
| calcite | -P4 | 38.0 | 3130 | 8940 | 1950 |
| | -P5 | 38.3 | 3330 | 7980 | 1680 |
| | -P6 | 38.3 | 3190 | 8380 | 1930 |
| | -P7 | 38.9 | <300 | 2690 | 550 |
| | P1 | 20.6 | 10.4 | 4230 | 20560 |
| | P2 | 20.5 | 10.6 | 4640 | 23577 |
| | P3 | 20.4 | 10.7 | 5200 | 18920 |
| dolomite | P4 | 20.9 | 10.4 | 5110 | 15860 |
| | P5 | 20.6 | 10.5 | 6050 | 17880 |
| | P6 | 22.5 | 9.4 | 6280 | 17540 |

open fractures are listed in Table 10. Although leaching of associated silicates and ferric oxyhydroxides in some samples may have contributed to the concentrations measured by AAS, the histograms are probably representative of the distribution of bulk elemental concentrations in these calcites.

At CRNL the (Sr/Ca) mole ratios in the ground water to depths of up to 350 m are relatively high ranging from 1.5-2.4 $x10^{-2}$. Variability is primarily due to large variations in Ca rather than in Sr concentrations. The (Sr/Ca) mole ratios are much lower in the fracture calcites ranging from $9.5x10^{-5}$ to $1.1x10^{-3}$.

Although CRNL ground water is at or near saturation with respect to calcite (Bottomley et al., 1984), it is clear that the fracture calcites are not in equilibrium with the Sr/Ca ratio of the ground water. Even if the minimum Sr distribution coefficient of 0.06 of Pingitore and Eastman (1986) is valid, calcites precipitating from the present day ground waters at CRNL should contain between about 600 and 1200 ppm Sr. However, measured concentrations are generally <300 ppm (Fig. 19). Therefore the bulk of the fracture calcite must have been formed prior to the development of the present day hydrogeochemical regime.

Concentrations of Fe and Mn in bulk fracture calcites are high and generally range between $10^3$ and $10^4$ ppm. Although these elements are most susceptible to contamination from associated oxides and oxyhydroxides, electron microprobe analyses of

Table 10. Microprobe analyses of patchy, flaky varieties of CRNL calcites from open fractures. Each result is the average of three measurements.

| Borehole and Depth (m) | Ca (%) | Mg ppm | Mn ppm | Fe ppm |
|---|---|---|---|---|
| CR1 - 232.38 | 39.18 | 970 | 4180 | 300 |
| CR1 - 252.23 | 39.93 | <300 | 3500 | 500 |
| CR2 - 105.75 | 39.43 | 1380 | 12580 | 940 |
| CR8 - 205.17 | 39.82 | 340 | 4770 | 950 |
| CR8 - 230.66 | 40.27 | 590 | 3510 | 650 |
| CR9 - 464.88 | 39.74 | <300 | 2960 | <300 |
| CR10 - 51.37 | 39.09 | <300 | 4860 | 1060 |
| CR12 - 78.17 | 39.81 | <300 | 3220 | 1030 |
| FS15 - 13.82 | 39.74 | <300 | 1870 | 610 |
| FS15 - 43.85 | 39.52 | 1000 | 5680 | 3640 |

the vein calcite shown in Plate V yielded similar Fe and Mg concentrations to those measured by AAS. In this example (FS15-13.82 m) 0.4 wt % Fe and 0.3% Mg were measured by electron microprobe (point P1 in Table 9) compared to 4400 ppm Fe and 3000 ppm Mg by AAS. The microprobe analyses indicate the dark zoned area in this sample is highly depleted in Mn (0.04%) compared to 0.8% Mn in the remainder of the vein. The Mn concentration of 4900 ppm measured by AAS may reflect an averaging effect produced by mixing of Mn-enriched and depleted portions of the vein material. Concentrations of Fe and Mn in the CRNL ground water are generally less than 50 ppb resulting in (Fe/Ca) and (Mn/Ca) mole ratios of less than $2.6 \times 10^{-3}$. Even at these low concentrations, however, the Fe and Mn contents of calcite precipitating from the present day ground waters could be greater than $10^3$ ppm because of the potentially large $k_t$ values for these elements. More precise measurements of Fe and Mn in ground water are needed to constrain maximum expected concentrations in modern calcites.

Recently it has been shown that the partitioning theory does not accurately describe the incorporation of Na and K into calcite. The concentrations of these elements are apparently controlled by adsorption-desorption equilibria on growing crystal surfaces with eventual accommodation in interstial lattice positions (Ishikawa and Ichikuni, 1984). Nevertheless as fluid salinity increases Na contents in precipitating calcites increase to a concentration of about 2500 ppm at $10^{o}/oo$

salinity. Sodium concentrations in the CRNL calcites are low (generally <300 ppm) indicating the calcites precipitated from fluids of very low salinity or the Na/Ca ratio of the fluid was much smaller than seawater. Alternatively Na in the original calcite could be lost if recrystallization took place.

Mole ratios of (Mg/Ca) range from 0.17 to 0.11 in CRNL ground waters. Based on these ratios and the $k_t$ values in Table 4, Mg concentrations in directly precipitated calcites could range over an order of magnitude - from 300 to 3000 ppm. Measured concentrations display a range in values considerably in excess of 300 ppm (Fig. 19). However, mineral sources other than calcite may contribute Mg to samples analyzed by AAS. For example, the Mg concentration of the calcite vein shown in Plate III was measured at 0.3 wt % by electron microprobe analysis compared to 7000 ppm by AAS. Non-calcite sources of Mg include fracture chlorite and patches of dolomite (possibly of exsolution origins) in some calcite veins.

Cathodoluminescence microscopy in conjunction with subsequent electron microprobe analyses have shown that the vein calcites may be compositionally non-uniform. Plate XIX is a cathodoluminescence photomicrograph of the central, coarse-grained region of a 1 cm wide calcite vein from CR7 - 137.34 m. Compositional zoning is evident within individual calcite crystals and in areas bordering pores and fractures in the central part of the vein. Electron microprobe analyses (Table 9) of several points within the zoned crystals indicate the darker,

non-luminescent regions are low in Mn compared to the yellow luminescent regions. This agrees with the well-known fact that Mn is an effective activator of calcite luminescence (Machel, 1985). Iron on the other hand is a quencher of luminescence. The cathodoluminescence and electron microprobe data indicate that during the final stages of precipitation of calcite vein CR7 - 137.34 m the fluid composition was rapidly changing to lower Mn concentrations. This change must have been rapid because these compositional changes are evident in individual calcite crystals. It is interesting to note that the most recent calcite which lines fractures and vugs in sample CR7 - 137.34 m is brightly luminescent (Plate XIXc) suggesting precipitation from a more Mn-rich fluid (assuming constant Ca concentration) than that which precipitated the dull Mn-poor calcite that immediately preceeded it. Obviously bulk chemical analyses of fracture calcites that are compositionally zoned are of limited value in interpreting the composition of the fluid using partition coefficient theory nor do they reveal the complex fluid history for some of these fractures.

Evidence for recent calcite precipitation from a fluid with a relatively large Mn/Ca mole ratio can be seen in the cathodoluminescence photomicrograph for a reopened calcite vein in sample CR9 - 574.33 m (Plate XX). In this example relatively brightly luminescent calcite overlies duller calcite containing numerous solution pits and inclusions of silicates (principally chlorite) near the contact with the more luminescent calcite.

This chlorite likely represents inclusions of chloritized wall rock material that was formerly in contact with the duller calcite prior to reactivation of the fracture. Although Mn concentrations measured by electron microprobe (Table 9) are high in both calcites Mn/Fe ratios are significantly higher in the more luminescent calcite. Four measurement points in the luminescent calcite have Mn/Fe ratios ranging from 7.9 to 26.7 whereas ratios for 5 measurement point in the duller calcite range from 2.7 to 5.7. Because of the quenching effect of Fe on calcite luminescence the Mn/Fe ratio can be an important factor in determining the brightness of luminescent calcite (Frank et al., 1982).

Manganese concentrations in the present day CRNL ground waters are low. Maximum values measured in the 600 m deep hydrogeochemistry borehole CR13 were 0.04 ppm but most ground water samples contained less than 0.03 ppm Mn (Bottomley et al., 1984). Maximum Mn/Ca mole ratios in the water and in calcite sample CR9 - 574.33 m are approximately 0.0016 and 0.0158, respectively. It is possible, therefore, that the brightly luminescent calcite in this sample precipitated from the present day ground water, given the uncertainty in the Mn $k_t$ value (Table 4) and the lack of constraint on the minimum Mn/Ca mole ratio of the CRNL ground water. This same uncertainty, however, precludes use of Mn data to show that the duller calcite precipitated from a fluid of different origins than that which precipitated the luminescent calcite. This distinction can be done on

the basis of differences in $^{18}O$ content between the two calcites. These calcites have been analyzed for $^{18}O$ and the results are discussed in a later section.

Microprobe analyses of calcites from open fractures (see SEM photos of selected samples, Plate XXI) show that without exception Mn is the most abundant minor element present (Table 10). Concentrations of Mg and Fe are generally low when compared to their concentration distributions in bulk calcite samples (Fig. 19). All of these 'open-fracture' samples are enriched in $^{18}O$ relative to the vein calcites and are believed to have formed from the recrystallization of hydrothermal calcite in recent meteoric waters (see section 6.3). Because of the large $k_t$ value for Mn (Table 4) calcite recrystallization may recycle Mn from one generation to the next. Although the $k_t$ value for Fe is greater than 1, Fe released during recrystallization may at least partially precipitate as a ferric oxyhydroxide rather than be coprecipitated in recrystallized calcite.

Occurrences of fracture calcite in core from the East Bull Lake and White Lake plutons are usually thin and accordingly are difficult to sample for chemical analysis by AAS. Nevertheless several selected calcites from EBL were analyzed by this method and the results are listed in Table 11. Manganese concentrations in the EBL calcites are 1-2 orders of magnitude lower than in the CRNL calcites and Sr concentrations are slightly lower in the EBL calcites. In contrast Na concentrations, although quite variable, are generally higher in the EBL calcites.

Table 11. Chemical composition of EBL fracture calcites (concentrations are in ppm except for Ca which is expressed as weight per cent CaO).

| Borehole | Depth (m) | CaO % | Mg | Fe | Mn | Na | Sr | I.R. (%) |
|---|---|---|---|---|---|---|---|---|
| EBL 1 | 192.54 | 47.8 | 4280 | 1600 | 75 | 13,700 | 190 | 65.8 |
| EBL 2 | 261.00 | 47.7 | <140 | 625 | 40 | 70 | 15 | 64.3 |
| EBL 2 | 625.15 | 37.4 | 2450 | 3970 | 215 | 1,300 | 35 | 65.4 |
| EBL 2 | 755.10 | 35.5 | 650 | 1060 | 295 | 1,530 | 95 | 58.0 |
| EBL 2 | 806.72 | 31.5 | 315 | 765 | 45 | 1,620 | 100 | 44.4 |
| EBL 4 | 115.76 | 50.5 | 515 | 770 | 85 | 3,170 | 90 | 41.5 |
| EBL 4 | 184.54 | 53.9 | 1370 | 2340 | 320 | 4,700 | 95 | 25.2 |
| EBL 4 | 184.57 | 50.0 | 3280 | 6090 | 640 | 3,000 | 120 | 46.3 |
| EBL 4 | 208.53(1) | 52.8 | 865 | 1260 | 210 | 490 | 70 | 33.8 |
| EBL 4 | 208.53(2) | 54.3 | 1065 | 1520 | 190 | 495 | 65 | 34.5 |
| EBL 4 | 208.53 ($Al(NO_3)_3$ rinsed) | 54.5 | 1020 | 1470 | 210 | 130 | 60 | 34.2 |

Although the Na data could suggest the EBL calcites precipitated from a more saline, Na/Cl water than that which precipitated the CRNL calcites, this can not be proven from the chemical data alone. The EBL ground waters exhibit a very large range in (Na/Ca) mole ratios ranging from 0.3 in the shallow $Ca/HCO_3$ ground waters to 280 in the deeper $Na/HCO_3$ ground waters. The deepest saline Na/Cl waters have (Na/Ca) mole ratios of 3.5-5.2 which are much larger than the ratios of 0.45-0.90 reported for the saline ground waters and brines in the Sudbury basin (Frape et al., 1984). Therefore, recently-precipitated EBL fracture calcites could have Na concentrations greater or less than that of marine calcites depending on whether they precipitated from the $Na/HCO_3$ or the $Ca/HCO_3$ or Na/Cl ground waters. Nevertheless the maximum Na concentration observed (13,700 ppm) is much too high to have been derived from any of the present day ground waters. Moreover the stable isotope data for the fracture calcites will show that most of these calcites are not in isotopic equilibrium with the present day ground waters. Therefore the higher Na concentration of the EBL calcites probably reflects their precipitation from an ancient fluid with a relatively high (Na/Ca) mole ratio compared to the present day ground waters.

Rare earth element (REE) concentrations in CRNL calcites, gneisses, and two ground water samples are listed in Table 12 and chondrite-normalized plots for these elements are shown in Figs. 20 and 21. Samples with element concentrations

Table 12. Rare earth element concentrations in CRNL calcites, whole rocks, and ground waters (mg $kg^{-1}$).

| Borehole and depth (m) | La | Ce | Nd | Sm | Eu | Gd | Dy | Yb |
|---|---|---|---|---|---|---|---|---|
| **Calcites** | | | | | | | | |
| CR3 - 22.22 | 162.7 | 198.1 | 73.1 | 11.1 | 1.6 | 6.3 | 1.7 | 1.3 |
| - 69.00 | 150.9 | 278.6 | 125.4 | 16.8 | 1.7 | 11.7 | 8.3 | 6.7 |
| - 130.13 | 51.4 | 91.1 | 47.5 | 8.8 | 1.0 | 10.4 | 11.6 | 9.4 |
| CR8 - 204.94 | 255.9 | 470.7 | 209.3 | 35.2 | 7.5 | 29.0 | 34.5 | 27.8 |
| - 205.05 | 330.3 | 654.4 | 307.3 | 51.1 | 10.9 | 41.4 | 44.7 | 36.1 |
| - 277.51 | 120.8 | 227.7 | 104.7 | 18.1 | 3.0 | 15.8 | 15.8 | 12.8 |
| - 292.32 | 282.3 | 626.1 | 304.3 | 52.2 | 9.3 | 46.5 | 50.8 | 41.0 |
| CR9 - 345.77 | 177.2 | 371.8 | 163.5 | 29.6 | 5.1 | 41.0 | 0.0 | 0.0 |
| - 351.16 | 100.6 | 227.1 | 118.1 | 23.0 | 4.0 | 23.5 | 33.8 | 27.3 |
| - 459.98 | 25.7 | 0.0 | 49.9 | 0.0 | 0.0 | 35.5 | 0.0 | 0.0 |
| - 492.43 | 95.1 | 16.2 | 36.0 | 4.1 | 0.0 | 2.6 | 0.0 | 0.0 |
| - 574.33 | 165.7 | 308.7 | 158.3 | 25.7 | 5.2 | 23.0 | 19.2 | 15.5 |
| CR10 - 51.37 | 4058.7 | 8400.4 | 4026.1 | 618.4 | 70.6 | 383.0 | 100.0 | 80.7 |
| CR12 - 77.90 | 4195.1 | 7561.8 | 3316.7 | 463.3 | 26.6 | 319.7 | 101.4 | 81.9 |
| FS15 - 13.82 | 349.3 | 735.5 | 321.1 | 52.8 | 8.5 | 44.0 | 40.1 | 32.4 |
| FS16 - 14.30 | 328.4 | 563.3 | 218.4 | 27.9 | 3.4 | 15.4 | 11.2 | 9.1 |
| **Whole Rocks** | | | | | | | | |
| CR1 - 108.4 | 13.3 | 27.9 | 15.7 | 3.2 | 2.3 | 6.4 | 0.0 | 0.0 |
| CR2 - 22.3 | 10.9 | 40.2 | 19.2 | 7.1 | 1.7 | 6.0 | 0.0 | 0.0 |
| CR8 - 58.0 | 40.2 | 74.0 | 31.1 | 4.4 | 1.2 | 2.8 | 2.9 | 2.3 |
| - 121.1 | 3.1 | 6.2 | 3.8 | 0.7 | 0.8 | 0.5 | 0.8 | 0.6 |
| - 184.5 | 23.9 | 50.7 | 27.0 | 4.4 | 2.9 | 3.3 | 3.8 | 3.1 |
| CR9 - 233.6 | 22.5 | 51.6 | 28.5 | 5.5 | 1.6 | 4.0 | 5.9 | 4.8 |
| - 448.3 | 54.3 | 104.6 | 41.2 | 6.9 | 1.3 | 5.5 | 5.0 | 4.0 |
| - 574.2 | 35.0 | 71.6 | 42.5 | 6.8 | 3.0 | 5.8 | 5.5 | 4.5 |
| CR14 - 29.1 | 13.3 | 31.6 | 12.9 | 2.1 | 0.9 | 1.6 | 1.6 | 1.3 |
| **Ground Waters** | | | | | | | | |
| CR13 - 86 m | 0.01 | 0.00 | 0.00 | 0.00 | 0.00 | 0.00 | 0.00 | 0.00 |
| - 341 m | 0.03 | 0.01 | 0.01 | 0.00 | 0.00 | 0.00 | 0.00 | 0.00 |

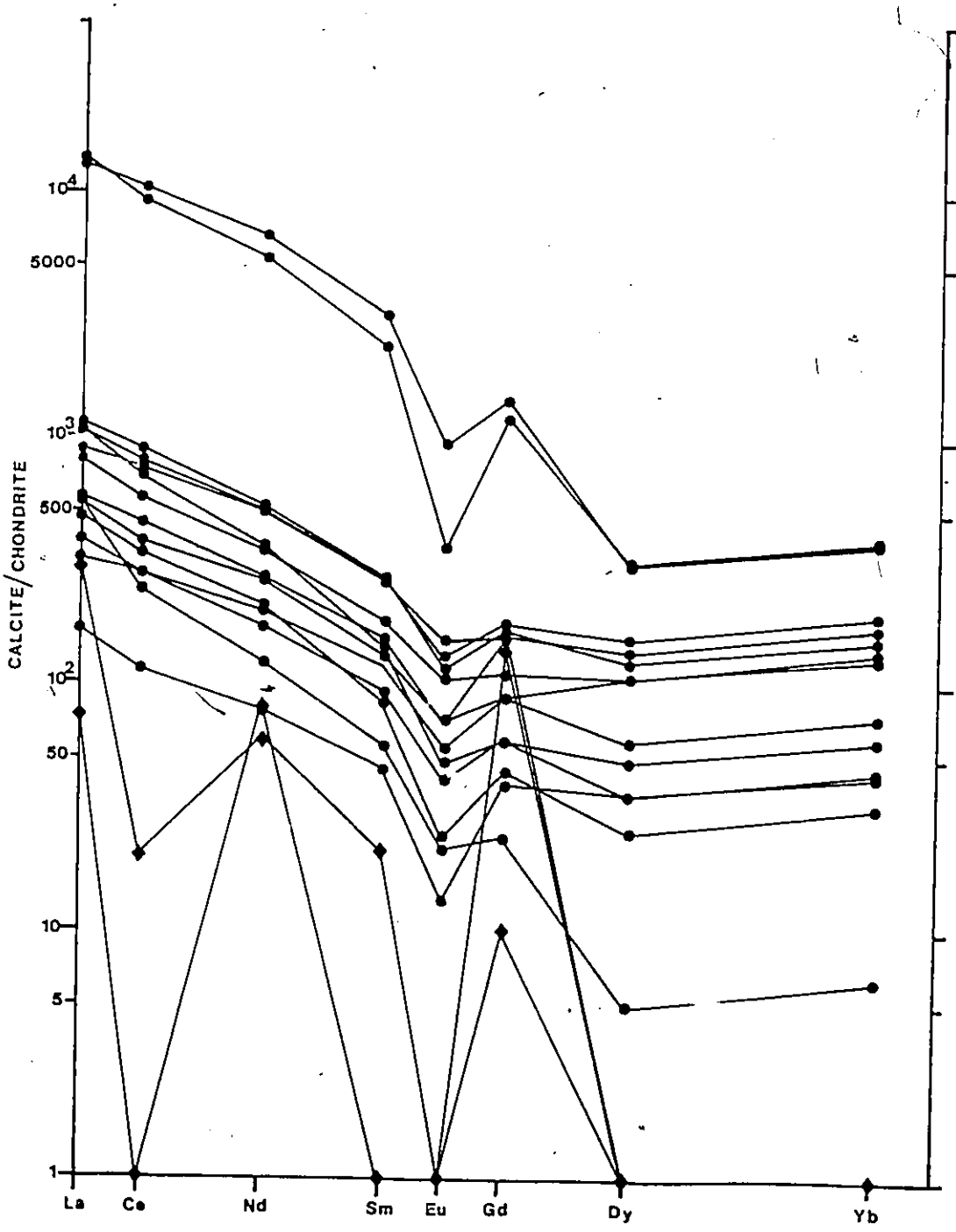


Fig. 20. Chondrite normalized plot of REE concentrations in CRNL calcites based on chondrite REE concentrations of Masuda et al. (1973). Diamond symbol indicates $^{18}O$-depleted calcite.

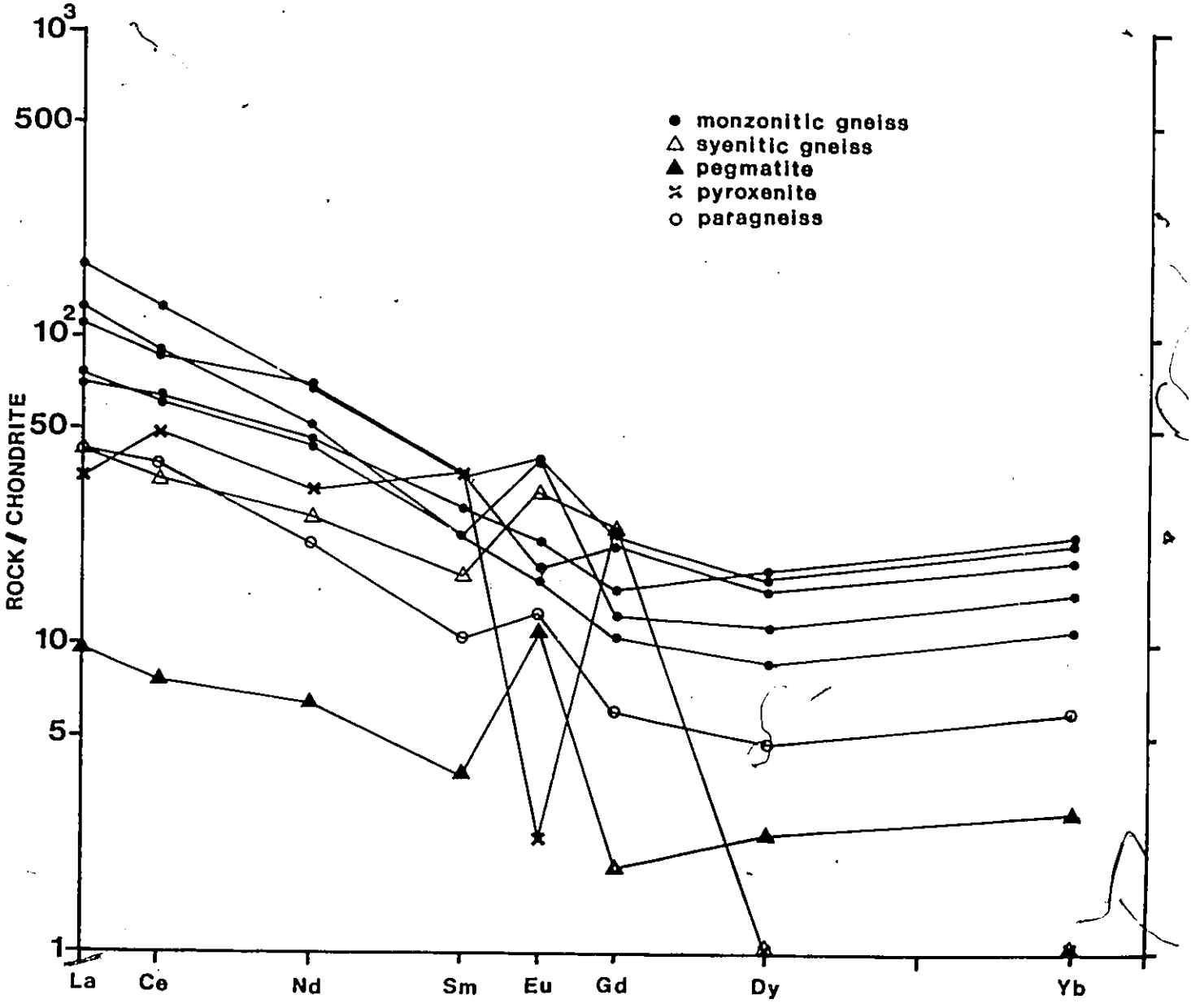


Fig. 21. Chondrite normalized plot of REE concentrations in CRNL whole rock samples.

less than the detection limit are shown with normalized ratios of one. The fracture calcites are enriched in REE relative to the host rocks although both generally exhibit similar light rare earth element (LREE) enrichment patterns. Two of the calcites contain very large concentrations of REE. These two calcites are also enriched in $^{18}O$ (>20°/oo) as the result of recrystallization in meteoric ground water as discussed in a following section. In contrast, two calcites with unusually light $\delta^{18}O$ values (~0°/oo) have low REE concentrations relative to the other calcites and strong negative Ce anomalies. Mild to strong negative Eu anomalies are present in most of the calcites. Whole rock samples have negative, positive or no Eu anomalies.

The similarity in REE patterns between the monzonitic orthogneisses and the calcites suggest that the REE in the calcites have been derived from these gneisses. The two low-REE calcites are obvious exceptions. The average Sm/Nd ratio of the calcites (excluding the low REE calcites) is 0.16 compared to 0.17 for the whole rock samples, excluding the pyroxenite. The average Sm/Nd ratio for granulite is 0.16 (Herman, 1970) further suggesting that the gneisses are the source of the REE contents in the calcites.

In Fig. 22 the calcite REE concentrations have been normalized against the average REE concentration in the five monzonitic-orthogneiss samples from boreholes CR8 and CR9. Most of the calcites display a relatively flat REE pattern with a

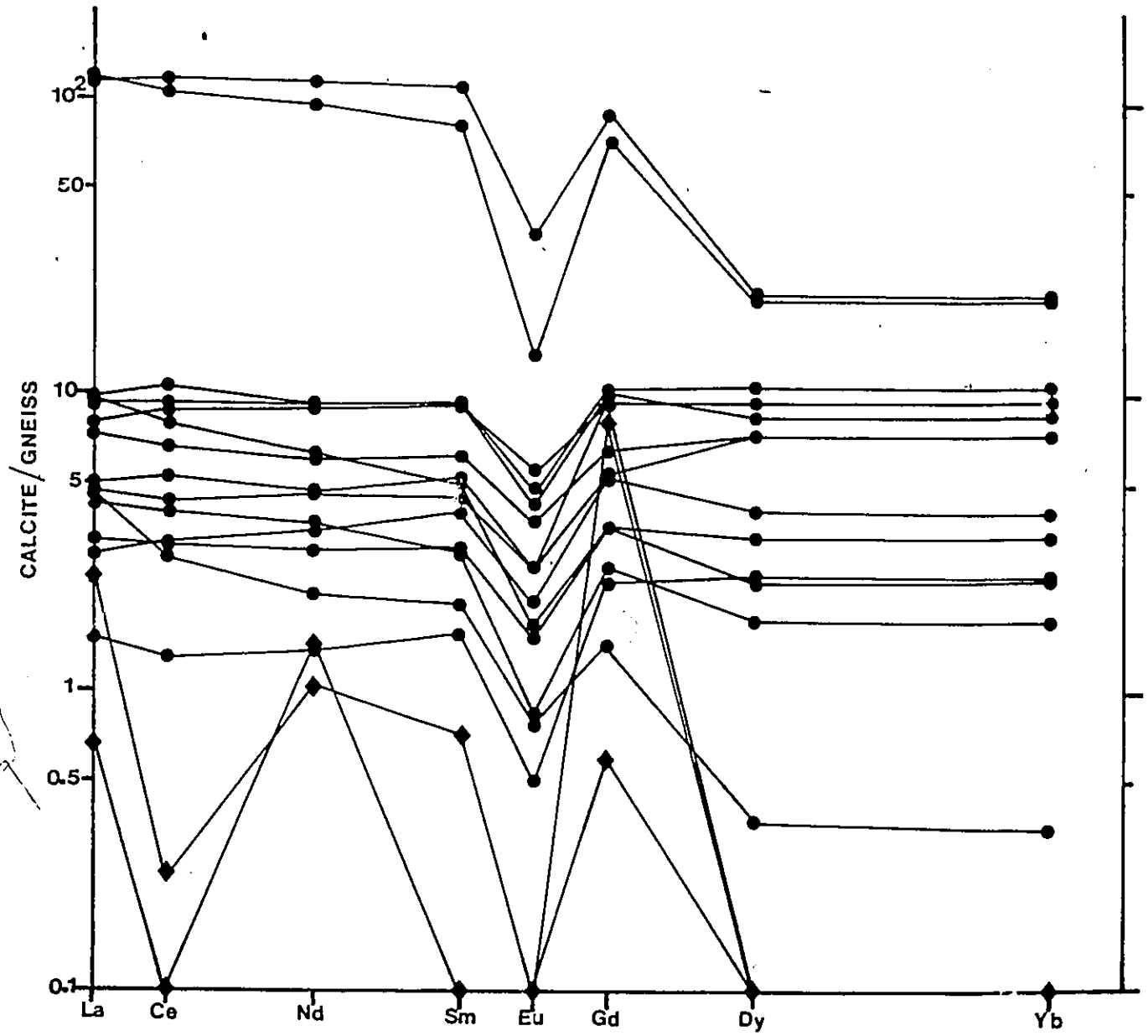


Fig. 22. Plot of CRNL calcite REE concentrations normalized against average REE concentration in CRNL orthogneisses. Diamond symbol indicates $^{18}O$-depleted calcite.

mild negative Eu anomaly suggesting Eu was slightly less mobile than the other REE during calcite precipiation. This could indicate the presence of $Eu^{+2}$ in solution which is probably too large to substitute as readily for $Ca^{2+}$ as $Eu^{3+}$ in calcite (Eby, 1975). The presence of a significant proportion of Eu in the +2 valency state would indicate that the fluid from which it precipitated was moderately reducing.

The large order of magnitude difference in REE concentrations between the fracture calcites and the host rocks suggests that the REE elements released by the alteration of the rocks are largely immobilized by the secondary fracture minerals. It is not likely, however, that the CRNL calcites are the only fracture mineral sinks for these elements. The mineral impurities (i.e. "insoluble residues") that accompany the calcite, such as ferric oxyhydroxides, are known to be efficient adsorbers of REE (Graf, 1984; Shaw and Wasserberg, 1985). Formation of REE minerals such as bastnaesite ($CeFCO_3$) in fractures in plutonic rocks has also been reported (Kamineni and Bonardi, 1983) and this has been attributed to recent interactions between ground water and monazite. In Fig. 23 the total REE concentration (ΣREE) in the fracture calcites have been plotted against their insoluble residue (I.R.) contents. There is a large amount of scatter in this plot suggesting the correlation between ΣREE and the I.R. is far from linear. Furthermore, variability in the I.R. content has had no apparent effect on the overall REE patterns. Therefore it is probable that both

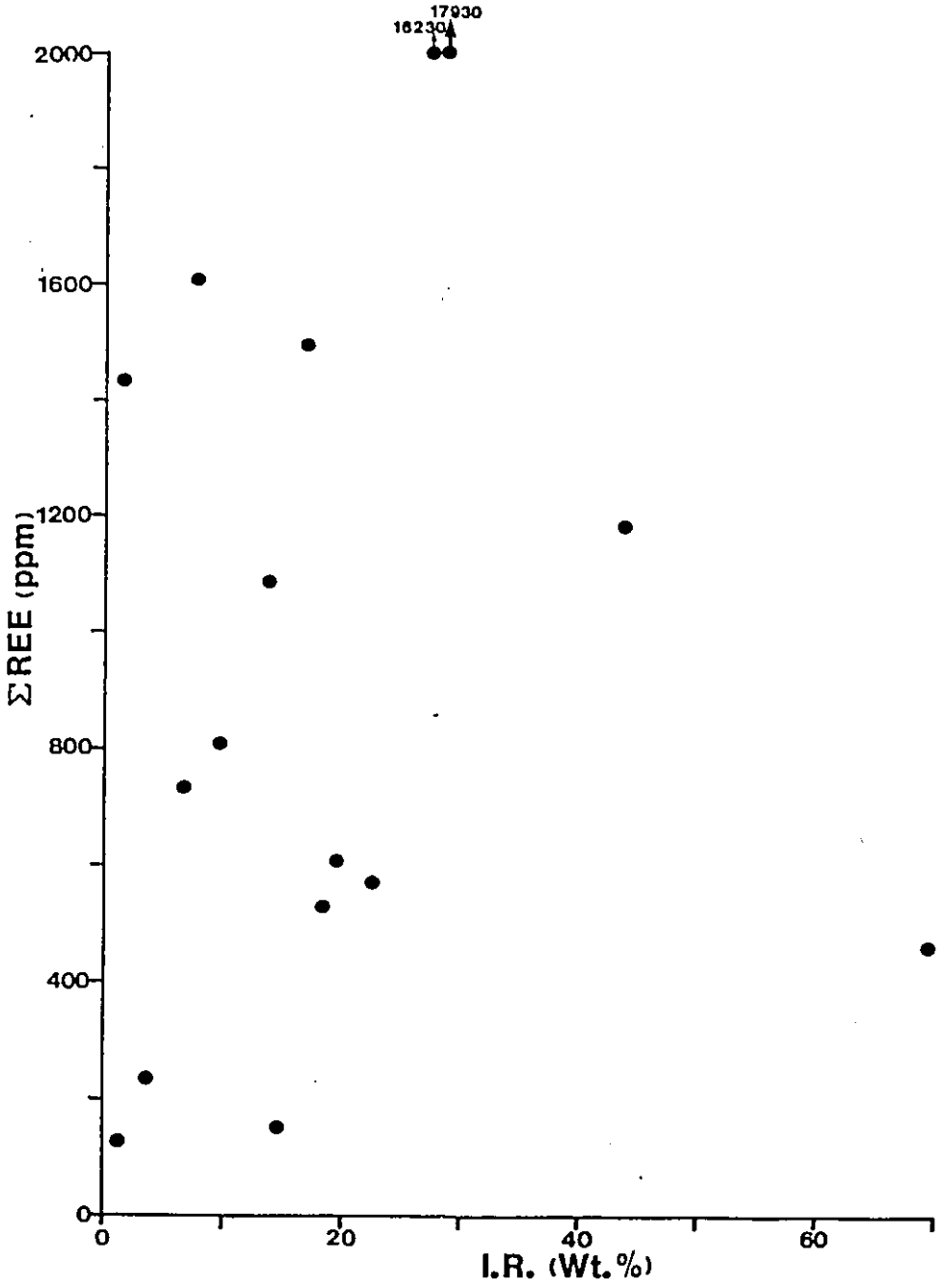


Fig. 23. Plot of the REE concentration vs. the insoluble residue content of CRNL calcites.

the fracture calcites and the insoluble residue have REE patterns similar in shape to that of the host gneisses.

Concentrations of REE in CRNL ground waters are near or below the detection limit of the analytical procedures used in this study. However, it is clear from the analyses of the sample from 341 m in borehole CR13 that the ground waters are enriched in La relative to the other REE. Because Ce and Nd concentrations in the monzonitic orthogneiss are similar to or greater than La concentrations it would appear that La is the most mobile REE in CRNL ground waters. The ionic radius of $La^{3+}$ is significantly larger than that of $Ce^{3+}$ or $Nd^{3+}$ which may make its substitution for $Ca^{2+}$ in calcite more difficult. Nevertheless the fracture calcites do not show any discrimination against La relative to Ce and Nd (Fig. 22). This suggests that either the hydrothermal calcites precipitated from a fluid that was also enriched in La relative to other LREE or, alternatively, REE complexation by $CO_3^{2-}$, $SO_4^{2-}$ or $Cl^-$ could have increased the effective (non-complexed) concentration of free $La^{2+}$ in the hydrothermal solution relative to other REE. Graf (1984) has shown that $La^{2+}$ can be expected to be less complexed than heavier REE in hydrothermal solutions resulting in relatively larger free $La^{2+}$ concentrations available for precipitation in calcite.

The two low REE calcites have distinctive REE patterns with strong negative Ce anomalies not observed in other calcite or rock samples. Seawater has a strong negative Ce anomaly apparently due to significant oxidation of $Ce^{3+}$ to $Ce^{4+}$ with subsequent incorporation primarily into Mn nodules (Addy, 1979;

Fleet, 1984). Highly oxidized meteoric waters might also be expected to have negative Ce anomalies. Moller et al. (1979) observed similar Ce anomalies in low REE hydrothermal calcites which they interpreted as forming from oxidized, meteoric water. Therefore the REE pattern in these calcites may reflect that of a fluid which had not interacted with the gneisses sufficiently to acquire the REE pattern of the gneisses. This would imply these calcites precipitated in a high meteoric water/rock environment. The $^{18}O$ contents of these calcites may support such an interpretation as discussed in a subsequent chapter.

## 6.3 ISOTOPIC COMPOSITIONS OF CHALK RIVER ROCKS AND FRACTURE CALCITES

### 6.3.1 Strontium

Ten whole rock samples were analyzed for their $^{87}Sr/^{86}Sr$ and Rb/Sr ratios (Table 13). Seven of these samples were orthogneisses which included syenitic, granodioritic, monzodioritic, granitic, and quartz monzonitic gneisses. The other three samples were comprised of a pyroxenite, metagabbro, and a pegmatite. The present day $^{87}Sr/^{86}Sr$ ratios of the orthogneiss samples range from 0.71085 to 0.72313. The pyroxenite and pegmatite values bracket the gneiss values with isotopic ratios of 0.70782 and 0.74498, respectively.

The $^{87}Sr/^{86}Sr$ and $^{87}Rb/^{86}Sr$ ratios for all whole rock samples are plotted in Fig. 24 and an isochron has been fitted to four of the seven gneiss samples using the method of York (1969). The slope of the isochron produces an age of 1345 ±

Table 13. Strontium isotope and Rb/Sr data for CRNL whole rock samples.

| Borehole and Depth (m) | $^{87}Sr/^{86}Sr$ | $^{87}Rb/^{86}Sr$ | Rock Description |
|---|---|---|---|
| CR1 - 108.4 | 0.71441 | 0.688 | brownish-grey medium grained quartz syenitic gneiss. |
| CR2 - 22.3 | 0.70782 | 0.109 | melanocratic, inequigranular, massive, non-foliated pyroxenite. |
| CR8 - 58.0 | 0.72313 | 1.004 | grey, fine-medium grained granodioritic gneiss. |
| CR8 - 73.7 | 0.71598 | 0.662 | medium-grained melanocratic monzodoritic augen gneiss. |
| CR8 - 121.1 | 0.74498 | 2.598 | coarse-grained, non-foliated granitic pegmatite. |
| CR8 - 184.5 | 0.71407 | 0.537 | fine-medium grained, pinkish grey granitic gneiss. |
| CR9 - 233.6 | 0.71085 | 0.367 | grey, medium-grained, garnetiferous quartz monzodioritic gneiss. |
| CR9 - 448.3 | 0.71250 | 0.468 | grey, medium-grained, garnetiferous quartz monzonitic gneiss. |
| CR9 - 574.2 | 0.72121 | 0.839 | grey, medium-coarse grained garnetiferous quartz monzonitic augen gneiss. |
| FS15 - 42.6 | 0.71670 | 0.629 | fine-grained, melanocratic, weakly foliated gabbro. |

22 Ma with an initial $^{87}Sr/^{86}Sr$ ratio of 0.70368. The mean square of weighted deviates (MSWD) of the isochron, as defined by Brooks et al. (1972), is 3.6 indicating there may be some scatter slightly in excess of experimental uncertainties. The pegmatite and pyroxenite samples plot well off the isochron as would be expected since they likely intruded the gneiss following the Grenville orogeny. The gabbro sample is also post "Grenvillian". Three of the gneisses appear not to have remained totally closed with respect to Rb or Sr as subsequent mobilization of these elements is suggested by the deviation of the gneisses from the isochron. The scale at which these rocks were open to gain or loss of Rb and Sr following emplacement is not clear and may have been variable. Although all samples were free of visible alteration, fracturing could be present in the rock near where the core samples were collected thus facilitating Rb or Sr migration between fracture fluids and the rock. This implies migration occurred either during or following the period of hydrothermal activity and is on the scale of centimetres. However, the uncommon syenitic gneiss lies well to the right of the isochron suggesting that either $^{87}Sr$ migrated out of or $^{87}Rb$ migrated into this gneiss. This migration may have occurred during the regional metamorphism of the Grenville orogeny and was probably on the scale of tens of metres. Such open system behavior is not uncommon for metamorphic rocks in the Grenville (Bell and Blenkinsop, 1980).

The Rb/Sr date of about 1300 Ma may represent the age of emplacement of the pluton into surrounding supracrustal metasedimentary rocks or the onset of the Grenvillian metamorphic

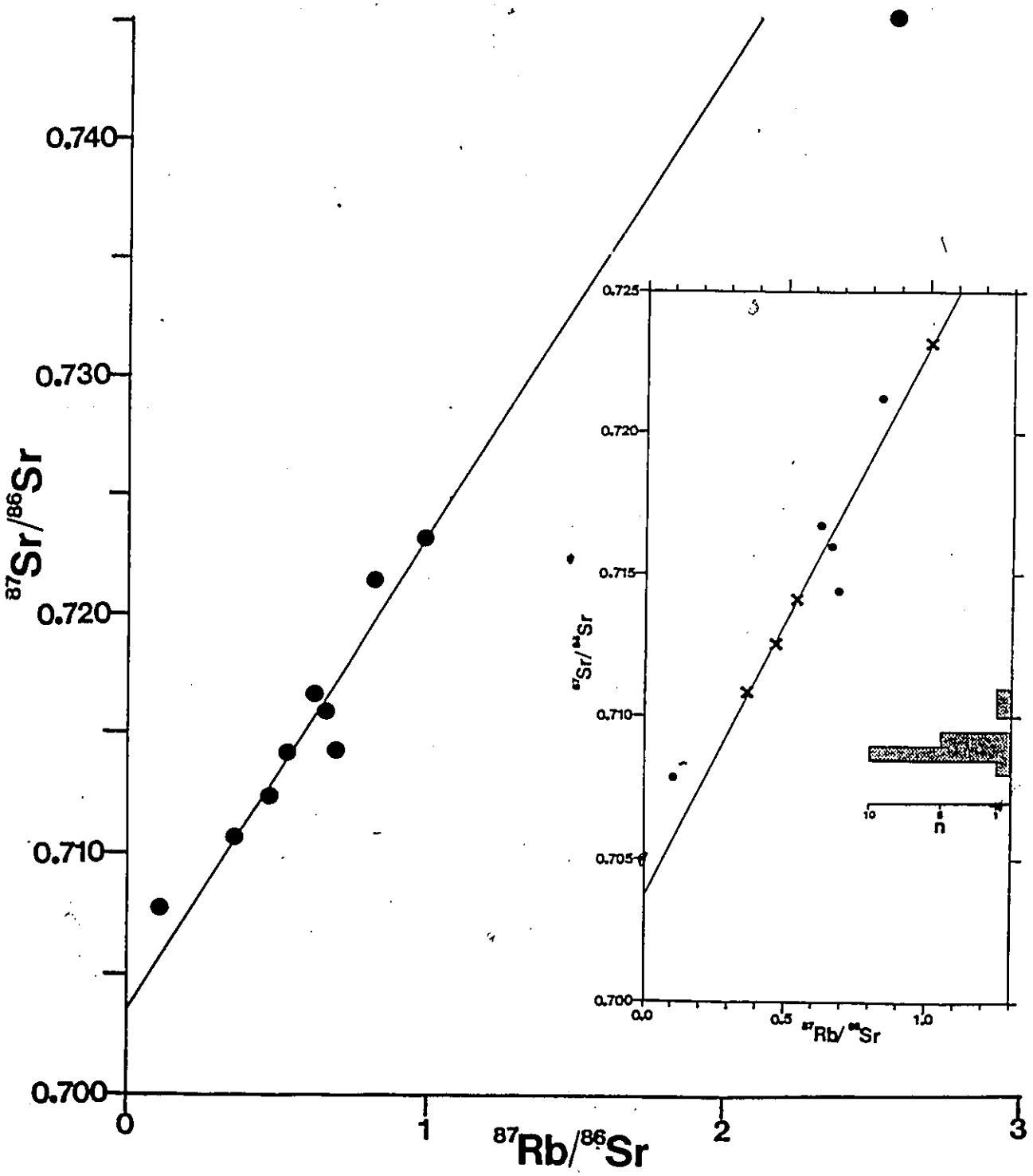


Fig. 24. Plot of CRNL whole rock $^{87}Sr/^{86}Sr$ and $^{87}Rb/^{86}Sr$ compositions. Insert is an enlargement of the isochron drawn to provide the best fit to four orthogneiss samples (crosses). The histogram shows the distribution of the $^{87}Sr/^{86}Sr$ ratios for the calcites.

event. However if the isochron is the result of metamorphism an age closer to 1100 Ma would be expected since this is the widely accepted period of peak metamorphism in this part of the Grenville (Baer, 1981). The Rb/Sr age of the Chalk River pluton is only slightly less than that of the nearby Algonquin batholith (1.5-1.4 Ga) which may have been subsequently remobilized by diapirism during the Grenville orogeny (Schwerdtner and Lumbers, 1980). Therefore, interpretation of the Rb/Sr age of the Chalk River pluton as the age of emplacement seems most reasonable especially if its emplacement was related to diapirism of the Algonquin batholith at the onset of the Grenville orogeny.

The low initial $^{87}Sr/^{86}Sr$ ratio of 0.70368 is similar to values of around 0.7030 - 0.7035 proposed for Grenville gneisses that may be the basement rocks for the Grenville Supergroup (Bell and Blenkinsop, 1980) and is distinctly lower than initial ratios of 0.709 - 0.715 for metagreywackes and paragneisses in the Ontario Gneiss Belt (see summary of Wu and Kerrich, 1986). The low initial ratio for the orthogneisses may indicate that these rocks were formed from a magma that was derived from the lower crust or upper mantle. Alternatively, the igneous precursor of the orthogneisses may have been derived from early Proterozoic metasediments perhaps containing a high percentage of volcanic detritus (and hence having a low Rb/Sr ratio). Such metasediments had initial ratios ranging from ~0.702 to ~0.705 (Wu and Kerrich, 1986). Some support for this latter suggestion is found in the high $Al_2O_3$ content of the monzonitic orthogneiss samples (Table 8.) The Al/(Na + Ca + K)

molar ratios for these rocks range from 1.14 - 1.47 which would suggest they were derived from peraluminous rocks, provided this ratio was not significantly altered during metamorphism. Accordingly the orthogneisses could have been derived from S-type granitic rocks that were formed by anatexis of early Proterozoic sedimentary rocks. Monzonitic-syenitic rocks in the Algonquin batholith have an average Al/(Na + Ca + K) ratio of 1.14 which is at the low end of the range for the CRNL gneisses (Wu and Kerrich, 1986).

The Sr isotopic compositions of the calcites are relatively uniform with a range of between 0.70825 and 0.71052 (Table 14). The mean value is 0.7090. These ratios are significantly less radiogenic than the present day whole rock values but more radiogenic than the initial ratio of the host gneisses. Because the calcite lattice cannot accommodate a significant amount of Rb, the $^{87}Sr/^{86}Sr$ of calcite records the isotopic composition of the fluid at the time of its precipitation. For the case of hydrothermal fluids the Sr isotopic composition of the fluid is usually similar to that of the host rocks (Stettler and Allègre, 1978) and hence the $^{87}Sr/^{86}Sr$ ratio of hydrothermal minerals low in Rb (such as calcite and fluorite) records the Sr isotopic composition of the wall rock at the time of vein mineral formation (Ruiz et al., 1984). Therefore, if the host rock is relatively rich in Rb it is possible to estimate a maximum age for the calcite (and a minimum age for the fracturing) using the Rb-Sr age dating equation:

$$(18) \qquad {}^{87}Sr/^{86}Sr = ({}^{87}Sr/^{86}Sr)_o + {}^{87}Rb/^{86}Sr\ (e^{\lambda t} - 1)$$

Table 14. Strontium isotopic composition of CRNL fracture calcites and ground waters.

| Borehole and Depth (m) | $^{87}Sr/^{86}Sr$ | Comments |
|---|---|---|
| Calcites | | |
| CR2 - 58.32 | 0.71052 | calcite vein stockwork |
| - 127.90 | 0.70868 | sealed vein |
| CR3 - 130.10 | 0.70867 | calcite/dolomite mixture |
| - 69.00 | 0.70894 | sealed vein in pyroxenite |
| CR8 - 184.88 | 0.70891 | sealed vein |
| - 285.38 | 0.70913 | patchy calcite - open fracture |
| CR9 - 75.75 | 0.70907 | open, sub-vertical fracture |
| - 351.16 | 0.70899 | sealed fracture in breccia zone |
| - 459.98 | 0.70879 | sealed vein with laumontite |
| - 492.43 | 0.70855 | sealed vein |
| - 574.33 | 0.70825 | first generation calcite in reopened vein |
| CR10 - 51.37 | 0.70895 | open, sub-vertical fracture |
| CR12 - 26.12 | 0.70864 | sealed fracture |
| - 26.38 | 0.71016 | duplicate samples |
| - 26.38 | 0.71011 | |
| - 26.42 | 0.70907 | open fracture |
| - 113.34 | 0.70899 | open fracture |
| FS16 - 14.30 | 0.70917 | open fracture |
| FS17 - 22.74 | 0.70939 | patchy calcite |
| Ground Waters | | |
| CR13 - 86 | 0.70929 | $Na/HCO_3$ water; $[Sr^{2+}]$ = 0.9 ppm |
| - 341 | 0.70920 | Na/Cl water; $[Sr^{2+}]$ = 1.7 ppm |

where $^{87}Sr/^{86}Sr$ and $^{87}Rb/^{86}Sr$ are the present day ratios of the gneiss and $(^{87}Sr/^{86}Sr)_o$ is the initial Sr isotopic ratio of the gneiss host rock at the time of hydrothermal mineral formation and which is recorded in the Sr isotopic ratio of the fracture calcite. This assumes, of course, that the Sr isotopic composition of the hydrothermal fluid was similar to the whole rock value and not controlled by a particularly soluble mineral phase with a distinctly different value (Ruiz et al., 1984).

Substitution of present day average $^{87}Sr/^{86}Sr$ and $^{87}Rb/^{86}Sr$ ratios of 0.71602 and 0.652, respectively for seven orthogneiss samples and a $(^{87}Sr/^{86}Sr)_o$ ratio of 0.709 results in an age of about 760 Ma for the hydrothermal calcite. However this age is not well constrained because it is sensitive to the $^{87}Rb/^{86}Sr$ ratio of the rocks which is quite low and variable (0.37 - 1.00) in the CRNL gneisses. Nevertheless the hydrothermal calcite must be several hundred million years old as is evident from an examination of $^{87}Sr/^{86}Sr$ development lines for 1345 Ma old gneiss as a function of the $^{87}Rb/^{86}Sr$ ratio (Fig. 25). Intersections of these lines with a horizontal line representing the average $^{87}Sr/^{86}Sr$ ratio of the fracture calcites indicate the hydrothermal calcite is at least 400 Ma old and quite possibly 700-800 Ma old if the average gneiss $^{87}Rb/^{86}Sr$ ratio of the gneiss (0.652) is considered. If so the calcite probably formed during a period of late Proterozoic fracturing and hydrothermal activity in this region of the Ottawa-Bonnechere graben system several hundred millions of

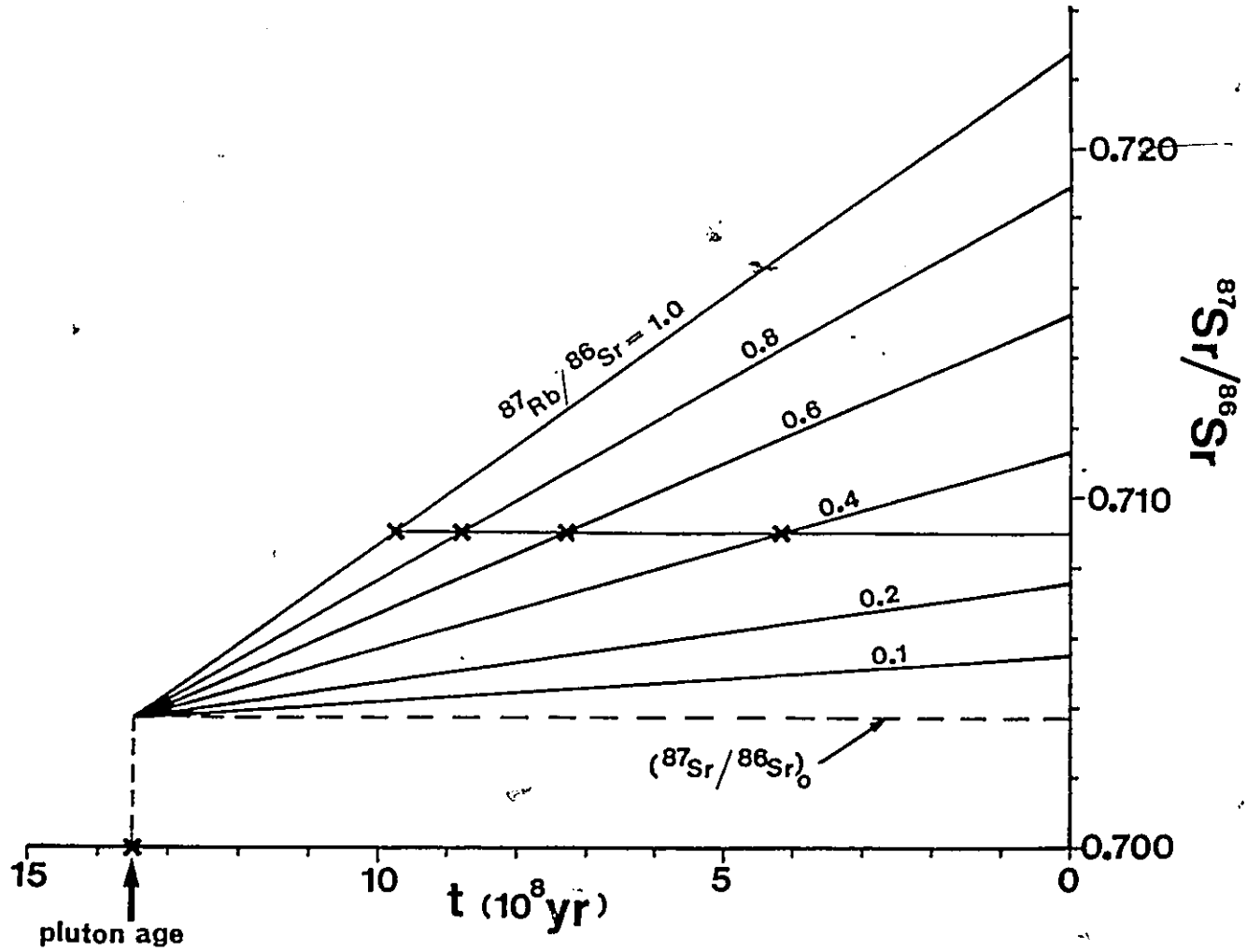


Fig. 25. Development trends in the $^{87}Sr/^{86}Sr$ ratio of the 1345 Ma old Chalk River pluton as a function of possible $^{87}Rb/^{86}Sr$ ratios for CRNL rocks. The dashed horizontal line is the initial $^{87}Sr/^{86}Sr$ ratio of the pluton (0.70368) and the solid horizontal line is the average present day ratio for CRNL fracture calcites.

years after the Grenville orogeny. Such a conclusion is not inconsistent with the previously noted long period of post-Grenville orogeny magmatism in the Grenville Province (Higgins, 1982) especially in regions near the Ottawa River Valley.

Both the $Na/HCO_3$ and Na/Cl ground waters at CRNL have $^{87}Sr/^{86}Sr$ ratios (0.70929 and 0.70920, respectively) that are similar to the fracture calcites. The similarity in Sr isotopic compositions of the CRNL ground waters and fracture calcites (Table 14) strongly suggests that calcite dissolution is a more important source of $Ca^{2+}$ and $Sr^{2+}$ in these waters than the incongruent dissolution of silicate minerals despite the substantial concentrations of both elements in the gneisses (Table 8). However the ground waters from CRNL that have been analyzed for $^{87}Sr/^{86}Sr$ are of the $Na/HCO_3$ and Na/Cl types. Shallow $Ca/HCO_3$ waters, such as those sampled in borehole CR7 (Fig. 4), could have more radiogenic $^{87}Sr/^{86}Sr$ ratios reflecting more significant contributions of silicate mineral $Sr^{2+}$. McNutt et al. (1987) showed that recent shallow, $Ca/HCO_3$ waters at EBL are characterized by relatively radiogenic and non-uniform $^{87}Sr/^{86}Sr$ ratios (0.710 - 0.721) compared to the $Na/HCO_3$ and Na/Cl waters and fracture calcites and laumontite that have relatively uniform ratios near 0.7125. Multiple mineral dissolution by chemically agressive low pH, recharge water may explain the variable $^{87}Sr/^{86}Sr$ ratios of the $Ca/HCO_3$ waters at EBL.

The high $Sr^{2+}$ concentration and $Sr^{2+}/Ca^{2+}$ mole ratios for the $Na/HCO_3$ waters at CRNL compared to the EBL $Na/HCO_3$

waters suggest the isotopic composition of $Sr^{2+}$ at CRNL is not buffered by an exchangeable $Sr^{2+}$ reservoir. The data are more consistent with a calcite recrystallization process. Solution and reprecipitation of calcite would lead to relatively large $Sr^{2+}/Ca^{2+}$ mole ratios (compared to the ratio in the unaltered calcite precursor) as well as impart the Sr isotopic signature of the calcite to the ground water. However, Davison (1982) has shown from inter-borehole tracer experiments at CRNL (between boreholes CR6 and CR7) using NaI as a tracer that exchangeable $Ca^{2+}$ is abundant on the fracture surfaces. While this supports the proposal that the $Ca/HCO_3$ to $Na/HCO_3$ ground water transition is the result of reversible ion exchange reactions, it also suggests that the exchangeable $Sr^{2+}$ concentrations on the fractures may be large ($Sr^{2+}$ was not measured in the ground water during the experiments). Therefore although calcite recrystallization is likely the predominant control on the $Sr^{2+}$ concentration and the $^{87}Sr/^{86}Sr$ ratio of the ground water, Sr isotopic buffering by exchangeable adsorbed Sr cannot be totally discounted.

### 6.3.2 Oxygen and Carbon

The distribution of the $\delta^{18}O$ and $\delta^{13}C$ values for the Chalk River calcites are shown in the histograms of Fig. 26. The actual measurements are listed in Appendix Table A2. Most of the $\delta^{13}C$ values range between -5.5 to -8.0°/oo although seve-

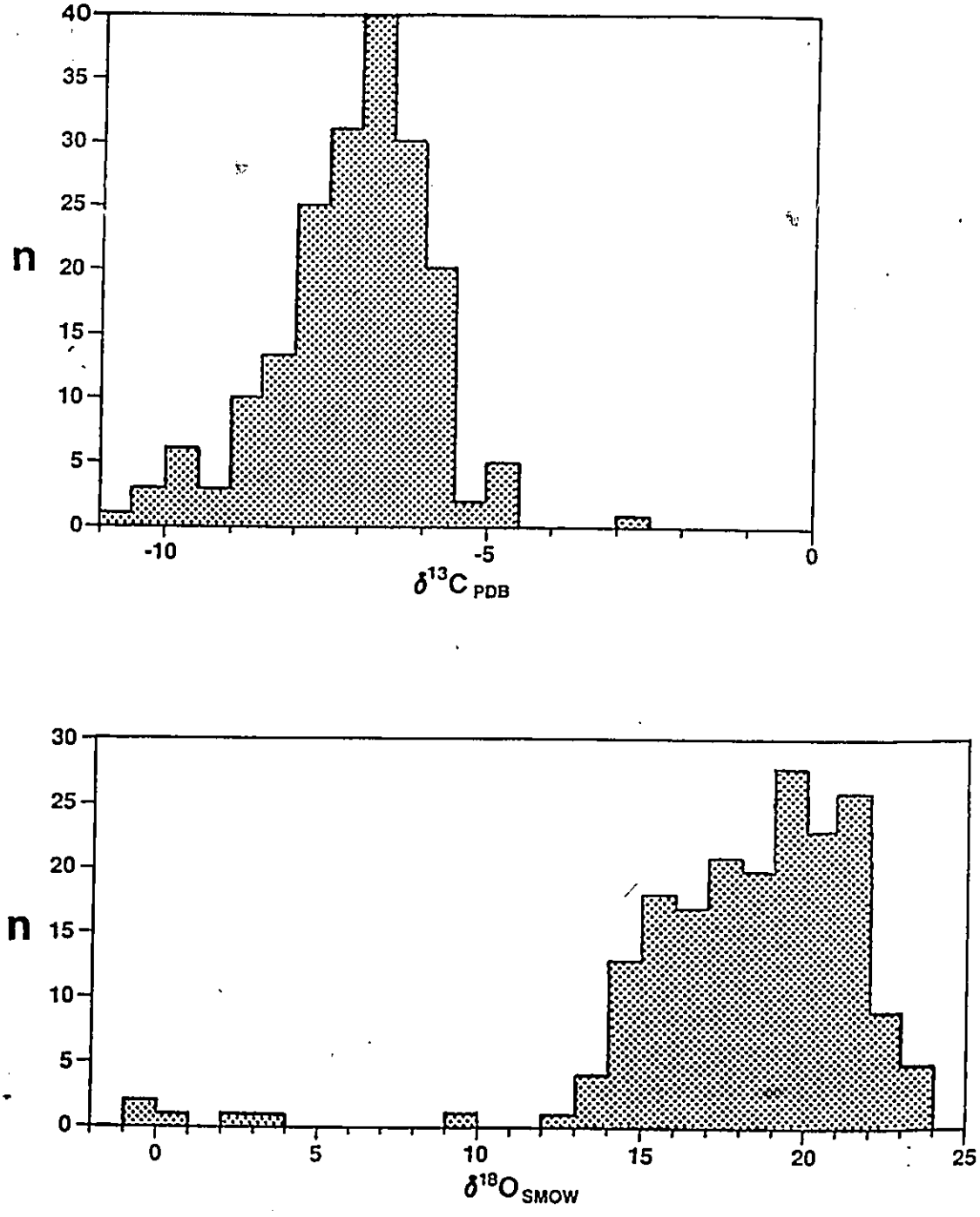


Fig. 26. Histograms of the $\delta^{13}C$ and $\delta^{18}O$ contents of CRNL calcites.

ral calcites are as light as -10°/oo. In contrast the $\delta^{18}O$ contents of the calcites exhibit a broad range with most values falling between 14 and 23°/oo (SMOW). Sealed vein calcites have $\delta^{18}O$ values that are generally <17°/oo. A few samples do not lie within the main population distribution. These calcites are very much lighter in $\delta^{18}O$ with values of about -1 to +9°/oo (SMOW).

The isotopic compositions of all CRNL calcites as a function of borehole depth are shown in Figs. 27 and 28. Most of the samples from CRNL were collected from boreholes CR8 and CR9 and the isotopic compositions of the calcites from only borehole CR-8 are shown in Fig. 29. Isotopic variations in shallow calcites from borehole CR-12 are shown in Fig. 30. Although there is no well defined depth relationship for either $\delta^{18}O$ or $\delta^{13}C$ there is a suggestion that the $\delta^{18}O$ values range over slightly lighter values and the $\delta^{13}C$ values range over slightly heavier values at greater depth. In the case of oxygen this observation might be the result of the slight decrease in the fractionation factor between calcite and water with increasing temperature at depth. In the case of carbon, biogenic $CO_2$ light in $^{13}C$ may be a more important source of calcite C as the soil zone is approached. Alternatively isotopic exchange may be a more important process in the shallow subsurface where rock permeability, and hence water/rock ratios, may be higher than at greater depths. However, the most important observation in these figures is the large variation in values for both isotopes

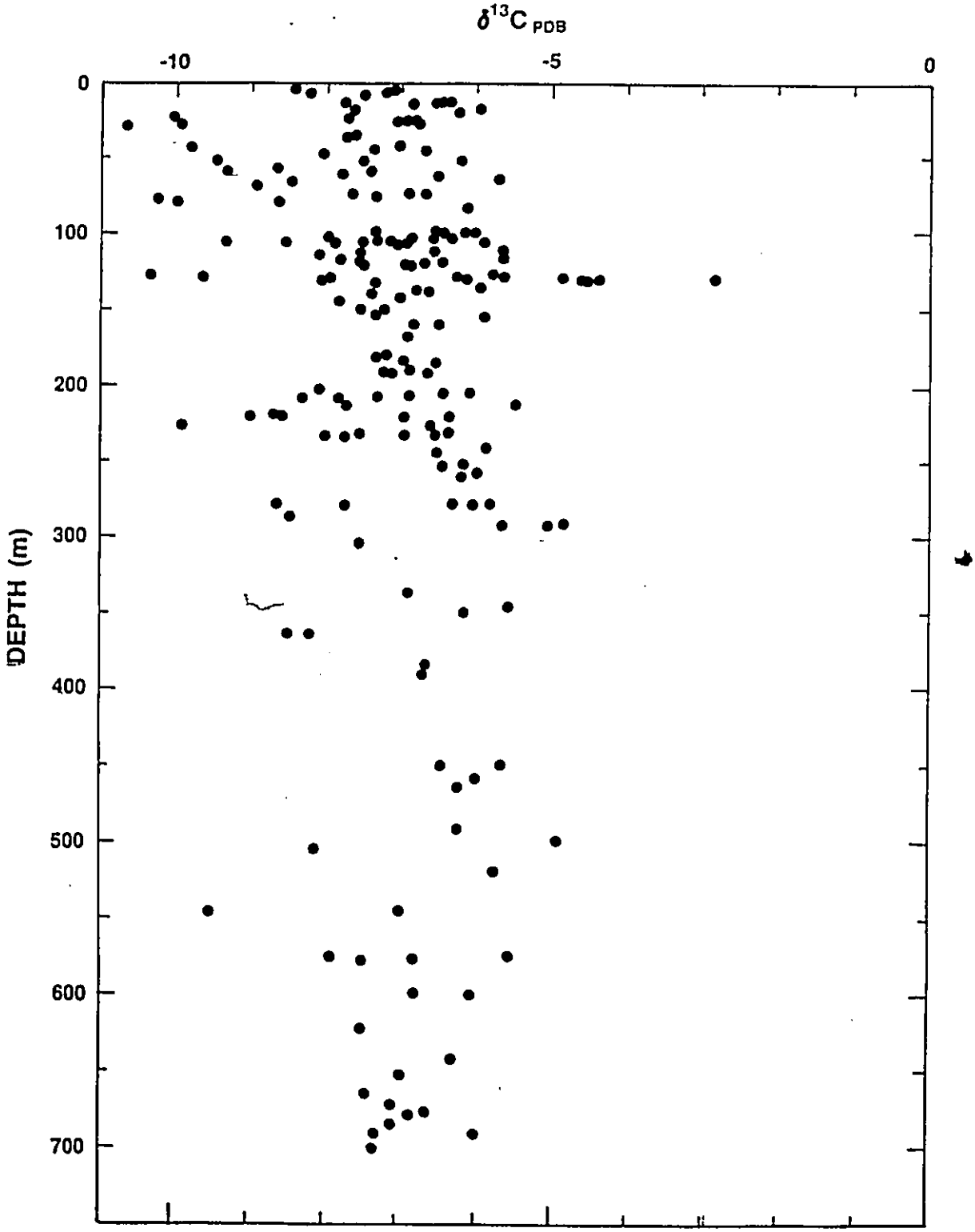


Fig. 27. Variations in the $\delta^{13}C$ contents of CRNL calcites with borehole depth.

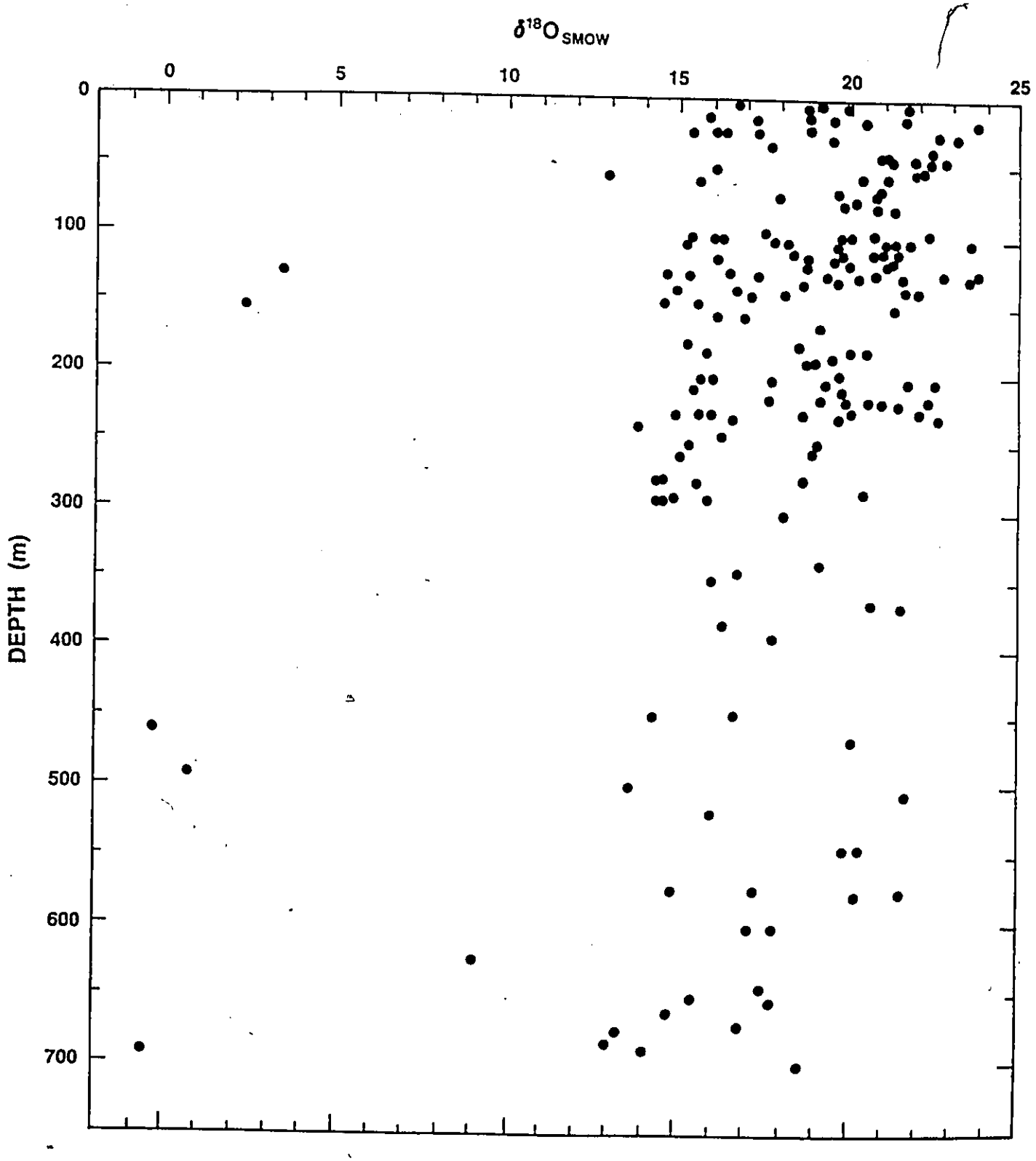


Fig. 28. Variations in the $\delta^{18}O$ contents of CRNL calcites with borehole depth.

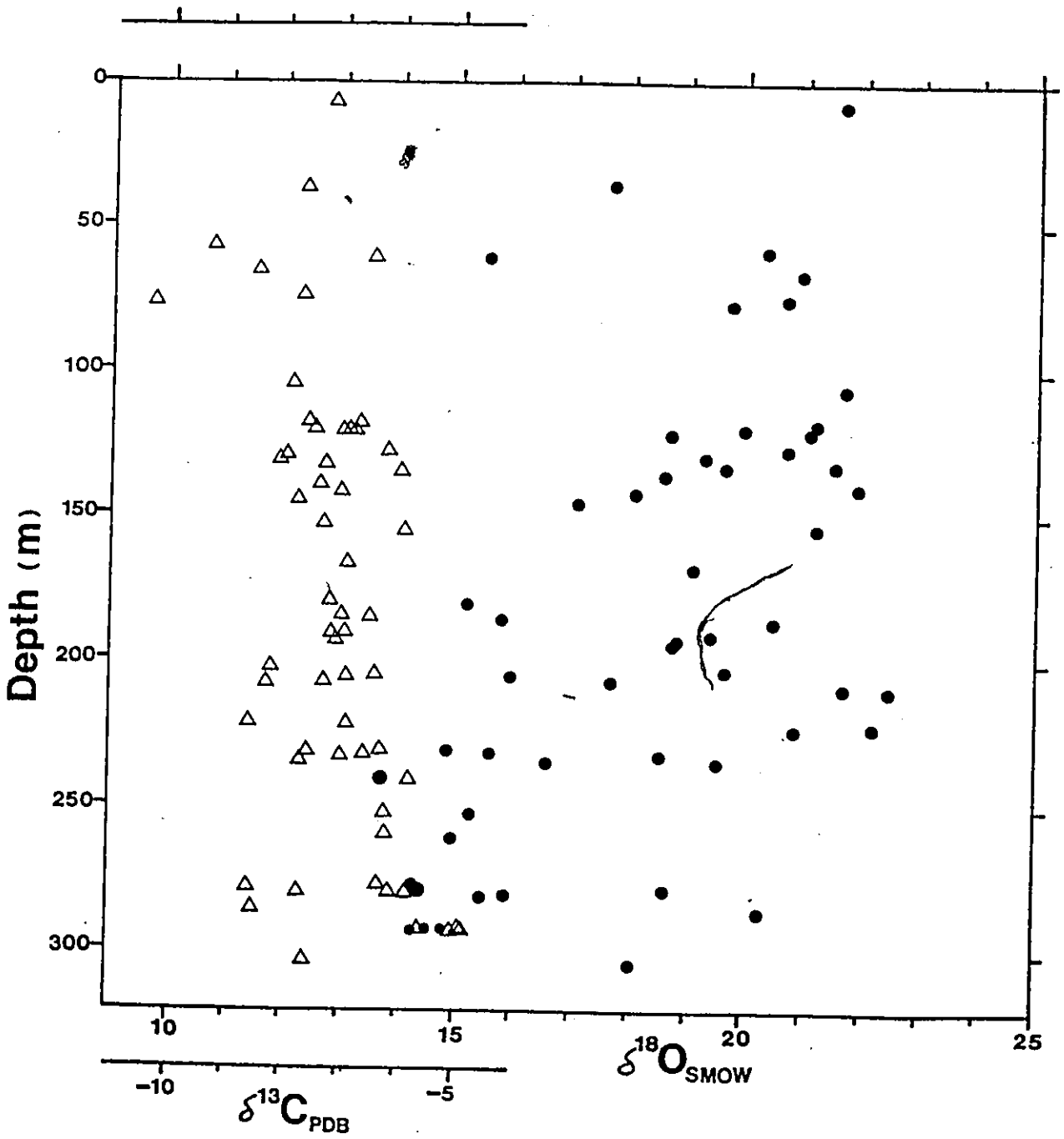


Fig. 29. Variations in the $\delta^{13}C$ (triangles) and $\delta^{18}O$ (solid dots) contents with depth of calcites from CRNL borehole CR8.

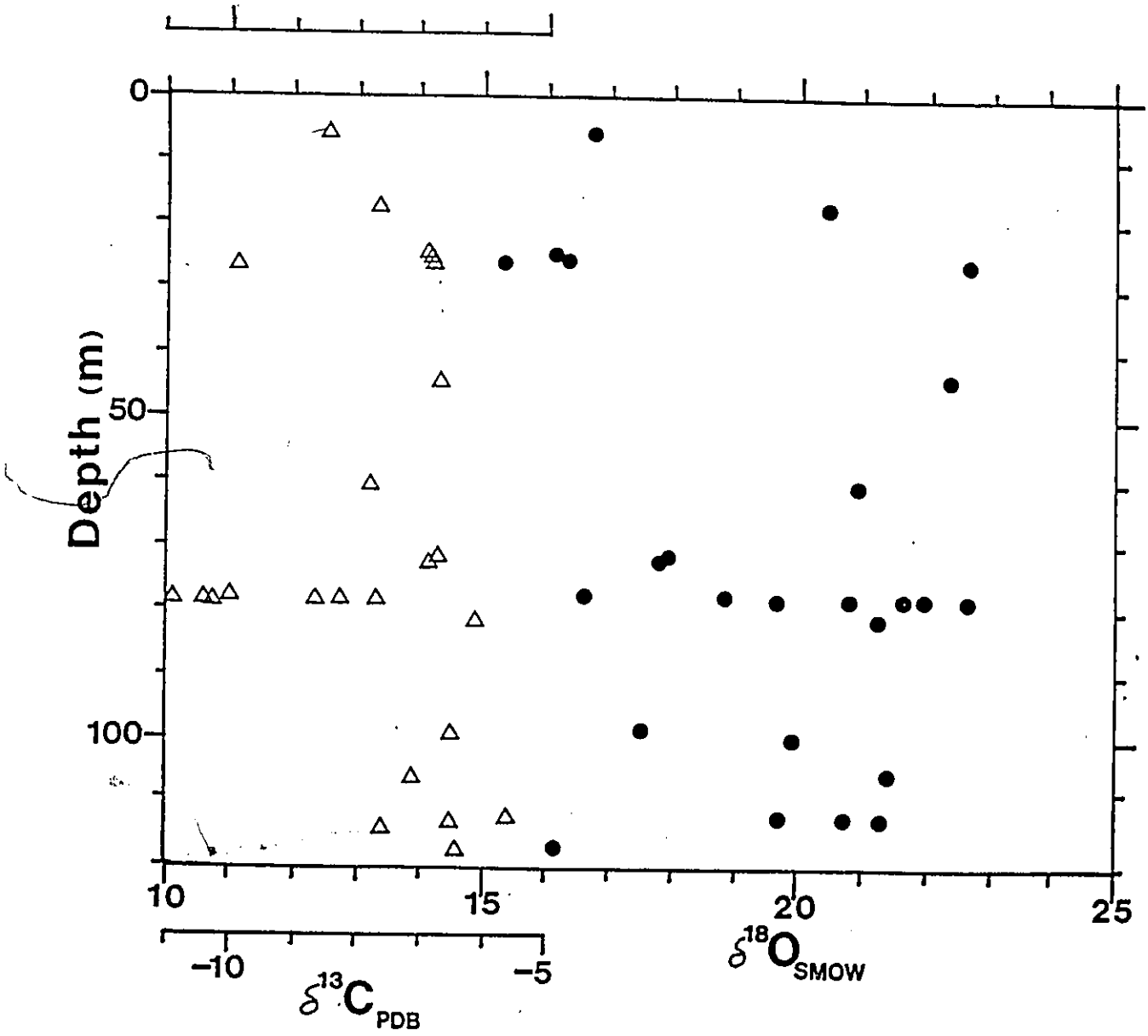


Fig. 30. Variations in the $\delta^{13}C$ (triangles) and $\delta^{18}O$ (solid dots) contents with depth of calcites from CRNL borehole CR12.

at any specific depth. Not only are there large isotopic variations between closely spaced fractures, there are also large variations within individual fractures. These intra-fracture variations are of two types: a) variations perpendicular to the plane of the fracture as the result of the precipitation of younger generations of calcite over older calcite, and b) variations within one calcite generation along the plane of the fracture.

An example of the first type of intra-fracture isotopic variation occurs in an open fracture at a depth of 574.3 m in borehole CR-9. Two generations of texturally distinct calcite in this fracture are evident both in transmitted light under the petrographic microscope and by cathodoluminescence (Plate XX). The older, massive calcite next to the gneiss host rock has a $\delta^{18}O$ of 14.8°/oo (SMOW) and a $\delta^{13}C$ of -5.6°/oo. The thin calcite layer overlying the massive calcite has a $\delta^{18}O$ of 21.5°/oo and a $\delta^{13}C$ of -7.9°/oo. The difference in isotopic composition of these two calcites in conjunction with the previously described chemical differences revealed by electron microprobe analyses and cathodoluminescence microscopy strongly suggests that these two generations of calcite formed at different times under different physicochemical conditions.

An example of the second type of intra-fracture variability occurs over a distance of about 25 cm in a sub-vertical fracture at a depth of 77 m in borehole CR-12. Calcite occurs in this fracture as a fine-grained, semi-continuous layer less

than 1 mm thick. The $\delta^{18}O$ of the calcite over this 25 cm section of the fracture varied by 6°/oo (16.6°/oo to 22.6°/oo) and the $\delta^{13}C$ by 3.2°/oo (-7.7°/oo to -10.9°/oo). It is clear from these complex, small scale inter- and intra-fracture isotopic variations that this feature is unlikely to have been produced by fluid mixing during a single hydrothermal event. Rather, I believe, the isotopic variation is the result of calcite recrystallization in meteoric ground waters and under variable water/rock ratios. This is discussed in detail in a later section.

## 6.4 FACTORS RESPONSIBLE FOR VARIATIONS IN THE CHEMICAL AND ISOTOPIC COMPOSITIONS OF CHALK RIVER CALCITES

Factor analysis with varimax rotation was employed to determine whether there were identifiable factors controlling the variations in the chemical and isotopic compositions of CRNL fracture calcites. The results of this analysis are shown in Table 15 which includes an interpretation of the nature of each factor.

The strong loading of Mg, Fe and Mn on factor 1, which accounts for 34.9% of the total variance, may represent variability in the concentrations of these elements in the original hydrothermal fluid. The scatter diagram of Mg vs. Fe (Fig. 31)

Table 15. Varimax rotated factor analysis of ORNL fracture calcites.

| | Factor 1 | Factor 2 | Factor 3 | Communality |
|---|---|---|---|---|
| $\delta^{13}C$ | 0.20992 | -0.81080 | -0.02937 | 0.70233 |
| $\delta^{18}O$ | 0.53847 | 0.61733 | -0.24164 | 0.72944 |
| log Ca | -0.12050 | 0.07135 | -0.78811 | 0.64073 |
| log Mg | 0.79504 | -0.01982 | 0.41804 | 0.80723 |
| log Na | 0.20061 | 0.14216 | 0.81040 | 0.71720 |
| log Mn | 0.88915 | 0.12458 | -0.06957 | 0.81094 |
| log Fe | 0.74073 | 0.23369 | 0.51309 | 0.86654 |
| log Sr | 0.07965 | 0.54447 | 0.34337 | 0.42070 |
| log Al | -0.43722 | 0.44261 | 0.69414 | 0.86889 |
| log I.R. | 0.19201 | 0.57497 | 0.36022 | 0.49722 |
| Depth | -0.28278 | -0.76833 | 0.04272 | 0.67212 |
| Eigenvalue | 3.83598 | 2.07813 | 1.81923 | |
| Per cent of variation explained | 34.9 | 18.9 | 16.5 | |
| Interpretation | high temperature water/rock interactions | low temperature calcite recrystallization & water/rock interactions | leaching of insoluble residue | |

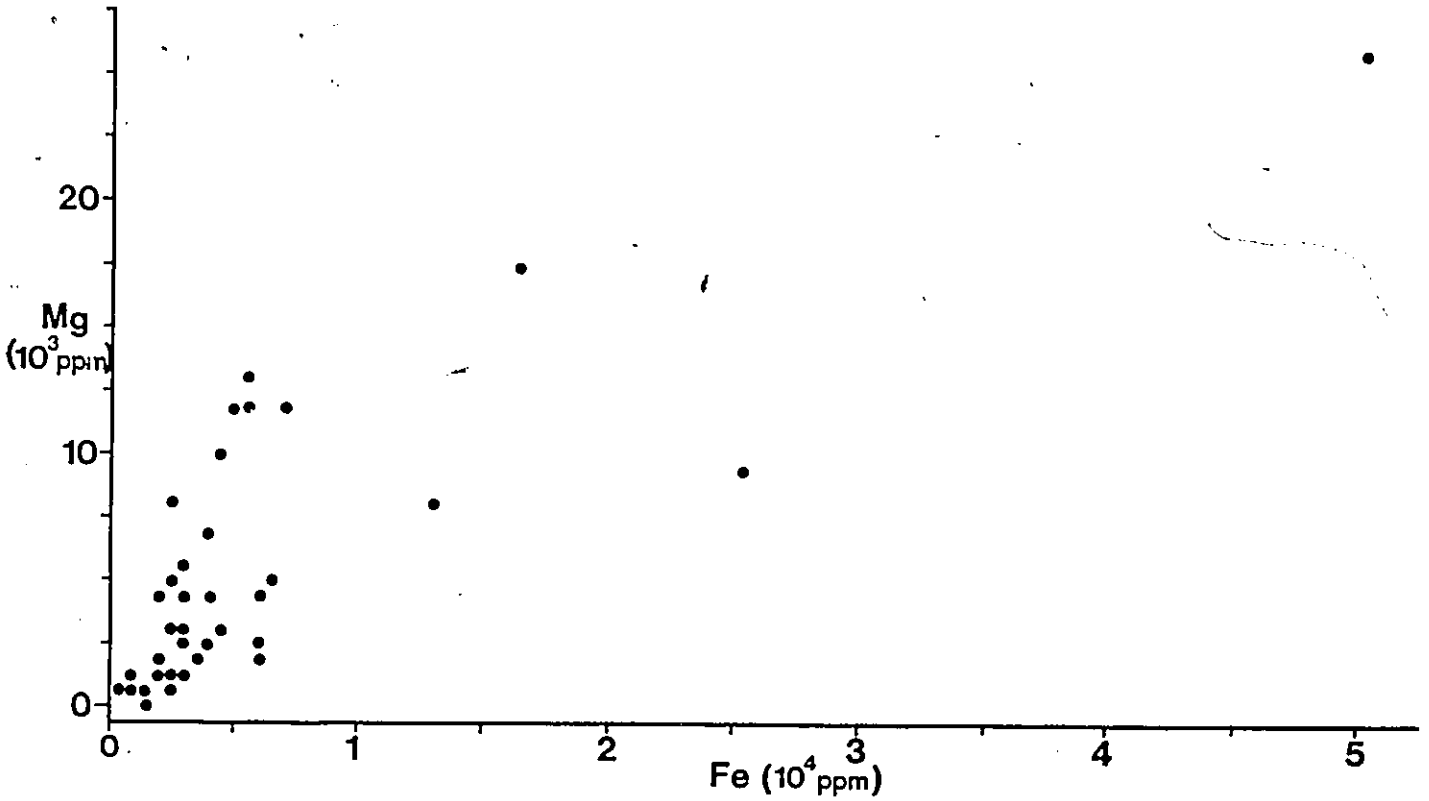


Fig. 31. Scatter diagram of Mg vs. Fe for CRNL fracture calcites.

shows a positive correlation between these two elements. A similar relationship exists between Mn and Mg or Fe. Accordingly factor 1 is interpreted as representing high temperature chemical interactions between hydrothermal fluids and the host rocks near the fractures. Depending on the water/rock ratio of individual fracture pathways, fluid chemistry may have been quite variable and strongly influenced by the composition of the local lithology (i.e., monzonites, granitic pegmatites, diabase, etc.). Indeed the previously presented microprobe analyses have clearly shown that the fluid composition in some fractures was not uniform during the precipitation of fracture calcite. It is also likely that the Mg and Fe content of the calcite was in part determined by the effectiveness of the previously formed fracture chlorite to fix these two elements as they were released to solution from the host rocks. The moderate loading of $^{18}O$ on this factor may indicate that isotopic exchange between the hydrothermal fluid and host rocks also occurred. This is discussed further in the following section.

Factor 2 is believed to represent low temperature water/rock interactions and calcite recrystallization. This is suggested by the antithetic loading of $^{18}O$ with $^{13}C$ and depth on this factor. Because permeability generally decreases with depth, calcite recrystallization should be more extensive at shallow depths. Low temperature recrystallization of hydro-

thermal calcite will result in an $^{18}O$ shift to more positive values. This is investigated more thoroughly in section 7.2.

Unlike the $\delta^{18}O$ values, $\delta^{13}C$ values of recrystallized calcites will tend to be shifted to more negative values (particularly at shallow depths) because of incorporation of biogenic carbon dissolved in the ground water. The loading of Sr on this factor is probably due to the relatively large $Sr^{2+}/Ca^{2+}$ mole ratios in the CRNL ground waters, particularly the $Na/HCO_3$ type. The scatter diagram of Sr concentration vs. $\delta^{13}C$ (Fig. 32) shows that $^{13}C$-rich hydrothermal calcite is characterized by low and relatively uniform Sr concentrations whereas recystallized calcite tends to have more variable but generally higher Sr contents. Although the large $Sr^{2+}/Ca^{2+}$ ratios of the ground water are primarily controlled by calcite recystallization, silicate dissolution is another source of ground water $Sr^{2+}$ as shown by the slightly more radiogenic isotopic composition of the ground water relative to the calcites (Table 14). The negative loading of depth on this factor suggests these water/rock interactions are most important at shallow depths. Moreover, because kaolinite is a probable product of these interactions (Fig. 7-10) the loading of insoluble residue on this factor suggests that water/rock interactions and calcite recrystallization are not totally independent processes and that they are spatially related.

Factor 3 may represent leaching of the insoluble residue as suggested by the strong loading of Na and Al on this

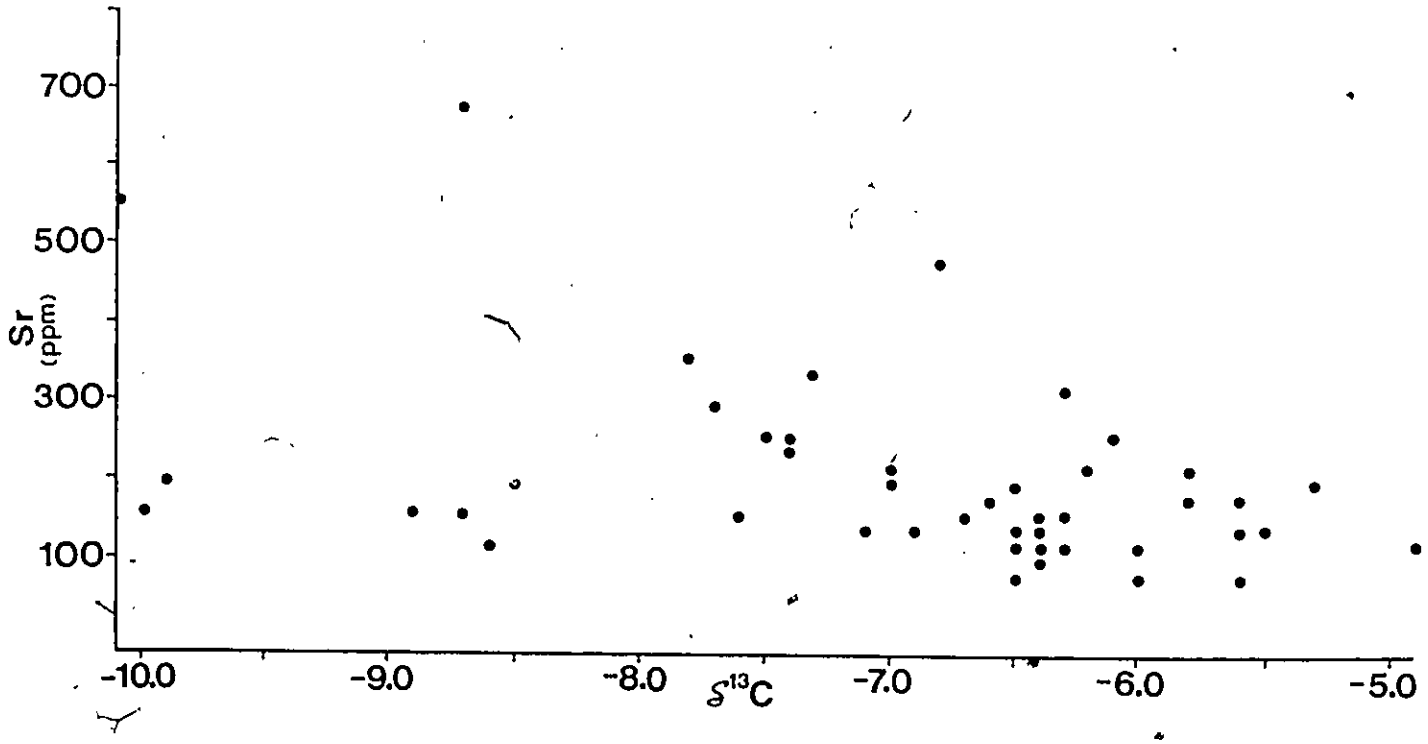


Fig. 32. Scatter diagram of Sr vs. $\delta^{13}C$ for CRNL fracture calcites.

factor and the complementary antithetic loading of Ca. Accordingly, Na concentrations in the calcites may be even lower than that shown in Fig. 19.

In summary it appears that two processes have been primarily responsible for most of the variability in the chemical and isotopic compositions of CRNL fracture calcites. High temperature water/rock interactions have controlled the magnitude of and the variability in the concentrations of Mg, Fe, and Mn in the hydrothermal calcites. Low temperature calcite recrystallization is responsible for the shifts in isotopic compositions and, in conjunction with water/rock (silicate) interactions, for the prevention of Sr depletion in calcite by maintaining a high $Sr^{2+}/Ca^{2+}$ mole ratio in solution.

# 7.0 ORIGINS OF CHALK RIVER FRACTURE CALCITES

## 7.1 CONDITIONS OF HYDROTHERMAL MINERAL FORMATION

The presence of laumontite with some of the calcites that have the lightest $\delta^{18}O$ values provides some geochemical constraints on the conditions in which this small group of light $^{18}O$ calcites formed. Laumontite is stable only at temperatures of less than 300°C and pressures of less than about 3 kb (Liou, 1971) and therefore the co-existing calcite must also have formed under these conditions. Furthermore laumontite will only form when the mole fraction of $CO_2$ in the fluid phase is low, <0.01 at 2 kb pressure (Thompson, 1971). The coexistence of laumontite and calcite in the same vein suggests a rapidly changing fluid composition during the precipitation of these minerals. In the case of the fracture infilling shown in Plate VIII the fluid composition must have changed with time from "$CO_2$-poor" to "$CO_2$-rich". Such conditions could occur in highly permeable zones that initially allowed large convectively-driven influxes of meteoric water through the fractures. If the C in the calcites was derived from a deep-seated $CO_2$ source then the initial convection of meteoric water into these zones could dilute the mole fraction of $CO_2$ to low enough values to enable laumontite precipitation. Fracture mineral formation would subsequently reduce fracture permeability and ground water flow rate possibly allowing the mole fraction of $CO_2$ to rise sufficiently to precipitate calcite.

If the above scenario is essentially correct then the lightest $^{18}O$ calcites may have formed from a hydrothermal fluid of meteoric origins that was not significantly affected by $^{18}O$ exchange with the host gneisses. Grenville basement gneisses generally have $\delta^{18}O$ values in the range of 6-9°/oo (see summary of Wu and Kerrich, 1986) and thus have the potential to shift meteoric hydrothermal fluids to more positive values. The calcite from 459.98 m in CR-9 has a $\delta^{18}O$ of -0.4°/oo. At 300°C the $^{18}O$ fractionation factor between calcite and water is about 5.5°/oo which means this calcite precipitated from ground water that was no heavier than -6°/oo. Because meteoric water is the only volumetrically important water type with a $\delta^{18}O$ of less than 0°/oo it can be reasonably concluded that meteoric water was a major component of the hydrothermal fluid. If the calcite-laumontite pair actually precipitated at 200°C then the $\delta^{18}O$ of the fluid was about -9°/oo.

Most of the apparently unaltered hydrothermal calcites have $\delta^{18}O$ values of 13 to 17°/oo. If these calcites formed from an unshifted meteoric hydrothermal fluid with a $\delta^{18}O$ of -6°/oo or less, then formation temperatures are constrained to <~100°C. The existence of the light $^{18}O$ calcite group, however, suggests that the heavier hydrothermal calcite may have formed from fluids richer in $^{18}O$ than -6°/oo. Such fluids could be produced by $^{18}O$ exchange with the gneisses under relatively low water/rock ratios. It is possible that both lower temperatures (retrograde exchange) and differences in fluid isotopic compositions

are responsible for the heavier hydrothermal calcites but it is not possible to determine which of the two was dominant.

The upper pressure boundary of 3 kb for the stability of laumontite corresponds to a depth of about 11 km if it is assumed fluid and lithostatic pressures are approximately equal. This can be compared to a burial depth of about 18 km during metamorphism based on pressure estimates of Dugal and Kamineni (1987). Hence the hydrothermal event responsible for laumontite formation occurred sometime after these rocks were uplifted to a depth of less than 11 km following metamorphism. If a cooling rate of 8°C $Myr^{-1}$ is realistic for the Grenville Province following metamorphism (Baer, 1981) then the required uplift of 11 km could have been achieved within 55 Myr of commencement. Accordingly hydrothermal vein formation at CRNL could have followed rather closely on the heels of metamorphism. Strontium isotopic data suggest, however, that the hydrothermal calcite formed at least 300-400 Ma after the peak in metamorphism indicating a late Proterozoic or younger age for these calcites.

The $\delta^{13}C$ values of the hydrothermal calcites show relatively little variation and are generally near -5 to -6°/oo. Mantle $CO_2$ is generally believed to have a $\delta^{13}C$ value of between -5 and -8°/oo (Javoy et al., 1986). Hydrothermal calcites that have precipitated in isotopic equilibrium with mantle C may exhibit a wide range in $\delta^{13}C$ values depending on the temperature, pH and $f_{O_2}$ of the hydrothermal solution (Ohmoto, 1972) and resulting in some uncertainty as to their origins and the $\delta^{13}C_{\Sigma C}$ of the parent solution. The relatively uniform and moderately

negative $\delta^{13}C$ values of the CRNL calcites, however, leave little doubt that the $\delta^{13}C_{\Sigma C}$ was very similar to that of the calcites themselves. This strongly suggests that mantle $CO_2$ was the source of C for the fracture calcites. Nevertheless there are some calcites that have much lighter $\delta^{13}C$ values than $-6^{o}/oo$. As will be discussed below this is believed to reflect relatively recent contributions (through recrystallization) of C derived from the isotopically light soil $CO_2$ reservoir which has been subsequently dissolved and partitioned amongst inorganic C species (primarily $HCO_3^-$) in the ground water.

The differences in both the $\delta^{18}O$ and $\delta^{13}C$ values of the calcite and dolomite components of carbonates can be used to estimate the temperature of formation of these minerals (Northrop and Clayton, 1966; Sheppard and Schwarcz, 1970; Matthews and Katz, 1977). This assumes, of course, that the dolomite and calcite are in isotopic equilibrium. The fractionation of $^{18}O$ and $^{13}C$ between metamorphic dolomite and calcite has been calibrated against the Mg-calcite solvus geothermometer over a temperature range of 100-600°C by Sheppard and Schwarcz (1970) who derived the following isotopic relationships:

$$(19) \qquad 10^3 \ln \alpha^{18}_{Do-Cc} = 0.45\ (10^6\ T^{-2}) - 0.40$$

$$(20) \qquad 10^3 \ln \alpha^{13}_{Do-Cc} = 0.18\ (10^6\ T^{-2}) + 0.17$$

Matthews and Katz (1977) have investigated the $^{18}O$ fractionation during hydrothermal dolomitization of $CaCO_3$ at temperatures of 252-295°C and have observed low fractionation values of $\leq 1^{o}/oo$ in this temperature range. This fractionation has been defined by the equation:

$$(21) \qquad 10^3 \ln \alpha^{18}_{Do-Cc} = 0.28\ (10^6\ T^{-2}) - 0.18$$

Temperatures of formation for the CRNL calcite-dolomite pairs have been calculated using equations 19-21 and are listed in Table 16. These samples were selected for isotopic analysis of both minerals on the basis of X-ray diffractograms which confirmed or suggested the presence of dolomite in the carbonate. Large variations in formation temperatures of 236-490°C and 315-528°C are calculated by the $^{18}O$ fractionation relationships of Matthews and Katz (1977) and Sheppard and Schwarcz (1970), respectively. With the exception of sample CR3-130 m the dolomite content of these samples is quite low which probably precludes high precision ($0.1^{o}/oo$) analysis of the dolomite component by this method (Walters et al., 1972). However, widely varying isotopic temperatures for the dolomite-calcite pair are not unusual (Sheppard and Schwarcz, 1970; Taylor and Bucher-Nurminen, 1986). Oxygen isotope temperatures calculated by the fractionation relationship of Northrop and Clayton (1966) are significantly higher than those listed in Table 16 and are considered unreasonable for these calcites when it is considered that laumontite has been observed in some fractures. The same is true for the C isotope temperatures in Table 16.

Table 16. Isotopic fractionations and temperatures (°C) for CRNL dolomite-calcite pairs

| Borehole and Depth (m) | $\Delta^{18}O$ (°/oo) | $\Delta^{13}C$ (°/oo) | $T^{1}_{18_O}$ | $T^{2}_{18_O}$ | $T^{1}_{13_C}$ | Wt % calcite | Wt % dolomite |
|---|---|---|---|---|---|---|---|
| CR2 - 127.90 | 0.3 | 0.3 | 490 | 528 | 904 | 74.9 | 5.0 |
| CR2 - 129.43 | 0.4 | 0.6 | 422 | 477 | 374 | 60.4 | 18.8 |
| CR3 - 130.13 | 0.9 | 0.3 | 236 | 315 | 904 | 31.4 | 56.5 |
| CR8 - 204.94 | 0.8 | -0.1 | 262 | 339 | - | 81.7 | 8.4 |
| CR8 - 205.05 | 0.3 | 0.2 | 490 | 528 | - | 59.8 | 16.2 |

1 Calculated from equations of Sheppard and Schwarcz (1970)

2 Calculated from equations of Matthews and Katz (1977)

Electron microprobe analyses were conducted on the calcite and dolomite components of sample CR3-130 m in order to determine whether the Mg-calcite solvus geothermometer of Goldsmith and Newton (1969) agreed with any of the isotopic temperatures. This sample, shown in Plate VI(b), consists of carbonate surrounding highly altered rock fragments in a brecciated fault zone. Cathodoluminescence spectroscopy of the sample shows that most of the calcite is present as vug infillings in dolomite (Plate XXII). The outer portions of dolomite crystals projecting into the vugs appear more luminescent than the core of the crystals suggesting that the transition from dolomite to calcite precipitation was rapid. Seven microprobe analyses of one such calcite vug (Table 9) show that the Mg concentration of the calcite is not uniform as points near the contact with the dolomite (P1, 2 and 7) are low in Mg compared to interior portions of the vug which average 1.31 mole % $MgCO_3$.

The Mg-calcite solvus equation is (Goldsmith and Newton, 1969):

$$(22) \quad X_{Mg} = \exp(0.847-3091/T) + (P-1)(0.17\times10^{-8}T - 0.33\times10^{-6})$$

where X = mole fraction of Mg in calcite

T = temperature in °K

P = pressure in bars

Substituting the average Mg concentration of 1.3 mole % $MgCO_3$ into this equation yields a temperature of about 325°C at atmospheric pressure or 310°C at 3 kb, the probable maximum

pressure at which the hydrothermal calcite could have formed. The iron concentrations in the carbonate are sufficiently low that temperature corrections for Fe (Bickle and Powell, 1977) are small. The Mg-calcite solvus temperature thus agrees well with the isotopic temperature calculated from the $^{18}O$ fractionation relationship of Matthews and Katz (1977), (Table 16). However, this temperature must be viewed with some caution in the absence of a suitable explanation for the low Mg content of the calcite near the dolomite contact which may suggest the dolomite and calcite were not in equilibrium at the time of their formation. Nevertheless, the relatively high dolomite content of sample CR3-130 m probably provides the best opportunity for determining formation temperatures of any of the CRNL fracture carbonates.

A formation temperature of about 300°C for the carbonate infilling in sample CR3-130 m would have considerable significance with regard to the origin of the fluid from which it formed because both the calcite and dolomite components of this sample are relatively rich in $\delta^{18}O$ (20.2 and 21.5°/oo, respectively). At 300°C the fractionation factor between calcite and water is only 5.5°/oo suggesting the $\delta^{18}O$ of the fluid was about 15°/oo (SMOW). The only mechanism by which such an $^{18}O$-rich fluid could be generated is through exchange with $^{18}O$-rich sedimentary rocks such as limestones. Marbles are a major component of the late Proterozoic Grenville Supergroup metasedimentary rocks which may have once covered the gneissic rocks in this

area (Schwerdtner and Lumbers, 1980). Lower Paleozoic carbonate rocks were also deposited in the Chalk River area. In either case meteoric waters circulating through such rocks in a hydrothermal convective flow system could have their $\delta^{18}O$ values shifted to much more positive values through exchange with carbonate rocks. Accordingly it appears that either two hydrothermal events are recorded in the isotopic compositions of CRNL fracture calcites, or the isotopic composition of the hydrothermal water during a single event was highly variable.

It should be noted that boreholes CR2 and CR3 shown in Fig. 4 were drilled to intersect the major east-northeast trending fault that cuts through Upper Bass Lake (see Fig. 3). This is a younger fault that cross cuts the predominant northwest trending faults in this area (Brown et al., 1982). Therefore, the $^{18}O$-rich fluid that apparently was present in this fault zone either did not infiltrate the fracture zones intersected by the other boreholes or it mixed with hydrothermal water that had retained its meteoric isotopic signature. The former alternative is favoured if a second hydrothermal event occurred shortly after the hydrothermal event which was responsible for most of the vein calcite at CRNL. The latter scenario is possible depending on the geology and topography of the area during the event because the juxtaposition of silicate and carbonate rock fluid pathways offers the possibility of hydrothermal meteoric waters with very different isotopic compositions. However, the restriction of these $^{18}O$-rich fracture calcites

(which are also $^{13}C$-rich) to the east-northeast trending fault argues for a second hydrothermal event that resulted in infiltration of $^{18}O$-shifted meteoric waters primarily through younger cross faults.

The common occurrence of calcite filling chlorite-lined fractures indicates a major change in fluid chemistry during the formation of these two minerals. Formation of the $Mg(OH)_2$ component in chlorite results in an acidic hydrothermal solution (Bischoff and Dickinson, 1975) yet the precipitation of calcite indicates a return to alkaline conditions. The common presence of quartz in the calcite veins suggests that although a decrease in fluid temperature could be responsible for quartz precipitation it could not by itself be responsible for the calcite because of the antithetic solubility-temperature relationships of these two minerals.

Hydration and/or carbonation reactions between wall rock silicate minerals and hydrothermal solutions are commonly invoked to explain the formation of vein calcite (Kerrich and Fyfe, 1981). While fluid/rock interactions were undoubtedly important in the precipitation of the hydrothermal calcites, the principal mechanism responsible for calcite precipitation may have been $CO_2$ degassing from a cooling, ascending hydrothermal fluid. Provided the ascent of the fluid was not extremely rapid $CO_2$ separation could occur without boiling of the fluid. Such a mechanism is feasible if the $CO_2$ source was the deep crust or upper mantle where the $CO_2$ would be present with $H_2O$ as a

supercritical fluid. Cooling of the fluid and mixing with meteoric water, possibly in a convectively-driven flow system associated with incipient rifting of the Ottawa River valley, would cause $CO_2$ immiscibility at pressures greater than the vapour curve of water (Takenouchi and Kennedy, 1964; Bowers and Helgeson, 1983). Continued cooling to temperatures of less than 300°C would decrease the mole fraction of $CO_2$ in the liquid phase which could result in calcite precipitation.

An alternative mechanism of $CO_2$ degassing and the one favoured here on the basis of textural and structural evidence (Plates II-VII), involves hydraulic fracturing of fracture pathways that became sealed primarily through the precipitation of quartz and other silicates. This process as described by Hedenquist and Henley (1985) and Nelson and Giles (1985) involves fluid boiling and degassing as the fluid pressure is relieved following fracturing. This mechanism results in brecciation of infilling materials and adjacent wallrock, calcification of lithic fragments in the breccia as well as in porous country rock which was permeated by a $CO_2$-rich vapour phase, and rapid calcite precipitation surrounding angular breccia fragments and overlying rough, angular fracture surfaces. All these features have been observed in the Chalk River core suggesting hydraulic fracturing may have been an important process responsible for vein calcite formation.

## 7.2 MODEL OF THE ISOTOPIC EVOLUTION OF FRACTURE CALCITES

Carbon and oxygen isotopic compositions of the CRNL calcites vary antithetically but the curvature of the trend is poorly constrained (Fig. 33). The shaded box in this figure outlines the expected maximum variation in the isotopic composition of calcite that could form in isotopic equilibrium with the $\delta^{18}O$ and $\delta^{13}C_{DIC}$ of the present day CRNL ground waters (Table 2) to depths of at least 500 m. The boundaries of this box are based on a 3°/oo variation in the ground water $\delta^{18}O$ (-10.5°/oo to -13.5°/oo), a 2.2°/oo variation in the $\delta^{13}C$ of the dissolved inorganic C which is predominantly bicarbonate (-13.8 to -16°/oo), and isotopic fractionation factors from eq. 9 for measured ground water temperatures of 8-20°C (Bottomley et al., 1984). Although many of the calcites are in apparent equilibrium with $\delta^{18}O$ of the present day ground waters, all of the calcites are significantly heavier in $\delta^{13}C$ (with one exception) than the calculated equilibrium range.

Although fluid boiling may have been an important factor in the precipitation of hydrothermal calcite, it can not explain the observed carbon-oxygen isotopic trend. Because $CO_2$ is markedly enriched in $^{18}O$ relative to coexisting water and slightly enriched in $^{13}C$ relative to calcite at temperatures greater than 200°C (Bottinga, 1968), progressive $CO_2$ loss from a hydrothermal fluid will result in a trend toward calcites that are significantly lighter in $^{18}O$ and slightly lighter in $^{13}C$. Such a positive correlation in the isotopic compositions of the calcites is not observed.

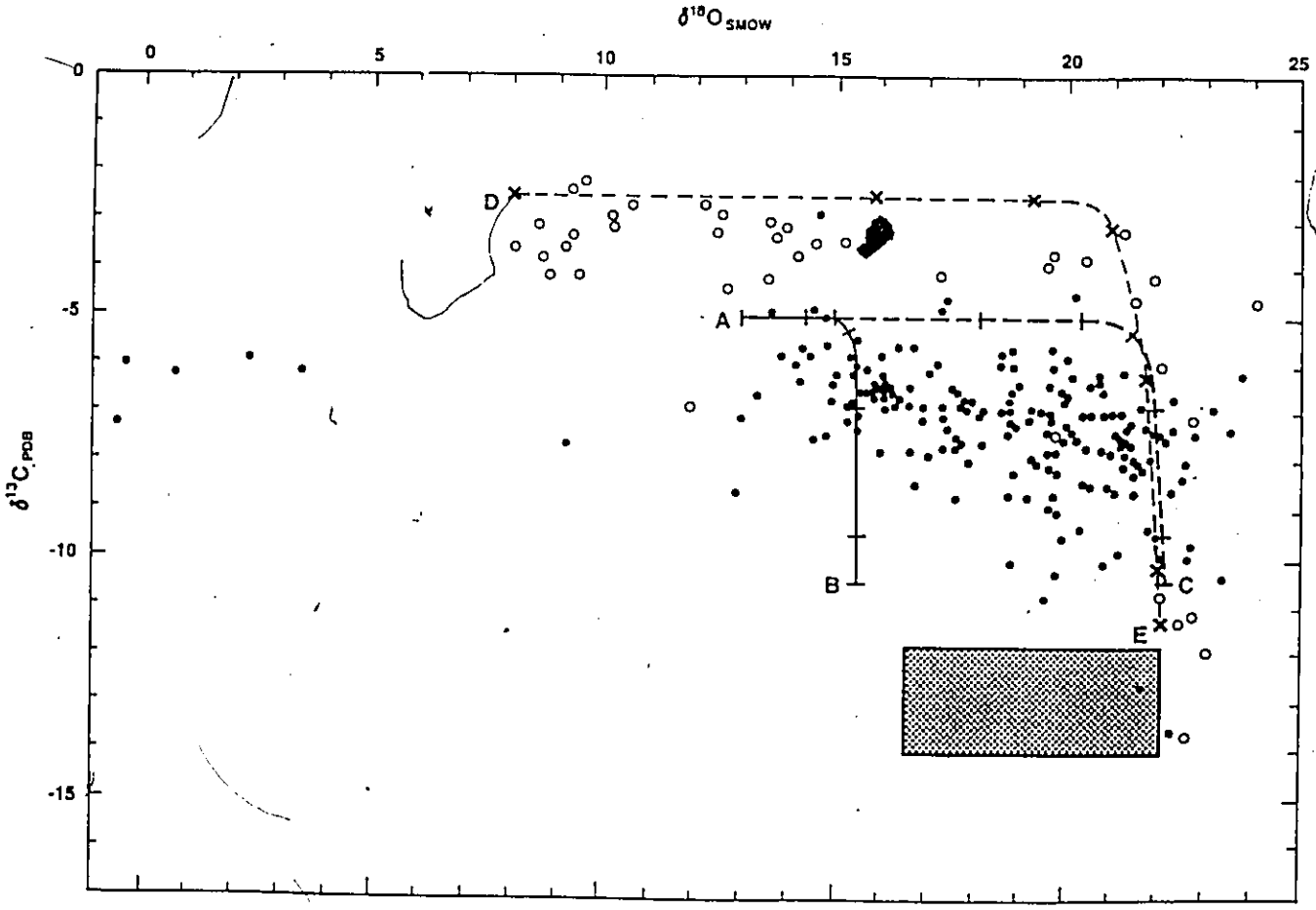


Fig. 33. Plots of $\delta^{13}C$ vs. $\delta^{18}O$ of CRNL (solid dots) and EBL (open circles) calcites. Curves AB and AC show the isotopic evolution of CRNL hydrothermal calcite, having a composition represented by point "A", during its recrystallization in meteoric water with a $\delta^{18}O$ of -14°/oo (AB) or -10°/oo (AC). Curve DE shows the isotopic evolution for EBL hydrothermal calcite having an initial composition represented by point "D" during its recrystallization in meteoric water with a $\delta^{18}O$ of -10°/oo. Tick marks on the CRNL curves and crosses on the EBL curve show the isotopic composition of the calcite when time-integrated closed system water/rock mole ratios of 10, $10^2$, $10^3$, $10^4$, $5x10^4$ and $10^5$, respectively, are attained (see text for further details).

The isotopic trend in Fig. 33 could be produced by one of three mechanisms:

1) mixing of hydrothermal fluids with cool, isotopically light meteoric waters at the time of calcite precipitation,
2) precipitation of recent calcite in equilibrium with the present day ground waters onto ancient hydrothermal calcite lining reactivated fractures, or
3) low temperature recrystallization of a low $^{18}O$, hydrothermal calcite under variable water/rock ratios.

Mixing of hydrothermal and meteoric fluid could produce a hyperbolic trend in the $\delta^{13}C$ and $\delta^{18}O$ relationship. The curvature of this mixing trend would be determined by the relative concentration of C in the two end members (Langmuir et al., 1978). However, a fluid mixing model by itself would be difficult to reconcile with the variabililty in calcite textures and with the fine-scale inter- and intra-fracture differences in isotopic composition. Moreover, fitting a mixing model to the data would imply that the calcites are coeval and that no subsequent isotopic alteration has occurred to them over several hundred million years. This requirement seems unreasonable in light of the high degree of fracturing of the rock and the apparent "openess" of the system to the infiltration of recent, meteoric waters (Raven, 1986).

Since the CRNL ground waters at relatively shallow depths are supersaturated with respect to calcite it might be

expected that recent calcite precipitation could occur as a thin layer on a passive hydrothermal calcite substrate without involving solution and reprecipitation of the older calcite. Calcite sampling at such a site would produce a mixed sample of two discrete calcite generations. While this mechanism can not be totally discounted it is incapable of explaining the origin of samples that are rich in $^{18}O$ and in equilibrium with the ground water $^{18}O$ but in disequilibrium with the ground water $\delta^{13}C_{DIC}$. This suggests that calcite precipitation occurs only after solution of a precursor fracture calcite at a thin microlayer near the calcite-water interface. This is consistent with U and Th isotopic measurements of fracture calcites from the CRNL site and elsewhere which show that U in a recrystallized outer layer often has a younger residence time than the U of the bulk sample (Milton and Brown, 1987). For example, the outer recrystallized layer of a fracture calcite from 250 m in CR13 was found to have mean age of 47,300 years compared to 152,800 years for the bulk sample.

The isotopic trend in Fig. 33 can be most simply explained by invoking the recrystallization of a hydrothermal calcite end member having a $\delta^{18}O$ of 13 to 16°/oo and a $\delta^{13}C$ of -5 to -6°/oo by ground waters with isotopic compositions and temperatures similar to the range in present day values and under variable water/rock ratios. Curves AB and AC show the predicted trends in the isotopic evolution of the original hydrothermal calcite (represented by the composition of point "A") as it recrystallizes under increasing water/rock ratios in

ground waters having $\delta^{18}O$ values of -14°/oo at 20°C and -10°/oo at 8°C, respectively. This combination of $\delta^{18}O$ and temperature values was selected to illustrate the maximum spread in isotopic compositions that could be produced from the range in values for these parameters measured at CRNL. In these calculations it is assumed that the system is open with respect to the ground water and hence to O but closed with respect to C. Obviously this assumption is more valid in the case of water oxygen than C because soil zone C is clearly a major component of the ground water DIC. However, the low bicarbonate concentrations in the CRNL ground waters (0.8-1.6 mM $L^{-1}$) would preclude any significant $^{13}C$ exchange in a totally open C system. This is not compatible with the observed shift to more negative $\delta^{13}C$ values as the $\delta^{18}O$ values increase. For the closed system evolution of the $\delta^{13}C$ values shown by curves AB and AC a bicarbonate concentration of 2 mM $L^{-1}$ with a $\delta^{13}C$ of -14.0°/oo was used in conjunction with a calcite-bicarbonate fractionation factor of 2°/oo. Because of the low bicarbonate concentration oxygen isotope exchange between water and calcite is essentially complete before any significant carbon isotope exchange occurs. Mole ratios of water/rock approaching $10^5$ are required to produce the lightest $\delta^{13}C$ calcites. It is worth noting that water/rock ratios calculated on the basis of O isotope exchange would underestimate the w/r ratios because of the attainment of O isotopic equilibrium (and the cessation of further exchange) at moderate w/r ratios ($10^3$-$10^4$). On the other hand, C isotope exchange continues to much larger w/r ratios because of the low C concentrations in these ground waters.

A system that is open with respect to O but closed to C may be understood by considering the role of diffusion during recrystallization as discussed by Veizer (1978, 1983), Brand and Veizer (1980), and Pingitore (1982). In the context of carbonate diagenesis, Pingitore (1982) made the distinction between physically and chemically open or closed systems and suggested a model whereby the water associated with reaction zones could be isolated, to varying degree, from the bulk solution of the aquifer. According to this model reaction zones are predominantly intragranular micropores that are too small to communicate with the macropore flow except via diffusion. A physically open system is defined in this model as a system that offers the potential for chemical exchange between micropores and macropores whereas a chemically open system obtains when ionic diffusion actually occurs in a physically open system because of the creation of a significant chemical gradient between the two water types. Therefore it is possible to have a reaction site that is chemically open to one element but relatively closed to another depending on the water chemistry.

Although the model of Pingitore (1982) was developed and discussed in terms of the diagenetic stabilization of aragonite in granular porous media the principles are equally applicable to calcite recrystallization in fractured rock. In this case the macropores are the fracture porosity of the bulk rock and the intragranular micropores (in the calcite) are analogous to the diffusion porosity of Norton and Knapp (1977). The rate of diffusion of a solute from the diffusion porosity to the fracture porosity is described by the following equation from Pingitore (1982):

(23) $$\frac{dq}{dt} = D(C_r - C_a)\, A/\ell$$

where $\frac{dq}{dt}$ = the quantity of material that diffuses per unit time

$D$ = diffusion coefficient of the solute

$C_r$ = ionic concentration in the reaction zone (micropore)

$C_a$ = ionic concentration in the aquifer (fracture porosity)

$A$ = effective pore area

$\ell$ = distance from reaction site to fracture porosity.

Because ionic diffusion coefficients in water are very similar the most variable term in the diffusion equation for a given environment is the concentration gradient. Diffusion is only an efficient mechanism for the transfer of ions when a concentration gradient between the reaction site and fracture porosity is maintained.

In the fractured rock at CRNL it is reasonable to assume that the system is physically open and that water in both the fracture and diffusion porosity of the fracture calcites is of recent meteoric origins with relatively uniform $\delta^{18}O$ values. This does not preclude slight $^{18}O$ shifts to more negative values in the diffusion porosity where w/r ratios may be very low. Because oxygen is the major component of the water molecule and not a solute the $\delta^{18}O$ concentration of the water involved in recent calcite recrystallization will be maintained at a

relatively constant value by the physically open nature of the meteoric ground water flow system. Compared to oxygen, however, the concentrations of C in the CRNL ground waters are low despite bicarbonate concentrations that are near saturation levels with respect to calcite. Although significant C concentration gradients are unlikely to exist between the reaction site and the bulk solution within the fracture, isotopic gradients may be appreciable. The $\delta^{13}C_{DIC}$ of the water at the reaction site will be rock-dominated and have a value similar to that of the precursor hydrothermal calcite (-5 to -6°/oo). In contrast the $\delta^{13}C_{DIC}$ of the water in the fracture porosity reflects the mixed origins of the DIC and has a value of -14°/oo or less because of the isotopically light biogenic C component. Hence the $\delta^{13}C$ of recrystallized fracture calcite may be in a state of isotopic disequilibrium with respect to the bulk solution provided:

1) the reaction site is within micropores which are too small to facilitate chemical exchange with the bulk solution, or
2) the reaction site is on a grain surface where the fracture flow rate is too slow relative to D to homogenize the $\delta^{13}C_{DIC}$ within the water of the fracture.

In other words, if the rate of dissolution-reprecipitation is greater than the isotopic diffusion rate the $\delta^{13}C$ of the recrystallized calcite will more closely resemble that of the

precursor calcite than the DIC. Such conditions may exist in low w/r environments such as in megafluid inclusions that are trapped within fractures by the formation of secondary minerals.

It was shown in a previous section that the Sr/Ca mole ratios of the CRNL ground waters are much greater than those of the fracture calcites and therefore calcite dissolution by itself could not be controlling the Sr/Ca ratio of the ground water. Although $Ca^{2+}$ adsorption is probably responsible for the evolution of $Ca/HCO_3$ to $Na/HCO_3$ type ground water, it is unlikely to be the reason for the high $Sr^{2+}/Ca^{2+}$ ratios because the affinity for $Sr^{2+}$ adsorption in ground water systems is similar or slightly greater than that of $Ca^{2+}$ (Grisak and Jackson, 1978). It is more probable that the high $Sr^{2+}/Ca^{2+}$ ratio is controlled by calcite recrystallization. Calcite dissolution followed by reprecipitation will concentrate $Sr^{2+}$ in solution becauses the distribution coefficient for $Sr^{2+}$ in calcite is $<<1$. In a completely closed system

$$(Sr^{2+}/Ca^{2+})_{solution} = (Sr/Ca)_{calcite}/k^{Sr^{2+}}_{calcite}.$$

If the maximum (Sr/Ca) ratios ($1.1 \times 10^{-3}$) measured in the CRNL fracture calcites are most representative of the unaltered hydrothermal calcite values and if one uses $k_{calcite} = 0.06$ (Pingitore and Eastman, 1986) then the $(Sr^{2+}/Ca^{2+})$ mole ratio in solution in a chemically closed system would be $\sim 1.8 \times 10^{-2}$. This compares favourably with the measured range of 1.5-2.4 x

$10^{-2}$ and suggests the large $(Sr^{2+}/Ca^{2+})$ ratios for the CRNL ground waters are the result of recrystallization under semi-closed conditions.

Calcite recrystallization also explains why the $^{87}Sr/^{86}Sr$ ratios of the calcites are relatively uniform despite their highly variable $\delta^{18}O$ values. Strontium released from the recrystallization of calcites buffers the $^{87}Sr/^{86}Sr$ ratio of the ground water in the fractures. Dissolution of silicate minerals in the host rocks would tend to produce more radiogenic Sr isotope ratios in the ground water and in recently precipitated calcites but this does not seem to be a major factor at the CRNL site. Apparently calcite-derived $Sr^{2+}$ quantitatively swamps $Sr^{2+}$ contributions to the ground water from silicate minerals. This combined with the fact that calcite discriminates against the incorporation of Sr in its lattice insures relatively uniform $^{87}Sr/^{86}Sr$ ratios for the calcites regardless of their age. If, as the C isotope data suggest, calcite recrystallization is generally a bulk solution disequilibrium reaction then it is likely that large $Sr^{2+}$ concentration gradients are present between the reaction sites and the ground water in the fracture porosity.

### 7.2.1 Model Sensitivity to Parameter Input Values

So far it has been shown that low temperature recrystallization of hydrothermal calcite in ground waters of approximately the present day isotopic composition could produce the observed isotopic variability of the fracture calcites. However, it is necessary to determine whether other combinations of fluid temperatures and isotopic compositions could produce the same trends before a recent low temperature recrystallization origin can be accepted.

Recrystallization in ground waters having isotopic compositions similar to present day values but at temperatures substantially higher than 20°C could not produce a large positive $^{18}O$ shift. The curves shown in Fig. 34 track the isotopic evolution of calcite having an initial $\delta^{18}O$ of $13^{o}/oo$ (SMOW) as it recrystallizes under increasing water/rock ratios. Curves for recrystallization temperatures of 5, 8, 20 and 40°C are shown. The isotopic composition of the water is $-10^{o}/oo$ for all cases. At temperatures greater than about 55°C recrystallization results in negative shifts toward $\delta^{18}O$ values that are lower than the initial value. The geothermal gradient at the CRNL site is about 25°C $km^{-1}$ which means most of the CRNL calcites are in contact with ground waters at temperatures of $\leq$15°C.

The assumption that the hydrothermal calcites have recrystallized in contact with meteoric ground water having isotopic compositions similar to that of the present day is more

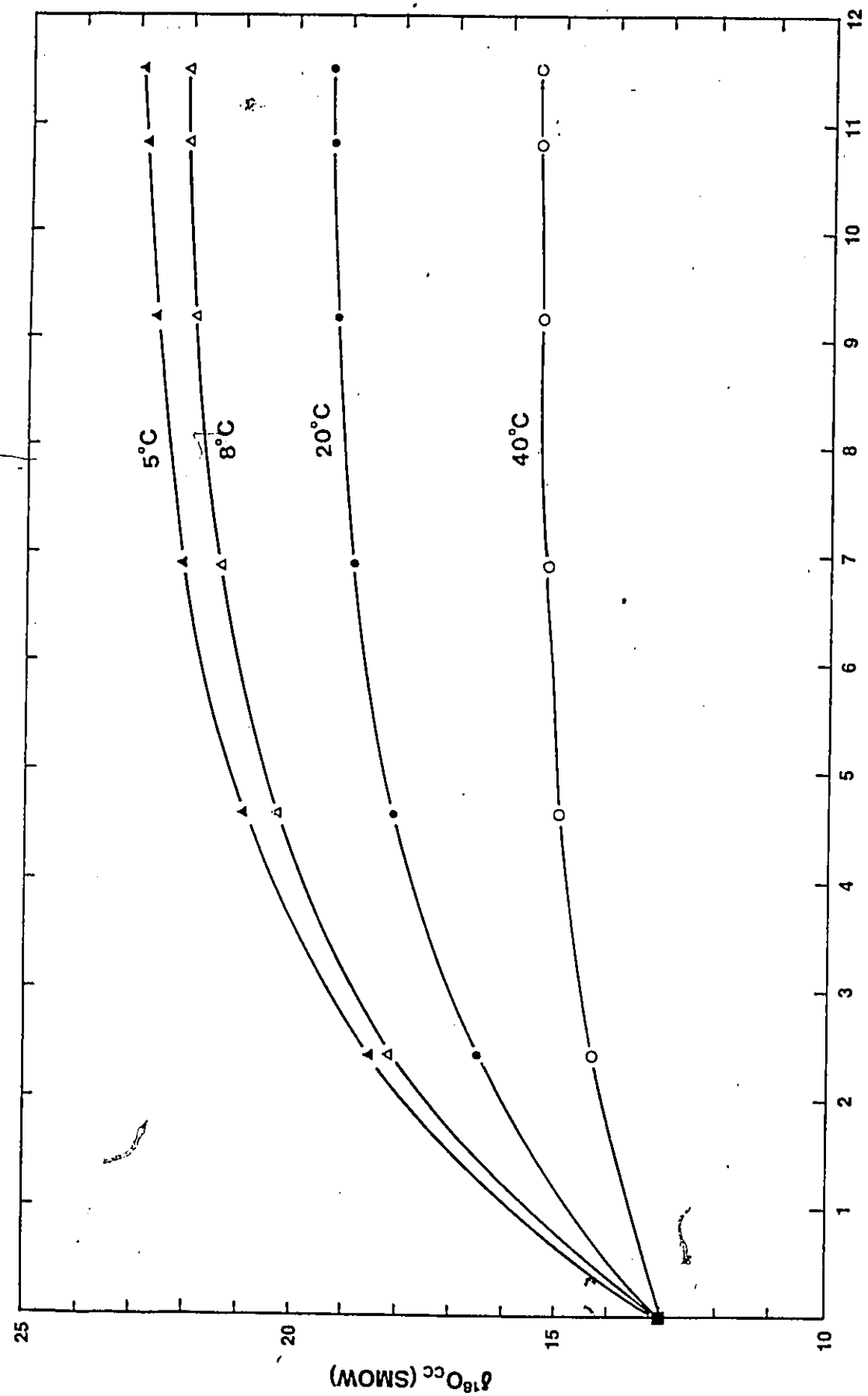


Fig. 34. The $\delta^{18}O$ of recrystallizing calcite as a function of increasing open system w/r mole ratios at temperatures of 5, 8, 20 and 40°C. The isotopic composition of the water is assumed to remain constant at -10°/oo.

difficult to verify. The CRNL area was at one time mantled with Lower Paleozoic sedimentary formations so it is possible that at one time formation waters or sea water infiltrated the crystalline basement rocks.

Because formation waters may be enriched in $^{18}O$ relative to the ambient, meteoric water because of isotopic exchange with $^{18}O$ rich sedimentary rocks such as carbonates (Clayton et al., 1966; Hitchon et al., 1969) it could be argued that the fracture calcites may have exchanged with waters much richer in $^{18}O$ than the present day waters. If this were the case then isotopic exchange would not be constrained to temperatures of <~20°C and relatively recent origins for the $^{18}O$ shift in the calcite could not be inferred. Figure 35 shows the change in the isotopic composition of a hydrothermal calcite as a function of the w/r ratio in ground waters with $\delta^{18}O$ values of 0, -5, -10 and -14°/oo and at temperatures of 20 and 40°C. It is clear that very large $^{18}O$ shifts could occur at low water/rock ratios if the $\delta^{18}O$ if the water were between -10 and 0°/oo.

In order to ascertain whether the $^{18}O$-enriched calcites may be the result of exchange with ancient relatively $^{18}O$-rich ground waters a number of calcites were analyzed for their $^{14}C$ content by accelerator mass spectrometry. Calcites that have exchanged only with ancient formation waters or sea water should be $^{14}C$-free (because of the short $^{14}C$ half life of 5730 yr.) whereas recently exchanged calcites would contain measurable $^{14}C$ activities provided the DIC of the ground water with

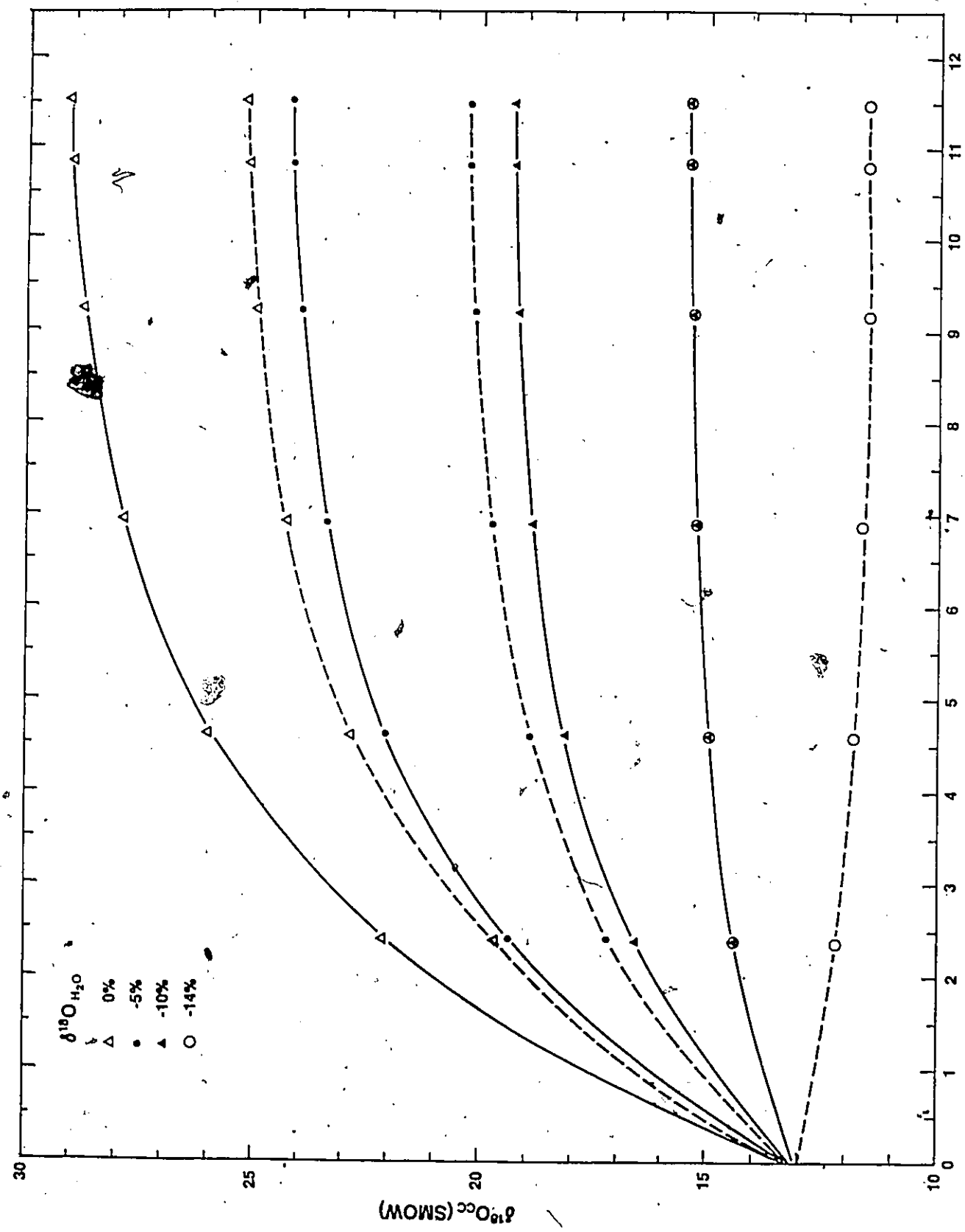


Fig. 35. The $\delta^{18}O$ of recrystallizing calcite as a function of increasing open system w/r mole ratios in water having constant $\delta^{18}O$ values of 0, -5, -10 and -14‰ and at temperatures of 20°C (solid curves) and 40°C (dashed curves).

which it is exchanging stable $^{13}C$ also contains $^{14}C$. The results of the $^{14}C$ analyses are listed in Table 17. Samples CR10-51.4 m, CR12-78.1 m, and FS17-57.4 m are from relatively shallow depths where ground water $^{14}C$ activities should be greater than 50% modern carbon (pmC) based on detailed sampling results from boreholes CR7 and CR13 (Table 2 and Bottomley et al., 1984). The two samples from borehole CR9-574.3 m a and b are from the inner zone and the relatively $^{18}O$-rich recrystallized outer layer, respectively. The $^{14}C$ activity of the ground water at this depth is expected (on the basis of $^{14}C$ trends in CR13) to be low (<10 pmC) but no uncontaminated ground water samples have been collected from depth to verify this assumption.

The $^{14}C$ results are the average of two machine-ready targets measured on different occasions. All results are corrected for natural, preparation and sputtering fractionation to a base of $\delta^{13}C = -25^{o}/oo$. The errors represent 68.3% confidence limits.

All samples contain easily measurable concentrations of $^{14}C$ which are within a relatively narrow range of 0.799-2.685 pmC. It is unlikely that these values are significantly affected by contamination with modern C because contamination associated with sample preparation at the Isotrace Laboratory is estimated to be less than 0.1 pmC (Beukens, 1986). The level of contamination associated with storage and handling of the core and extraction of the calcites from the fractures has,

Table 17. The $^{14}C$ activity of some CRNL fracture calcites. Results are expressed in per cent modern carbon (pmC). Uncorrected radiocarbon ages using the Libby $^{14}C$ mean life of 8033 years are also listed.

| Borehole and Depth (m) | Weight (mg) | $^{14}C$ Activity (pmC) | $^{14}C$ Age (years BP) |
|---|---|---|---|
| CR9 - 574.3a (inner layer) | 220 | 0.799 ± 0.036 | 38,790 ± 370 |
| CR9 - 574.3b (outer layer) | 365 | 1.582 ± 0.056 | 33,310 ± 280 |
| CR10 - 51.4 | 223 | 0.886 ± 0.053 | 37,970 ± 490 |
| CR12 - 78.1 | 253 | 1.371 ± 0.057 | 34,460 ± 340 |
| FS17 - 57.4 | 166 | 2.685 ± 0.089 | 29,060 ± 270 |

however, not been quantified. The radiocarbon "ages" reported in Table 17 are maximum ages since initial $^{14}C$ activities in the calcites of 100 pmC have been assumed. Because ground water $^{14}C$ activities are highly variable and almost always significantly less than 100 pmC this is clearly not a very realistic assumption. However, if it can be assumed that the total contamination of the calcite is less than 0.1 pmC then it follows that at least a component of these calcites formed in the late Pleistocene and quite possibly in the Holocene. It is also clear that samples CR10, CR12, and FS17 did not precipitate directly from post-glacial recharge water.

It is instructive to compare the $\delta^{13}C$ shifts of samples CR10, CR12, and FS17 with their $^{14}C$ activities since their $\delta^{18}O$ values suggest they have extensively exchanged isotopes with meteoric ground waters. Because these samples were collected from depths of 51-78 m where the $^{14}C$ activity of the ground water is at least 50 pmC (Bottomley et al., 1984) recent stable isotope exchange should be accompanied by the incorporation of $^{14}C$ into the calcite provided the w/r ratios are large enough not to limit the supply of $^{14}C$. This enrichment ($\varepsilon$) in $^{14}C$ should be approximately double the depletion in $^{13}C$ (i.e. $\varepsilon\ ^{14}C \approx 2\varepsilon\ ^{13}C‰$ or $0.2\varepsilon\ ^{13}C‰$) (Craig, 1954). If the original calcite was ancient hydrothermal calcite then it would have contained no $^{14}C$ and would have had a $\delta^{13}C$ of near $-5‰$ at the onset of low temperature recrystallization with meteoric ground water. The $\delta^{13}C$ values of these calcites now range from -7.4 to

$-8.7^{o}/oo$, a shift of $2.4-3.7^{o}/oo$ in $^{13}C$ which should be accompanied by $^{14}C$ activities of 0.48-0.74 pmC if $^{14}C$ decay is neglected. These activities are similar to but slightly less than the measured activities of 0.89-2.69 pmC. Matrix diffusion of $^{14}C$ from the ground water into the calcite may be an additional mechanism of $^{14}C$ enrichment for these calcites. In any event, the $^{14}C$ activities are consistent with the magnitude of the $^{13}C$ shift and are compatible with a recent recrystallization hypothesis to explain the isotopic compositions of CRNL fracture calcites.

In an open O system when the $\delta^{18}O$ of the ground water is buffered by the external reservoir the $\delta^{18}O$ of the recrystallized calcite is sensitive to the initial $\delta^{18}O$ value only at relatively low w/r ratios. For example, if the initial $\delta^{18}O$ value ($\delta^{18}O_r^i$) for the CRNL calcites had been assumed to be $16^{o}/oo$ rather than $13^{o}/oo$ then an open system w/r ratio of only 3.0 would be required to produce a $\delta^{18}O_r^f$ of $20^{o}/oo$ rather than 4.2 as as indicated in Fig. 33 (for $\delta^{18}O_w^i = -10^{o}/oo$). However the maximum $\delta^{18}O_r^f$ values that can be produced with increasing w/r ratios (at constant $\delta^{18}O_w^i$) are the same regardless of the assumed value of $\delta^{18}O_r^i$ because at high w/r ratios $\delta^{18}O_r^f$ is controlled by $\delta^{18}O_w^i$ and the $^{18}O$ fractionation factor between calcite and water. For $\delta^{18}O_w^i = -14^{o}/oo$, $\delta^{18}O_r^f$ would actually decrease with increasing w/r ratios if a $\delta^{18}O_r^i$ of $16^{o}/oo$ had been assumed in Fig. 33. Based on this analysis it is unlikely that the maximum w/r ratios calculated for the CRNL site are significantly influenced by the uncertainty in $\delta^{18}O_r^i$.

The $^{13}C$ fractionation factor between dissolved bicarbonate or carbonate and calcites is small and insensitive to variations in temperature. Therefore, unlike $^{18}O$, $\delta^{13}C$ values of recrystallized calcite are essentially free of significant temperature effects. However variations in DIC concentrations and $\delta^{13}C_{DIC}$ values may have a major effect on w/r ratios calculated from $^{13}C$ trends of recrystallized calcite. Figure 36 shows the influence of varying the $\delta^{13}C$ of the dissolved bicarbonate on the $\delta^{13}C$ of the recrystallized calcite as the w/r ratio increases. The curves have been constructed for a constant bicarbonate concentration of 2 mM $L^{-1}$ and with a calcite-bicarbonate fractionation factor of $2^{o}/oo$. The initial $\delta^{13}C$ of the calcite was $-5^{o}/oo$ in all cases. At $\delta^{13}C_{DIC}$ values greater than $-7^{o}/oo$ calcite recrystallization would result in a positive $\delta^{13}C$ shift rather than the observed negative shift. If $\delta^{13}C_{DIC}$ values less than -14‰ (used in the construction of the curves in Fig. 33) were involved in calcite recrystallization then calculated, time-integrated water/rock ratios of less than $10^5$ could have produced the lightest $\delta^{13}C$ values for the calcites. However, even at an unlikely $\delta^{13}C_{DIC}$ concentration of $-20^{o}/oo$ w/r ratios of at least $10^4$ are required to produce the lightest values.

At constant $\delta^{13}C_{DIC}$ the w/r ratio required to produce a specific $\delta^{13}C$ shift in the calcite decreases as the DIC concentration increases. Concentrations of DIC in ground water are highly variable. In the saline ground waters and brines from

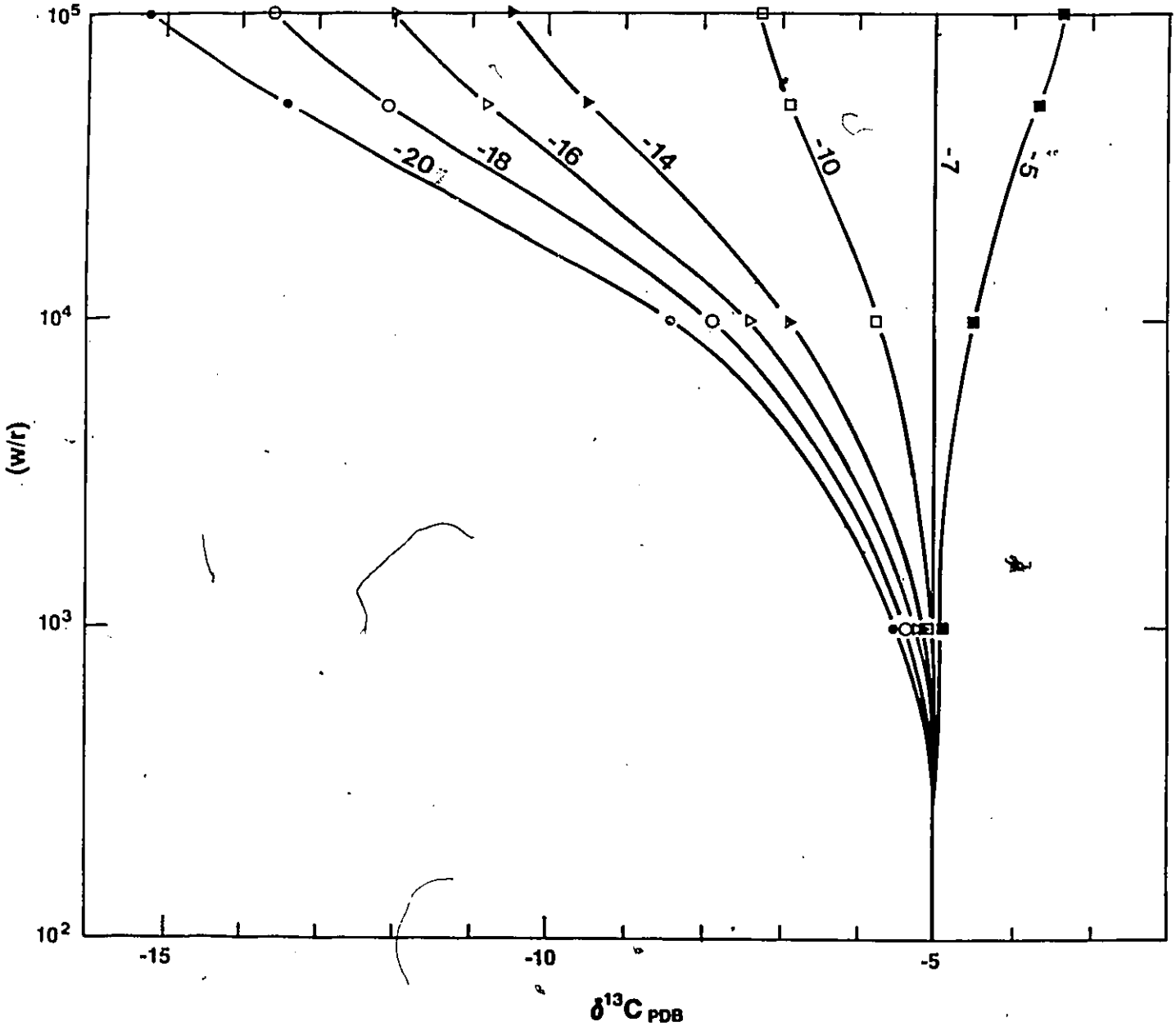


Fig. 36. The $\delta^{13}C$ of recrystallizing calcite as a function of the closed system w/r mole ratios in waters with $\delta^{13}C_{DIC}$ values of -5, -7, -10, -14, -16, -18 and -20‰. A constant bicarbonate concentration of 2 mM $L^{-1}$ has been assumed.

the Canadian Shield DIC concentrations are buffered to values of less than 0.5 mM $L^{-1}$ by the high $Ca^{2+}$ concentrations in these waters (Frape et al., 1984). At the other extreme some formation waters have extremely large DIC concentrations in excess of 1000 mg $L^{-1}$ (16.4 mM $L^{-1}$ or ~$3x10^{-4}$ moles C/mole $H_2O$). Ground waters from the AECL research areas generally have DIC concentrations well below 500 mg $L^{-1}$ (8.2 mM $L^{-1}$). Figure 37 shows the effect of increasing DIC concentration on the $\delta^{13}C$ of recrystallized calcite as a function of the w/r ratio. At DIC concentrations of 500-1000 mg $L^{-1}$ w/r ratios approaching ~$10^4$ would be required to produce the lightest calcites rather than $10^5$ for concentrations of 2 mM $L^{-1}$ (~122 mg $L^{-1}$). At high DIC concentrations values of $\delta^{13}C_{DIC}$ are generally greater than $-14^{o}/oo$. Therefore the combined effects of high DIC concentrations and low $\delta^{13}C_{DIC}$ values on the $\delta^{13}C$ of the calcite normally need not be considered.

In the previous section it was proposed that C isotope exchange during calcite recrystallization was a bulk solution disequilibrium process. Although this process would not significantly affect the DIC concentration used in equation 15 to determine the water/rock ratio required to produce a particular $\delta^{13}C$ shift, the effective $\delta^{13}C_{DIC}$ involved in recrystallization would be greater than the bulk solution value. The value of the effective $\delta^{13}C_{DIC}$ is difficult to specify because it would depend on the steepness of the isotopic gradient between the reaction site and bulk solution. Nevertheless it is clear from Fig.

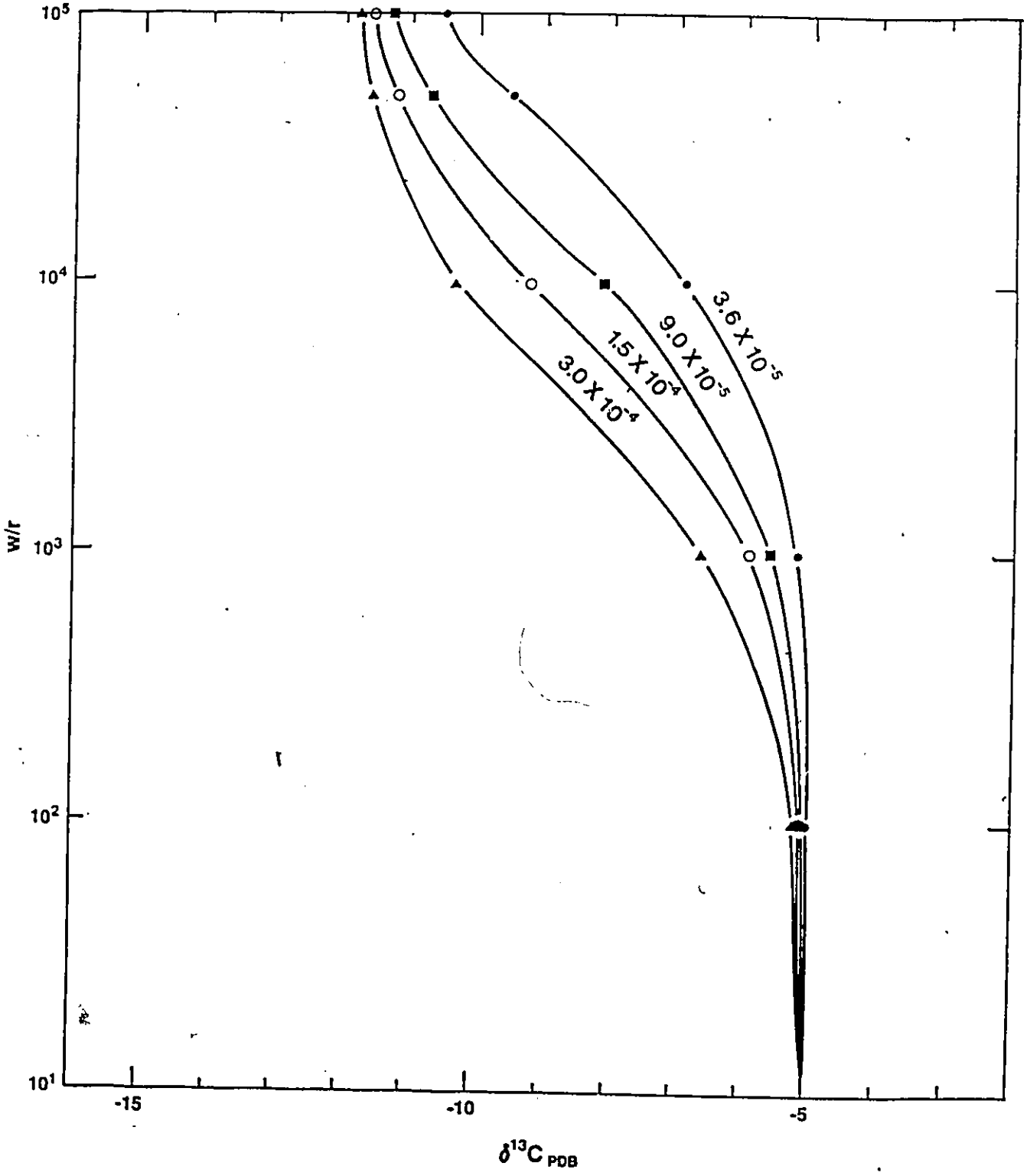


Fig. 37. The $\delta^{13}C$ of recrystallizing calcite as a function of the closed system w/r mole ratios in waters with DIC concentrations of $3.6x10^{-5}$, $9.0x10^{-5}$, $1.5x10^{-4}$ and $3.0x10^{-4}$. A constant $\delta^{13}C_{DIC}$ ($HCO_3^-$) of -14°/oo has been assumed.

36 that use of the bulk solution $\delta^{13}C_{DIC}$ value is conservative. Use of an isotopically heavier effective $\delta^{13}C_{DIC}$ value, which reflects the memory effect of the calcite precursor, would require even greater w/r mole ratios than those indicated in Fig. 33 to produce calcites with the lightest $\delta^{13}C$ values.

In summary it is concluded that the isotopic shifts observed in the CRNL calcites were likely produced by low temperature exchange with meteoric ground waters having temperatures, isotopic compositions, and DIC concentrations similar to present day values. Accordingly, maximum w/r mole ratios of at least $10^4$ are inferred for those calcites lightest in $\delta^{13}C$. Because the magnitude of the $^{18}O$ shift is sensitive to the $\delta^{18}O$ of the ground water, the participation in the exchange of O isotopes of ancient, relatively $^{18}O$-enriched meteoric waters (of possible formation water origins) can not be discounted. However, the presence of $^{14}C$ in $^{18}O$-rich calcites from open fractures indicates that C isotope exchange is a geologically recent phenomenum. Accordingly recent O isotope exchange should also be anticipated since there is more O than C in present day ground waters. Nevertheless a component of ancient O isotope exchange to the overall $^{18}O$ shift remains a possibility.

### 7.2.2 Isotopic Evidence for the Bulk Solution Disequilibrium Recrystallization Model

Plots of the $\delta^{18}O$ and $\delta^{13}C$ values of the CRNL calcites against their $^{87}Sr/^{86}Sr$ ratios are shown in Fig. 38. There is no apparent correlation between $\delta^{18}O$ and $^{87}Sr/^{86}Sr$. Two calcite samples from the light $^{18}O$ group have $^{87}Sr/^{86}Sr$ ratios that are similar to the heavier hydrothermal calcites and to the $^{18}O$-rich calcites which are believed to have undergone extensive isotopic exchange with meteoric waters. In contrast, the plot of $\delta^{13}C$ versus $^{87}Sr/^{86}Sr$ suggests a possible mixing trend between two reservoirs, one that has a relatively low $^{87}Sr/^{86}Sr$ ratio but is rich in $^{13}C$ and the other containing more radiogenic Sr but which is depleted in $^{13}C$. The two samples with the most radiogenic Sr isotopic ratios do not lie on the mixing line. However, both these samples had large insoluble residue contents and hence may have been contaminated with relatively radiogenic silicate Sr.

Mixing is also suggested in the plot of $^{87}Sr/^{86}Sr$ versus 1/Sr (Fig. 39'). In this type of plot a mixing trend should approximate a straight line. If the two most radiogenic Sr samples are ignored the CRNL calcite data approximate a straight line fairly well. It could be argued that contamination of the calcites with radiogenic silicate Sr could produce the same straight-line relationship. However, if this were the case one might expect that calcites with the lowest Sr concentrations should be most sensitive to silicate contamination.

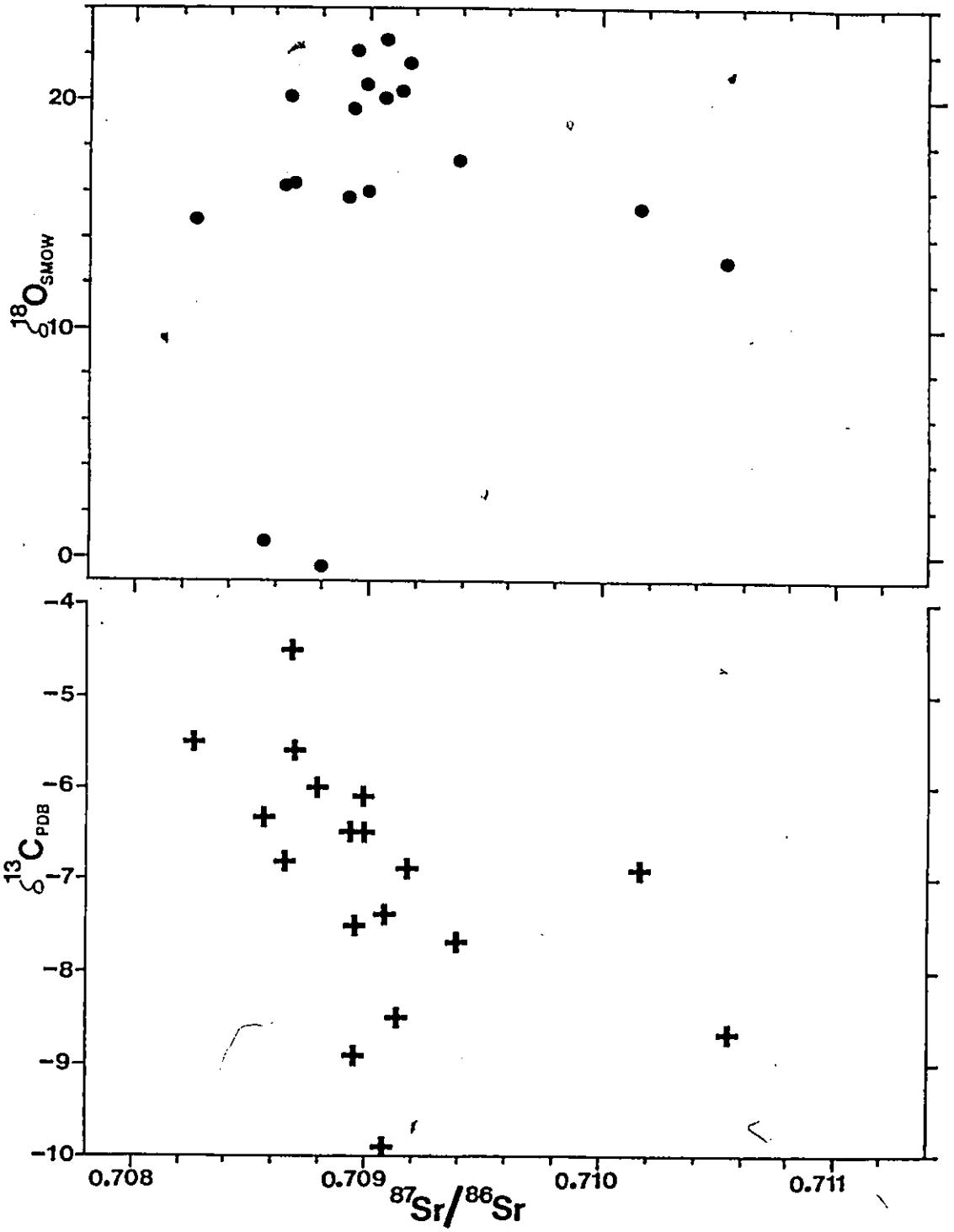


Fig. 38. Plots of $\delta^{18}O$ (top) and $\delta^{13}C$ (bottom) vs. the $^{87}Sr/^{86}Sr$ ratios of CRNL calcites.

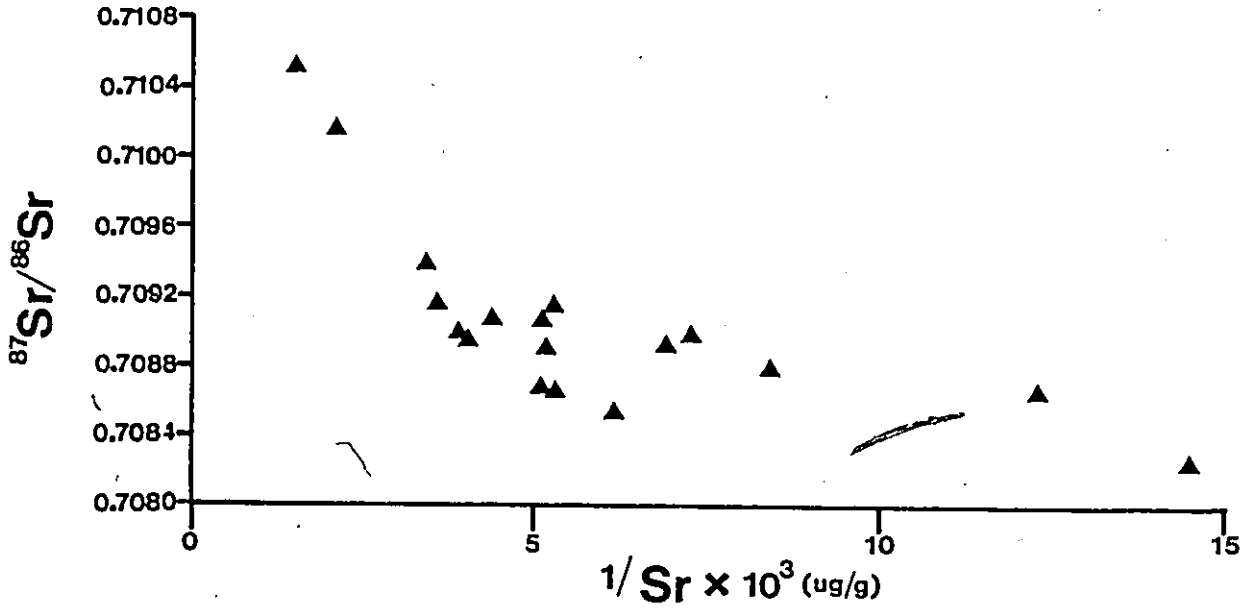


Fig. 39. Plot of $^{87}Sr/^{86}Sr$ vs. the reciprocal of the Sr concentration (1/Sr) of CRNL calcites.

However, the data indicate the opposite, showing a positive linear correlation between the Sr concentration and the isotopic ratio. Moreover silicate contamination could not produce the inverse relationship between $\delta^{13}C$ and $^{87}Sr/^{86}Sr$ shown in Fig. 38.

The relationships between $^{18}O$, $^{13}C$, and $^{87}Sr/^{86}Sr$ are consistent with the previously described bulk solution disequilibrium recrystallization model. Hence it is proposed that the mixing suggested by the $\delta^{13}C$-$^{87}Sr/^{86}Sr$ plot involves participation of the the present day meteoric ground water in the fractures and micropore, or "messenger film", water (Brand and Veizer, 1980) within the diffusion porosity or along grain boundaries of the calcite. The fracture water at depths of less than ~400 m at CRNL has a $^{87}Sr/^{86}Sr$ ratio of 0.7092-0.7093 (Table 14) and a $\delta^{13}C$ of less than $-13.8^{o}/oo$ (Table 5). In a chemically closed or semi-closed system the $\delta^{13}C$ value and $^{87}Sr/^{86}Sr$ ratio of the micropore water will be similar to that of the dissolving calcite. If this calcite is not yet extensively recrystallized it will have a $\delta^{13}C$ of -4 to $-6^{o}/oo$ and a $^{87}Sr/^{86}Sr$ of 0.708-0.709. Hence, the isotopic compositions of the fracture and micropore waters are compatible with end member compositions inferred from the mixing trend in Fig. 39. Furthermore it is clear that calcites which have recrystallized in more open environments should have both C and Sr isotopic compositions that more closely approach those of the ground water in the fractures.

In an earlier chapter it was suggested that the relatively large $Sr^{2+}/Ca^{2+}$ mole ratios of the CRNL ground waters could be primarily the result of calcite recrystallization. Because calcite discriminates against the incorporation of $Sr^{2+}$ during its precipitation, Sr released during calcite recrystallization will result in $Sr^{2+}/Ca^{2+}$ ratios in the ground water that are much larger than in the parent calcite. However, the presence of silicate-derived $Sr^{2+}$ results in ground water $^{87}Sr/^{86}Sr$ ratios that are slightly greater than that of the parent calcite. Calcites that have precipitated from ground waters (fracture water) with the present day $Sr^{2+}/Ca^{2+}$ ratios and Sr isotopic compositions should be relatively rich in both Sr and $^{87}Sr$. Micropore water in the calcite however, should have lower Sr/Ca and $^{87}Sr/^{86}Sr$ ratios. Calcite that precipitated from a mixture of fracture and micropore waters should have compositions that fall along a mixing line joining the two end members on a $^{87}Sr/^{86}Sr$ vs 1/Sr plot. Such a trend is in fact observed for the CRNL calcites (Fig. 39).

The relationships between the Sr and C concentrations in the calcites and their isotopic compositions suggest a chemically semi-closed environment of recrystallization with respect to these two elements. However, because water is mainly composed of oxygen, a system that is physically open with respect to water will also be chemically open with respect to oxygen. Hence the $^{18}O$ content of recrystallized calcite depends mostly

on the water/rock ratio of the system and not on the $\delta^{18}O$ of the precursor calcite.

Isotopically exchanged calcites are present in fractures at depths of at least 500 m at CRNL suggesting fracture interconnectivity must be extensive to enable the infiltration of meteoric waters to these depths. Alternatively, the presence of juxtaposed fracture calcites that have retained their hydrothermal isotopic signatures show that most of the meteoric ground water flux has occurred along discrete fractures having larger effective apertures, a finding which is consistent with the 500 fold variation in apertures of present day open fractures (Raven, 1986).

## 7.3 METEORIC GROUND WATER FLUX THROUGH THE CHALK RIVER PLUTON

The maximum isotopic water/rock ratios recorded by the CRNL calcites are very large compared to ratios calculated for silicate plutonic rocks where convective hydrothermal systems were formerly operative. Water/rock mole ratios for these systems are generally less than 5 (Taylor, 1974). In seawater-dominated hydrothermal systems involving the alteration of mid ocean ridge basalts, water/rock mole ratios greater than 50 have been calculated for saponite-rich pillow breccias (Stakes and O'Neil, 1982). However, in the present study the low temperature exchangeable O and C resides in only a small fraction of the total volume of the pluton. Hence the water/rock ratios determined here are not directly comparable to those

for hydrothermally altered, batholith-size rock masses reported in other studies. The mass of fracture calcite in the CRNL core must be small when it is considered that the fracture or flow porosity of plutonic rock is of the order of $10^{-4}$ (Norton and Knapp, 1977). If the volume of fracture calcite is assumed to be the same or similar to that of the fracture porosity then on average 1 $m^3$ of fractured rock would contain 2-3 moles of calcite and 5-6 moles of water. Because water/rock ratios of the order of at least $10^5$ are required to produce those calcites with the lightest $\delta^{13}C$ values, the time-integrated flux of meteoric water through these fractures must have been sufficient to flush this unit volume of rock $\sim 5 \times 10^4$ times which is equivalent to about 4500 L of water. This is a minimum estimate for the maximum volumes of water involved since large amounts of water may circulate through these fractures without exchanging. The actual water/rock ratio in an open system as a function of time (t), is independent of isotopic quantities, and is calculated from the following general equation (Gregory and Criss, 1986):

$$(24) \qquad \frac{w}{r} = (X_w + ut)/(\Sigma X_i)$$

where $X_w$ = mole fraction of water

$X_i$ = mole fraction of the $i^{th}$ exchangeable mineral

$u$ = ground water flow rate.

If the rate constant for isotopic exchange between calcite and water is small compared to "u" large volumes of water could pass through the fracture without affecting the isotopic composition of the calcite. Moreover it is assumed in the derivation of the isotopic water/rock ratio (Eq. 11) that isotopic equilibrium is attained which in fact may not actually be achieved. As a result of these considerations Gregory and Criss (1986) concluded that the calculated isotopic w/r ratio will always be less than the actual ratio (Eq. 24).

An estimate of the average minimum amount of meteoric water that has circulated through the upper ~500 m of the orthogneiss can be calculated from the median $\delta^{13}C$ value of $-7^{o}/oo$ as shown in the cumulative frequency plot of Fig. 40. From Fig. 33 it can be seen that a time-integrated water/rock ratio of $\sim 10^{4}$ is required to produce a $\delta^{13}C$ value of $-7^{o}/oo$. Therefore 1 $m^3$ of idealized, uniformly fractured orthogneiss would have been flushed by 450 L of ground water. Hence the total volume of ground water that has circulated through the orthogneiss is about half the volume of the pluton itself.

Taylor (1974) concluded that the volume of heated meteoric water in fossil hydrothermal systems was typically approximately the same as the volume of altered rock. Because individual hydrothermal systems can exist for several tens of thousands of years the volume of water involved is not unreasonable and requires infiltration of only a few per cent of the mean annual precipitation. The major problem in hydrothermal

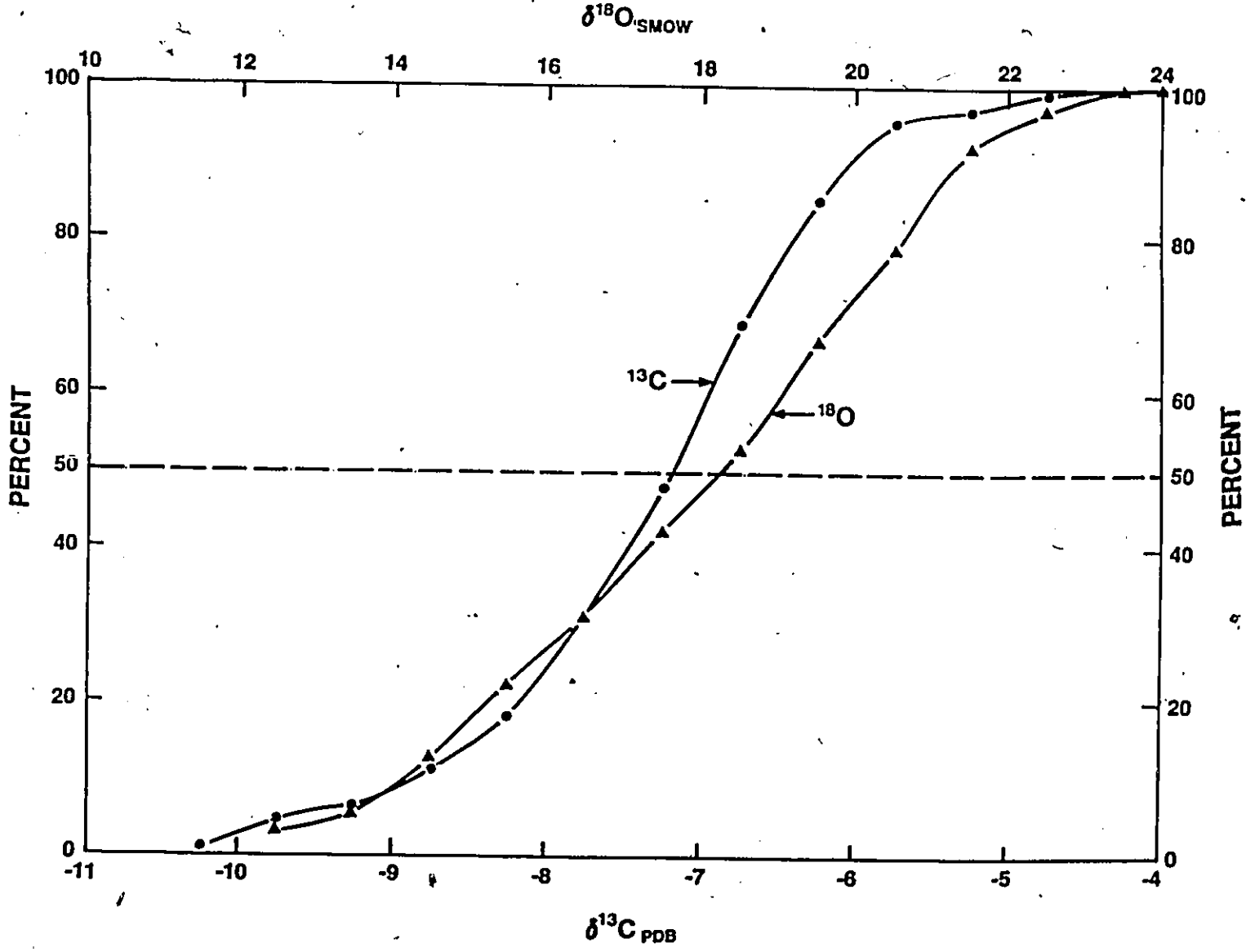


Fig. 40. Cumulative frequency plots for the $\delta^{13}C$ and $\delta^{18}O$ contents of CRNL calcites.

systems is actually to provide enough heat energy to maintain the convective system (Taylor, 1974). The volume of water involved in the low temperature recrystallization of the CRNL calcites is thus of the same order as that involved in hydrothermal systems. Clearly the permeability and hydraulic gradients have been sufficiently large to force large volumes of meteoric water through the CRNL rocks without the benefit of significant thermal gradients that are present in convective hydrothermal systems.

## 8.0 ISOTOPIC COMPOSITION OF CHALK RIVER FRACTURE PYRITES

Fracture calcites are sometimes accompanied by pyrite and they appear to be coeval and cogenetic (Plates IV and XII). The sulphur isotopic compositions of several fracture pyrites have been determined and are listed in Table 18 and the distribution of the $\delta^{34}S$ values is shown in the histogram of Fig. 41. The $\delta^{34}S$ values vary widely from -25 to +46°/oo although most analyses are less than 0°/oo or slightly positive.

The S for pyrite formation might have been supplied from two possible sources. It could have been leached from country rocks by hydrothermal fluids and re-precipitated in the fractures. Although the host gneisses are low in S (<0.06%), metasedimentary rocks richer in S may have been present at the time of hydrothermal activity. While a country rock source can not be discounted, the coexistence of hydrothermal calcite with a mantle C isotopic signature suggests the origin of the S was hydrolyzed mantle $SO_2$. Because mantle sulphur has a $\delta^{34}S$ value near 0°/oo, the $\delta^{34}S$ of the total sulphur in solution ($\delta^{34}S_{\Sigma S}$) from this source would also have been near 0°/oo. Crustal rifting over a mantle "hotspot" may have enabled mantle volatiles such as $CO_2$ and $SO_2$ to penetrate the crust and mix with meteoric ground waters in a convective hydrothermal flow system.

The negative $\delta^{34}S$ values, which can be explained by the partitioning of S isotopes between reduced and oxidized S species, are a common characteristic of many hydrothermal sulphide deposits. Moreover, large variations in the negative $\delta^{34}S$

Table 18. Sulphur isotopic composition of CRNL fracture pyrites

| Borehole & Depth (m) | $\delta^{34}S_{CDT}$ | Comments |
|---|---|---|
| CR1 - 108.35 | -22.8 | patchy $FeS_2$ on chlorite |
| 128.35 | 44.8 | patchy $FeS_2$ on chlorite in diabase |
| 128.50 | 29.6 | patchy $FeS_2$ with calcite |
| 212.97 | -16.0 | $FeS_2$ patch on calcite |
| 244.62 | 6.2 | platy $FeS_2$ on chlorite |
| 251.83 | -16.24 | platy, slickensided $FeS_2$ (Plate XIIIc) |
| CR2 - 57.21 | -25.2 | large fine-grained patch on black chlorite |
| CR8 - 65.02 | +7.0 | patchy $FeS_2$ in calcite-open fracture |
| 77.57 | -4.3 | patchy $FeS_2$ with calcite |
| 104.72 | -18.2 | patchy $FeS_2$ with calcite |
| 121.08 | 14.9 | patchy $FeS_2$ with calcite |
| 132.75 | -2.0 | patchy $FeS_2$ with calcite |
| 153.00 | -17.6 | patchy $FeS_2$ with calcite |
| 167.17 | -7.8 | fine $FeS_2$ cubes in vug in calcite |
| 192.75 | 46.0 | thick, fine-grained patch with calcite (Plate XIIc) |
| 221.26 | -0.8 | patchy $FeS_2$ |
| 234.00 | -15.3 | patchy $FeS2_2$ on slickensided calcite |
| 302.82 | -11.4 | large patches of $FeS_2$ with calcite |
| CR9 - 220.82 | 3.3 | fine $FeS_2$ cubes |
| 233.65 | 2.5 | patchy $FeS_2$ |
| CR11 - 114.63 | -9.5 | open fracture with calcite |
| 118.90 | 10.5 | patchy $FeS_2$ on chlorite |
| 121.17 | 14.0 | patchy, fine-grained $FeS_2$ (Plate XIIb) |
| CR12 - 77.81 | -8.2 | platy $FeS_2$ with calcite |
| 81.35 | -21.2 | platy $FeS_2$ |
| 105.39 | 10.5 | patchy $FeS_2$ in calcite |
| FS16 - 14.3 | 3.4 | fine $FeS_2$ in chlorite and calcite |
| PAF std. | 27.9 | accepted value 27.8 |
| FRED std. | 1.0 | accepted value 1.0 |

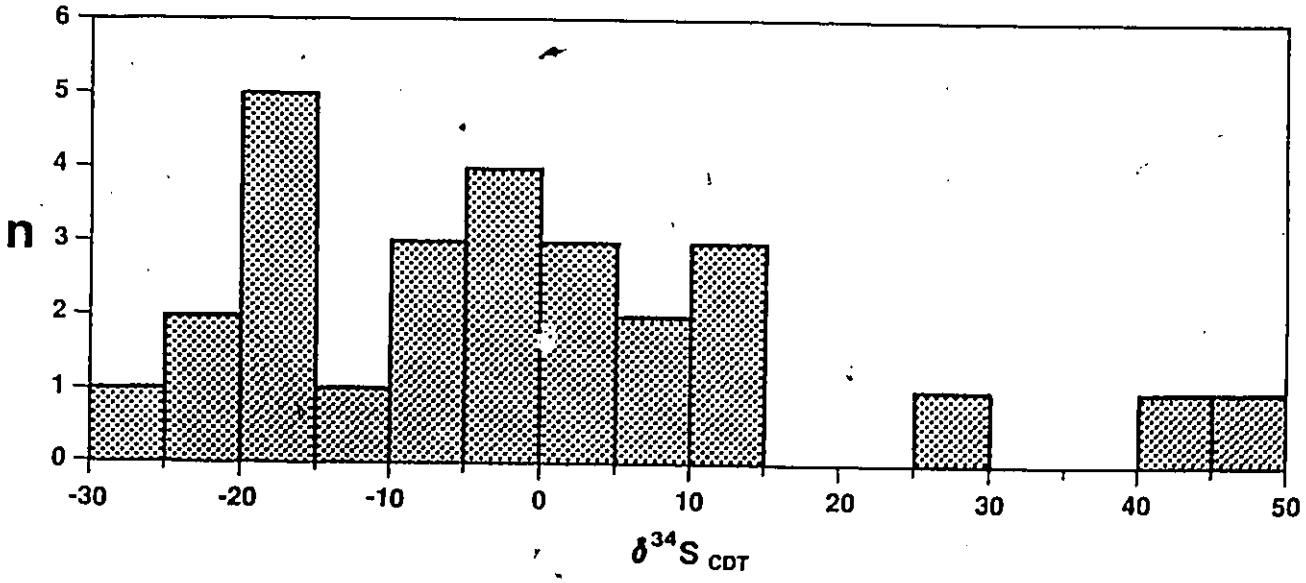


Fig. 41. Histogram of the $\delta^{34}S_{CDT}$ values of CRNL fracture pyrites.

values of hydrothermal sulphides may result from small variations in fluid pH under moderately reducing conditions (Ohmoto, 1972). Although dissimilatory sulphate reduction by bacteria can produce similar distributions in $\delta^{34}S$ values as evidenced by S isotope distributions in sedimentary sulphide deposits (Schwarcz and Burnie, 1973), bacterial sulphate reduction was probably not significant at the time of formation of these fracture pyrites because of the low levels of organic C in these gneissic rocks. Furthermore, because organic C is very light in $\delta^{13}C$, oxidation of organic matter during sulphate reduction normally results in associated calcites with light $\delta^{13}C$ values ($<\sim-15^{o}/oo$). Such light $\delta^{13}C$ values have not been measured in the CRNL calcites.

The highly positive $\delta^{34}S$ pyrites are more problematic because these sulphides could not form from a fluid with a $\delta^{34}S_{\Sigma S}$ of near $0^{o}/oo$ unless the amount of S removed from the hydrothermal fluid by precipitation in some fractures was a significant fraction of the total S concentration initially in solution. Under these conditions the $\delta^{34}S_{\Sigma S}$ would increase continuously and very heavy sulphides could eventually form. This process is described by the previously mentioned Rayleigh distillation equation (Eq. 4) and is applicable to systems that become closed with respect to the S source. Figure 42 shows the nature of the $\delta^{34}S$ increase as a function of the fraction of S remaining in solution as the result of sulphide precipitation in a closed system. A constant fractionation factor of $25^{o}/oo$

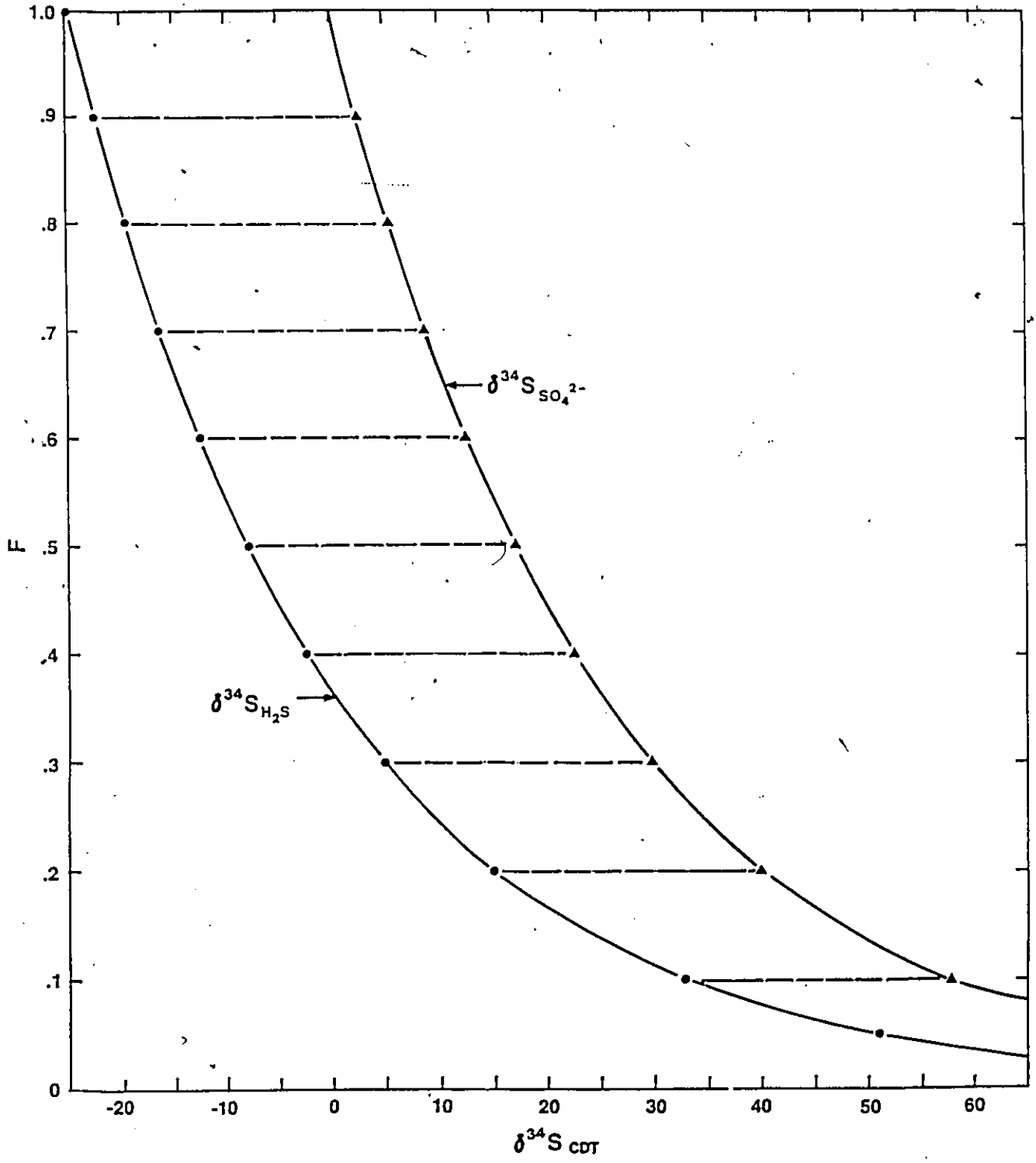


Fig. 42. Rayleigh distillation curves for the $\delta^{34}S$ of $H_2S$ and $SO_4^{2-}$ in a closed system as a function of the fraction of S remaining in solution. A constant fractionation factor ($\alpha_{SO_4^{2-} - H_2S}$) of 25‰ has been assumed as well as an initial $\delta^{34}S_{TS}$ of 0‰.

between sulphate and sulphide has been assumed in the construction of these curves as well as an initial $\delta^{34}S_{\Sigma S}$ of $0^{o}/oo$ in the fluid. Under these conditions the S content of the fluid would have to be reduced to less than 10% of the original concentration in order to produce the heaviest $\delta^{34}S$ values. It appears as though some fractures in the CRNL gneisses behaved as closed or semi-closed environments with respect to the flux of hydrothermal sulphur through them. This suggests that even at this early stage in the history of fracture flow in the gneiss variable fluid/rock ratios were influencing the isotopic composition of fracture minerals, in this case sulphides.

Although calcites are vulnerable to low temperature recrystallization and isotopic exchange with meteoric waters this is not the case with sulphides which will therefore retain their original hydrothermal isotopic signatures. It is possible to reconstruct the original pH-$f_{O_2}$ of the hydrothermal fluid on the basis of the $\delta^{34}S$ of the pyrite and the $\delta^{13}C$ of the cogenetic fracture calcite (Ohmoto, 1972). However sulphide samples used for this purpose must not have precipitated in a closed environment and calcite samples must have retained their original $\delta^{13}C$ values. It is also necessary to assume a temperature of formation, total C and S concentrations in the fluid, and values for $\delta^{34}S_{\Sigma S}$ and $\delta^{13}C_{\Sigma C}$. Reasonable values for the latter two values are $0^{o}/oo$ and -4 to $-8^{o}/oo$, respectively, if the S and C are mantle derived. Concentrations of C and S in the hydrothermal fluid are unknown but Ohmoto (1972) has suggested that

values of $10^{-2}$ - $10^{0}$m for C and $10^{-3}$ - $10^{-1}$ m for S are typical for hydrothermal ore-forming fluids. Fortunately the pH-$f_{O_2}$ reconstruction is not particularly sensitive to order of magnitude variability in C and S concentrations.

On Fig. 43 I have plotted $\delta^{34}S$ values for sulphides that have been unaffected by possible Rayleigh distillation effects and $\delta^{13}C$ values for hydrothermal calcites that have not been $^{18}O$-enriched through recrystallization processes. These values plot within a relatively restricted region of near neutral pH and of moderately reducing $f_{O_2}$ ($f_{O_2}$ ~$10^{-37}$). The temperature of 250°C used in the construction of Fig. 43 is near the maximum temperature of calcite formation at CRNL. At lower temperatures, $f_{O_2}$ values inferred from the $\delta^{34}S$ and $\delta^{13}C$ data would be considerably smaller. This figure also constrains the $\Sigma S$ concentration to at least ~0.001 mole/$kg_{H_2O}$ since at concentrations less than this value the stability field of $FeS_2$ would shrink to pH values less than the stability boundary for calcite.

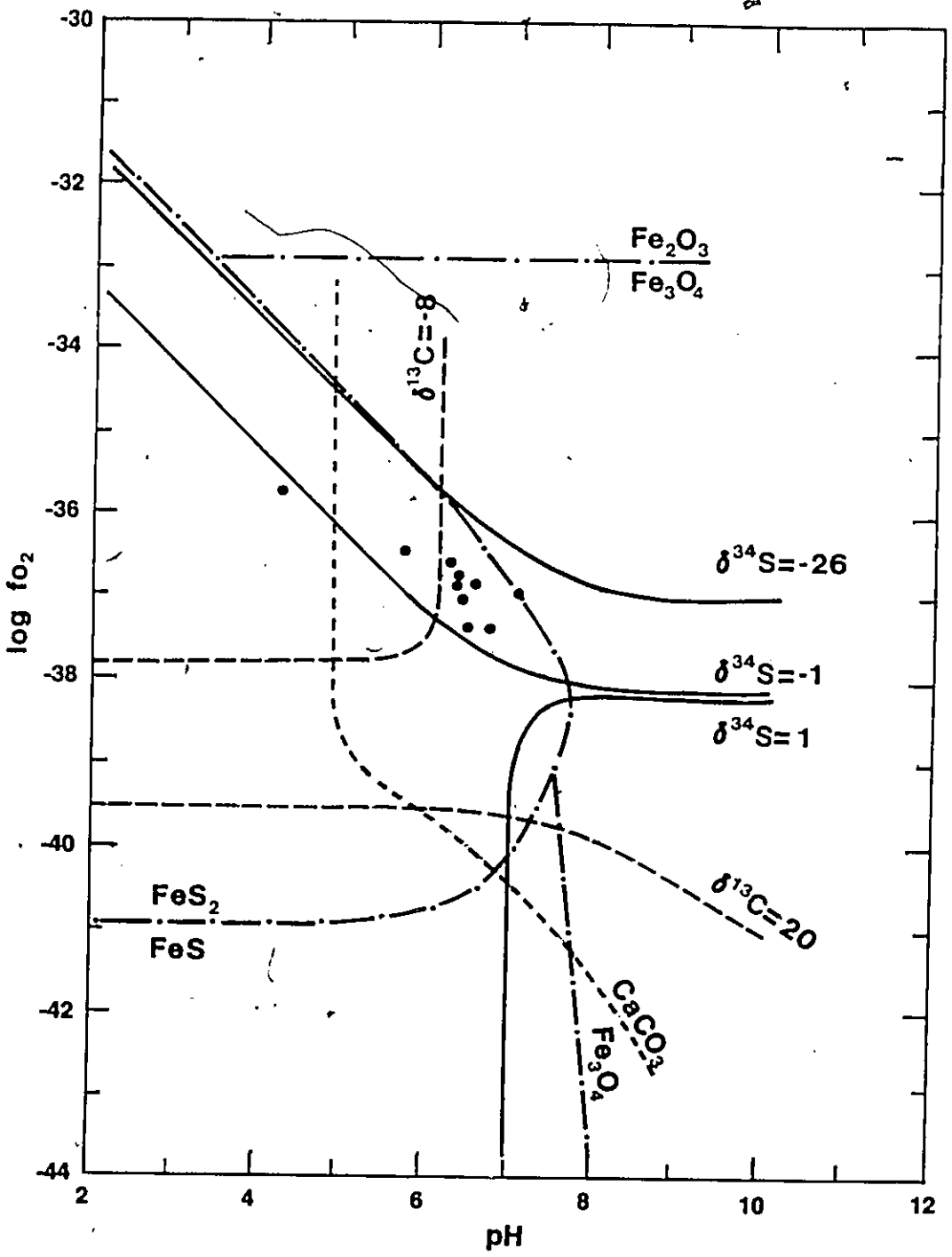


Fig. 43. Plot of $\delta^{13}C$ and $\delta^{34}S$ values of coexisting calcites and pyrites on a pH-$f_{O_2}$ diagram for the carbon and sulphur systems at 250°C (Ohmoto, 1972). $\delta^{13}C_{\Sigma C}$ and $\delta^{34}S_{\Sigma S}$ values of $-7^{o}/oo$ and $0^{o}/oo$, respectively, have been assumed (see text).

## 9.0 ISOTOPIC COMPOSITION OF EAST BULL LAKE FRACTURE CALCITES

Calcite is much less abundant as a fracture mineral in EBL core compared to core from CRNL and fewer samples have been analyzed. Moreover specific zones that have been sampled for ground water have also been sampled for fracture calcites resulting in some sampling bias towards high permeability zones. The results of the $^{13}C$ and $^{18}O$ analyses of these calcites are listed in Table 19.

The $\delta^{13}C$ and $\delta^{18}O$ distributions of the EBL calcites are shown in Fig. 44. Most of the $\delta^{13}C$ values are greater than $-5^{o}/oo$ with a peak in the distribution at about $-4^{o}/oo$. Most of the $\delta^{13}C$ values lighter than $-10^{o}/oo$ occur at shallow depths of $\leq$~20 m which clearly suggests that C derived from soil zone $CO_2$ is an important component of many (but not all) near-surface calcites (Fig. 45). Below a depth of 125 m the $\delta^{13}C$ of the calcites are, with one exception, greater than $-5^{o}/oo$.

As in the case of the CRNL calcites the EBL calcites have non-uniform $\delta^{18}O$ values which range from 7.5 to $24.1^{o}/oo$. Large variations in $\delta^{18}O$ occur to depths of at least 450 m and are also present in individual samples (Fig. 46). For example, a thick calcite infilling from a depth of 208.53 m in borehole EBL-4 (Table 19) was found to be approximately $10^{o}/oo$ richer in $\delta^{18}O$ on the outer surfaces that were in direct contact with ground water than the centre of the infilling. This particular sample was a calcite vein that was not in tight contact with the wall rock on either surface.

Table 19. Carbon and oxygen isotopic compositions of EBL fracture calcites.

| Borehole and Depth (m) | $\delta^{13}C_{PDB}$ | $\delta^{18}O_{SMOW}$ | Comments |
|---|---|---|---|
| EBL-1 165.95 | -4.6 | 21.3 | patchy calcite with $FeS_2$-open fracture |
| 192.54 | -2.6 | 12.0 | |
| 192.54 | -3.2 | 12.3 | calcite vein |
| 194.72 | -3.8 | 8.5 | calcite with chlorite-closed fracture |
| 406.30 | -6.0 | 22.0 | patchy calcite with laumontite |
| 407.40 | -3.8 | 8.2 | sealed calcite vein with laumontite |
| 410.93 | -4.4 | 12.5 | patchy calcite with $FeS_2$ |
| 501.61 | -3.2 | 10.0 | |
| 512.68 | -3.1 | 13.9 | patchy calcite with quartz and laumontite |
| 630.40 | -3.6 | 7.5 | patchy calcite with laumontite |
| 838.76 | -3.0 | 13.5 | patchy calcite, open fracture |
| EBL-2 6.37 | -11.8 | 23.1 | patchy calcite |
| 9.58 | -6.9 | 11.8 | patchy calcite with laumontite |
| 11.81 | -10.8 | 21.9 | patchy calcite with laumontite |
| 14.87 | -4.1 | 21.9 | bottom - vein calcite |
| 14.87 | -7.0 | 22.7 | top - flaky calcite |
| 15.21 | -4.6 | 24.1 | patchy calcite - open fracture |
| 15.58 | -11.3 | 22.5 | patchy calcite |
| 17.08 | -13.5 | 22.6 | calcite with quartz and laumontite |
| 112.67 | -4.3 | 9.0 | vein with $FeS_2$ & laumontite (Plate XVIIa) |
| 118.76 | -11.22 | 22.7 | thick calcite wedge in open fracture |
| 123.62 | -7.4 | 19.6 | coarse crystalline calcite |
| 261.00 | -3.5 | 8.7 | thick, massive, clear calcite vein |
| 625.15 | -2.3 | 9.0 | |
| 755.10 | -2.2 | 9.4 | calcite vein with $FeS_2$ |
| 758.92 | -3.0 | 8.1 | patchy calcite |
| 806.72 | -2.7 | 10.4 | thick patchy calcite |
| 819.30 | -2.9 | 12.4 | filmy calcite with $FeS_2$ on chlorite |
| EBL-4 112.46 | -4.2 | 13.5 | quartz-calcite vein (Plate XVIc) |
| 115.76 | -4.2 | 8.5 | sealed quartz-calcite vein |
| 122.13 | -3.1 | 21.2 | patchy calcite with pyrrhotite |
| 168.80 | -4.0 | 17.4 | patchy calcite with quartz & chlorite (Plate XVIb) |
| 168.98 | -3.3 | 15.8 | patchy calcite on chlorite |
| 184.54 | -3.8 | 19.5 | |
| 184.57 | -3.7 | 14.1 | |
| 208.53 | -3.6 | 19.6 | vein, top contact |
| 208.53 | -2.9 | 9.9 | vein, centre |
| 208.53 | -3.4 | 14.6 | vein, bottom contact |
| 446.35 | -3.4 | 13.6 | patchy calcite with laumontite (Plate XVIIb) |
| 455.98 | -3.4 | 15.2 | patchy calcite on chlorite, open fracture |
| 459.55 | -3.7 | 20.4 | patchy calcite on chlorite, open fracture |

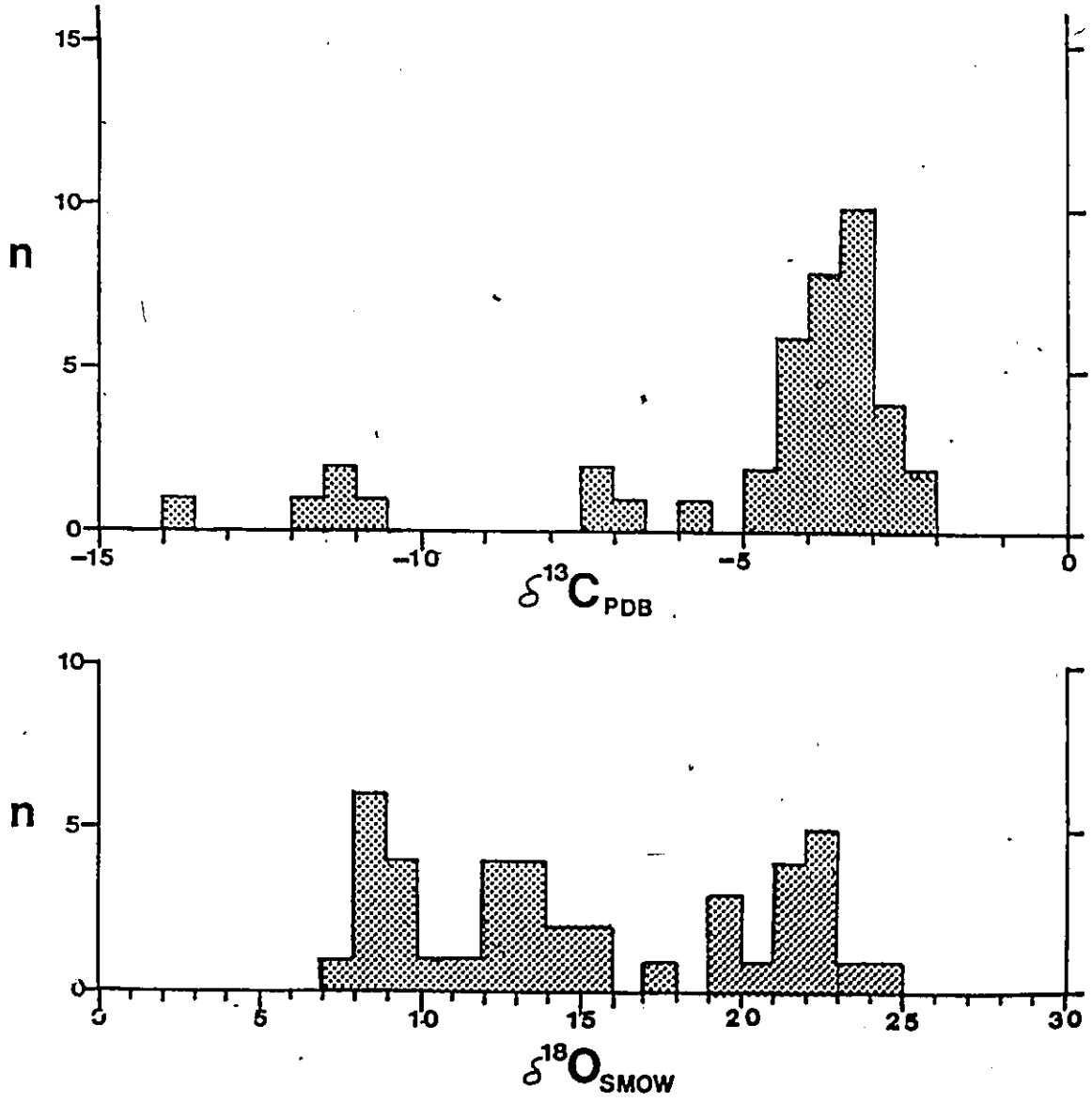


Fig. 44. Histograms of the $\delta^{13}C$ and $\delta^{18}O$ contents of EBL calcites.

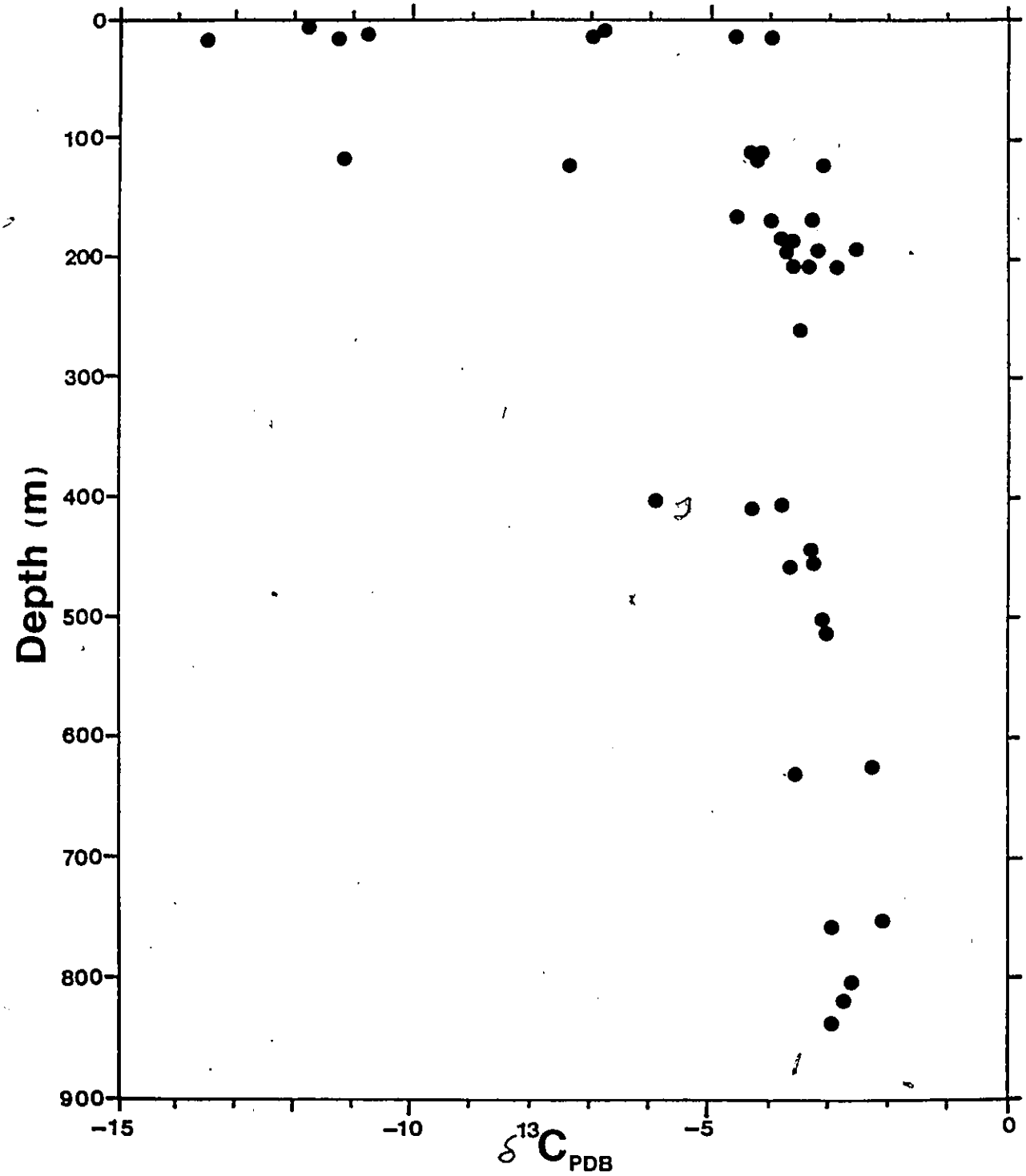


Fig. 45. Variations in the $\delta^{13}C$ contents of EBL calcites with borehole depth.

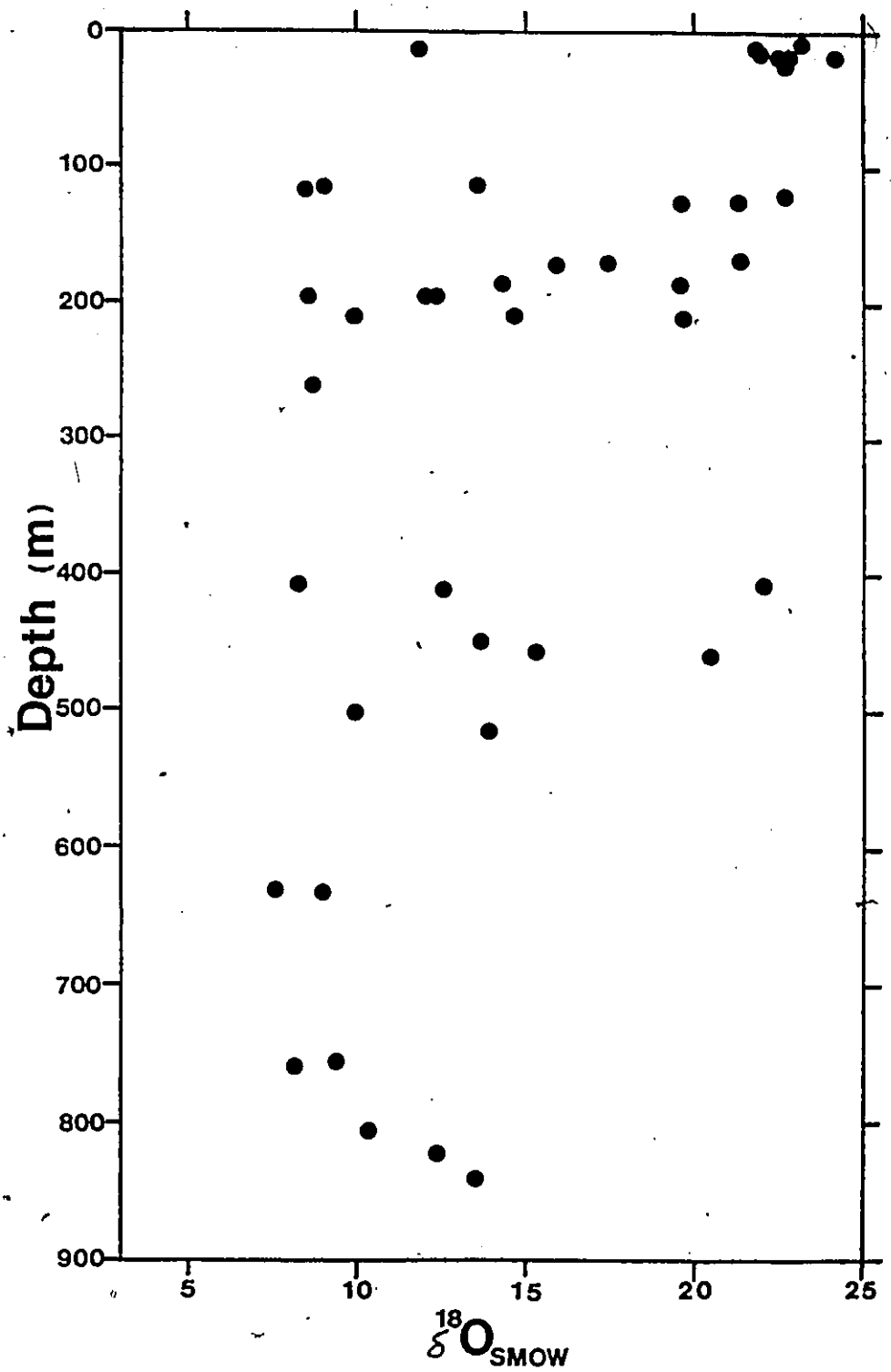


Fig. 46. Variations in the $\delta^{18}O$ contents of EBL calcites with borehole depth.

The lightest $\delta^{18}O$ values (7 to 10°/oo) are believed to be calcites that have not exchanged isotopically with meteoric water. These calcites also have $\delta^{13}C$ values of >-5°/oo. The isotopic data are consistent with a hydrothermal origin for this calcite and its association with laumontite suggests a temperature of formation of less than 300°C. At 300°C the $^{18}O$ fractionation factor between calcite and water is 5.5°/oo indicating that the $\delta^{18}O$ of the fluid from which it formed could have ranged from less than 1.5 to 4.5°/oo. However, these are maximum values since minimum temperatures of laumontite formation are poorly constrained. Indeed, laumontite precipitation from spring waters has been documented at temperatures of <50°C. In any case a meteoric origin for the hydrothermal fluid is inferred if these calcites formed at temperatures of less than about 200°C. A marine origin for the fluid is possible if the laumontite formed at temperatures greater than this value although the fluid would have to have been enriched by several °/oo through $^{18}O$ exchange with the host rocks if formation temperatures were near 300°C.

The $\delta^{13}C$ values for most of the EBL calcites are significantly heavier than the CRNL calcites. This could be a consequence of higher pH for the fluids in the EBL pluton at the time of calcite precipitation compared to the CRNL pluton and does not require that the $\delta^{13}C_{\Sigma C}$ values of the two sites be significantly different. Mafic rocks are more reactive to fluids than granitic rocks resulting in higher fluid pH. Even today

meteoric ground water in the EBL pluton has maximum pH values that are much larger (>10) than those of the CRNL ground waters (<9) (Table 3). Therefore pH contrasts between the two sites may have been the parameter controlling the differences in $\delta^{13}C$ values of the hydrothermal calcites. It is unlikely, however, that the carbon initially dissolved in meteoric recharge water was the major source of calcite C since such waters normally have $\delta^{13}C_{DIC}$ values significantly lighter than $-5^{o}/oo$ because of major inputs of biogenic $CO_2$. Both the heavy $\delta^{13}C$ and light $\delta^{18}O$ values are most simply explained by additions of deep crustal or mantle $CO_2$ to a hydrothermal system dominated by meteoric water.

It is apparent from Figs. 45 and 46 that significant shifts in the $^{18}O$ and $^{13}C$ contents of the hydrothermal calcites have subsequently occurred in specific zones. The large positive shifts in $\delta^{18}O$ values from the baseline values of $<10^{o}/oo$ are almost certainly the result of low temperature exchange with cool, meteoric ground water. These large $^{18}O$ shifts are accompanied by large negative $^{13}C$ shifts only at relatively shallow depths. Hence isotopic equilibrium between the present day ground water and the fracture calcites is approached only in the shallow subsurface. These observations suggest that the isotopic shift is the result of solution-reprecipitation processes and that the magnitude of the shift is controlled by the time-integrated water/rock ratio of the flow system in the EBL pluton.

Although fewer EBL fracture calcites have been analyzed, the $^{18}O$-$^{13}C$ relationship observed for the CRNL calcites also appears to exist at EBL (Fig. 33). The isotopic evolution curve "D-E" for the EBL calcites was drawn assuming that hydrothermal calcite having an initial $\delta^{18}O$ of $8^{o}/oo$ (SMOW) and a $\delta^{13}C$ of $-2.5^{o}/oo$ recrystallized in a meteoric ground water flow system that was isotopically open with respect to O but closed with respect to C. It is also assumed that the $\delta^{18}O$ of the ground water was $-10^{o}/oo$ and that recrystallization occurred at a temperature of 8°C. This $\delta^{18}O$ value of $-10^{o}/oo$ is slightly larger than the maximum value measured for the present day ground waters in the pluton. Furthermore, a DIC concentration of 3 mM $L^{-1}$ with a $\delta^{13}C$ of $-15^{o}/oo$ has been assumed. As with the CRNL isotopic evolution curves, tick marks on curve "D-E" correspond to w/r ratios of 10, $10^2$, $10^3$, $10^4$, $5x10^4$, and $10^5$. While the lightest $\delta^{13}C$ values for the EBL calcites appear to require w/r ratios as large as the maximum values calculated for the CRNL calcites ($\sim 10^5$), these high values are mainly restricted to depths of less than 25 m (Fig. 45). Most of the other isotopic values could be produced by w/r ratios of $<10^3$ to $10^4$. The cumulative frequency plot for the EBL calcites indicates that the median $\delta^{13}C$ value is $\sim -4^{o}/oo$ (Fig. 47). This suggests that an average w/r ratio for the EBL pluton is close to $\sim 10^3$, as opposed to $\sim 10^4$ for the CRNL pluton. Therefore the lower average w/r ratio for the EBL pluton is consistent with the results of borehole hydraulic testing which have shown that the EBL pluton has a relatively low permeability except where intersected by major structural discontinuities..

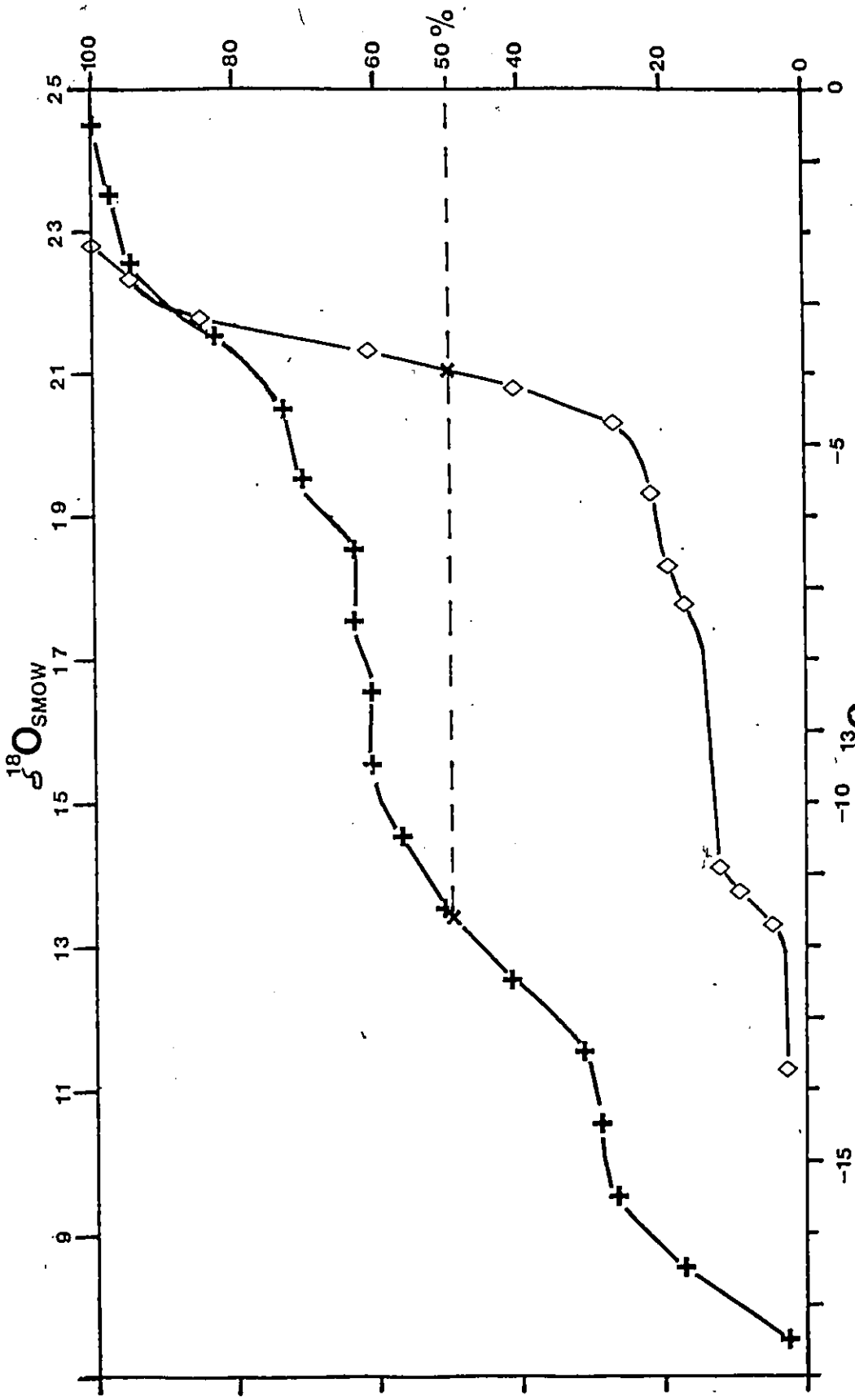


Fig. 47. Cumulative frequency plots for the $\delta^{13}C$ (diamonds) and $\delta^{18}O$ (crosses) contents of EBL calcites.

## 10. ISOTOPIC COMPOSITION OF WHITE LAKE CARBONATES

The isotopic compositions of fracture calcites from the White Lake pluton and of the marbles into which it intrudes are listed in Table 20. The $\delta^{13}C$ values for the fracture calcites are variable and unlike the CRNL and EBL fracture calcites several of these samples have values greater than $0^{o}/oo$. The $\delta^{18}O$ values range from 15.3 to $21.8^{o}/oo$. The calcite fraction of the marbles on the northern periphery of the pluton have $\delta^{13}C$ values ranging from $-0.1^{o}/oo$ to $6.2^{o}/oo$ while the dolomite component ranges from $0.2^{o}/oo$ to $6.6^{o}/oo$. With the exception of samples WLS-5, 8, and 9 the dolomite component is slightly richer in $^{13}C$ and $^{18}O$ than the coexisting calcite fraction. The differences in $\delta$ values between the calcite and dolomite pairs are, however, non uniform. Samples with the calcite component richer in $^{13}C$ and $^{18}O$ than the dolomite are clearly disequilibrium assemblages.

Sample WLS-3 was a tremolite-rich sample low in carbonate but the other samples had carbonate contents greater than 80% by weight. Calcite was the predominant carbonate component except for sample WLS-4. The differences in $^{18}O$ and $^{13}C$ of coexisting calcite and dolomite have been used to estimate their temperature of formation from the equations of Sheppard and Schwarcz (1970) in (Eqs. 19 and 20) and Matthews and Katz (1977) (Eq. 21). and the results of these calculations are shown in Table 21. The general lack of agreement between the O and C isotopic thermometers suggests the calcite and dolomite formed

Table 20. Carbon and oxygen isotopic composition of White Lake carbonates

| Fracture Calcites- WL Pluton Borehole and Depth (m) | | $\delta^{13}C_{PDB}$ | $\delta^{18}O_{SMOW}$ | Comments |
|---|---|---|---|---|
| WL1- | 18.1 | -2.2 | 16.6 | patchy calcite on inclined open fracture |
| | 33.2 | -0.5 | 16.5 | patchy calcite with $Fe_2O_3$ - open |
| | 33.5 | -0.7 | 16.0 | filmy calcite |
| | 34.1 | -2.0 | 16.1 | calcite on $Fe_2O_3$, sub-vertical |
| | 34.8 | -5.4 | 21.8 | patchy calcite, vertical open fracture |
| | 36.6 | -4.4 | 17.7 | patchy calcite, inclined open fracture |
| | 65.8 | 0.2 | 15.3 | patchy calcite on quartz-chlorite vein |
| | 67.4 | 3.0 | 20.2 | patchy calcite with $Fe_2O_3$ |
| | 71.3 | 1.4 | 18.6 | patchy calcite with $Fe_2O_3$ |
| | 72.7 | 2.5 | 19.6 | patchy calcite with $Fe_2O_3$ (Plate XVIIIb) |
| | 72.7 | -1.4 | 21.2 | patchy calcite with $FeS_2$, open (Plate XVIIIc) |
| | 72.7 | 2.1 | 15.5 | sealed vein (Plate XVIIIa) |
| | 73.78 | 0.7 | 16.4 | patchy calcite with $Fe_2O_3$, open |
| | 73.83 | 0.8 | 15.5 | coarse, crystalline calcite vein |
| | 73.88 | 0.6 | 18.2 | patchy calcite with $FeS_2$, open |
| WL2- | 9.8 | -4.6 | 17.7 | patchy calcite with $Fe_2O_3$, open |
| | 14.2 | -3.2 | 18.7 | patchy calcite with $Fe_2O_3$, open |
| | 20.7 | -4.9 | 18.4 | patchy calcite |
| WL3- | 4.6 | -5.6 | 18.5 | calcite with chlorite, reactivated vein |
| WL4- | 30.5 | -3.2 | 22.1 | calcite vein |

| Marbles Sample No. | | | | Wt % |
|---|---|---|---|---|
| WLS-1 | 4.7 | 23.5 | calcite | 64.9 |
| WLS-1 | 5.1 | 23.7 | dolomite | 30.8 |
| WLS-2 | 3.0 | 26.8 | calcite | 63.1 |
| WLS-2 | 3.4 | 27.3 | dolomite | 24.9 |
| WLS-3 | -0.1 | 19.5 | calcite | 1.0 |
| WLS-3 | 0.2 | 19.8 | dolomite | 0.5 |
| WLS-4 | 2.0 | 21.6 | calcite | 8.3 |
| WLS-4 | 3.2 | 22.9 | dolomite | 72.2 |
| WLS-5 | 1.2 | 23.3 | calcite | 80.4 |
| WLS-5 | 0.9 | 22.5 | dolomite | 11.1 |
| WLS-6 | 4.9 | 21.2 | calcite | 77.8 |
| WLS-6 | 5.3 | 21.6 | dolomite | 15.0 |
| WLS-7 | 1.1 | 18.2 | calcite | 12.3 |
| WLS-7 | 1.8 | 18.6 | dolomite | 49.3 |
| WLS-8 | 6.2 | 26.0 | calcite | 73.5 |
| WLS-8 | 6.3 | 25.7 | dolomite | 22.5 |
| WLS-9 | 5.8 | 25.2 | calcite | 65.4 |
| WLS-9 | 5.9 | 24.7 | dolomite | 27.7 |
| WLS-10 | 6.1 | 26.7 | calcite | 71.5 |
| WLS-10 | 6.6 | 27.2 | dolomite | 21.5 |

Table 21. Isotopic fractionations and temperatures (°C) for White Lake dolomite-calcite pairs

| Sample | $\Delta^{18}O$ (°/oo) | $\Delta^{13}C$ (°/oo) | $T^{1}_{18}O$ | $T^{2}_{18}O$ | $T^{1}_{13}C$ | Wt % Calcite | Wt % Dolomite |
|---|---|---|---|---|---|---|---|
| WLS-1 | 0.2 | 0.4 | 593 | 585 | 612 | 64.9 | 30.8 |
| WLS-2 | 0.5 | 0.4 | 434 | 369 | 612 | 63.1 | 24.9 |
| WLS-3 | 0.3 | 0.3 | 529 | 491 | 904 | 1.0 | 0.5 |
| WLS-4 | 1.3 | 1.2 | 242 | 162 | 145 | 8.3 | 72.2 |
| WLS-5 | -0.8 | -0.4 | - | - | - | 80.4 | 11.1 |
| WLS-6 | 0.4 | 0.4 | 477 | 422 | 612 | 77.8 | 15.0 |
| WLS-7 | 0.4 | 0.7 | 477 | 422 | 310 | 12.3 | 49.3 |
| WLS-8 | -0.3 | 0.1 | - | - | - | 73.5 | 22.5 |
| WLS-9 | -0.5 | 0.1 | - | - | - | 65.4 | 27.7 |
| WLS-10 | 0.5 | 0.5 | 434 | 369 | 465 | 71.5 | 21.5 |

[1] calculated from equations of Sheppard and Schwarcz (1970)

[2] calculated from equations of Matthews and Katz (1977)

in isotopic disequilibrium. There is also large variability in formation temperatures calculated by either the O or C equation with an average temperature of ~400°C (Matthews and Katz, 1977) or 455°C (Sheppard and Schwarcz, 1970) calculated on the basis of $^{18}O$ differences and 480°C using $^{13}C$. Samples nearer the pluton contact are, however, more depleted in $^{18}O$ and $^{13}C$ relative to more distant samples. The range in $\delta^{18}O$ values between sample sites is about $8^{o}/oo$ and the $^{13}C$ range is about $7^{o}/oo$. It is likely that isotopic depletion of the marbles is related to the intrusion of pluton and could be caused by decarbonation reactions or by isotopic exchange with magmatic hydrothermal fluids during contact metamorphism (Valley, 1986).

The isotopic compositions of the marbles and of the fracture calcites from the pluton are shown in the $^{13}C$-$^{18}O$ plot of Fig. 48 which suggests that many of these samples lie along the same trend line and are genetically related. This could be produced by isotopic exchange between the marble and thermal fluids convectively driven by the heat of the intrusion and is analagous to the previously described isotopic alteration of hydrothermal fracture calcite by cool meteoric ground waters. However, in this case the $^{18}O$ shift experienced by the $^{18}O$-rich marbles is in the opposite direction to that of the low $^{18}O$ hydrothermal fracture calcites at CRNL.

The curve drawn in Fig. 48 was constructed to demonstrate how the isotopic composition of the White Lake marbles could be lowered by exchange with ground water by contact meta-

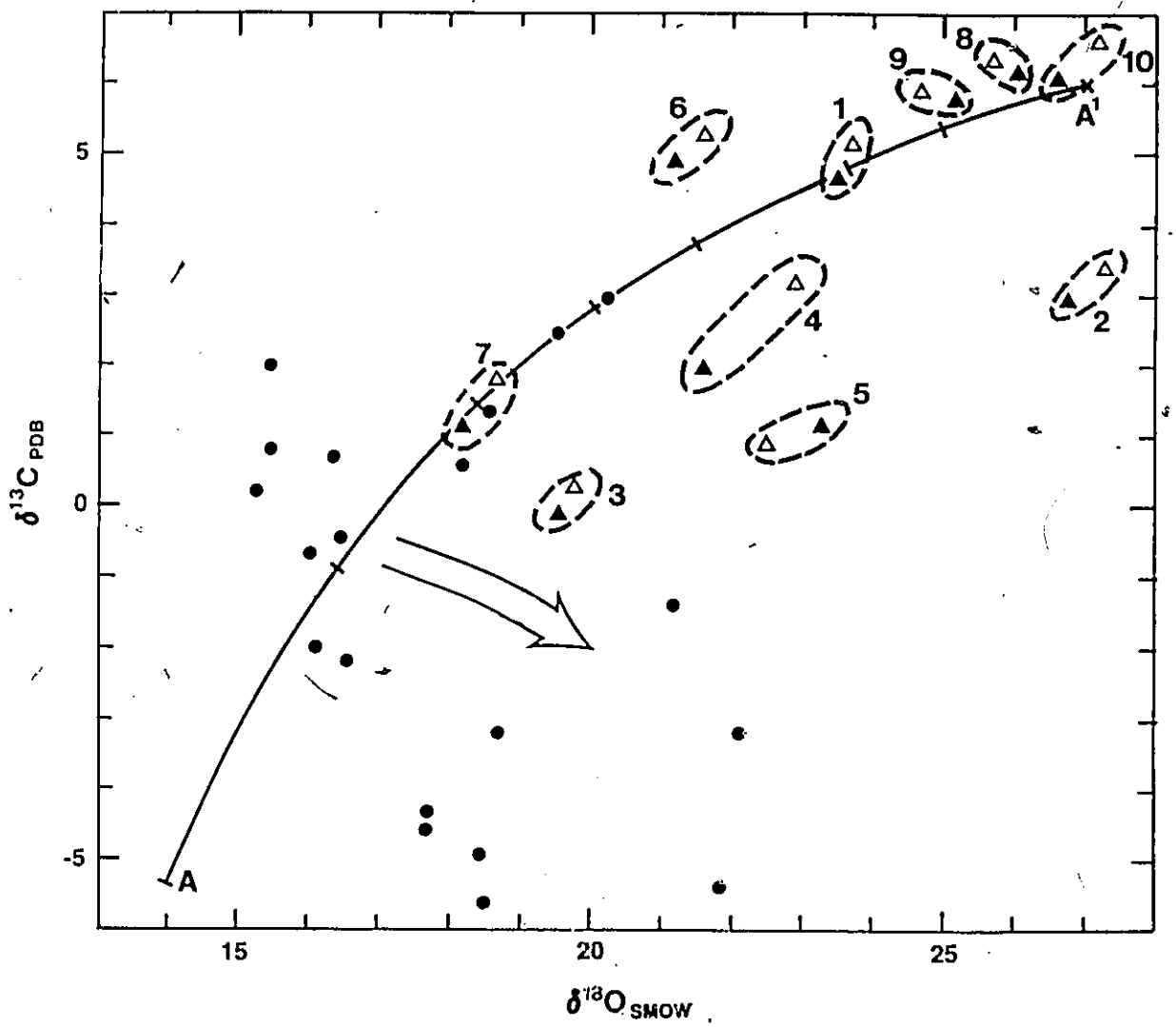


Fig. 48. Plot of $\delta^{13}C$ vs. $\delta^{18}O$ for White Lake fracture calcites (solid dots) and marble calcites (solid triangles) and dolomites (open triangles) from sites shown in Fig. 6. Curve AA' represents the isotopic composition of secondary calcites formed by mixing O and C derived from the marble (point A') with magmatic $CO_2$ having a $\delta^{13}C$ of -5°/oo dissolved in a thermal water (400°C) with a $\delta^{18}O$ of 10°/oo (SMOW). Tick marks represent closed system water/rock mole ratios of 0.5, 1, 2, 3, 5, 10 and 50 (see text). Arrow indicates isotopic trend for fracture calcites that have subsequently exchanged with low temperature meteoric waters.

morphism during intrusion of the pluton. In this example a temperature of 400°C has been assumed and $CO_2$ is taken as the dominant C species in solution. The mole fraction of $CO_2$ in the fluid ($X_{CO_2}$) has been estimated at 0.1 for modelling purposes and is based on the curvature of the trend shown in Fig. 48 (Taylor and Bucher-Nurminen, 1986). Unexchanged carbonate rock is represented by the isotopic composition of point A[1] ($\delta^{18}O$ = 27°/oo and $\delta^{13}C$ = 6°/oo). Exchange with magmatic $CO_2$ associated with the plutonism and having a $\delta^{13}C$ of -5°/oo is assumed. The $\delta^{18}O$ of the fluid is taken as +10°/oo which could be produced by an $^{18}O$ shift of meteoric water by exchange with the $^{18}O$-rich country rocks. This does not preclude however, the possibility of a significant component of magmatic water (~+5°/oo) in this fluid. Furthermore, the modelled curve assumes closed system exchange which would be a good approximation if a convective hydrothermal system was established at the time of intrusion. Water/ rock mole ratios of 0.5, 1, 2, 3, 5, 10 and 50 are shown as tick marks on the curve, in increasing order toward lighter isotopic compositions.

The limitations of the existing data base for the White Lake pluton preclude rigorous constraints on the parameter values used in the construction of the isotope exchange curve. Nevertheless fluid mixing and isotopic exchange between magmatic and sedimentary C reservoirs would appear to be a viable explanation for the origin of the fracture calcites in the White Lake pluton. It is necessary to mention however that similar coupled

trends in $\delta^{13}C$-$\delta^{18}O$ plots can result from Rayleigh volatilization of $CO_2$ during high temperature decarbonation of sedimentary carbonates (Valley, 1986). This arises from the fact that at 400°C both $^{13}C$ and $^{18}O$ isotopes are preferentially incorporated in $CO_2$ relative to calcite.

Curve AA' in Fig. 49 shows the expected trend in the isotopic evolution of carbon in calcite from its initial value of 6°/oo during the Rayleigh distillation of $CO_2$ from the rock as calculated by the following relationship from Broecker and Oversby (1971):

$$(25) \qquad \delta^{13}C_{cc} = \delta^{13}C^{i}_{cc} - 1000\,(1 - F^{\alpha-1})$$

where $\alpha$ is the fractionation factor for C between calcite (cc) and $CO_2$ and F is the fraction of carbonate remaining in the rock. Curve BB' is the trend in the $\delta^{18}O$ of marble calcite during Rayleigh distillation of $CO_2$. Note that during Rayleigh volatilization the $^{13}C$ depletion is small until F is reduced to about 50%. A similar relationship occurs if dolomite-$CO_2$ fractionation factors are used. In contrast the carbonate contents of the White Lake marbles are, with one exception, greater than 80% by weight yet large variations in both $^{13}C$ and $^{18}O$ are observed (Fig. 49). This suggests that decarbonation is not the primary cause of isotopic depletions in these marbles.

Positive $\delta^{13}C$ values in hydrothermal calcites can not in themselves be used as criteria for the recognition of a sedimentary C component since $\delta^{13}C$ values as high as ~20°/oo are possible for calcites if the hydrothermal fluid is alkaline and

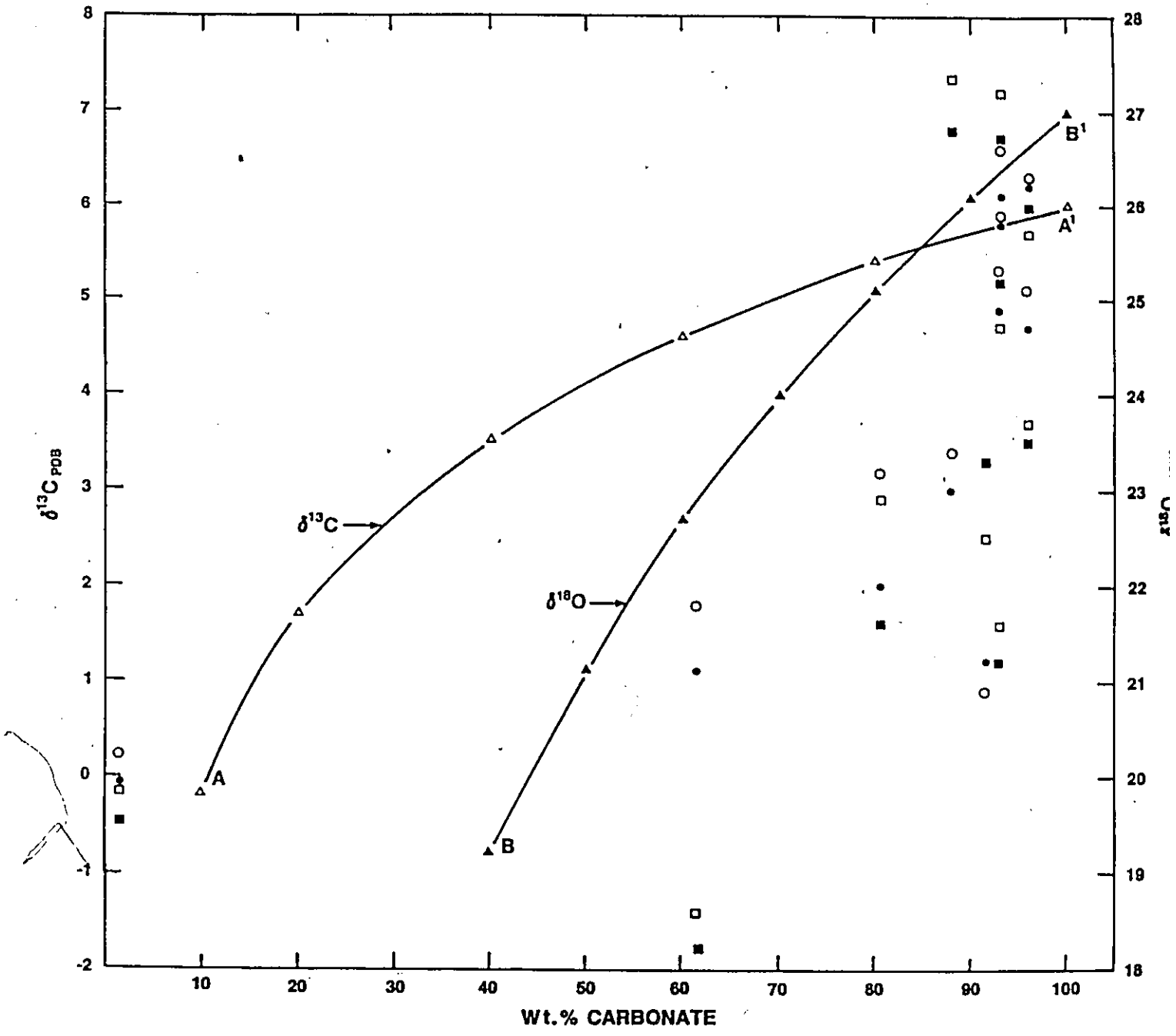


Fig. 49. Plot of the $\delta^{13}C$ of the calcite (solid dots) and dolomite (open circles) components and the $\delta^{18}O$ of the calcite (solid squares) and dolomite (open squares) components as a function of the carbonate content (wt %) of White Lake marbles (Fig. 6). Curves AA' and BB' represent the $\delta^{13}C$ and $\delta^{18}O$, respectively, of marble during the progressive Rayleigh distillation of $CO_2$ (see text). Note lack of correlation between predicted distillation trends and measured isotopic values.

has low $f_{O_2}$ (Ohmoto, 1972). However the apparent coupling of $^{18}O$-$^{13}C$ depletions in the marbles to isotopic trends in the fracture calcites suggests that fluid interactions with the marble country rock was an important source of C for the fracture calcites in the pluton.

A secondary trend of $^{18}O$ enrichment as the result of isotope exchange between the fracture calcites and recent meteoric ground water should also be expected if the model proposed for the isotopic evolution of fracture calcites at CRNL and EBL is of general applicability. Such a trend may be present in the White Lake data (Fig. 48) but additional drilling and fracture calcite sampling would be required to verify this. Unlike the CRNL and EBL calcites the isotopic composition of the hydrothermal calcites at White Lake are more variable because of their mixed isotopic origins. Consequently isotopic shifts due to low temperature exchange reactions are more difficult to identify than at CRNL or EBL.

# 11. IMPLICATIONS OF THE RESULTS OF THIS STUDY TO THE CANADIAN CONCEPT FOR NUCLEAR WASTE DISPOSAL

Within the Canadian Nuclear Fuel Waste Management Program considerable effort has been expended on assessing the potential for the long term release and transport of radionuclides by ground water from the waste disposal vault to the biosphere. Atomic Energy of Canada Ltd. has developed a computer code (SYVAC) to quantify radionuclide release rates and to estimate radiation exposures for individuals who reside in areas where radionuclides may eventually reach the surface (Sherman et al., 1985). Simulations have been performed for up to $10^7$ years after disposal.

The geosphere submodel of this code calculates the transport of radionuclides from the vault and through fractured plutonic rock which is the host medium for the waste vault. In this submodel ground water transit times are calculated based on borehole measurements of the hydraulic conductivity of the plutons at the AECL research areas and using (at depths of <200 m) equivalent porous medium flow modelling methods. It has not been determined whether construction of discrete or stochastic fracture flow models would provide more realistic results.

Stable isotope analyses of CRNL fracture calcites show that even in highly fractured rock such as the CRNL pluton ground water movement is controlled by flow channelling along

discrete fractures. Some of these pathways have experienced large time-integrated water/rock ratios while other portions of the same fracture appear to have remained sealed since the precipitation of hydrothermal calcite several hundred million years ago. Analyses of the $^{234}U/^{230}Th$ activity ratios of CRNL fracture calcites (Milton and Brown, 1987) and their $^{14}C$ activities have shown that some calcites have recrystallized in the last 50,000 years and that, in fact, this process has continued to the present time. Thus the isotopic record of CRNL fracture calcites is clearly incompatible with an equivalent porous medium interpretation of ground water flow in the pluton and would argue for the adoption of a discrete fracture flow model in the SYVAC computer code. Groundwater velocities calculated by this model may be significantly greater than those calculated by porous media models.

It should also be clear that ground water pathways in fractured rock are not static systems but rather they adjust to changing hydrochemical regimes (which may alter the nature of fracture infillings) or stress conditions in the upper crust. Therefore long term predictions ($>\sim 10^4$ years) on the nature of ground water flow in the pluton are inheritantly problematical.

The stable isotope compositions of fracture calcites from the CRNL, EBL, WL (White Lake), and WNRE (Whiteshell Nuclear Research Establishment on the Lac du Bonnet batholith) research areas are shown in $\delta^{13}C$-$\delta^{18}O$ co-ordinate space as general fields within which most of the data from each site plot (Fig. 50). Arrows in the CRNL, EBL, and WL fields indicate the pre-

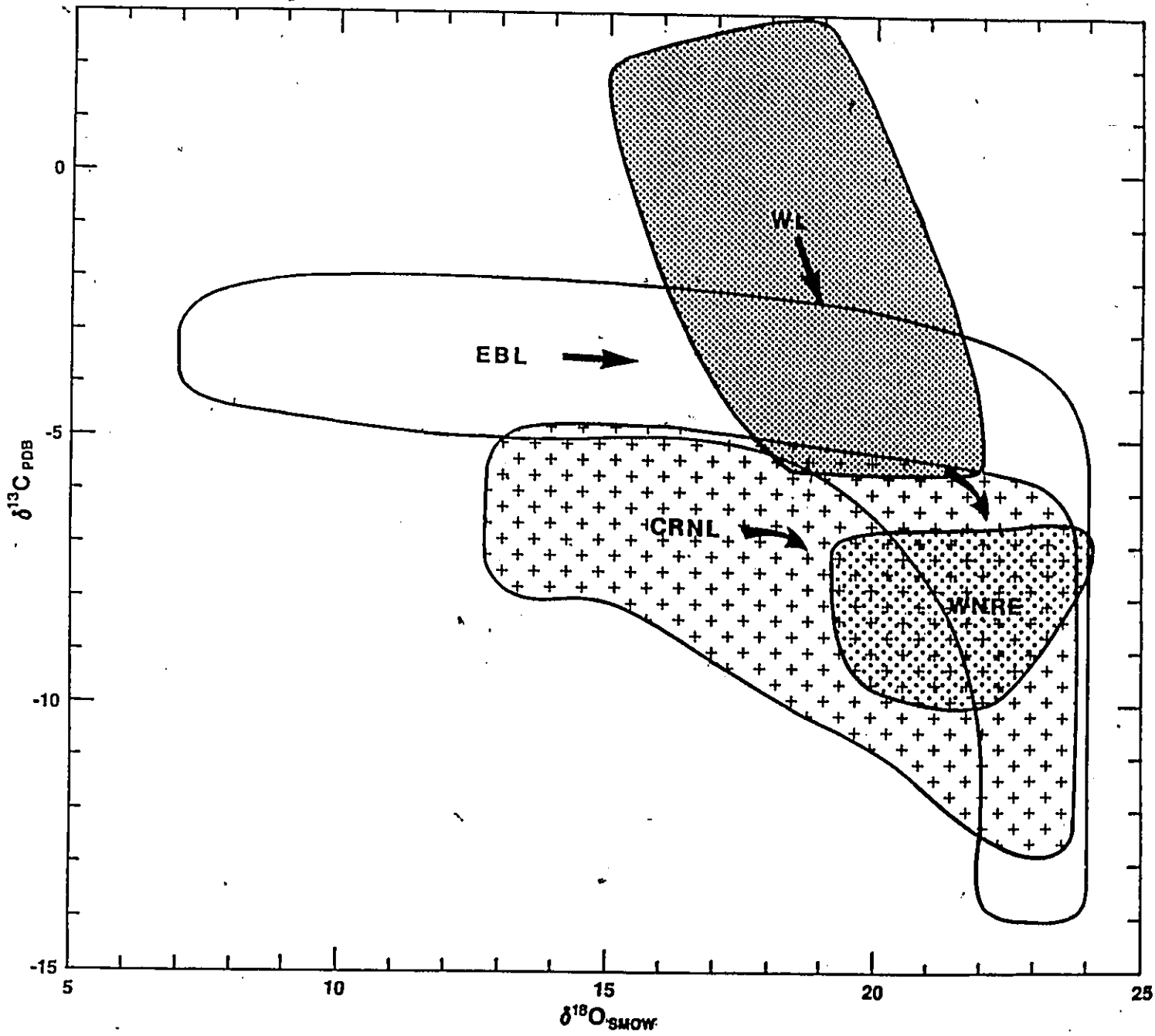


Fig. 50. Comparison of the $\delta^{13}C$ and $\delta^{18}O$ values of fracture calcites from the CRNL, EBL, WL, and WNRE research areas. Arrows indicate the present directional trend in the isotopic evolution of the calcites. The WNRE field is based on data of Bottomley et al. (1980).

sent day evolutionary trends in the isotopic compositions of these calcites as the result of recrystallization. The nature of these trends is to produce recrystallized calcites that approach to varying degrees isotopic equilibrium with the $\delta^{18}O$ and $\delta^{13}C_{DIC}$ of the ambient ground water. Recrystallized calcites tend to be heavier in $\delta^{18}O$ and lighter in $\delta^{13}C$ than the precursor calcites at each site. However the magnitude of the isotopic shift of individual calcites has been controlled by the time-integrated water/rock ratios along individual flow channels in the fractures. The isotopic data from all research areas are thus complementary and support the conclusion that ground water movement and radionuclide transit times in fractured plutonic rock would be most accurately described by discrete fracture flow modelling.

# 12. CONCLUSIONS

Based on the chemical and isotopic data, and on the textural evidence collected during the course of this investigation it can be concluded that the fracture calcites in the CRNL core are of hydrothermal origins. The Sr isotopic data indicate this hydrothermal activity probably occurred several hundred million years after emplacement of the host plutonic rocks approximately 1345 Ma ago. Based on the occasional co-existence of laumontite with calcite it is likely that calcite precipitation occurred at temperatures of <300°C. Isotope geothermometry on calcite-dolomite pairs provides contradictory estimates of precipitation temperatures and it is apparent that the C and O compositions are not in isotopic equilibrium.

Chemical and isotopic analyses of the calcites indicate they are not in equilibrium with the present day ground waters. Strontium concentrations in the calcites are much lower than predicted on the basis of the (Sr/Ca) mole ratios of the ground water if it were assumed the calcites were recent precipitates. In addition, there is no evidence that the calcites formed from saline solutions with high (Na/Ca) mole ratios. The REE contents of the calcites are much larger than the host rocks but the chondrite-normalized REE patterns are similar. Both are enriched in LREE and are characterized by a steep slope in the LREE enrichment pattern. It is clear that the REE contents of the calcites were derived from the host pluton.

The $\delta^{18}O$ of the CRNL fracture calcites exhibit a broad range in values from 14-23°/oo (SMOW) except for a small group of samples that are much lighter in $\delta^{18}O$ (0 to +9°/oo). In contrast most of the $\delta^{13}C$ values fall in a narrow range between -5.5 to -8.8°/oo. There is no well defined depth relationship for either isotope but sharp inter- and intra-fracture isotopic variations occur that are unlikely to be primary features produced by fluid mixing during the formation of the hydrothermal calcites. The large isotopic variations, particularly in the case of $^{18}O$, are interpreted to be the result of recrystallization in recent meteoric ground water under variable water/ rock ratios. This recrystallization has occurred in a system that is physically open to water (i.e. a "single pass" system) and chemically open with respect to oxygen. However, because of low DIC concentrations in the ground water, the system approximates a closed system with respect to C. Mole ratios of water/ rock approaching $10^5$ have been required to produce those calcites that are lightest in $\delta^{13}C$.

Recrystallization of fracture calcite is a bulk solution disequilibrium process in which much of the C in the recrystallized calcite is inherited from the precursor calcite. In this regard this process is entirely analogous to the recrystallization of high-Mg marine calcites in diagenetic sedimentary environments that are physically open to flushing of the pore space by meteoric ground waters. The presence of small amounts of $^{14}C$ in isotopically exchanged calcites indicates that recrystallization is an ongoing process even at the present time.

Calcite recrystallization controls the (Sr/Ca) mole ratio of the ground water and its Sr isotopic composition. The dissolution of silicates is not a major source of dissolved $Sr^{2+}$ in the $Na/HCO_3$ or Na/Cl waters at CRNL. Nevertheless the present day ground water has a slightly more radiogenic $^{87}Sr/^{86}Sr$ ratio than the end member hydrothermal calcite. Consequently the $^{87}Sr/^{86}Sr$ of recrystallized calcites depends on the extent of mixing between micropore and macropore (fracture) water at the site of recrystallization. It is evident, however, that, as in the case of C, the Sr isotopic ratio of the precursor calcite is the dominating control on the Sr isotopic composition of recrystallized calcite.

Fracture calcites from East Bull Lake pluton exhibit similar trends in $\delta^{13}C$-$\delta^{18}O$ co-ordinate space as the CRNL calcites. However the largest isotopic shifts in the EBL calcites are mainly restricted to the higher permeablility zones in the shallow subsurface (<25 m deep). Isotopic shifts as the result of recent recrystallization are not as apparent in the fracture calcites of the White Lake pluton because of the wider range in the initial $\delta^{13}C$ and $\delta^{18}O$ values of the original hydrothermal calcite. This variability resulted from the mixing of magmatic and sedimentary C reservoirs caused by the intrusion of the pluton into permeable carbonate country rocks.

Large inter- and intra-fracture isotopic shifts over short distances are consistent with the concept of flow channeling in fractures. Fracture calcites that occur within the

channel are subject to higher water/rock ratios than calcite that is isolated from the active flow channels. It is necessary to stress, however, water/rock ratios calculated on the basis of isotopic shifts are time-integrated values because flow pathways within fractures may vary as the result of changing stress regimes in the crust, filling of old pathways by the formation of fracture minerals, or by changes in ground water chemistry that could lead to the dissolution of old infillings and the reactivation of previously sealed pathways.

The results of this investigation are relevant to the Canadian concept for the disposal of nuclear wastes in plutonic rock in two respects. Firstly, isotopic analyses of fracture calcites can differentiate fractures that have experienced large time-integrated water/rock ratios from those that have not. Therefore this technique may be able to identify zones within a potential plutonic repository that have been less permeable to ground water flow than others over geologic time scales. Secondly, the isotopic data support the adoption and application of discrete fracture ground water flow models within the CNFWMP to describe and predict ground water flow in fractured plutonic rock even at shallow depths.

## REFERENCES

Addy, S.K. (1979). Rare earth element patterns in manganese nodules and micronodules from northwest Atlantic. Geochim. Cosmochim. Acta 43, 1105-1115.

Al-Aasm, I. and Veizer, J. (1986a). Diagenetic stabilization of aragonite and low-Mg calcite, 1. Trace elements in rudists. J. Sed. Petrology 56, 138-152.

Al-Aasm, I. and Veizer, J. (1986b). Diagenetic stabilization of aragonite and low-Mg calcite, 2. Stable isotopes in rudists. J. Sed. Petrology 56, 763-770.

Arima, M., Kerrich, R. and Thomas, A. (1986). Sapphirine-bearing paragneiss from the northern Grenville province in Labrador, Canada: protolith composition and metamorphic P-T conditions. Geology 14, 844-847.

Baer, A.J. (1981). Two orogenies in the Grenville Belt? Nature 290, 129-131.

Bell, K. and Blenkinsop (1980). Whole rock Rb-Sr studies in the Grenville province of Southeastern Ontario and Western Quebec - A summary report. In Current Research Part C, GSC Paper 80-1C, 152-154.

Bell, K. and Blenkinsop (1984). Multiple collection in solid-source mass spectrometry. Geoscience Canada 11, 50-52.

Beukens, R. (1986). Research activities - radiocarbon dating. Isotrace Newsletter 3, 8-10.

Bickle, M.J. and Powell, R. (1977). Calcite-dolomite geothermometry for iron-bearing carbonates. The Glockner area of the Tauern window, Austria, Contrib. Mineral. Petrol. 59, 281-292.

Bischoff, J.L. and Dickson, F.W. (1975). Seawater-basalt interaction at 200°C and 500 bars: implications for origin of sea floor heavy metal deposits and regulation of seawater chemistry. Earth Planet. Sci. Letters 25, 385-397.

Bodine, M.W., Holland, H.D. and Bocsik, M. (1965). Co-precipitation of manganese and strontium with calcite. In Problems of Postmagmatic Ore Deposition - Proc. Symp., Prague, 2, 401-406.

Boles, J.R. and Combs, D.S. (1977). Zeolite facies alteration of sandstones in the Southland syncline, New Zealand. Am. J. Sci. 277, 982-1012.

Bottinga, Y. (1968). Calculation of fractionation factors for carbon and oxygen exchange in the system calcite-carbon dioxide-water. Jour. Phys. Chemistry 72, 800-808.

Bottomley, D., Graham, B. and Ross, J. (1980). Investigations into the geochemistry of groundwater in Precambrian crystalline rocks. A.E.C.L. Tech. Rec. TR-122, 36 pp.

Bottomley, D.J., Ross, J.D. and Graham, B.W. (1984). A borehole methodology for hydrogeochemical investigations in fractured rock. Water Resources Research 20, 1277-1300.

Bottomley, D.J., Ross, J.D. and Clarke, W.B. (1984). Helium and neon isotope geochemistry of some ground waters from the Canadian Precambrian Shield. Geochim. Cosmochim. Acta 48, 1973-1985.

Bottomley, D.J., Gascoyne, M., Ross, J.D. and Ruttan, J.T. (1986). Hydrogeochemistry of the East Bull Lake pluton, Massey, Ontario. A.E.C.L. Tech. Rec. TR-382, 28 pp.

Bowers, T.S. and Helgeson, H. (1983). Calculation of the thermodynamic and geochemical consequences of nonideal mixing in the system $H_2O$-$CO_2$-NaCl on fluids at high pressures and temperatures. Geochim. Cosmochim. Acta 47, 1247-1275.

Brand, U., and Veizer, J. (1980). Chemical diagenesis of a multicomponent carbonate system - 1: Trace elements. J. Sed. Petrology 50, 1219-1236.

Brand, U. and Veizer, J. (1981). Chemical diagenesis of a multicomponent carbonate system - 2: Stable isotopes. J. Sed. Petrology 51, 987-997.

Broecker, W.S. and Oversby, V.M. (1971). Chemical Equilibria in the Earth. McGraw-Hill Book Co., New York, 318 pp.

Brooks, C., Hart, S.R. and Wendt, I. (1972). Realistic use of the two-error regression treatments as applied to rubidium-strontium data. Reviews of Geophysics and Space Physics 10, 551-577.

Brown, P.A., Misiuro, J. and Maxwell, G. (1979). The geological and tectonic history of the Chalk River area, S.E. Ontario. GSC Internal Rept. 6D-INT-909.

Brown, P.A., Rey, N.A.C., McEwen, J.H. and Lau, J.S.O. (1982). The role of fracture characterization in data synthesis modeling. A.E.C.L. Tech. Rec. TR-191, 89 pp.

Brown, S.R. (1987). Fluid flow through rock joints: the effect of surface roughness. J. Geophys. Res. 92, 1337-1347.

Burke, K. and Dewey, J.F. (1973). Plume-generated triple junctions: key indicators in applying plate tectonics to old rocks. J. Geol. 81, 406-433.

Catto, N.R., Patterson, R.J. and Gorman, W.A. (1981). Late Quarternary marine sediments at Chalk River, Ontario. Can. J. Earth Sci. 18, 1261-1267.

Clayton, R.N., Friedman, I., Graf, D.L., Mayeda, T.K., Meents, W.F. and Shimp, N.F. (1966). The origin of saline formation waters: I. Isotopic composition. J. Geophys. Res. 71, 3869-3882.

Clayton, R.N. and Mayeda, T. (1963). The use of bromine pentafluoride in the extraction of oxygen from oxides and silicates for isotopic analysis, Geochim. Cosmochim. Acta 27, 43-52.

Clayton, R.N., O'Neil, J.R. and Mayeda, T.K. (1972). Oxygen isotope exchange between quartz and water. J. Geophys. Res. 77, 3057-3067.

Cole, D.R. and Ohomoto, H. (1986). Kinetics of isotopic exchange at elevated temperatures and pressures. In: Stable Isotopes in High Temperature Geological Processes (J.W. Valley, H.P. Taylor, Jr., J.R. O'Neil eds.), Reviews in Mineralogy 16, 41-90.

Craig, H. (1954). Carbon-13 in plants and the relationships between carbon-13 and carbon-14 variations in nature. J. Geol. 62, 115-149.

Craig, H. (1961). Isotope variations in meteoric waters. Science 133, 1702-1703.

Criss, R.E. and Taylor Jr., H.P. (1983). An $^{18}O/^{16}O$ and D/H study of tertiary hydrothermal systems in the southern half of the Idaho batholith. Geol. Soc. Am. Bull. 94, 640-663.

Criss, R.E. and Taylor Jr., H.P. (1986). Meteoric hydrothermal systems. In: Stable Isotopes in High Temperature Geological Processes (J.W. Valley, Jr., H.P. Taylor, Jr., J.R. O'Neil eds.), Reviews in Mineralogy 16, 373-425.

Dansgaard, W. (1964). Stable isotopes in precipitation. Tellus 16, 436-468.

Dardenne, M. (1967). Etude experimental de la distribution du zinc dans les carbonates de calcium. Bull. Bur. Rech. Geol. Min. 5, 75-110.

Davison, C.C. (1981). Physical hydrogeologic measurements in fractured crystalline rock-summary of 1979 research programs at WNRE and CRNL. A.E.C.L. Tech. Rec. TR-161, 108 pp.

Davison, C.C. (1982). Field-scale tracer migration experiments in fractured crystalline rock at CRNL. In: Chemistry and Geochemistry - Proceedings of the Thirteenth Information Meeting of the Nuclear Fuel Waste Management Program. A.E.C.L. Tech. Rec. TR-201, 325-339.

Davison, C.C., Keys, W.S. and Paillet, F.L. (1982). Use of borehole-geophysical logs and hydrologic tests to characterize crystalline rock for nuclear-waste storage, Whiteshell Nuclear Research Establishment, Manitoba, and Chalk River Nuclear Laboratory, Ontario, Canada. Officer of Nuclear Waste Isolation Rept.-418, 103 pp.

Drever, J.I. (1982). The Geochemistry of Natural Waters. Prentice-Hall Inc., Englewood, New Jersey, 388 pp.

Dugal, J.J.B., Lau, J.S.O. and Raven K.G. (1979). A progress report on the White Lake experimental test site. A.E.C.L. Tech. Rec. TR-16, 78 pp.

Dugal, J.J.B. and Kamineni, D.C. (1984). Lithology, fracture intensity, and fracture filling of drill core from the Chalk River research area, Chalk River, Ontario. Unpublished Geological Survey of Canada Report, 50 pp.

Eslinger, E.V. (1971). Mineralogy and oxygen isotope ratios of hydrothermal low grade metamorphic argillaceous rocks. Ph.D. thesis, Case Western Reserve University, Cleveland, Ohio, 205 pp.

Eslinger, E.V. and Savin, S.M. (1973). Mineralogy and oxygen isotope geochemistry of thermally altered rocks in the Ohaki-Broadlands, New Zealand geothermal area. Am. J. Sci. 273, 240-267.

Eby, G.N. (1975). Abundance and distribution of rare-earth elements and yttrium in the rocks and minerals of the Oka carbonatite complex, Quebec. Geochim. Cosmochim Acta 39, 597-620.

Ejeckam, R.B., Sikorsky, R.I., Kamineni, D.C. and McCrank, G.F.D. (1985). Subsurface geology of the East Bull Lake research area (RA7) in northeastern Ontario. A.E.C.L. Tech. Rec. TR-348, 35 pp.

Emerich, K., Ehhalt, D.H. and Vogel, J.C. (1970). Carbon isotope fractionation during the precipitation of calcium carbonate. Earth Planet Sci. Lett. 8, 363-371.

Epstein, S., Graf, D.L. and Degens, E.T. (1964). Oxygen isotope studies on the origin of dolomites. In Isotopic and Cosmic Chemistry (H. Craig et al., eds.). North Holland Pub. Co., Amsterdam, 169-180.

Fleet, A.J. (1984). Aqueous and sedimentary geochemistry of the rare earth elements. In Rare Earth Element Geochemistry (P. Henderson, ed.) Elsevier Pub. Co., Amsterdam, 343-373.

Forester, R.W. and Taylor Jr., H.P. (1977). $^{18}O/^{16}O$, D/H and $^{13}C/^{12}C$ studies of the tertiary igneous complex of Skye, Skye, Scotland. Amer. J. Sci. 277, 136-177.

Frank, J.R., Carpenter, A.B. and Oglesby, T.W. (1982). Cathodoluminescence and composition of calcite cement in the Taum Sauk limestone (Upper Cambrian), Southeast Missouri. J. Sed. Petrology 52, 631-638.

Frape, S.K., Fritz, P. and McNutt, R.H. (1984). Water-rock interaction and chemistry in groundwaters from the Canadian Shield. Geochim. Cosmochim. Acta 48, 1617-1627.

Friedman, I. and O'Neil, J.R. (1977). Compilation of stable isotope fractionation factors of geochemical interest. In: Data of Geochemistry (M. Fleischer, ed.). U.S. Geol. Surv., Prof. Paper, 440-KK(6th ed.).

Fritz, P., Gale, J.E. and Reardon, E.J. (1979). Comments on carbon-14 dating of groundwaters in crystalline environments. Geoscience Canada 6, 10-14.

Garlick, G.D. (1969). The stable isotopes of oxygen. In: Handbook of Geochemistry (K.J. Wedepohl ed.), Springer-Verlag, New York, N.Y., Sect. 8-B, 1-26.

Gascoyne, M. (1983). Trace-element partition coefficients in the calcite-water system and their paleoclimatic significance in cave studies. Jour. Hydrol. 61, 213-222.

Goldsmith, J.R. and Newton, R.C. (1969). P-T-X relations in the system $CaCO_3$-$MgCO_3$ at high temperatures and pressures, Am. Jour. Sci. 267-A, 160-190.

Graf Jr., J.L. (1984). Effects of Mississippi Valley-type mineralization on REE patterns of carbonate rocks and minerals, Viburnum Trend, Southeast Missouri, J. Geology 92, 307-324.

Gregory, R.T. and Criss, R.E. (1986). Isotopic exchange in open and closed systems. In: Stable Isotopes in High Temperature Geological Processes (J.W. Valley, Jr., H.P. Taylor, Jr., J.R. O'Neil eds.), Reviews in Mineralogy 16, 91-140.

Grisak, G. and Jackson, R.E. (1978). An appraisal of the hydrogeological processes involved in shallow subsurface radioactive waste management in Canadian terrain. Scientific Series No. 84, Inland Waters Directorate, Environment Canada, Ottawa.

Hamilton, K.T. (1984) Petrology of drill core from borehole CR-9 at the Chalk River test site. A.E.C.L. Tech. Rec. TR-290, 31 pp.

Hedenquist, J.W. and Henley, R.W. (1985). Hydrothermal erruptions in Waiotapu geothermal system, New Zealand: their origin, associated breccias, and relation to precious metal mineralization. Econ. Geol. 80, 1640-1668.

Herman, A.G. (1970). Yttrium and the Lanthanides. In: Handbook of Geochemistry (K.H. Wedepohl ed.), II (5), 57-71 B to M, SpringerVerlag, Berlin, Heidelberg, New York.

Higgins, M.D. (1982). Magmatism in the Grenville Province since the Grenville orogeny. Geoscience Canada 9, 118-121.

Hitchon, B. and Friedman, I. (1969). Geochemistry and origin of formation waters in the Western Canada sedimentary basin, I. Stable isotopes of hydrogen and oxygen. Geochim. Cosmochim. Acta 33, 1321-1349.

Hoefs, J. (1973). Stable Isotope Geochemistry. Springer-Verlag, Berlin, Heidelberg, New York, 140 pp.

Ishikawa, M. and Ichikuni, M. (1984). Uptake of sodium and potassium by calcite. Chem. Geol. 42, 213-222.

James, R.S. and Born, P. (1985). Geology and geochemistry of the East Bull Lake intrusion, District of Algoma, Ontario. Can. J. Earth Sci. 22, 968-979.

Javoy, M., Pineau, F. and Delorme, H. (1986). Carbon and nitrogen isotopes in the mantle. Chem. Geol. 57, 41-62.

Kamineni, D.C. and Bonardi, M. (1983). Bastnaesite in fractures of the Eye-Dashwa Lakes pluton, Atikokan, Northwestern Ontario. Can. Mineralogist, 21, 115-119.

Kamineni, D.C. and Stone D. (1983). The ages of fractures in the Eye-Dashwa pluton, Atikokan, Canada. Contrib. Mineral. Petrol. 83, 237-246.

Kamineni, D.C., McCrank G.F.D., Stone, D., Ejeckam, R.B., Flindall, R. and Sikorsky, R. (1984). Geology of the central plateau of the East Bull Lake pluton, Northeastern Ontario. In: Current Research, Part B, Geological Survey of Canada, Paper 84-1B, 75-83.

Kamineni, D.C. (1986). A petrochemical study of calcic amphiboles from the East Bull Lake anorthosite-gabbro layered complex, District of Algoma, Ontario. Contrib. Mineral. Petrol. 93, 471-481.

Kamineni, D.C. (1986). Distribution of the U, Th, and rare-earth elements in the Eye-Dashwa Lakes pluton - A study of some analogous elements. Chem. Geol. 55, 361-373.

Kamineni, D.C. (1987). Halogen-bearing minerals in plutonic rocks: A possible source of chlorine in saline groundwater in the Canadian Shield. In: Saline Water and Gases in Crystalline Rocks (P. Fritz and S.K. Frape eds.). Geol. Assoc. of Can. Spec. Paper 33.

Kamineni, D.C., McCrank, G.F. and Stone, D. (1987). Multiple alteration events in the East Bull Lake anorthosite-gabbro layered complex, N.E. Ontario: evidence from fracture mineralogy and $^{40}Ar$-$^{39}Ar$ dating. Applied Geochemistry 2, 73-80.

Kay, G.M. (1942). Ottawa-Bonnechere graben and Lake Ontario homocline. Bull. Geol. Soc. Am. 53, 585-646.

Kerrich, R. and Fyfe, W.S. (1981). The gold-carbonate association: source of $CO_2$ and $CO_2$ fixation reactions in Archaean lode deposits. Chem. Geol. 33, 265-294.

Killingley, J.S. (1983). Effects of diagenetic recrystallization on $^{18}O/^{16}O$ values of deep-sea sediments. Nature 301, 594-597.

Kinsman, D.J.J. (1969). Interpretation of $Sr^{2+}$ concentrations in carbonate minerals and rocks. J. Sed. Petrology 39, 486-508.

Kulla, J.B. and Anderson, T.F. (1978). Experimental oxygen isotope fractionation between kaolinite and water. U.S.G.S. open file report 78-701, 234-235.

Kumarapelli, P.S. and Saull, V.A. (1966). The St. Lawrence valley system. Can. J. Earth Sci. 3, 639-658.

Langmuir, C.H., Vocke Jr., R.D., Hanson, G.H. and Hart, S.R. (1978). A general mixing equation with applications to Icelandic basalts. Earth Planet. Sci. Lett. 37, 380-392.

Larson, S.A. and Tullborg, E.L. (1984). Stable isotopes of fissure-filling calcites from Finnsjon, Uppland, Sweden. Lithos 17, 117- 125.

Liou, J.G. (1971). P-T stabilities of laumontite, wairakite, lawsonite, and related minerals in the system $CaAl_2Si_2O_8$--$SiO_2$-$H_2O$. J. Petrology 12, 379-411.

Lorens, R.B. (1981). Sr, Cd, Mn, and Co distribution coefficients in calcite as a function of calcite precipitation rate. Geochim. Cosmochim. Acta 45, 553-561.

Lumbers, S.B. (1973). No. 21, Mattawa-Deep River area, District of Nipissing and County of Renfrew. In: Summary of Field Work, 1973. Geological Branch, Ont. Dept. Mines, Miscellaneous Paper 56 (V.G. Milne, D.F. Hewitt, and W.J. Wolfe, eds.), 144-147.

Machel, H.G. (1985). Cathodoluminescence in calcite and dolomite and its chemical interpretation. Geoscience Canada 12. 139-147.

Majid, A.H. and Veizer, J. (1986). Deposition and chemical diagenesis of Tertiary carbonates, Kirkuk oil field, Iraq. AAPG Bull. 70, 898-913.

Magaritz, M. and Taylor Jr., H.P. (1976). $^{18}O/^{16}O$ and D/H studies along a 500 km traverse across the Coast Range batholith and its country rocks, central British Columbia. Can. J. Ear. Sci. 13, 1514-1536.

Masuda, A., Nakamura, N. and Tanaka, T. (1973). Fine structures of mutually normalized rare-earth patterns of chondrites. Geochim. Cosmochim. Acta 37,. 239-248.

Matsuhisa, Y., Goldsmith, J.R. and Clayton, R.N. (1979). Oxygen isotopic fractionation in the system quartz-albite-anorthite-water. Geochim. Cosmochim. Acta 43, 1131-1140.

Matthews, A. and Katz, A. (1977). Oxygen isotope fractionation during the dolomitization of calcium carbonate. Geochim. Cosmochim. Acta 41, 1431-1438.

McCrea, J.M. (1950). The isotopic chemistry of carbonates and a paleotemperature scale. J. Chem. Phys. 18, 849.

McIntire, W.L. (1963). Trace element partition coefficients - a review of of theory and applications to geology. Geochim. Cosmochim. Acta 27, 1209-1264.

McNutt, R.H. (1987). $^{87}Sr/^{86}Sr$ ratios as indicators of water/rock interactions: application to brines found in Precambrian age rocks from Canada. In: Saline Water and Gases in Crystalline Rocks (P. Fritz and S.K. Frape eds.). Geol. Assoc. of Can. Spec. Paper 33.

McNutt, R.H., Gascoyne, M. and Kamineni, D.C. (1987). $^{87}Sr/^{86}Sr$ values in groundwaters of the East Bull Lake pluton, Superior Province, Ontario, Canada. Applied Geochem. 2, 93-101.

Mereu, R.F., Wang, D., Kuhn, O., Forsyth, D.A., Green, A.G., Morel, P., Buchbinder, G.G.R., Crossley, D., Schwarz, E., du Berger, R., Brooks, C. and Clowes, R. (1986). The 1982 COCRUST seismic experiment across the Ottawa-Bonnechere graben and Grenville Front in Ontario and Quebec. Geophys. J. Royal Astr. Soc. 84, 491-514.

Michard, G. (1968). Coprecipitation de l'ion manganeaux avec le carbonate de calcium. Comptes Rendus Acad. Sci. Paris, Ser. D 167, 1685- 1688.

Milton, G.M. and Brown, R.M. (1987). U series dating of calcite coatings in ground water flow systems of the Canadian Shield. Isot. Geosci. 65, 57-65.

Moller, P., Rajagopalan, G. and Germann, K. (1976). A geochemical model for dolmitization based on material balance: Part II. Geol. Jahrb. B-20, 57-76.

Moller, P., Morteani, G., Hoefs, J. and Parekh, P.P. (1979). The origin of ore-bearing solutions in the Pb-Zn veins of the Western Harz, Germany, as deduced from rare earth element and isotope distributions in calcite. Chem. Geol. 26, 197-215.

Morgan, J.W. and Wandless, G.A. (1980). Rare earth element distributions in some hydrothermal minerals: evidence for crystallographic control. Geochim. Cosmochim. Acta 44, 973-980.

Nelson, C.E. and Giles, D.L. (1985). Hydrothermal eruption mechanisms and hot spring gold deposits. Econ. Geol. 80, 1633-1639.

Nesbitt, H.W. (1979). Mobility and fractionation of the rare earth elements during weathering of a granodiorite. Nature 279, 206-210.

Nesbitt, H.W. (1980). Characterization of mineral-solution interactions in Carboniferous sandstones and shales of the Illinois sedimentary basin. Am. J. Sci. 280, 607-630.

Northrup, D.A. and Clayton, R.N. (1966). Oxygen-isotope fractionations in systems containing dolomite. J. Geol. 74, 174-196.

Norton, D. and Knapp, R. (1977). Transport phenomena in hydrothermal systems: the nature of porosity. Am. J. Sci. 277, 913-936.

Novakowski, K.S., Flavelle, P.A., Raven, K.G. and Cooper, E.L. (1985). Determination of groundwater flow pathways in fractured plutonic rock using a radioactive tracer. Int. J. Appl. Radiat. Isot. 36, 399-404.

Novakowski, K.S., Evans, G.V., Lever, D.A. and Raven, K.G. (1985). A field example of measuring hydrodynamic dispersion in a single fracture. Water Resources Research 21, 1165-1174.

Ohmoto, H. (1972). Systematics of sulphur and carbon isotopes in hydrothermal ore deposits. Econ. Geol. 67, 551-579.

O'Neil, J.R. and Taylor Jr., H.P. (1969). Oxygen isotope equilibrium between muscovite and water. J. Geophys. Res. 74, 6012-6022.

O'Neil, J.R., Clayton, R.N. and Mayeda, T.K. (1969). Oxygen isotope fractionation in divalent metal carbonates. J. Chem. Phys. 51, 5547-5558.

O'Neil, J.R. (1977). Stable isotopes in mineralogy. Phys. Chem. Minerals 2, 105-123.

Pingitore Jr., N.E. (1982). The role of diffusion during carbonate diagenesis. J. Sed. Petrology 52, 27-39.

Pingitore Jr., N.E. and Eastman, M.P. (1986). The co-precipitation of $Sr^{2+}$ with calcite at 25°C and 1 atm. Geochim. Cosmochim. Acta 50, 2195-2203.

Plummer, L.N., Jones, B.F. and Truesdell, A.H. (1976). WATEQF: A FORTRAN IV version of WATEQ, a computer program for calculating chemical equilibrium of natural waters, U.S. Geol. Surv. Water Resour. Invest. 76-13.

Rasmuson, A. and Neretnieks, I. (1986). Radionuclide transport in fast channels in crystalline rocks. Water Resources Research 22, 1247-1256.

Raven, K.G. (1980). Studies in fracture hydrology at Chalk River Nuclear Laboratories: 1977-79. AECL Tech. Rec. TR-113, 93 pp.

Raven, K.G. and Gale, J.E. (1985). Water flow in a natural rock fracture as a function of stress and sample size. Int. J. Rock Mech. Min. Sci. and Geomech. 22, 251-261.

Raven, K.G. (1986). Hydraulic characterization of a small ground water flow system in fractured monzonitic gneiss. IWD Scientific Series No. 149, Environment Canada, Ottawa, 133 pp.

Raven, K.G., Bottomley, D.J., Sweezey, R.A., Smedley, J.A. and Ruttan, T.J. (1987). Hydrogeological characterization of the East Bull Lake research area. IWD Scientific Series, Environment Canada, Ottawa.

Reardon, E.J. and Fritz, P. (1978). Computer modelling of ground water $^{13}C$ and $^{14}C$ isotope compositions. J. Hydrol. 36, 201-224.

Reardon, E.J. and Reimer, J.D. (1982). A laboratory investigation of crystalline rock-water interactions. A.E.C.L. Tech. Rec. TR-137.

Reeder, R.J. and Grams, J.C. (1987). Sector zoning in calcite cement crystals: implications for trace element distributions in carbonates. Geochim. Cosmochim. Acta 51, 187-194.

Rosenbaum, J. and Sheppard, S.M.F. (1986). An isotopic study of siderites, dolomites and ankerites at high temperatures. Geochim. Cosmochim. Acta 50, 1147-1150.

Rudnick, R.L., McLennan, S.M. and Taylor, S.R. (1985). Large ion lithophile elements in rocks from high-pressure granulite facies terrains. Geochim. Cosmochim. Acta 49, 1645-1655.

Ruiz, J., Jones, L.M. and Kelly, W.C. (1984). Rubidium-strontium dating of ore deposits by Rb-rich rocks using calcite and other common Sr-bearing minerals. Geology 12, 259-262.

Sands, C.D. and Drever, J.I. (1978). Authigenic laumontite in deep-sea sediments. In: Natural Zeolites: Occurrence, Properties, Use. (L.B. Sand and F.A. Mumston, eds.). Pergamon Press, Elmsford, New York, 269-275.

Schwarcz, H.P. and Burnie, S.W. (1973). Influence of sedimentary environments on sulfur isotope ratios in clastic rocks: a review. Mineral. Deposita 8, 264-277.

Schwerdtner, W.M. and Lumbers, S.B. (1980). Major diaperic structures in the Superior and Grenville Provinces of the Canadian Shield. In: The Continental Crust and its Mineral Deposits (D.W. Stangway, ed.). Geol. Assoc. Can. Spec. Paper 20, 149-180.

Shaw, H.F. and Wasserburg, G.J. (1985). Sm-Nd in marine carbonates and phosphates: implications for Nd isotopes in seawater and crustal ages. Geochem. Cosmochem. Acta 49, 503-518.

Sheppard, S.M.F., Nielson, R.L. and Taylor Jr., H.P. (1969). Oxygen and hydrogen isotope ratios of clay minerals from porphyry copper deposits. Econ. Geol. 64, 755-777.

Sheppard, S.M.F. and Schwarcz, H.P. (1970). Fractionation of carbon and oxygen and magnesium between coexisting metamorphic calcite and dolomite. Contrib. Mineral. Petrol. 26, 161-198.

Sheppard, S.M.F. and Taylor Jr., H.P. (1974). Hydrogen and oxygen isotope evidence for the origins of water in the Boulder batholith and the Butte ore deposits, Montana. Econ. Geol. 69, 926-946.

Sheppard, S.M.F. (1986). Characterization and isotopic variations in natural waters. In: Stable Isotopes in High Temperature Geological Processes (J.W. Valley, H.P. Taylor, Jr., J.R. O'Neil, eds.). Reviews in Mineralogy 16, 165-183.

Sherman, G.R., Donahue, D.C., King, S.G. and So, A. (1985). SYVAC-2 - a systems variability analysis code for assessment of nuclear fuel waste disposal concepts. A.E.C.L. Tech. Rec. TR-317.

Silver, L.T., Bickford, M.E., van Schmus, W.R., Anderson, J.L., Anderson, T.H. and Madaris Jr., L.G. (1977). The 1.4-1.5 by transcontinental anorogenic plutonic perforation of North America. Geol. Assoc. Am., Abstracts with programs, 9, 1176-1177.

Somers, G. (1984). Geochemistry and petrogenesis of the White Lake pluton, Southeast Ontario. M.Sc. thesis, University of Western Ontario, London, Ont., 159 pp.

Stakes, D.S. and O'Neil, J.R. (1982). Mineralogy and stable isotope geochemistry of hydrothermally altered oceanic rocks. Earth and Planet Sci. Lett. 57, 285-304.

Stettler, A. and Allègre, C.J. (1978). $^{87}Rb$-$^{87}Sr$ studies of waters in a geothermal area: The Cantal, France. Ear. Planet. Sci. Lett. 38, 364-372.

Storey, C.C. and Vos, M.A. (1981). Industrial minerals of the Pembroke Renfrew area, Part 2. Ontario Geological Survey Mineral Deposits Circular 22, 145-161.

Sverjensky, D.A. (1981). Isotopic alteration of carbonate host rocks as a function of water to rock ratio - an example from the Upper Mississippi Valley zinc-lead district. Econ. Geol. 76, 154-172.

Takenouchi, S. and Kennedy, A.C. (1964). The binary system $H_2O$-$CO_2$ at high temperatures and pressures. Am. J. Sci. 212, 1055-1074.

Taylor, B.E. and Bucher-Nurminen, K. (1986). Oxygen and carbon isotope and cation geochemistry of metasomatic carbonates and fluids - Bergell aureole, Northern Italy. Geochim. Cosmochim. Acta 50, 1267-1279.

Taylor Jr., H.P. and Forester, R.W. (1971). Low O-18 igneous rocks from the intrusive complexes of Skye, Mull and Ardnamurchan, Western Scotland. J. Petrol. 12, 465-497.

Taylor Jr., H.P. (1974). The application of oxygen and hydrogen isotope studies to problems of hydrothermal alteration and ore deposition. Econ. Geol. 69, 843-883.

Taylor Jr., H.P. (1977). Water/rock interaction and the origin of $H_2O$ in granitic batholiths. J. Geol. Soc. London 133, 509-558.

Thompson, A.B. (1971). $P_{CO_2}$ in low-grade metamorphism; zeolite, carbonate, clay mineral, prehnite relations in the system $CaO-Al_2O_3-SiO_2-CO_2-H_2O$. Contrib. Mineral. & Petrol. 33, 145-161.

Truesdell, A.H. and Hulston, J.R. (1980). Isotopic evidence on environments of geothermal systems. In: Handbook of Environmental Isotope Geochemistry (P. Fritz and J. Ch. Fontes, eds.), Vol. 1, The Terrestrial Environment, A. Elsevier Scientific Publishing Co., Amsterdam, Oxford, New York, 179-226.

Turi, B. and Taylor Jr., H.P. (1971). An oxygen and hydrogen isotope study of a granodiorite pluton from the Southern California batholith. Geochim. Cosmochim. Acta 35, 383-406.

Valley, J.W. (1986). Stable isotope geochemistry of metamorphic rocks. In: Stable Isotopes in High Temperature Geological Processes. Reviews in Mineralogy 16, 445-489.

Veizer, J., Lemieux, B., Jones, B., Gibling, M.R. and Savelle, J. (1978). Paleosalinity and dolomitization of a lower Paleozoic carbonate sequence, Somerset and Prince of Wales Island, Arctic Canada. Can. J. Ear. Sci. 15, 1448-1461.

Veizer, J. Holser, W.T. and Wilgus, C.K. (1980). Correlation of $^{13}C/^{12}C$ and $^{34}S/^{32}S$ secular variations. Geochim. Cosmochim. Acta 44, 579-587.

Veizer, J. (1983a). Chemical diagenesis of carbonate rocks: theory and application of trace element technique. In: Stable Isotopes in Sedimentary Geology (M.A. Arthur, T.F. Anderson, I.R. Kaplan, J. Veizer, and L.S. Land, eds.). SEPM Short Course Notes 10, SEPM, pp. III/1 - III/100.

Veizer, J. (1983b). Trace elements and isotopes in sedimentary carbonates. Reviews in Mineralogy 11, 265-300.

Veizer, J., Compston, W., Clauer, N. and Schidlowski, M. (1983c). $^{87}Sr/^{86}Sr$ in Late Proterozoic carbonates: evidence for a mantle event at ~900 Ma ago. Geochim. Cosmochim. Acta 47, 295-302.

Veizer, J., Fritz, P. and Jones, B. (1986). Geochemistry of brachiopods: oxygen and carbon isotopic records of Paleozoic oceans. Geochim. Cosmochim. Acta 50, 1679-1696.

Walters Jr., L.J., Claypool, G.E. and Choquette, P.W. (1972). Reaction rates and $\delta^{18}O$ variation for carbonate-phosphoric acid preparation method. Geochim. Cosmochim. Acta 36, 129-140.

Wenner, D.B. and Taylor Jr., H.P. (1971). Temperatures of serpentinization of ultramafic rocks based on $^{18}O/^{16}O$ fractionation between coexisting serpentine and magnetite. Contrib. Mineral. Petrol. 32, 165-185.

Wigley, T.M.L. (1975). Carbon 14 dating of groundwater from closed and open systems. Water Resources Research 11, 324-328.

Wright, J.B. (1969). A simple alkalinity ratio and its applications to the questions of non-orogenic granite genesis. Geol. Mag. 106, 370-384.

Wu, T.W. and Kerrich, R. (1986). Combined oxygen isotope-compositional studies of some granitoids from the Grenville Province of Ontario, Canada: implications for source regions. Can. J. Ear. Sci. 23, 1412-1432.

Wuschke, D.M., Gillespie, P.A., Mehta, K.K., Heinrich, W.F., LeNeveu, D.M. Guvanasen, V.M., Sherman, G.R., Donahue, D.C., Goodwin, B.W., Andres, T.H. and Lyon, R.B. (1985). Second interim assessment of the Canadian concept for nuclear fuel waste disposal, vol. 4: post closure assessment. A.E.C.L. Report AECL-8373-4, 154 pp.

Yeh, H.W. and Savin, S.M. (1977). Mechanisms of burial metamorphism of argillaceous sediments: 3. O-isotope evidence. Geol. Soc. Am. Bull. 88, 1321-1330.

York, D. (1969). Least squares fitting of a straight line with correlated errors. Earth Planet. Sci. Lett. 5, 320-324.

# APPENDICES

Table A1. Chemical compositions of CRNL fracture calcites

| Borehole and Depth (m) | Ca (%) | Mg | Fe | Mn | Na | Sr | I.R. (%) | Al | Zn |
|---|---|---|---|---|---|---|---|---|---|
| | | ---------- | | ppm | ---------- | | | ppm | ppm |
| CR2 - 58.32 | 31.2 | 1760 | 6200 | 3710 | 160 | 680 | 24.6 | 830 | |
| - 115.91 | 21.7 | 1200 | 2680 | 4450 | 140 | 180 | 43.6 | 4880 | |
| - 127.90 | 28.9 | 12980 | 5290 | 5480 | 110 | 200 | 3.1 | 100 | |
| CR3 - 22.22 | 21.9 | 26040 | 50590 | 3610 | 1020 | 550 | 69.3 | 14180 | |
| - 69.00 | 32.1 | 990 | 900 | 1480 | 240 | 150 | 19.6 | 490 | |
| - 130.13 | 19.0 | 98270 | 19020 | 7550 | 260 | 80 | 3.5 | 78 | |
| CR6 - 212.13 | 35.6 | 5630 | 2990 | 2070 | 180 | 140 | 19.5 | | <10 |
| CR8 - 139.26 | 30.6 | 340 | 650 | 2640 | 90 | 250 | 7.0 | 250 | |
| - 184.88 | 35.5 | 2170 | 2060 | 950 | 110 | 190 | 15.8 | | <10 |
| - 192.78 | 38.6 | 3150 | 2280 | 3040 | 120 | 130 | 36.1 | | <10 |
| - 204.94 | 29.2 | 12090 | 5480 | 3700 | 110 | 140 | 13.5 | 600 | |
| - 205.05 | 24.3 | 9780 | 4610 | 4550 | 110 | 100 | 16.9 | 440 | |
| - 205.67 | 30.4 | 900 | 2260 | 2110 | 70 | 130 | 31.2 | 1150 | |
| - 207.62 | 31.3 | 1290 | 2800 | 4660 | 270 | 330 | 9.5 | 890 | |
| - 221.56 | 28.1 | 2220 | 4030 | 2900 | 330 | 180 | 46.3 | | 15 |
| - 230.45 | 38.1 | 860 | 1440 | 1140 | 60 | 110 | 19.4 | | |
| - 230.66 | 28.4 | 2340 | 2920 | 2497 | 170 | 160 | 12.6 | 1780 | |
| - 232.82 | 31.0 | 4370 | 4030 | 2300 | 140 | 220 | 23.7 | 590 | |
| - 240.28 | 31.0 | 7840 | 13030 | 1060 | 190 | 220 | 72.9 | | |
| - 259.55 | 34.9 | 5020 | 6710 | 3220 | 140 | 220 | 54.3 | | |
| - 277.51 | 38.3 | 490 | 610 | 2330 | 30 | 120 | 18.2 | 280 | |
| - 278.85 | 37.6 | 7870 | 2570 | 3240 | 50 | 170 | 9.8 | | |
| - 285.38 | 38.8 | 540 | 1050 | 4060 | 30 | 190 | 17.3 | | |
| - 292.32 | 29.9 | 4600 | 2050 | 3120 | 140 | 120 | 1.3 | 80 | |
| CR9 - 75.75 | 34.1 | 2620 | 3100 | 1490 | 210 | 230 | 23.7 | | 15 |
| - 345.77 | 27.4 | 11830 | 4950 | 3930 | 110 | 130 | 9.6 | 770 | |
| - 351.16 | 31.4 | 4580 | 6130 | 2890 | 100 | 260 | 22.6 | 2230 | |
| - 448.39 | 31.1 | 1060 | 2780 | 1470 | 150 | 70 | 22.8 | 1260 | |
| - 459.98 | 30.0 | 110 | 40 | 40 | 100 | 120 | 1.2 | 5640 | |
| - 492.43 | 31.6 | 190 | 1340 | 170 | 80 | 160 | 14.4 | 1060 | |
| - 574.33 | 29.4 | 3130 | 3070 | 3510 | 140 | 70 | 6.5 | 310 | |
| CR10 - 51.37 | 32.0 | 2750 | 6000 | 2250 | 100 | 250 | 28.5 | 2480 | |

Table A1 (cont'd.)

Table A1. Cont'd.

| Borehole and Depth (m) | Ca (%) | Mg | Fe | Mn | Na | Sr | I.R. (%) | Al | Zn |
|---|---|---|---|---|---|---|---|---|---|
| | | ---------- | | ppm | ---------- | | | ppm | ppm |
| CR12 - 24.92 | 35.2 | 11570 | 7050 | 5130 | 90 | 140 | 24.1 | | 20 |
| - 26.12 | 34.8 | 7010 | 4040 | 2350 | 140 | 190 | 33.1 | | 10 |
| - 26.38 | 27.6 | 17300 | 16700 | 2950 | 220 | 480 | 47.1 | | 100 |
| - 26.42 | 36.6 | 1150 | 1870 | 3510 | 40 | 200 | 5.0 | | 50 |
| - 44.36 | 30.8 | 9250 | 25630 | 3410 | 260 | 160 | 84.7 | | |
| - 77.90 | 26.2 | 4410 | 3050 | 1080 | 320 | 160 | 28.3 | 4640 | |
| - 78.19 | 30.9 | 1880 | 1830 | 1260 | 180 | 150 | 30.1 | | 155 |
| - 98.98 | 37.5 | 650 | 1080 | 1530 | 40 | 110 | 23.8 | | |
| - 113.30 | 32.0 | 960 | 1160 | 1660 | 70 | 140 | 5.5 | 480 | |
| - 116.95 | 37.0 | 4960 | 2380 | 2620 | 70 | 110 | 26.3 | | |
| FS15 - 13.44 | 30.2 | 1790 | 3260 | 1920 | 110 | 160 | 47.2 | | |
| - 13.81 | 29.9 | 3320 | 4400 | 4920 | 70 | 320 | 7.3 | 750 | |
| - 15.80 | 36.0 | 520 | 2490 | 2320 | 140 | 70 | 31.8 | | 15 |
| FS16 - 14.30 | 31.8 | 1320 | 2970 | 1560 | 100 | 350 | 43.7 | 1810 | |
| FS17 - 22.74 | 36.2 | 720 | 1380 | 160 | 50 | 300 | 24.2 | | 10 |

Table A2. Carbon and oxygen isotopic compositions of CRNL fracture calcites

| Borehole and Depth (m) | $\delta^{13}C_{PDB}$ | $\delta^{18}O_{SMOW}$ | Comments (see footnotes) |
|---|---|---|---|
| CR1 - 4.50 | -7.1 | 19.1 | patchy, grey on incl. O.F. |
| 5.99 | -7.5 | 19.9 | patchy, on chl. - sub. vert O.F. |
| 125.86 | -10.3 | 23.3 | patchy, on chl. - sub. vert |
| 128.50 | -9.7 | 22.6 | patchy, crys. - sub. horiz. O.F. |
| 208.79 | -7.9 | 19.2 | th. patchy, crys. - incl. F. |
| 212.97 | -7.7 | 19.7 | w.$FeS_2$, chl. - sub. horiz. O.F. |
| 223.12 | -8.6 | 21.4 | patchy, on chl. - incl. F. |
| 227.46 | -6.6 | 20.0 | patchy, - incl. F. |
| 227.60 | -9.9 | 22.0 | patchy, - incl. F. |
| 232.38 | -8.0 | 22.5 | patchy, - incl. F. |
| 244.62 | -6.5 | 16.2 | patchy w.$FeS_2$ on chl. - sub. horiz. F. |
| 252.23 | -6.4 | 19.0 | patchy w.$FeS_2$ on chl. - vert. F. |
| 257.20 | -6.0 | 18.9 | patchy, on slick. chl. |
| CR2 - 58.32 | -8.7 | 12.9 | vein stockwork |
| 104.82 | -9.4 | 21.8 | platy - horiz. F. |
| 105.48 | -8.6 | 21.0 | irreg. F. |
| 105.61 | -7.6 | 21.2 | patchy w.$Fe_2O_3$ - incl. O.F. |
| 105.75 | -5.8 | 20.0 | sealed vein |
| 105.75 | -7.3 | 23.4 | patchy, w.$Fe_2O_3$ - incl. O.F. |
| 105.75 | -6.9 | 18.1 | patchy, on chl. - incl. O.F. |
| 113.53 | -5.8 | 18.6 | patchy, crys. - incl. F. |
| 115.91 | -5.6 | 18.8 | sealed vein - in diabase |
| 117.78 | -7.8 | 21.2 | hematized, brecciated zone-sub.horiz.F. |
| 127.90 | -5.6 | 16.4 | composite cc-do. |
| 127.90 | -5.3 | 16.9 | cc fraction |
| 127.90 | -5.0 | 17.6 | do fraction |
| 128.47 | -5.8 | 15.3 | in diabase |
| 128.50 | -2.8 | 14.7 | w. $Fe_2O_3$ - in diabase |
| 129.32 | -4.8 | 17.3 | patchy - sub. horiz. F. |
| 129.43 | -4.6 | 17.3 | composite cc-do w.chl. - vert. F. |
| 129.43 | -4.8 | 17.4 | cc fraction w.chl. - vert. F. |
| 129.43 | -4.2 | 18.2 | do fraction w.chl. - vert. F. |
| 181.30 | -7.3 | 18.5 | crystals in porous, altered zone |
| 183.60 | -7.2 | 20.0 | crys. - vuggy, sub. horiz. F. |
| CR3 - 22.22 | -10.1 | 18.8 | vein edge w. qtz. - incl. F. |
| 22.22 | -10.2 | 18.8 | vein centre w. qtz. - incl. F. |
| 69.00 | -8.9 | 19.6 | stockwork, sealed veins |
| 98.20 | -6.2 | 20.7 | patchy w. $Fe_2O_3$ |
| 98.31 | -7.3 | 22.2 | patchy, crys. |
| 129.46 | -6.1 | 3.4 | w.$Fe_2O_3$-sealed vein in altered diabase |

(Table A2. cont'd.)

Table A2 (cont'd.)

| Borehole and Depth (m) | $\delta^{13}C_{PDB}$ | $\delta^{18}O_{SMOW}$ | Comments |
|---|---|---|---|
| CR3 - 130.13 | -4.4 | 23.5 | composite cc-do, brecciated zone-sealed vein |
| 130.13 | -4.5 | 20.2 | cc fraction, brecciated zone-sealed vein |
| 130.13 | -4.2 | 21.5 | do fraction, brecciated zone-sealed vein |
| CR6 - 103.06 | -6.4 | 16.1 | ox. zone - vert. O.F. |
| 103.40 | -7.9 | 17.8 | patchy - incl., irreg. O.F. |
| 212.13 | -5.5 | 15.4 | brecciated qtz. - cc. vein on chl. |
| CR7 - 99.21 | -6.0 | 19.7 | patchy, on chl. - incl. F. |
| 107.26 | -7.1 | 19.6 | massive, on chl. - incl. F. |
| 137.34 | -6.7 | 14.9 | vein centre, sealed vein - horiz. |
| 137.34 | -6.8 | 16.6 | vein edge, sealed vein - horiz. |
| 137.36 | -12.6 | 21.6 | patchy - sub. horiz. O.F. |
| CR8 - 6.51 | -7.2 | 21.6 | filmy, white - incl. O.F. |
| 36.34 | -7.7 | 17.6 | on chl, ox. zone |
| 57.80 | -9.3 | 20.3 | patchy, grey, on chl. - incl. F. |
| 61.21 | -6.5 | 15.5 | th. crys., w.$FeS_2$ - incl. reopened vein |
| 65.02 | -8.5 | 20.9 | w.$FeS_2$ - sub. horiz. O.F. |
| 73.89 | -7.7 | 20.7 | th. patchy cc |
| 77.57 | -10.3 | 19.8 | filmy, w. $FeS_2$ |
| 104.72 | -7.9 | 21.7 | patchy - sub. vert. O.F. |
| 117.83 | -7.6 | 21.2 | patchy, white - incl. O.F. in peg. |
| 119.28 | -6.7 | 20.0 | filmy, white - sub. vert. O.F. |
| 120.51 | -7.5 | 21.1 | patchy - incl. O.F. in peg. |
| 120.64 | -7.0 | 21.2 | patchy - incl. O.F. in peg. |
| 121.08 | -6.9 | 18.7 | granular w.$FeS_2$ - incl. O.F. in peg. |
| 121.24 | -6.8 | 18.7 | th., on chl. w. $FeS_2$ |
| 127.92 | -6.2 | 20.7 | filmy - sub. vert. O.F. |
| 128.93 | 8.0 | 19.3 | th., patchy - incl. O.F. |
| 131.73 | -8.1 | 21.5 | filmy, white - incl. O.F. |
| 132.75 | -7.3 | 19.6 | patchy - incl. F. |
| 135.43 | -6.0 | 18.6 | patchy, grey, on chl. - incl. F. |
| 139.26 | -7.4 | 21.9 | filmy - sub. vert. O.F. |
| 142.10 | -7.0 | 18.1 | patchy - sub. vert. O.F. |
| 145.51 | -7.8 | 17.1 | |
| 153.00 | -7.3 | 21.2 | patchy - incl. O.F. |
| 154.90 | -5.9 | 2.4 | vuggy, w. $FeS_2$ on chl. - sub. vert. F. |
| 167.17 | -6.9 | 19.1 | patchy, on chl. - sub. vert. O.F. |
| 180.23 | -7.2 | 15.2 | patchy, grey - incl. O.F. in peg. |
| 184.63 | -7.0 | 20.5 | patchy |
| 184.88 | -6.5 | 15.8 | sealed vein |
| 189.90 | -6.9 | 19.4 | patchy - sub. horiz. F. |
| 191.05 | -7.2 | 18.9 | patchy w.$FeS_2$ on chl.-incl. O.F. in peg. |
| 192.75 | -7.1 | 18.8 | w.$FeS_2$ - irreg. incl. F. in peg. |
| 202.24 | -8.2 | 19.7 | patchy, grey - incl. O.F. in peg. |

(Table A2. cont'd.)

TABLE A2. (cont'd.)

| Borehole and Depth (m) | $\delta^{13}C_{PDB}$ | $\delta^{18}O_{SMOW}$ | Comments |
|---|---|---|---|
| CR8 - 204.94 | -6.4 | 16.0 | cc fraction, sub. vert. C.F. in peg. |
| 204.94 | -6.5 | 17.2 | do fraction, sub. vert. C.F. in peg. |
| 205.05 | -6.1 | 15.6 | composite cc-do, carb. matrix of peg. |
| 205.05 | -6.4 | 16.0 | cc fraction, carb. matrix of peg. |
| 205.05 | -6.2 | 16.8 | do fraction, carb. matrix of peg. |
| 205.67 | -6.9 | 17.7 | coarse crystals in carb. amph. |
| 207.62 | -7.3 | 21.7 | patchy, on chl. in amph. |
| 207.74 | -8.3 | 22.5 | patchy, grey - sub. vert. O.F. in diabase |
| 221.26 | -8.6 | 22.2 | patchy, w.$FeS_2$ - sub. vert. F. |
| 221.56 | -6.9(-6.4) | 20.9(20.5) | patchy, grey on chl. - sub. vert. F. |
| 230.45 | -6.3 | 14.9 | patchy, on chl. - sub. vert. O.F. |
| 230.66 | -7.6 | 18.6 | patchy, w.$FeS_2$ - vert. O.F. |
| 231.37 | -6.6 | 15.6 | patchy - horiz. F. |
| 232.82 | -7.0 | 19.6 | vein in peg. |
| 234.00 | -7.7 | 16.6 | platy, slick., grey - vert. F. |
| 240.28 | -5.8 | 13.8 | th. massive - incl. F. |
| 251.96 | -6.2 | 15.3 | th. sealed vein - incl. F. |
| 259.55 | -6.2 | 15.0 | w. $Fe_2O_3$ on chl. - sub. vert. vein |
| 277.27 | -6.3 | 14.3 | crys. - incl. F. |
| 277.51 | -8.6 | 18.7 | coarse crystals in vug |
| 278.85 | -5.8 | 14.5 | carb. matrix in brecciated, altered zone |
| 279.00 | -7.7 | 15.9 | vein |
| 279.30 | -6.1 | 15.5 | granular, crys. - vert. O.F. |
| 285.38 | -8.5 | 20.4 | patchy, grey on chl. - sub. vert. O.F. |
| 292.01 | -5.0 | 14.8 | carb. matrix in brecciated zone |
| 292.32 | -4.9 | 14.5 | vein |
| 292.60 | -5.6 | 14.3 | patchy - incl. F. in ox. zone |
| 302.82 | -7.6 | 18.1 | patchy w.$FeS_2$ on chl. - sub. vert. O.F. |
| CR9 - 6.36 | -8.2 | 18.8 | on chl. - incl. irreg. O.F. |
| 35.75 | -7.6 | 17.7 | patchy on chl. - sub. vert. O.F. |
| 75.75 | -7.4 | 20.1 | patchy - sub. vert. O.F. |
| 149.79 | -7.3(-7.5) | 15.5(14.5) | th. patchy, crys. - sub. vert. |
| 159.20 | -6.5 | 16.1 | patchy, grey - incl. F. |
| 160.18 | -6.8 | 16.9 | patchy on chl. |
| 192.78 | -6.7 | 15.8 | massive - C.F. |
| 219.71 | -8.7 | 17.6 | filmy - incl. F. |
| 219.77 | -8.7 | 19.1 | patchy - sub. horiz. F. |
| 220.82 | -9.0 | 19.8 | patchy - sub. horiz. F. |
| 336.15 | -6.9 | 19.2 | th. vein on chl. - in peg. |

(Table A2 cont'd.)

TABLE A2. (cont'd.)

| Borehole and Depth (m) | $\delta^{13}C_{PDB}$ | $\delta^{18}O_{SMOW}$ | Comments |
|---|---|---|---|
| CR9 - 345.77 | -5.6 | 16.7 | sub-vert. F. in alteration zone |
| 351.16 | -6.1 | 16.0 | C.F. in brecciated, oxidized zone |
| 363.84 | -8.2 | 21.5 | sub. vert. O.F. in peg. |
| 363.90 | -8.5 | 20.6 | patchy - sub. horiz. O.F. |
| 390.74 | -6.7 | 17.8 | patchy, grey, slick. - incl. F. |
| 448.22 | -5.6 | 14.3 | massive - sub. horiz. F. |
| 448.39 | -6.5 | 16.7 | coarse crys. - sub. horiz. F. in porous zone |
| 459.98 | -6.0 | -0.4 | sealed vein w. laum. crystals |
| 464.88 | -6.2 | 20.1 | patchy, on chl. - sub.vert. O.F. in diabase |
| 492.43 | -6.3 | 0.7 | sealed lense in porous altered rock |
| 500.40 | -5.0 | 13.6 | patchy, clear, slick. on chl.-sub.vert. F. |
| 505.78 | -8.1 | 21.6 | patchy, crys. w.$Fe_2O_3$-sub.horiz. F. |
| 520.39 | -5.8 | 16.0 | th., massive - sub.vert. F. in ox. zone |
| 545.40 | -7.0 | 20.4 | patchy - sub. vert. O.F. |
| 545.92 | -9.6 | 19.9 | granular - incl. O.F. |
| 574.33 | -5.6 | 14.8 | inner layer incl. O.F. in alteration zone |
| 574.33 | -7.9 | 21.5 | outer layer incl. O.F. in alteration zone |
| 576.70 | -6.8 | 17.3 | filmy - incl. O.F. |
| 577.48 | -7.5 | 20.2 | sub. vert. O.F. |
| 599.15 | -6.8 | 17.9 | patchy, flaky - sub. vert. O.F. |
| 599.21 | -6.1 | 17.1 | sub. horiz. sealed vein |
| 623.52 | -7.6 | 9.1 | patchy, on chl. in brecciated peg. |
| 641.97 | -6.4 | 17.5 | patchy - incl. F. |
| 652.98 | -7.0 | 15.5 | sealed F. - on chl. |
| 663.77 | -7.5 | 14.8 | sub. vert. F. in diabase |
| 672.20 | -7.1 | 16.9 | patchy, brown - incl. F. in peg. |
| 676.42 | -6.6 | 13.3 | slick., on chl. - vert. F. |
| 676.94 | -6.9 | 17.8 | patchy, orange, w.$FeS_2$ on chl. - sub.vert. |
| 685.52 | -7.1 | 13.0 | platy, on chl. - sub. horiz. F. in gabbro |
| 689.99 | -6.0 | 14.1 | patchy, grey on chl.-sub.vert. F. in diabase |
| 691.47 | -7.3 | -0.6 | prismatic crystals on chl. - incl. F. |
| 700.09 | -7.4 | 18.7 | patchy, on chl. - sub. vert. F. |
| CR10 - 51.37 | -7.5 | 22.1 | patchy, on chl. - sub. vert. O.F. |
| 51.70 | -6.2 | 16.0 | cc in breccia matrix (sealed) |
| 51.70 | -9.5 | 21.9 | vert. F. in matrix w.$Fe_2O_3$ |
| CR11 - 102.24 | -6.8 | 15.3 | filmy, grey - incl. F. |
| 102.62 | -6.7 | 16.0 | sub. vert. F. |
| 114.63 | -8.1 | 19.6 | th. cc. w.$FeS_2$ - inclined O.F. |
| CR12 - 6.12 | -8.5 | 16.7 | patchy - vert. O.F. |
| 17.75 | -7.7 | 20.4 | patchy, grey on chl. - incl. F. in ox. zone |
| 24.92 | -6.9 | 16.1 | carb. brecciated zone (sealed) |
| 26.12 | -6.8(-7.0) | 16.3(17.4) | vein w. chl. - sealed |
| 26.38 | -6.8 | 15.3 | carb. gneiss matrix |

(Table A2 cont'd.)

TABLE A2. (cont'd.)

| Borehole and Depth (m) | $\delta^{13}C_{PDB}$ | $\delta^{18}O_{SMOW}$ | Comments |
|---|---|---|---|
| CR12 - 26.42 | -9.9 | 22.6 | th., patchy, porous, soft-sub.horiz.O.F. |
| 44.36 | -6.7(7.4,7.4) | 22.3(21.9,22.7) | vein in diabase |
| 60.72 | -7.8 | 20.9 | patchy, granular - incl. F. |
| 72.34 | -6.7 | 17.9 | patchy - vert. O.F. |
| 72.38 | -6.9 | 17.8 | patchy - sub. vert. O.F. |
| 77.81 | -10.0 | 20.8 | patchy, slick., w.$FeS_2$-sub.vert. O.F. |
| 78.02 | -7.7 | 16.6 | patchy - sub. vert. O.F. |
| 78.07 | -8.3 | 18.8 | patchy - sub. vert. O.F. |
| 78.17 | -10.4 | 21.9 | patchy - sub. vert. O.F. |
| 78.19 | -8.7 | 19.7 | patchy - sub. vert. O.F. |
| 78.23 | -10.3 | 21.6 | patchy - sub. vert. O.F. |
| 78.27 | -10.9 | 22.6 | patchy - sub. vert. O.F. |
| 81.35 | -6.1 | 21.2 | patchy - incl. O.F. |
| 98.98 | -6.5 | 19.9 | patchy w. $FeS_2$ - vert. O.F. |
| 105.39 | -7.1 | 21.4 | patchy w. $FeS_2$ - sub. vert. O.F. |
| 112.04 | -5.6 | 19.7 | patchy, on chl. - O.F. |
| 113.34 | -6.5 | 20.7 | th., on chl. - incl. O.F. |
| 113.61 | -7.6 | 21.3 | granular, patchy, grey - irreg. O.F. |
| 116.95 | -6.4 | 16.1 | th. sealed vein |
| CR13 - 383.4 | -6.7 | 16.3 | chip sample, depth approximate |
| CR14 - 28.96 | -10.7 | 19.5 | patchy - sub. horiz. O.F. |
| CR21 - 28.28 | -6.8 | 23.1 | patchy - sub. horiz. O.F. |
| FS15 - 13.44 | -6.4 | 19.6 | patchy, white, on chl. - incl. O.F. |
| 13.82 | -6.3 | 15.8 | inner layer - massive, vein |
| 13.82 | -6.5 | 18.8 | outer layer - patchy |
| 15.80 | -6.0 | 17.2 | clear, hard - in peg. |
| 42.61 | -7.0 | 20.8 | th. crusty w. chl. and $Fe_2O_3$-sub. vert. |
| 43.85 | -9.8 | 21.1 | flaky w.$Fe_2O_3$ - sub. vert. O.F. |
| 46.40 | -8.0 | 21.2 | patchy, grey, on chl. - incl. O.F. |
| FS16 - 14.30 | -7.8 | 19.5 | inner layer on chl. - incl. O.F. |
| 14.30 | -6.8 | 21.6 | outer layer on chl. - incl. O.F. |
| 20.02 | -6.2 | 23.8 | patchy, on chl.-sub. vert. O.F. in ox. zone |
| 39.55 | -13.5 | 22.3 | patchy, w.$Fe_2O_3$ on chl.-sub. vert. O.F. |
| FS17 - 22.74 | -7.7 | 17.4 | patchy, grey w.$FeS_2$ - incl. F. |
| 57.41 | -7.4 | 21.1 | crumbly, on chl. - vert. O.F. |

Abbreviations: incl. - inclined; O.F. - open fracture; C.F. - closed fracture; vert. - vertical; horiz. - horizontal; chl. - chlorite; crys. - crystalline; th. - thick; ox. - oxidized; qtz. - quartz; cc. - calcite; do. - dolomite; w. - with; carb. - carbonatized; irreg. - irregular; peg. - pegmatite, slick. - slickensided; laum. - laumontite.

PLATE I. Typical NQ-3 core of fractured granitic augen gneiss from CRNL borehole CR7.

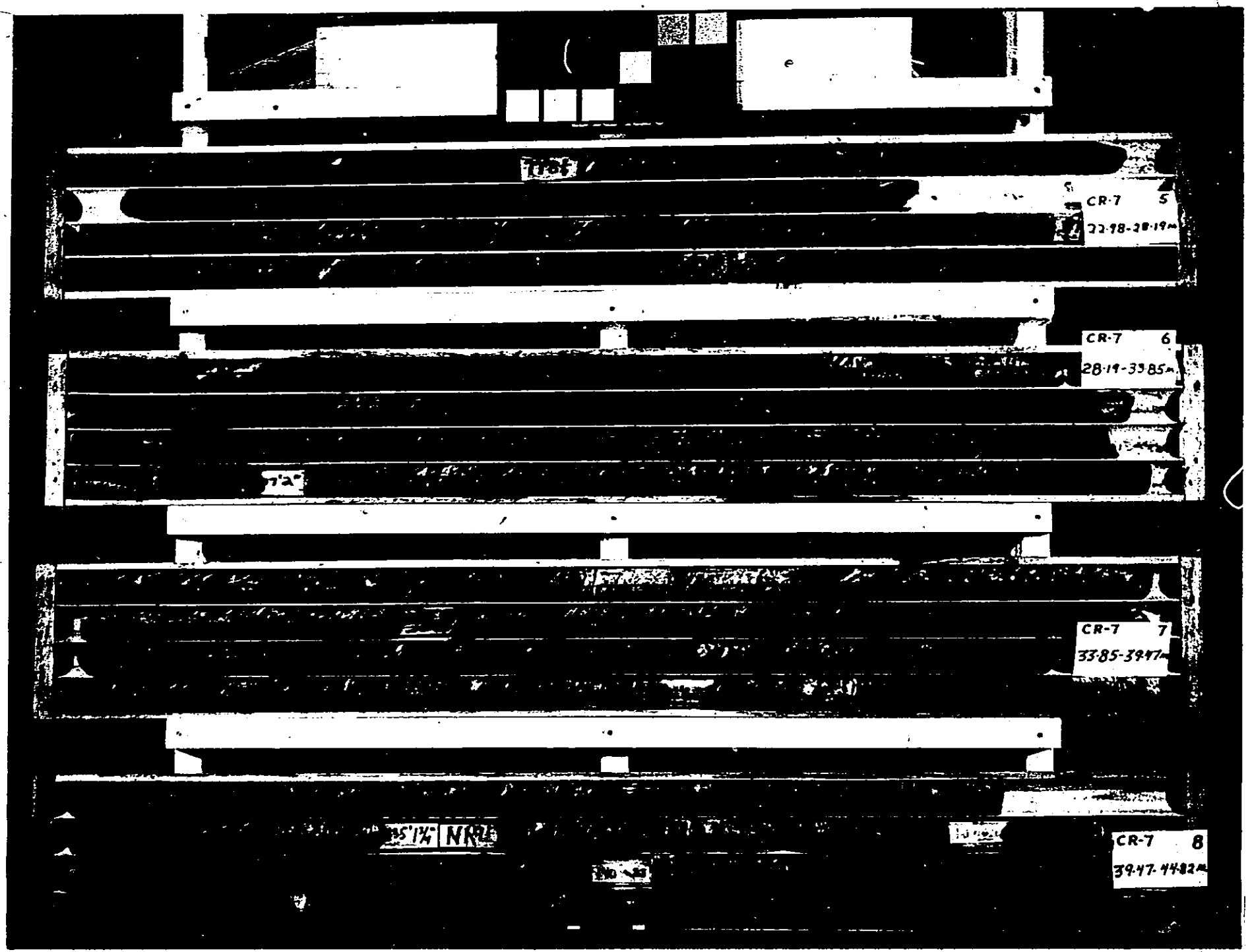
CR-7 5
22.98-28.19m
CR-7 6
28.19-33.85m
CR-7 7
33.85-39.47m
CR-7 8
39.47-44.82m

PLATE II. Examples of sealed calcite veins as viewed under the petrographic microscope (crossed polars):
a) medium-grained equigranular calcite and fine-grained quartz vein in granitic gneiss at 292.32 m in CR8 (field of view is 14 mm across);
b) fine-grained brecciated calcite vein surrounded by quartz in a chlorite-lined fracture at 212.13 m in CR6 (field of view is 14 mm across);
c) fine-grained calcite vein containing fragments of granitic gneiss at 184.88 m in CR8 (field of view is 14 mm across).

a

b

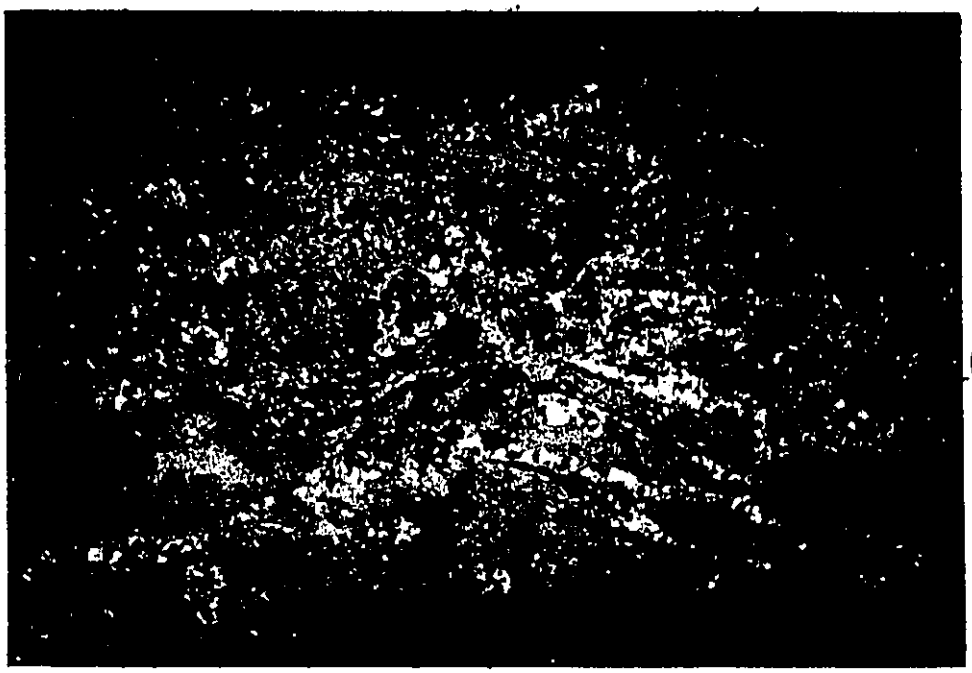

c

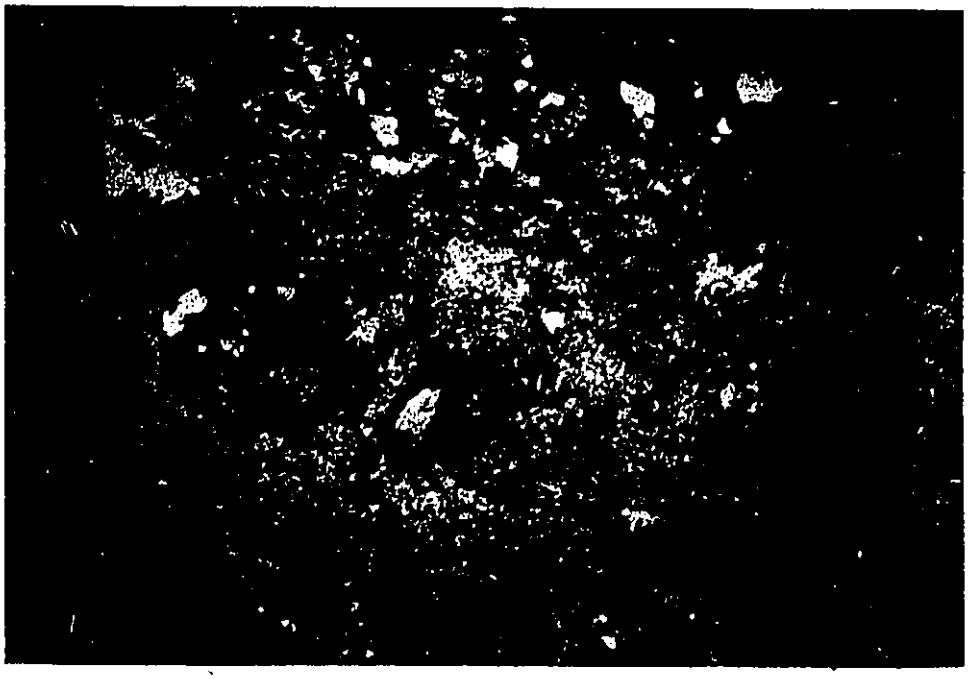

PLATE III. Chlorite-lined fracture sealed with calcite at 26.12 m in CR12:
a) binocular microscope photograph (field of view is 7 mm across);
b) photomicrograph (crossed polars). Field of view is 14 mm across.
c) SEM image of vein showing calcite (cc), pyrite ($FeS_2$), K feldspar (kf) and chlorite (chl) (vertical bar scale is 1 mm).

a

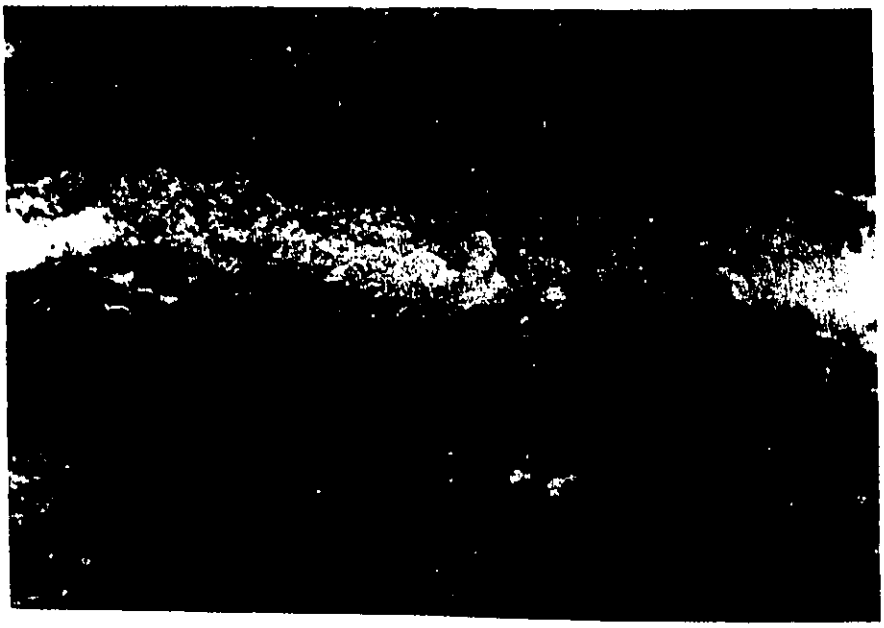

b

c

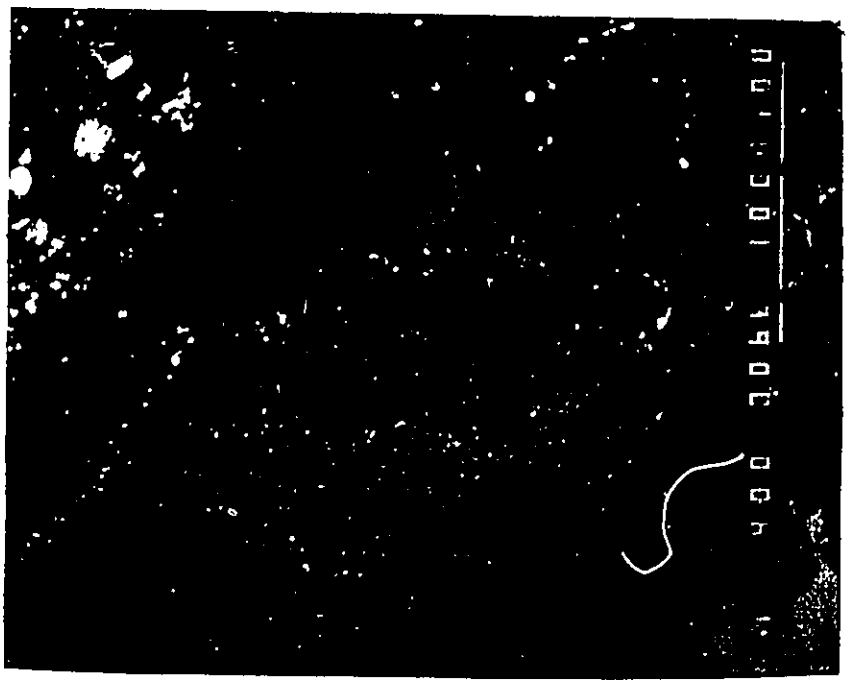

PLATE IV. Scanning electron microscope image of the chlorite-lined sealed fracture at 26.12 m in CR12:
a) SEM image of vein showing the presence of quartz-ofeldspathic material (kf, qtz), pyrite, and calcite (cc);
b) back scattered electron map of the Ca distribution (calcite) in the vein;
c) back scattered electron map of Si distribution (silicates) in the vein.

PLATE IV
a–c

a

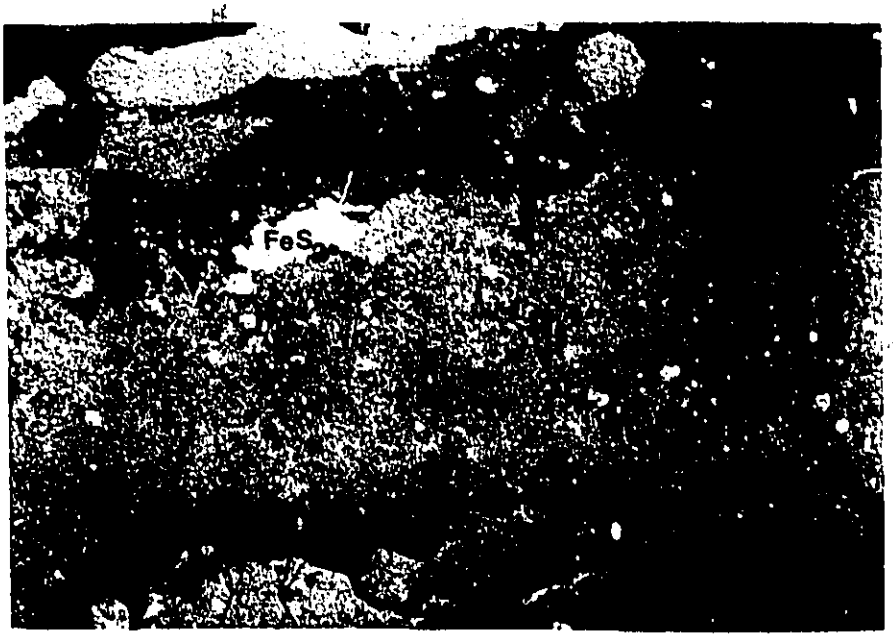


b

c

PLATE V. a) Two generations of calcite in a reopened sub-vertical fracture in monzonitic gneiss at 13.74-13.90 m in FS15. Younger patchy calcite overlies vein calcite. The field of view is 18 mm across.
b) Photomicrograph (crossed polars) showing the coarse-grained calcite (cc) vein in monzonitic gneiss. The field of view is 14 mm across.
c) SEM image of the calcite (cc) vein showing growth zonation and quartz (qtz) inclusions (black oval-shaped objects). Vertical bar scale is 1 mm.

a

b

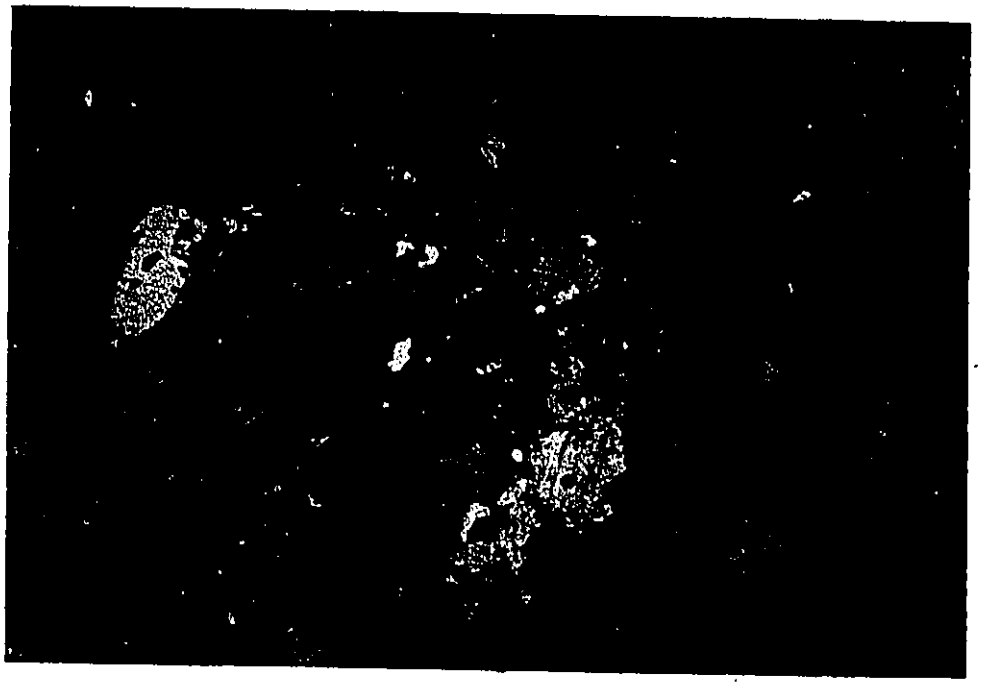

c

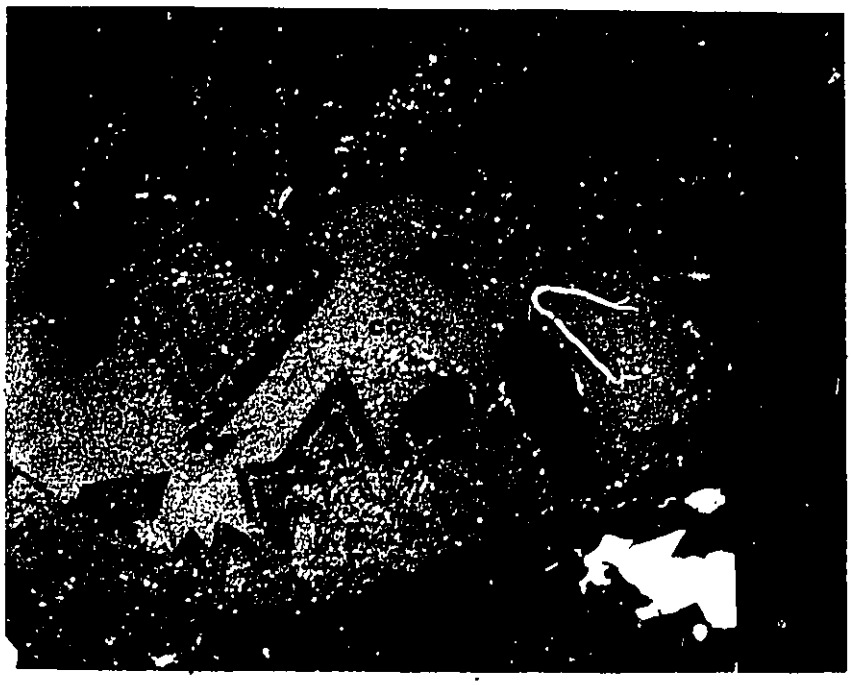

PLATE VI.

a) Sealed calcite lense in altered, porous granitic gneiss at 492.43 m in CR9. The field of view is 18 mm across.
b) Calcite/dolomite matrix surrounding lithic fragments in highly altered, brecciated fault zone at 130.13 m in CR3. The field of view is 18 mm across.
c) Calcified lithic fragment in brecciated zone at 14.9 m in CR12. The field of view is 18 mm across.

a

b

c

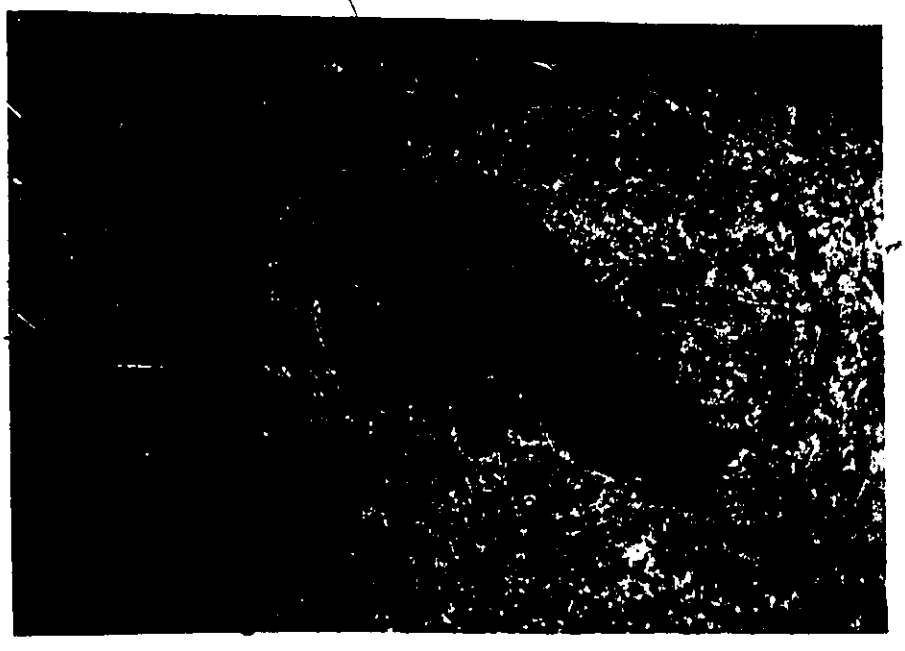

PLATE VII. a) Iron rich oxidation zone next to a sealed calcite vein in monzonitic gneiss at 345.77 m in CR9. The field of view is 7 mm across.

b) Photomicrograph of the calcite (cc) vein showing angular wall rock fragments projecting into the calcite (plain polarized light). The field of view is 2.8 mm across.

c) Photomicrograph (plain polarized light) of brown muscovite (phengite?) in altered feldspar in the oxidation zone next to the calcite vein. Note the unaltered garnet (gn) crystals. The field of view is 2.8 mm across.

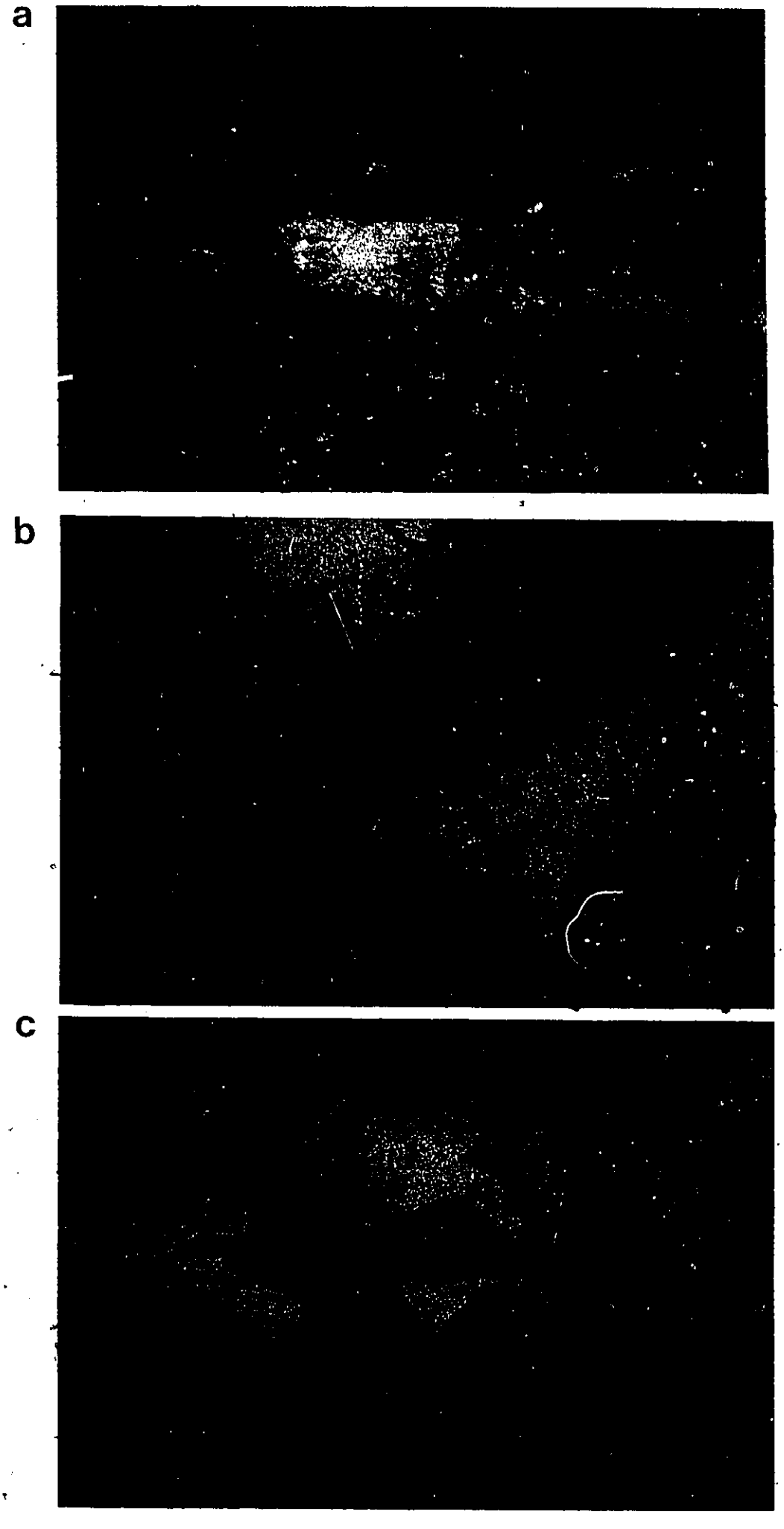
a
b
c

PLATE VIII. a) Calcite (cc) vein with laumontite (lau) in sealed fracture at 459.98 m in CR9. The field of view is 18 mm across.
b) Prismatic crystal of laumontite surrounded by calcite. The field of view is 7 mm across.
c) Individual prismatic crystals of laumontite extracted from the calcite vein. The field of view is 3 mm across.

a

b


c

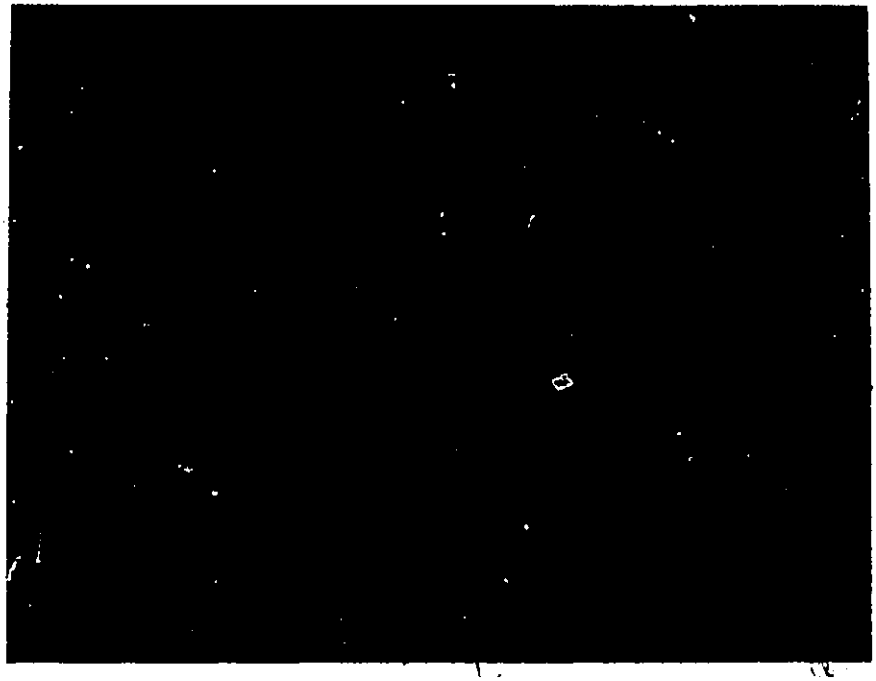

PLATE IX. a) Photomicrograph (plain polarized light) of an altered calcic pyroxene phenocryst near a fracture in a diabase dyke at 128.47 m in CR2. The field of view is 1.4 mm across.
b) Cathodoluminescent image of the phenocryst showing the extent of phenocryst calcification.

a

b

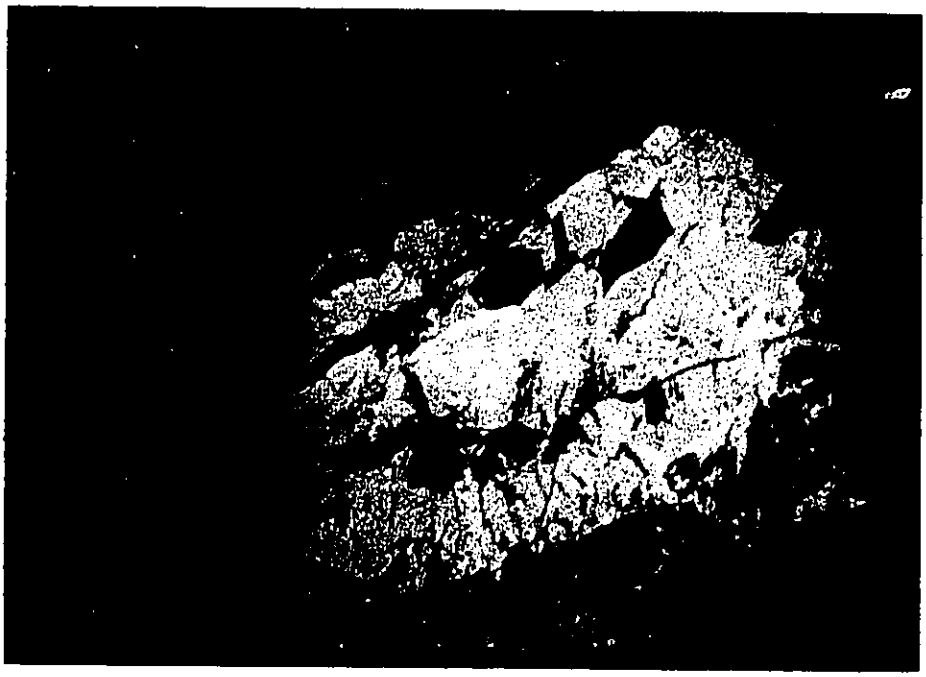

PLATE X.

a) Coarse-grained euhedral calcite crystals in an open sub-horizontal fracture in granitic gneiss at 277.54 m in CR8. The field of view is 18 mm across.

b) Coarse-grained subhedral calcite crystals in a vug of granitic pegmatite at 277.51 m in CR8. The field of view is 18 mm across.

c) Coarse grained subhedral calcite crystals from an irregular curved fracture in amphibolite at 205.67 m in CR8. The field of view is 18 mm across.

a

b

c

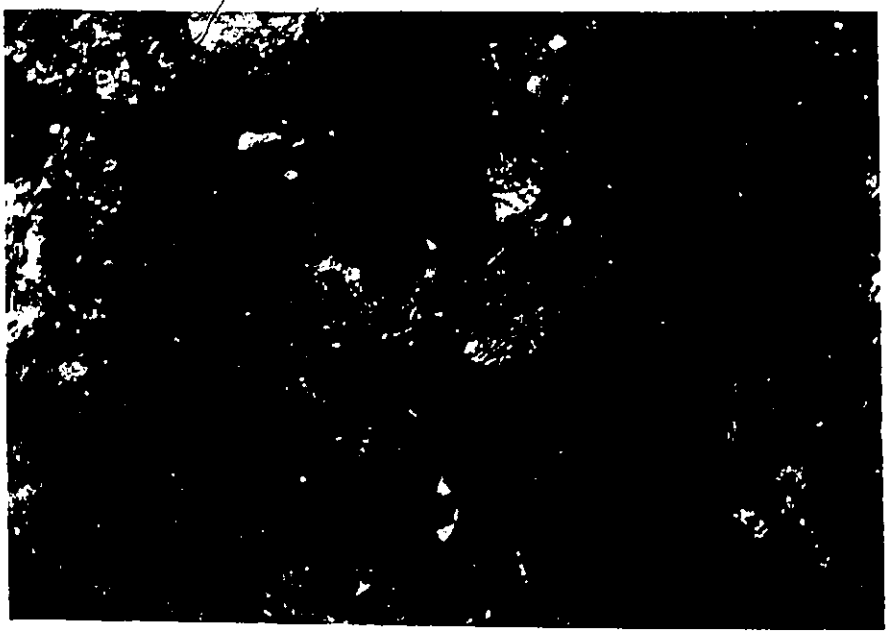

PLATE XI. a) Faintly slickensided calcite on chlorite in a sub-vertical fracture in pegmatite at 285.38 m in CR8. The field of view is 18 mm across.
b) Flaky calcite on chlorite in a sub-vertical open fracture at 51.4 m in CR10. The field of view is 18 mm across.
c) Patchy calcite overlying the calcite vein shown in PLATE V (a). The field of view is 18 mm across.

a

b

c

PLATE XII. a) Fine grained pyrite cubes embedded in "sugary" calcite in a fracture at 99 m in CR12. The field of view is 3 mm across.
b) Patchy aggregate of fine grained pyrite ($FeS_2$) on chlorite in a fracture at 121 m in CR11. The field of view is 18 mm across.
c) Fine grained pyrite with patchy calcite (cc) in a rough irregular fracture in pegmatite at 192.75 m
in CR8. The field of view is 18 mm across.

a

b

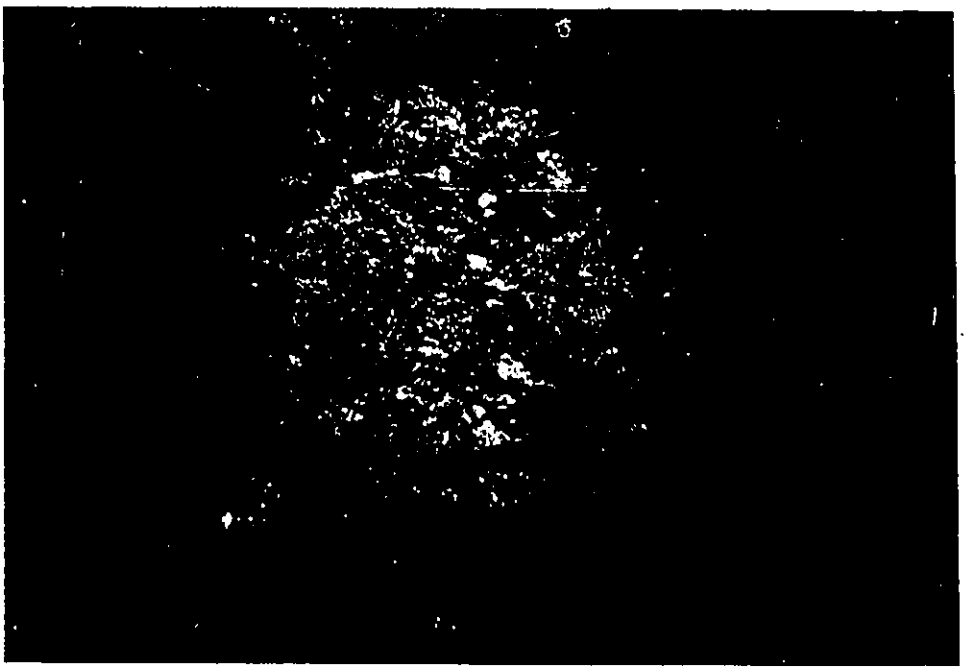

c

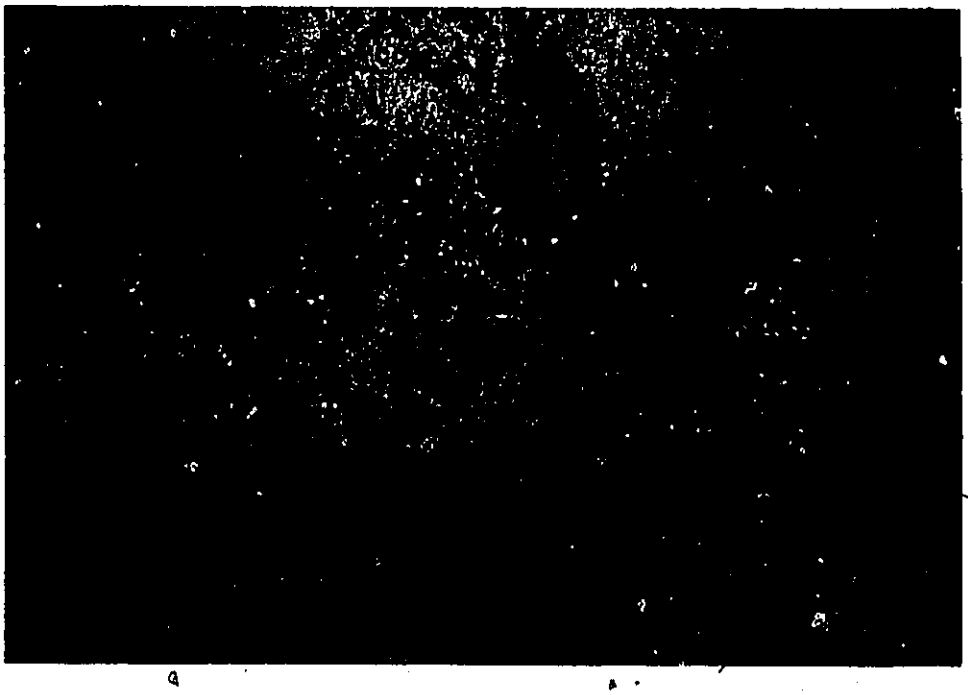

PLATE XIII. Examples of slickensided fracture calcites and pyrites from CRNL core:

a) Faintly slickensided flaky calcite on a sub-vertical open fracture at 51.4 m in CR10. The field of view is 18 mm across.

b) Strongly slickensided "greasy" calcite in a sub-horizontal fracture at 77.8 m in CR12. The field of view is 18 mm across.

c) Strongly slickensided platy pyrite with bluish calcite on chlorite in a fracture at 251.83 m in CR1. The field of view is 18 mm across.

a

b

c

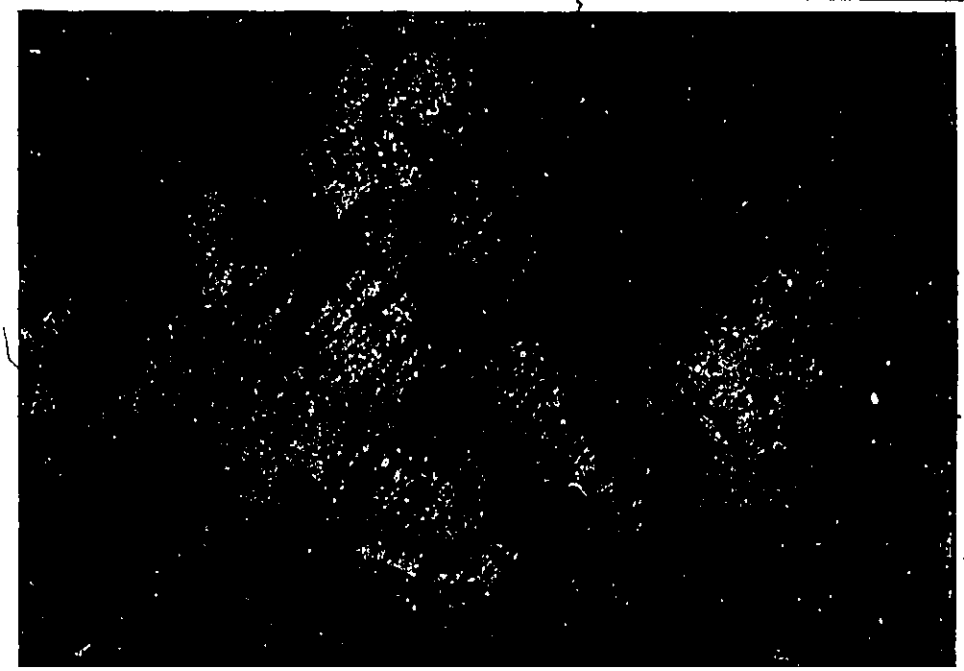

PLATE XIV. SEM images of open-fracture minerals on a fracture in granitic gneiss at 279.3 m in CR8:
a) calcite rhombohedra;
b) chlorite (chl) flakes on K feldspar (kf);
c) clumps of chlorite on K feldspar and calcite (cc) surrounding a probable solution pit.

PLATE XIV
a–c

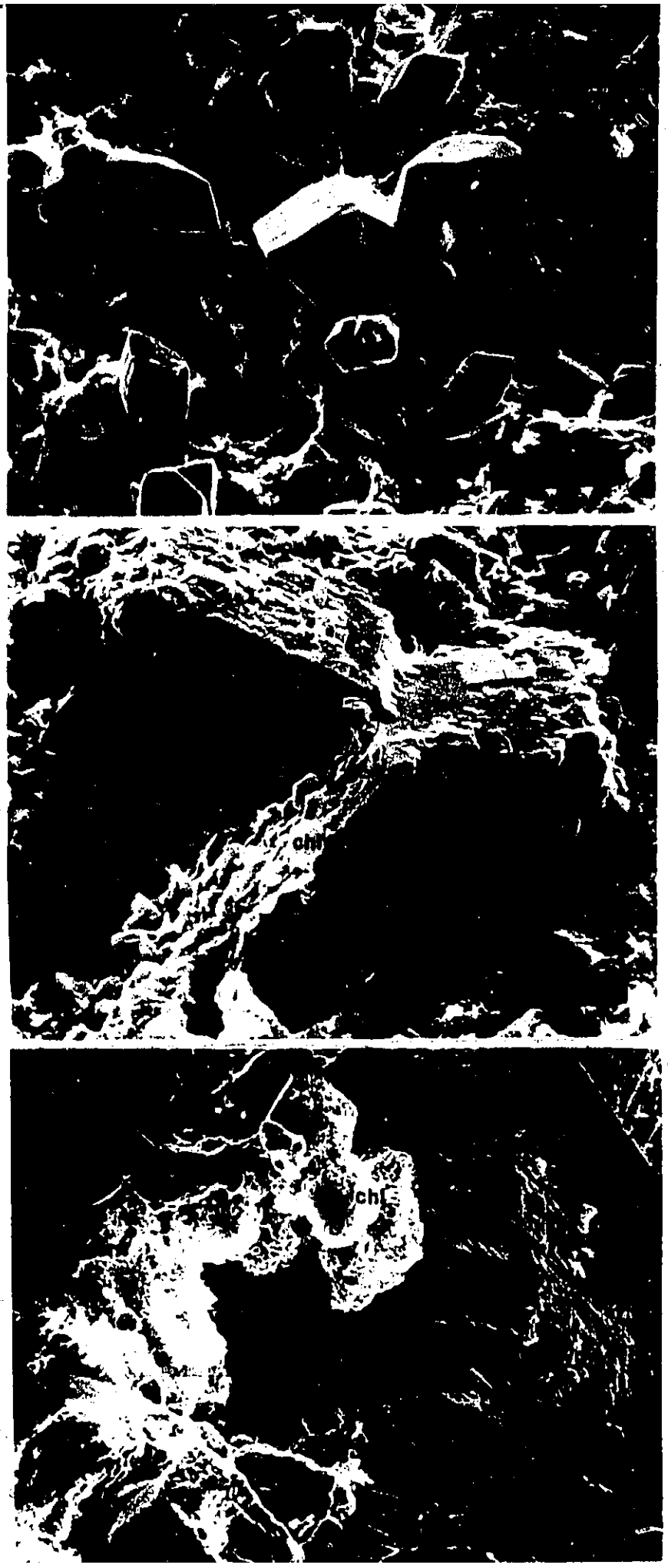

PLATE XV. a) Edge view of younger, brownish, flaky calcite overlying a reopened calcite vein at 574.3 m in CR9. Field of view is 18 mm across.
b) Edge view of younger, brownish, granular calcite (cc3) overlying a reopened calcite vein at 545.9 m in CR9. The field of view is 18 mm across.
c) Clear calcite crystals overlying a reopened calcite vein at 520.39 m in CR9. The field of view is 7 mm across..

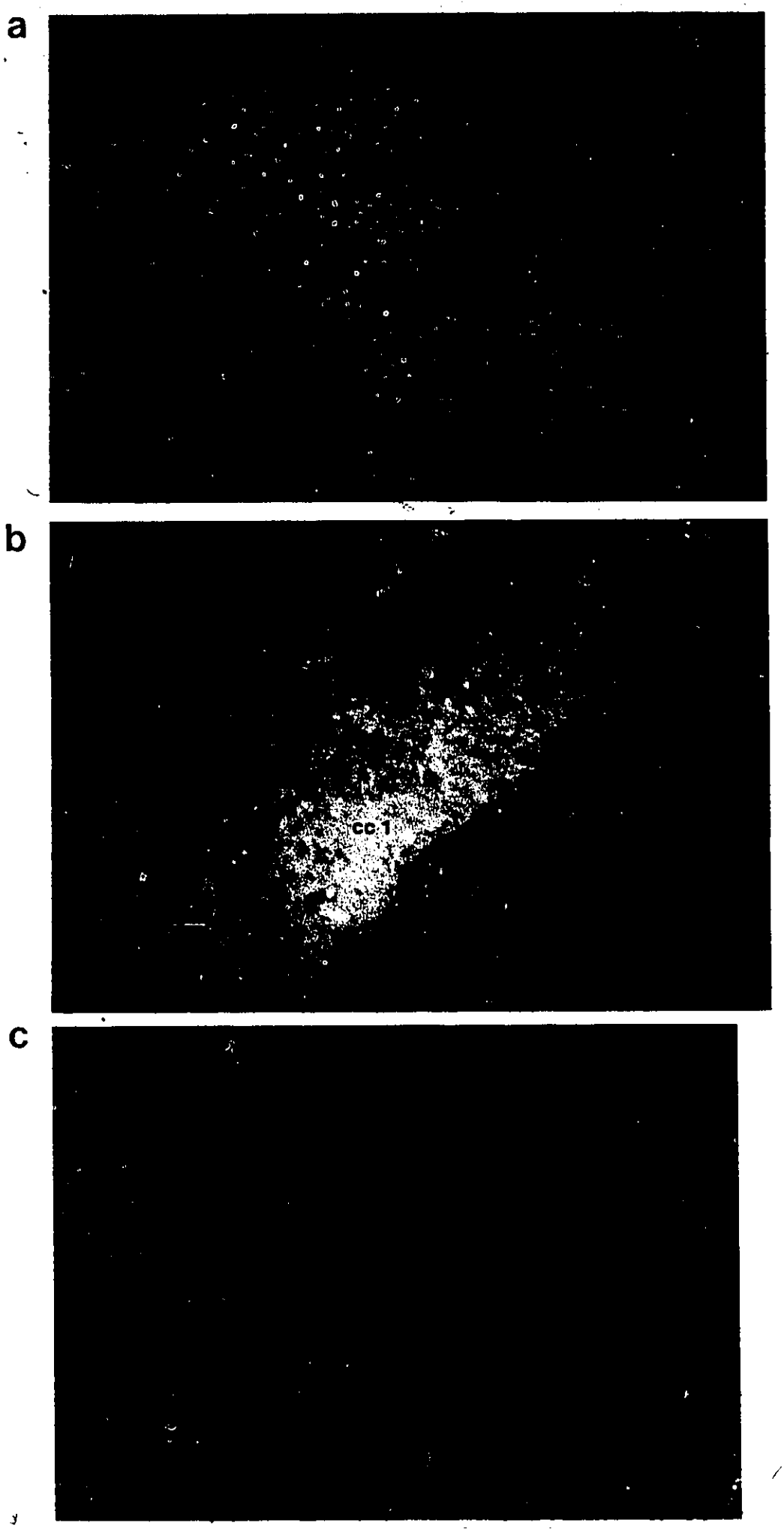
a
b
cc 1
c

PLATE XVI. Examples of fracture calcite from EBL core (field of view 18 mm across in a-c).
a) Sealed calcite vein at 185.6 m in EBL4.
b) Patchy calcite on a sub-vertical fracture at 168.8 m in EBL4.
c) Sub-hedral calcite crystals in vein calcite at 112.46 m in EBL4.

a

b

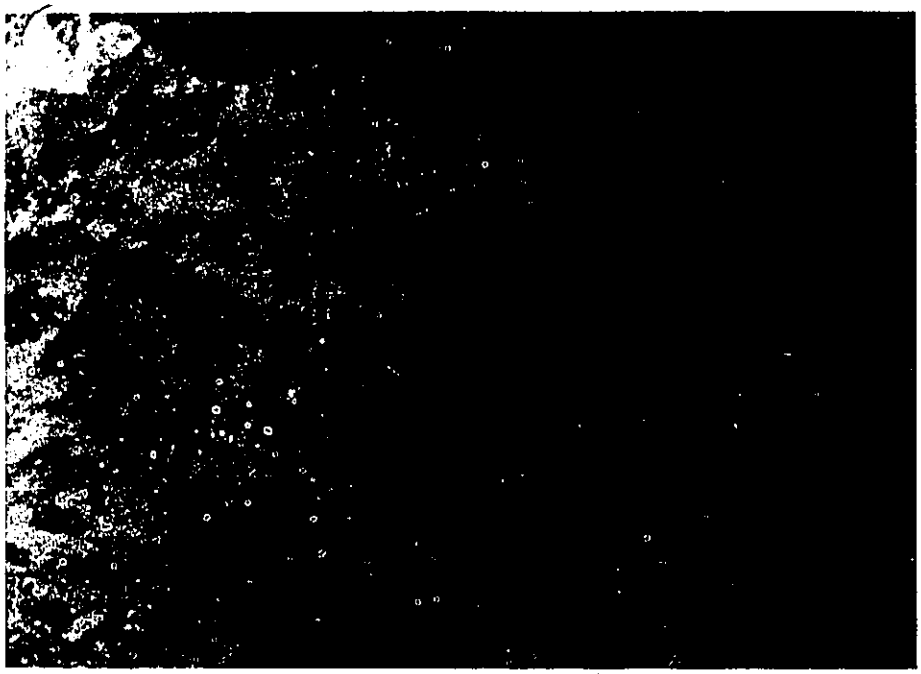

c

PLATE XVII. a) Fine grained pyrite crystals in a fracture at 112.67 m in EBL2. The field of view is 7 mm across.
b) Patchy calcite (cc) with pinkish laumontite (lau) on a fracture at 446.35 m in EBL4. The field of view is 18 mm across.
c) Platy laumontite in a fracture at 654.2 m in EBL1. The field of view is 18 mm across.

a

b

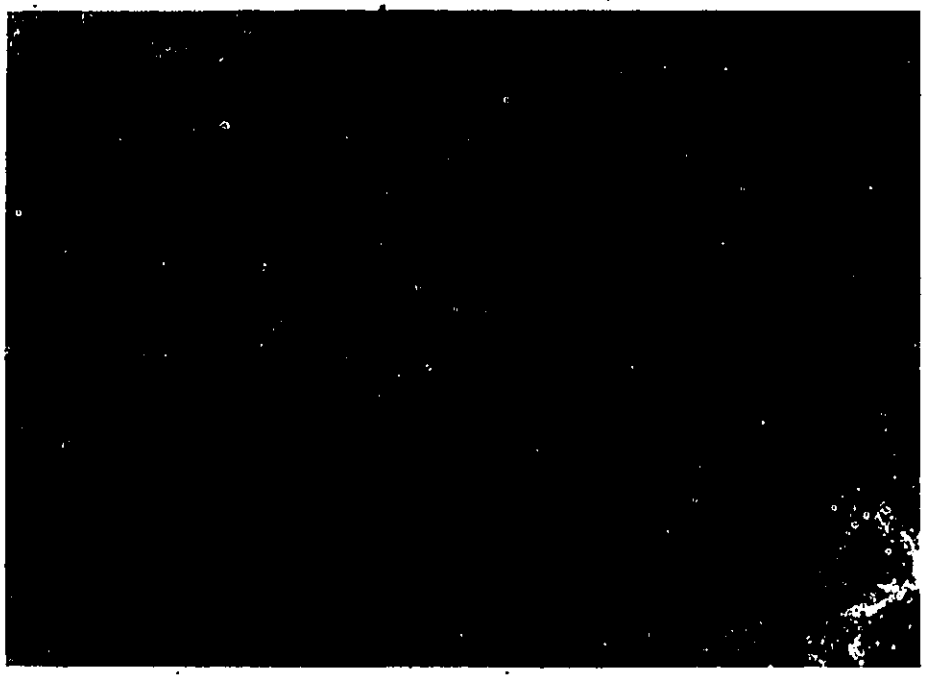

c

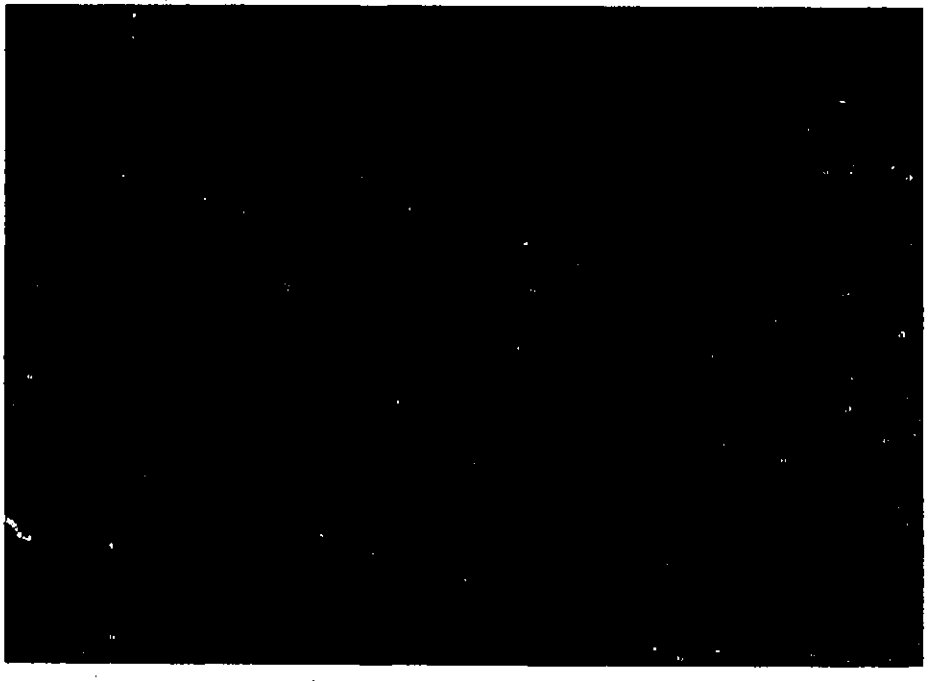

PLATE XVIII. Examples of fracture calcites from the White Lake core:

a) Sealed calcite vein cross-cutting an older quartzofeldspathic vein at 72.7 m in WL1. The field of view is 18 mm across.

b) Platy, ferric oxide-stained calcite on an open fracture at 72.7 m in WL1. The field of view is 18 mm across.

c) Patchy granular calcite overlying ferric oxide-stained, slickensided calcite on an open fracture at 72.7 m in WL1. The field of view is 18 mm across.

a

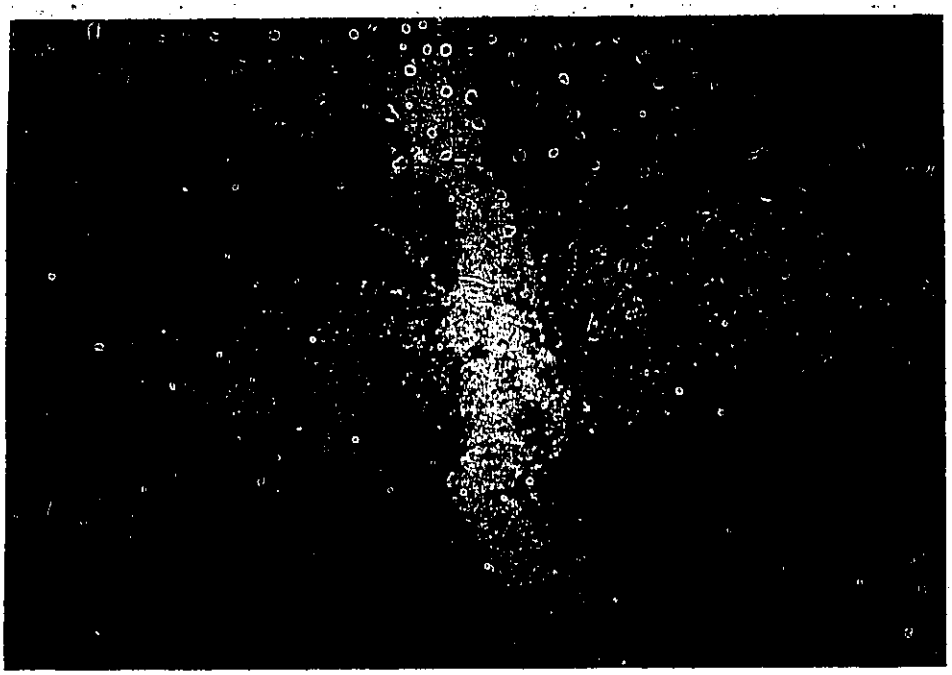

b

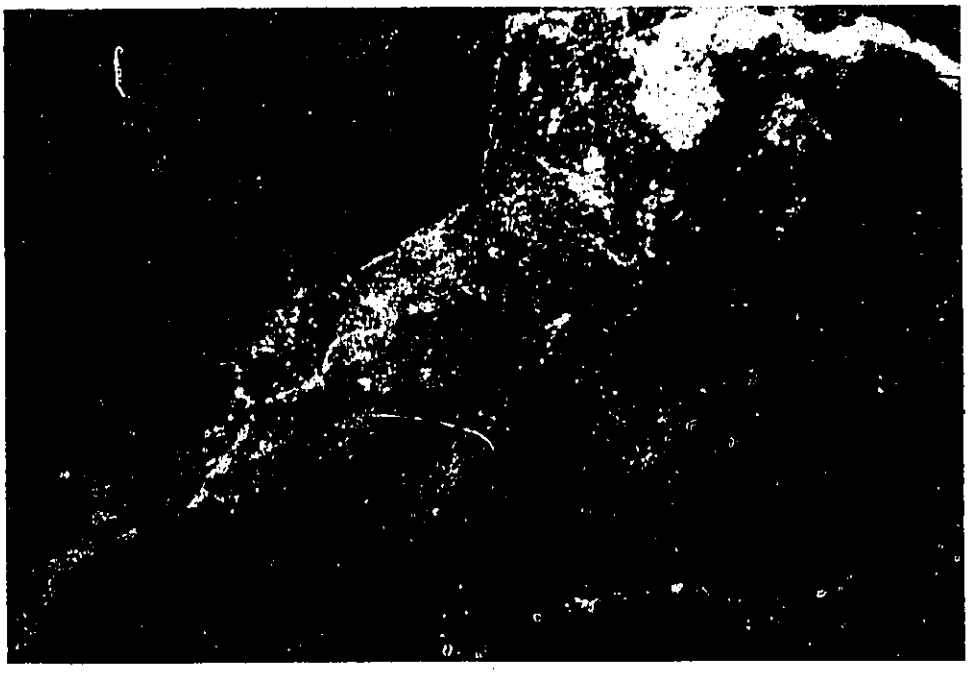

c

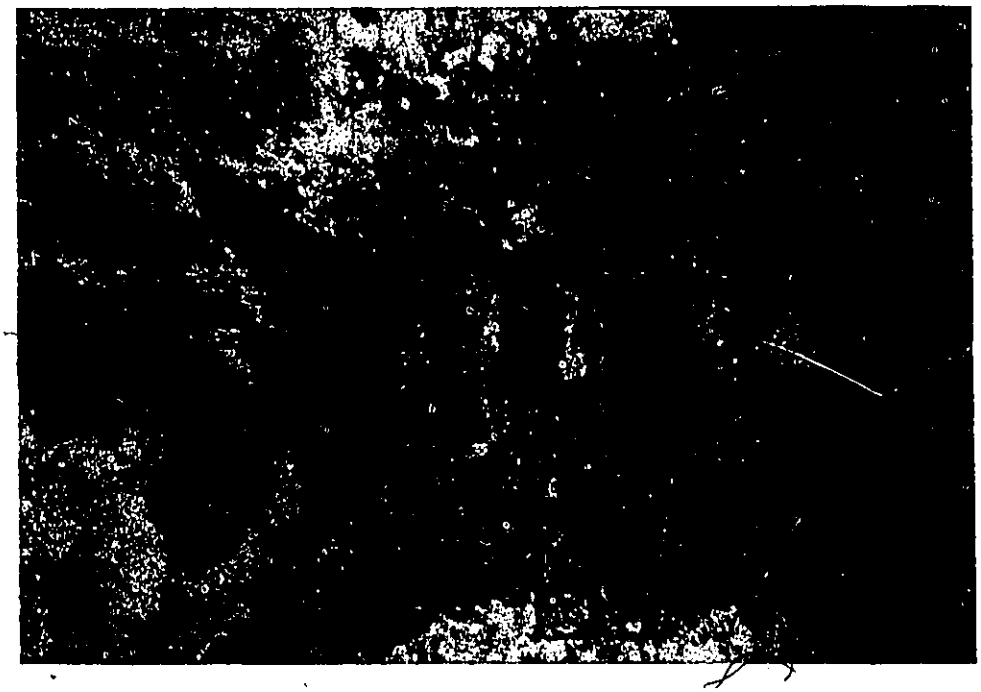

PLATE XIX. a) Photomicrograph of coarse-grained calcite crystals in a sealed vein in granitic gneiss at 137.34 m in CR7 (crossed polars). The field of view is 2.8 mm across.

b) Cathodoluminescent image of the vein showing compositional zoning within individual crystals. Electron microprobe analyses were conducted at the points shown (see Table 9).

c) Cathodoluminescent image of the medial suture of the vein and central vug showing fine scale compositional banding. The field of view is 2.8 mm across.

a

b

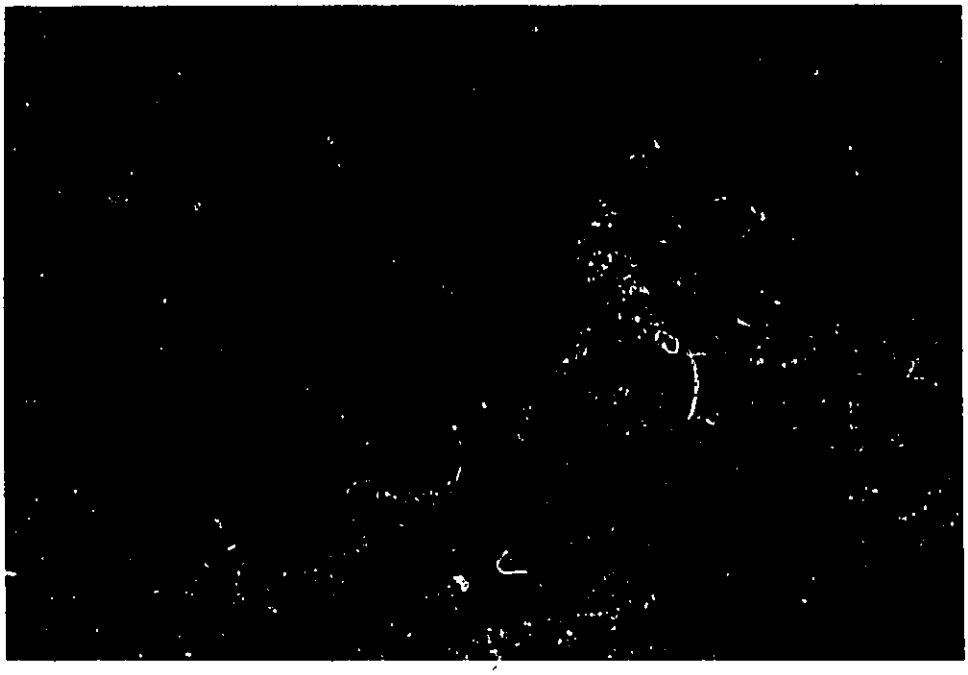

c

PLATE XX. a) Photomicrograph (crossed polars) of a reopened calcite vein at 574.33 m in CR9 showing a younger flaky calcite layer (cc2) overlying the vein (cc1). Note the "corroded" fine-grained texture of top portion of the underlying vein. The field of view is 2.8 mm across.

b) Cathodoluminescent image of the vein showing the brighter calcite layer relative to the darker underlying vein. The field of view is 2.8 mm across.

c) Cathodoluminescent image of the calcite vein showing points analyzed by the electron microprobe and chlorite (chl). The field of view is 1.4 mm across.


a


b

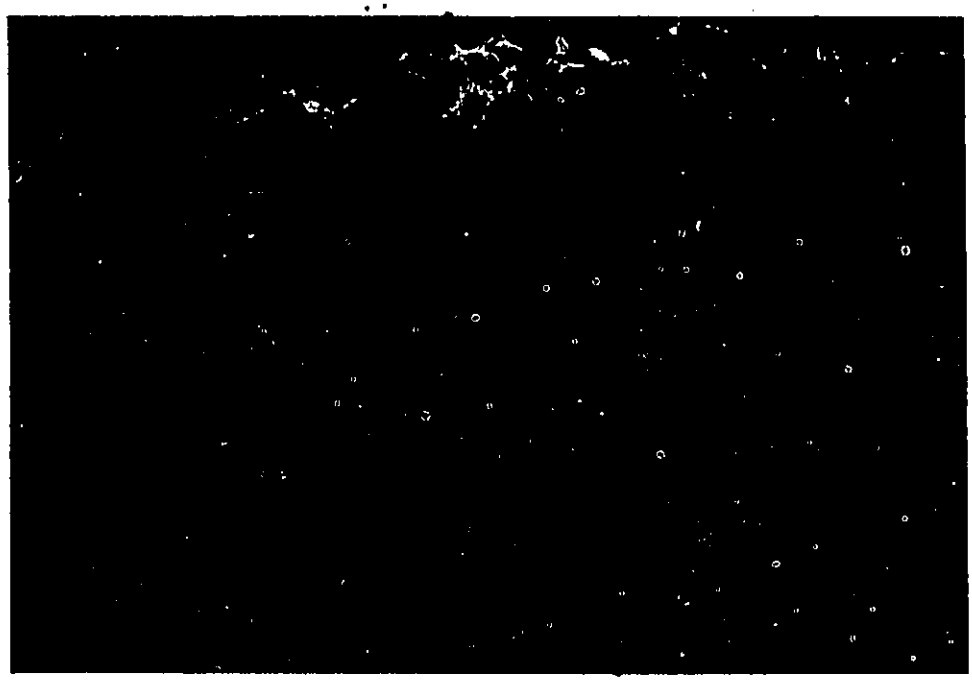

PLATE XXI. SEM images of open fracture calcites analyzed by the electron microprobe (Table 10):

a) "step and kink" dissolution pattern in calcite from CR9 - 464.88 m
b) calcite crystal in fine-grained calcite matrix from CR1 - 232.38 m
c) fine-grained calcite from CR10 - 51.37 m
d) spheroidal calcite from FS15 - 43.85 m
e) laumontite crystal on calcite from CR9 - 464.88 m
f) calcite crystals surrounded by patchy calcite from CR8 - 205.17 m

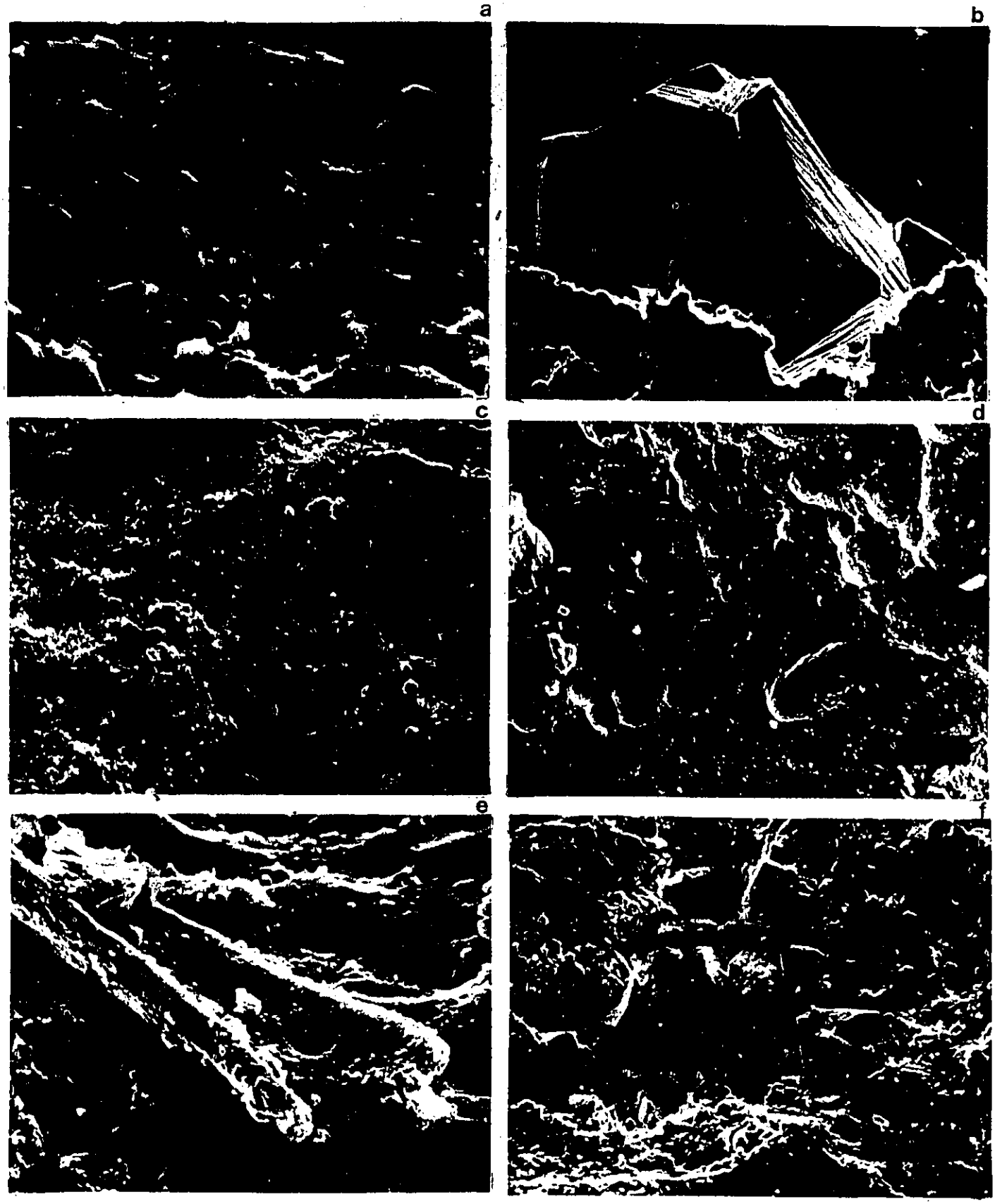
a
b
c
d
e
f

PLATE XXII. Cathodoluminescent image of vug filled with calcite (yellow) surrounded by dolomite (do) cystals. The sample is from a sealed (with carbonate) brecciated
fault zone at 130 m in CR3. The field of view is 2.8 mm across.